

Corrosion Testing of a Plutonium-Loaded Lanthanide Borosilicate Glass Made with Frit B

Chemical Engineering Division

About Argonne National Laboratory

Argonne is a U.S. Department of Energy laboratory managed by The University of Chicago under contract W-31-109-Eng-38. The Laboratory's main facility is outside Chicago, at 9700 South Cass Avenue, Argonne, Illinois 60439. For information about Argonne, see www.anl.gov.

Availability of This Report

This report is available, at no cost, at <http://www.osti.gov/bridge>. It is also available on paper to the U.S. Department of Energy and its contractors, for a processing fee, from:

U.S. Department of Energy
Office of Scientific and Technical Information
P.O. Box 62
Oak Ridge, TN 37831-0062
phone (865) 576-8401
fax (865) 576-5728
reports@adonis.osti.gov

Disclaimer

This report was prepared as an account of work sponsored by an agency of the United States Government. Neither the United States Government nor any agency thereof, nor The University of Chicago, nor any of their employees or officers, makes any warranty, express or implied, or assumes any legal liability or responsibility for the accuracy, completeness, or usefulness of any information, apparatus, product, or process disclosed, or represents that its use would not infringe privately owned rights. Reference herein to any specific commercial product, process, or service by trade name, trademark, manufacturer, or otherwise, does not necessarily constitute or imply its endorsement, recommendation, or favoring by the United States Government or any agency thereof. The views and opinions of document authors expressed herein do not necessarily state or reflect those of the United States Government or any agency thereof, Argonne National Laboratory, or The University of Chicago.

ANL-06/35

ARGONNE NATIONAL LABORATORY
9700 South Cass Avenue
Argonne, IL 60439-4837

**CORROSION TESTING OF A PLUTONIUM-LOADED LANTHANIDE
BOROSILICATE GLASS MADE WITH FRIT B**

by

W. L. Ebert

Chemical Engineering Division
Argonne National Laboratory
9700 South Cass Avenue
Argonne, Illinois 60439-4837

June 2006

INTENTIONALLY LEFT BLANK

CONTENTS

	<u>Page</u>
ACKNOWLEDGEMENTS	viii
ABSTRACT	1
1. INTRODUCTION	2
1.1 Background: Mechanistic Model for HLW Glass Degradation and the Rate Expression	3
1.2 Technical Methods.....	5
2. TESTING	10
2.1 Preparation of Glass Test Specimens.....	10
2.2 Glass Composition Analyses	13
2.3 Testing Equipment.....	14
2.4 Test Execution	16
3. IMMERSION TEST RESULTS AND DISCUSSION	19
3.1 Comparison with Rates in Defense HLW Glass Degradation Model.....	25
3.2 Model Coefficients Based on the Release of Si.....	33
3.3 Model Coefficients Based on the Release of B	33
3.4 Comparison with the Simplified Rate Expression Used in the Defense HLW Glass Degradation Model	34
3.5 Fitting Test Results with Rate Equation	36
3.6 Tests in Demineralized Water at 90 and 120 °C	39
3.7 Concentrations of Pu, Gd, and Hf in Test Solutions	40
4. VAPOR HYDRATION TEST RESULTS AND DISCUSSION	47
5. ADDITIONAL COMMENTS.....	59
5.1 Homogeneity of Pu LaBS-B Glass	59
5.2 Leachant Solutions	59
5.3 Dissolution Rates Compared with Defense HLW Glass Degradation Model	60
5.4 Model Coefficient Values.....	61
5.5 Effect of HLW Glass on LaBS Glass Dissolution	62
5.6 Recommendations for Further Work	63
5.7 Estimated Impact of Pu LaBS Glass on HLW Inventory Used in TSPA	64
6. CONCLUSIONS	65
REFERENCES	66
APPENDIX A: Glass Test Specimens	68
APPENDIX B: Data and Results for Immersion Tests at 40 °C	77
APPENDIX C: Data and Results for Immersion Tests at 70 °C	86
APPENDIX D: Data and Results for Immersion Tests at 90 °C	95
APPENDIX E: Propagation of Errors.....	104
APPENDIX F: Test Data for Vapor Hydration Tests.....	114

TABLES

	<u>Page</u>
1. Test Matrix for Immersion Tests with Pu LaBS-B Glass.....	7
2. Leachant Solution Compositions and Initial pH Values	8
3. Test Matrix for Vapor Hydration Tests.....	9
4. Compositions of Pu LaBS-B, Frit X, and SRL 418 Glasses	14
5. Rate Equations for Forward Rates Based on Si Release	26
6. Rate Equations for Forward Rates Based on B Release.....	26
7. Summary of Experimental Results and Numerical Regression for Si Release	29
8. EDS Compositions of Phases on Surface of Vapor-Hydrated SRL 418 Glass.	50
9. EDS Compositions of Phases in Outer Layers of Vapor-Hydrated SRL 418 Glass	53
10. Results of XRD Analyses of Vapor-Reacted SRL 418 Glass	54
11. Summary of EDS Results.....	58
12. Si Concentrations Measured in Blank Tests Conducted at Different Temperatures	60
13. Comparison of Model Coefficient Values η and E_a Measured for Various Glasses	61
14. Impact of the Estimated Plutonium Content in Pu LaBS Glass on TSPA-LA Inventory	64
A1. Measured Dimensions of Monolithic Pu-LaBS-B Glass Test Specimens	70
A2. Measured Composition of Frit X Glass.....	74
A3. Measured Composition of SLR 418 Glass	75
A4. Measured Composition of Pu LaBS-B Glass	76
B1. Test Data for Tests at 40 °C.....	79
B2. Results of Static Dissolution Tests at 40 °C: Measured Concentrations in Test Solutions	81
B3. Results of Static Dissolution Tests at 40 °C: Calculated Masses in Test Solutions	82
B4. Results of Static Dissolution Tests at 40 °C: Measured Concentrations in Acid Soak Solutions.....	83
B5. Results of Static Dissolution Tests at 40 °C: Calculated Masses in Acid Soak Solutions	84
B6. Results of Static Dissolution Tests at 40 °C: Normalized Elemental Mass Losses.....	85
C1. Test Data for Tests at 70 °C.....	88

TABLES (cont.)

	<u>Page</u>
C2. Results of Static Dissolution Tests at 70 °C: Measured Concentrations in Test Solutions	90
C3. Results of Static Dissolution Tests at 70 °C: Calculated Masses in Test Solutions	91
C4. Results of Static Dissolution Tests at 70 °C: Measured Concentrations in Acid Soak Solutions	92
C5. Results of Static Dissolution Tests at 70 °C: Calculated Masses in Acid Soak Solutions	93
C6. Results of Static Dissolution Tests at 70 °C: Normalized Elemental Mass Losses	94
D1. Test Data for Tests at 90 °C	97
D2. Results of Static Dissolution Tests at 90 °C: Measured Concentrations in Test Solutions	99
D3. Results of Static Dissolution Tests at 90 °C: Calculated Masses in Test Solutions	100
D4. Results of Static Dissolution Tests at 90 °C: Measured Concentrations in Acid Soak Solutions	101
D5. Results of Static Dissolution Tests at 90 °C: Calculated Masses in Acid Soak Solutions	102
D6. Results of Static Dissolution Tests at 90 °C: Normalized Elemental Mass Losses	103
E1. Summary of Solution Concentrations, Volumes, and Specimen Areas and Their Uncertainties	110
E2. Summary of Variance in Each Term, Uncertainty, and Relative Uncertainty	112
F1. Test Data for Vapor Hydration Tests	114

FIGURES

	<u>Page</u>
1. Schematic Drawing of How Bar of Pu LaBS-B Glass Was Cut into Coupon Specimens for Testing.....	11
2. SEM Photomicrograph of LaBS-B Glass.....	12
3. Photograph of Teflon and Steel Test Vessels and Assemblies for Immersion Tests	15
4. Schematic Drawing of VHT Specimens Suspended from Support Rod	17
5. NL(i) vs. Reaction Time for Tests with Pu LaBS-B Glass at 40 °C and pH 3.70, pH 4.88, pH 6.09, pH 8.56, pH 9.40, and pH 10.89	21
6. NL(i) vs. Reaction Time for Tests with Pu LaBS-B Glass at 70 °C and pH 3.73, pH 4.89, pH 6.10, pH 8.58, pH 9.37, and pH 10.87.....	22
7. NL(i) vs. Reaction Time for Tests with Pu LaBS-B Glass at 90 °C and pH 3.74, pH 4.89, pH 6.13, pH 8.60, pH 9.18, and pH 10.87	23
8. Comparison of Rates Representing the pH and Temperature Dependence in the Defense HLW Glass Dissolution Model with Measured Dissolution Rates of Pu LaBS-B Glass in Tests at 40 °C, 70 °C, and 90 °C.	27
9. Regression Fit of NR(Si) Results to Determine Dependence on pH and Temperature at 40 °C, 70 °C, and 90 °C.	28
10. Regression Fit of NR(B) Results to Determine Dependence on pH and Temperature at 40 °C, 70 °C, and 90 °C.....	33
11. Comparison of Forward Dissolution Rate Models for Pu LaBS-B Glass Based on Releases of Si and B at 90 °C	34
12. Comparison of Defense HLW Glass Model with Analogous Rate Equations for Pu LaBS-B Glass Based on Releases of Si and B at 90 °C	36
13. NL(Si) Results Fitted by Linear Regression and by Regression to Glass Dissolution Equations for Tests at 70 °C in pH 10.87 Solution, 90 °C in pH 10.87 Solution, 70 °C in pH 9.37 Solution, 90 °C in pH 9.18 Solution, 70 °C in pH 8.58 Solution, and 90 °C in pH 8.60 Solution.....	38
14. Results of Tests Conducted in Demineralized Water through 5 Days and through 91 Days.....	39

FIGURES (cont.)

		<u>Page</u>
15.	Results of PCTs Conducted at SRNL with Pu LaBS-B Glass at 90 °C and 21,000 m ⁻¹	40
16.	Concentrations of Gd, Hf, and Pu in the Test Solutions at 40 °C, 70 °C, and 90 °C	42
17.	Ratios NL(Gd)/NL(Si), NL(Hf)/NL(Si), and NL(Pu)/NL(Si) for Test Series MLB1-90, MLB2-90, MLB3-90, MLB4-90, MLB5-90R, and MLB6-90.....	43
18.	Distributions of Gd, Hf, and Pu Between Test Solutions and Acid Soak Solutions	44
19.	Ratios NL(Gd)/NL(Si), NL(Hf)/NL(Si), and NL(Pu)/NL(Si) for Tests Conducted in Demineralized Water at 90 and 120 °C.	46
20.	Vapor-Reacted Pu-LaBS-B Glass Contacting SRL 418 Glass, and Separated	48
21.	Vapor-Reacted SRL 418 Glass.....	48
22.	SEM Photomicrographs of Alteration Phases Formed on Surface of Vapor-Hydrated SRL 418 Glass.....	49
23.	SEM Photomicrograph of Vapor-Reacted SRL 418 Glass	51
24.	SEM Photomicrographs of Outermost and Interior Alteration Layers Formed on Vapor-Reacted SRL 418 Glass.....	52
25.	SEM Photomicrographs of Alteration Phases Formed on Pu LaBS-B Glass Contacted with SRL 418 Glass in VHT at 200 °C.....	55
26.	SEM Photomicrographs of Alteration Phases Formed on Pu LaBS-B Glass Specimen B7b.....	57

ACKNOWLEDGMENTS

This report provides a compilation and summary of work performed under the auspices of the Savannah River National Laboratory through Memorandum Purchase Order AC45709V under the technical guidance of Dr. James C. Marra (SRNL). Solution analyses were conducted by Yifen Tsai; SEM analyses were performed by Nancy Dietz and Jeffery Fortner; technical and analytical assistance was provided by Delbert Bowers, Mark Clark, Jeffery Emery, and Alice Essling, all scientists in the Argonne National Laboratory Chemical Engineering Division. Quality Assurance oversight was provided by Roberta Riel and technical oversight by James Cunnane. Work at Argonne National Laboratory is supported by the U.S. Department of Energy, Office of Nuclear Engineering, Science and Technology under contract W-31-109-Eng-38.

CORROSION TESTING OF A PLUTONIUM-LOADED LANTHANIDE BOROSILICATE GLASS MADE WITH FRIT B

W. L. Ebert

ABSTRACT

Laboratory tests were conducted with a lanthanide borosilicate (LaBS) glass made with Frit B and added PuO₂ (the glass is referred to herein as Pu LaBS-B glass) to measure the dependence of the glass dissolution rate on pH and temperature. These results are compared with the dependencies used in the Defense HLW Glass Degradation Model that was developed to account for HLW glasses in total system performance assessment (TSPA) calculations for the Yucca Mountain repository to determine if that model can also be used to represent the release of radionuclides from disposed Pu LaBS glass by using either the same parameter values that are used for HLW glasses or parameter values specific for Pu LaBS glass. Tests were conducted by immersing monolithic specimens of Pu LaBS-B glass in six solutions that imposed pH values between about pH 3.5 and pH 11, and then measuring the amounts of glass components released into solution. Tests were conducted at 40, 70, and 90 °C for 1, 2, 3, 4, and 5 days at low glass-surface-area-to-solution volume ratios. As intended, these test conditions maintained sufficiently dilute solutions that the impacts of solution feedback effects on the dissolution rates were negligible in most tests. The glass dissolution rates were determined from the concentrations of Si and B measured in the test solutions. The dissolution rates determined from the releases of Si and B were consistent with the “V” shaped pH dependence that is commonly seen for borosilicate glasses and is included in the Defense HLW Glass Degradation Model. The rate equation in that model (using the coefficients determined for HLW glasses) provides values that are higher than the Pu LaBS-B glass dissolution rates that were measured over the range of pH and temperature values that were studied (i.e., an upper bound). Separate coefficients for the rate expression in acidic and alkaline solutions were also determined from the test results to model Pu LaBS-B glass dissolution directly.

The releases of Gd, Hf, and Pu from the glass were also measured. The release of Pu was significantly less than Si at all temperatures and pH values (on a normalized basis). More Gd than Pu or Hf was released from the glass in acidic solutions, but more Pu than Gd or Hf was released in alkaline solutions. Almost all of the released Gd remained in solution in tests conducted in Teflon vessels, whereas about half of the released Pu and Hf became fixed to the Teflon. In tests conducted in Type 304L stainless steel vessels, most of the released Gd, Hf, and Pu became fixed to the steel. The aqueous concentrations of Gd, Hf, and Pu decreased from about 2×10^{-5} , 2×10^{-8} , and 1×10^{-7} M in tests solutions near pH 3.7 to about 1×10^{-9} , 8×10^{-10} , and 1×10^{-8} M in test solutions near pH 10.8, respectively, in the 90 °C tests in Teflon vessels (the solutions were not filtered prior to analysis).

Vapor hydration tests (VHTs) were conducted at 120 and 200 °C with Pu LaBS-B glass and SRL 418 glass, which was made to represent the HLW glass that will be used to macro-encapsulate LaBS glass within the waste form. Some VHTs were conducted with specimens of Pu LaBS-B and SRL 418 glasses that were in contact to study the effect of the solution generated as HLW glass dissolves on the corrosion behavior of Pu LaBS-B glass. Other VHTs were conducted in which the glasses were not in contact. The Pu LaBS-B glass is more durable than the HLW glass under these accelerating test conditions, even when the glasses are in contact. The presence of the SRL 418 glass did not promote the dissolution of the Pu LaBS-B glass significantly. However, Gd, Hf, and Pu were detected in alteration phases formed on the Pu LaBS-B glass surface and in (or on) phases formed by SRL 418 glass degradation, such as analcime. This indicates that Gd, Hf, and Pu were transported from the LaBS glass, through the water film formed on the specimens, and to the SRL 418 glass during the test. The disposition of the PuO₂ inclusion phases as the Pu LaBS-B glass dissolved was not determined. They were observed in the glass underlying the alteration layers, but were not detected among the alteration phases.

1. INTRODUCTION

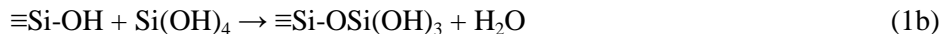
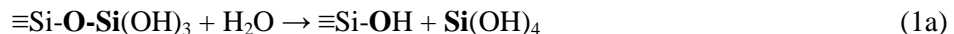
The work described in this report was conducted under the auspices of the Savannah River National Laboratory (SRNL) through memorandum purchase order AC45709V to support the development of analysis/model reports to assess the likely performance of lanthanide borosilicate (LaBS) glass waste forms developed to immobilize plutonium. The technical objectives were to measure the degradation rate of a LaBS glass containing PuO_2 as a function of temperature and pH under conditions in which the feedback from dissolved glass (primarily dissolved Si) is small, and identify alteration phases that form as LaBS glass dissolves (either alone or in the presence of HLW glass) and the disposition of Pu. The dismantling of nuclear weapons has resulted in an excess of weapons-useable Pu that will be either irradiated in a nuclear reactor as mixed-oxide (MOX) fuel or disposed as waste. A lanthanide borosilicate (LaBS) glass is being formulated to immobilize the Pu destined for disposal in the federal high-level radioactive disposal system at Yucca Mountain. The proposed Pu disposal form is Pu-bearing LaBS glass that is macro-encapsulated within HLW glass made with tank waste at the Savannah River Site. The LaBS glass will contain Pu at concentrations that are much higher than typical borosilicate high-level radioactive waste (HLW) glasses designed for tank wastes (about 10 mass% in Pu LaBS compared with less than 0.1 mass% in HLW glass), and will be the dominant contributor to the ^{239}Pu inventory of HLW in the repository (see discussion in Section 5.7). The Pu LaBS glass must be sufficiently durable to ensure that the total amount of Pu released from the repository will remain within regulated limits. Laboratory tests are being conducted to demonstrate that Pu LaBS glass will be acceptable for disposal in the DOE repository at Yucca Mountain and that its contribution to the Pu source term can be quantified in total system performance assessment (TSPA) calculations. The proposed approach is to show that the Defense HLW Glass Degradation Model developed for use in performance assessment calculations can be used directly (or slightly modified) to include the impact of Pu LaBS waste forms on repository performance. That model provides the rate at which the silicate glass matrix dissolves such that Pu and other radionuclides become available for transport as either dissolved species or colloids.

Use of the same model for HLW glasses and Pu LaBS glass is reasonable because both are aluminoborosilicate glasses and the dissolution of the silicate matrix occurs through hydrolysis of Si–O bonds (in alkali solutions). The major difference is the absence of alkali metals in Pu LaBS glass. The lack of alkali metals is expected to enhance the chemical durability of Pu LaBS glass relative to borosilicate glass due to both structure effects (e.g., alkali metals terminate the silicate network in HLW glasses) and chemical effects (e.g., the release of alkali metals leads to an increase in the solution pH). Because Pu LaBS glass will be encapsulated in HLW glass, dissolution of HLW glass will control the chemistries of groundwater solutions that may eventually contact LaBS glass. Therefore, it is important to understand the corrosion behavior of LaBS glass in solutions other than those produced by dissolution of LaBS glass alone. Several vapor hydration tests (VHTs) were conducted to gain insight into the impact of HLW glass dissolution on the dissolution behavior of LaBS glass. For example, dissolution of HLW glass will result in highly alkaline solutions with high alkali metal contents that can lead to the formation of zeolites and other alteration phases that could affect the durability of Pu LaBS glass.

The development of the Defense HLW Glass Degradation Model used in TSPA is first discussed in detail to show how the results of tests conducted with LaBS glass relate to the Model. The technical methods and test results of the immersion tests are then presented and discussed. The measured rates are compared directly with the rates used to develop the model. Model parameter values are determined from the results of tests with a LaBS glass containing Pu and compared with values used in the Model. The amounts of Gd, Hf, and Pu released under different test conditions are determined to evaluate the possible separation of Pu from the neutron absorbers Gd and Hf under repository conditions. Finally, the results of scoping vapor hydration tests (VHTs) are discussed with regard to the insight they provide regarding the relative durabilities of LaBS glasses and HLW glasses.

1.1 BACKGROUND: MECHANISTIC MODEL FOR HLW GLASS DEGRADATION AND THE RATE EXPRESSION

The mechanistic model developed for dissolution of aluminosilicate minerals (Aagaard and Helgeson 1982) was adapted to model dissolution of borosilicate HLW glasses (Grambow 1985). The dissolution of compositionally complex HLW glasses is modeled to be dominated by the hydrolysis of Si–O bonds, which are by far the most abundant bonds in HLW glasses; HLW glasses typically contain between about 35 and 50 mass% SiO₂. The net hydrolysis and condensation reactions are given in Equations 1a and 1b:



Dissolution occurs due to hydrolysis of the bond between a silicon atom that is part of the structure and an oxygen atom of an adjacent OSi(OH)₃ group (see Lasaga and Gibbs 1990). These are shown in bold font in Equation 1a. A hydrogen bond is formed between an H atom of the incoming water molecule and the oxygen, and a bond forms between the oxygen atom of the water and the Si atom of the terminal Si(OH)₃ group (shown in bold font in Eq. 1a). The activated complex is illustrated in Equation 1c:



The original bond between the O and Si (shown in bold font in Eqs. 1a and 1c) is broken, the H atom is transferred from the water to the oxygen of the glass to form a silanol group, and the OH of the water bonds with the Si atom (shown in bold font) to form a molecule of orthosilicic acid (H₄SiO₄) that is released into solution. The reactions in Equations 1a and 1b are written for Si, but analogous hydrolysis reactions occur with other elements in the glass network (e.g., Al–O–Si, B–O–Si, U–O–Si, etc.) to release other species into solution. The reverse reaction can occur, as shown in Equation 1b, and becomes more significant as the concentration of orthosilicic acid increases. The net rate is the difference between the rates of the forward and reverse reactions in Equations 1a and 1b, and can be expressed in terms of the forward reaction rate using non-equilibrium thermodynamics as (Aagaard and Helgeson 1982)

$$\text{rate}_G = \text{rate}_f \cdot \left(1 - \frac{Q}{K}\right), \quad (2)$$

where Q and K are the ion activity product and solubility product of the solution, respectively. The subscript G is used to denote the net rate of glass dissolution and the subscript f is used to denote the forward rate. The term in parentheses is referred to as the chemical affinity term. Glass dissolution is usually modeled by including only orthosilicic acid in the Q and K terms. When the solution is very dilute and the value of Q is near 0, the value of the affinity term is 1 and dissolution occurs at the so-called forward rate, rate_f , which depends on the glass composition, pH, and temperature. As the concentration of orthosilicic acid increases, the value of Q increases (and the value of the affinity term decreases) and the net rate becomes less than the forward rate. In the limit where orthosilicic acid reaches its solubility limit and $Q = K$, the value of the affinity term (and the rate) becomes zero.

The expression used for the forward rate is empirical. Tests have shown the forward rate to have a power law dependence on the pH and an Arrhenius dependence on the temperature. A rate coefficient term k_0 is used to account for the dependence on glass composition, and the effects of other variables are included explicitly. The forward rate is expressed as

$$rate_f = k_0 \cdot 10^{\eta \cdot pH} \cdot \exp\left(\frac{-E_a}{RT}\right), \quad (3)$$

where η is the coefficient for the pH dependence and E_a is the coefficient for the temperature dependence, R is the ideal gas constant, and T is the temperature in Kelvin. Inserting Equation 3 into Equation 2 gives the net dissolution rate as

$$rate_G = k_0 \cdot 10^{\eta \cdot pH} \cdot \exp\left(\frac{-E_a}{RT}\right) \cdot \left(1 - \frac{Q}{K}\right). \quad (4)$$

In the Defense HLW Glass Degradation model developed for TSPA, the rate expression in Equation 4 was simplified by combining the k_0 and $(1 - Q/K)$ terms into a single term k_E . Experimentally determined values of k_E were used to provide maximum and minimum values for the dissolution rate under extreme but repository-relevant conditions (Bechtel SAIC, LLC, BSC 2004):

$$rate_G = k_E \cdot 10^{\eta \cdot pH} \cdot \exp\left(\frac{-E_a}{RT}\right). \quad (5)$$

Values of η and E_a were determined from the results of tests under conditions in which the pH, temperature, and/or the value of $(1 - Q/K)$ were constant (or nearly so). For tests conducted at a constant temperature but at different pH values, Equation 5 can be further simplified by combining the k_E and temperature terms in a constant, C , and taking the common logarithm:

$$\log rate_G = C + \eta \times pH. \quad (6)$$

The pH dependence of the dissolution rate (i.e., the value of η) can be determined from the slope of a plot of rate vs. pH under conditions where the temperature and affinity term remain constant, which is most conveniently done in dilute solutions. Once the pH dependence is known, the temperature dependence can be determined from the ratio of the rates measured at the same pH but different temperatures:

$$\frac{rate_{T_1}}{rate_{T_2}} = \exp\left(\frac{E_a/R}{1/T_2 - 1/T_1}\right). \quad (7a)$$

Rearranging to solve for E_a ,

$$E_a = \ln\left(\frac{rate_{T_1}}{rate_{T_2}}\right) \times R \times \left(1/T_2 - 1/T_1\right). \quad (7b)$$

Separate coefficient values η_{acid} , E_{a_acid} , $\eta_{alkaline}$, and $E_{a_alkaline}$ were determined for use in the Defense HLW Glass Degradation Model from the dissolution rates of a glass in dilute acidic and alkaline solutions. Both η and E_a are determined from the **relative rates** measured at different pH and temperature values and are characteristic values of the glass. The value of k_E is determined from an absolute rate and is sensitive to the environment as well as to the glass. In the Defense HLW Glass Degradation model, a range of k_E values is used to capture the impacts of variables that are not directly taken into account in the model, including the various HLW glass compositions, or that can change over

time, such as the amount of water contacting the glass and the dissolved silica concentration. Values of k_E were determined for use in the model by applying Equation 5 to the rates measured under various test conditions in which the glass was corroded in aqueous solutions, by dripping water, and by water vapor. Maximum values of k_E were determined from the rates measured in immersion tests for acidic solutions and from the rates measured in 7-day product consistency tests (PCTs) for alkaline solutions. Minimum values were determined from the results of unsaturated (drip) tests for acidic solutions and from vapor hydration tests for alkaline solutions. The maximum values of k_E correspond to the unlikely conditions in which large volumes of water are present in a breached waste package, whereas the minimum values correspond to the more likely conditions of dripping water and water vapor. For TSPA calculations, the values of k_{E_acid} and $k_{E_alkaline}$ are treated as stochastic and selected from triangular distributions in which the minimum values are the most probable and the maximum values are the least probable. The glass dissolution rate is calculated as the sum of the rates calculated with the expressions for acidic and alkaline solutions:

$$rate_G = k_{E_acid} \times 10^{\eta_{acid} pH} \times \exp\left(\frac{-E_{a_acid}}{RT}\right) + k_{E_alkaline} \times 10^{\eta_{alkaline} pH} \times \exp\left(\frac{-E_{a_alkaline}}{RT}\right). \quad (8)$$

Whereas the dissolution mechanism in alkaline solutions is well understood, less is known about borosilicate glass dissolution in acidic solutions. Application of Equation 5 to acidic solution is empirical, and neither the role of the affinity term nor which species affect the rate in acidic solutions is known. [NOTE: We believe that hydrolysis of aluminum-oxygen bonds drives glass dissolution in acidic solutions through a mechanism that is analogous to that shown for silicon-oxygen bonds in Equation 1. Similar to $\text{Si}(\text{OH})_4$ in Eqs. 1a and 1b, dissolved Al (probably $\text{Al}(\text{OH})_4^-$) is expected to have the greatest impact on the dissolution rate in acidic solutions. However, because dissolved Al is readily consumed by sparingly soluble secondary phases such as $\text{Al}(\text{OH})_3$, the value of the affinity term is expected to remain near 1 as the glass dissolves. That is, the value of K for the acid leg will be fixed at some value by the glass, but the value of Q will become fixed at a value much less than K by the formation of secondary phases. Although alteration phase formation is known to affect the dissolution rate in alkaline solutions, those phases fix the Si concentration at values that are high enough that the values of $(1-Q/K)$ remain significantly less than 1.] The static dissolution tests used in this testing activity were designed to maintain values of $(1 - Q/K)$ near 1 by using low glass-surface-area-to-solution-volume ratios and short test durations.

Most of the tests conducted with Pu LaBS-B glass in this activity were intended to provide data that could be compared with data used to develop the Defense HLW Glass Degradation Model and with the rates calculated by the model to determine if the model can be used to adequately take into account the impact of disposed Pu LaBS glass on repository performance. Separate values of k_E , η , and E_a for acidic and alkaline solutions are also derived from the test results to model the Pu LaBS glass dissolution rate directly. Other tests are conducted to gain insight into the long-term corrosion behavior of Pu LaBS glass.

1.2 TECHNICAL METHODS

Tests were conducted with a LaBS glass made using “Frit B” and added PuO_2 that was provided by Savannah River National Laboratory (SRNL). That glass is referred to as Pu LaBS-B glass in this report to distinguish it from LaBS glasses made previously with Frit A and with new frit compositions that are being developed to increase the solubility of Pu in the glass (e.g., Frit X). A non-radioactive glass that represents the HLW glass likely to be used to encapsulate the LaBS glass was also provided by SRNL. This surrogate HLW glass is referred to as SRL 418 in this report. The work was separated into 4 subtasks, which are described below.

1.2.1 Subtask A: Assay of Pu LaBS-B Glass, LaBS-X Frit Glass, and SRL 418 Glass

The compositions of the Pu LaBS-B and SRL 418 glasses provided by SRNL were measured by dissolving the glasses in acid and analyzing the solutions. The composition of a LaBS glass made with Frit X (without added Pu) was also measured. Samples were taken randomly from bars of each glass provided by SRNL and crushed. Shards of crushed glass of approximately 50 mg were dissolved in a mixture of HCl, HNO₃, and HF using a procedure commonly used by the Argonne National Laboratory Analytical Chemical Laboratory (ACL) to dissolve glasses for assay analysis. The resulting solutions were diluted with demineralized water and analyzed for cations with inductively coupled plasma-mass spectrometry (ICP-MS).

1.2.2 Subtask B: Examination of Pu LaBS-B Glass

A sample was cut from the bar of Pu LaBS-B glass and examined with a scanning electron microscope (SEM) to characterize the distribution of PuO₂ inclusions in the glass. The orientation of the sample relative to the bar it was cut from was noted. The distribution of the PuO₂ in the test specimens could affect the test results, and it was suspected that most of the PuO₂ could be segregated at the bottom of the glass bar, having settled by gravity when the glass was made.

1.2.3 Subtask C: Immersion Tests with Pu LaBS-B Glass

Three series of immersion tests were conducted following standard operating procedures for conducting the tests, preparing the specimens, analyzing the test solutions, etc. The test method is based on the American Society for Testing and Materials (ASTM) test method C1220, which is itself based on the former Materials Characterization Center test number 1 (MCC-1). These are referred to simply as immersion tests in this report. The first series of immersion tests (Series C1) was conducted to measure the dependence of the forward dissolution rate on the pH and temperature. Three acidic and 3 alkaline solutions were used to estimate the pH dependence. The second (Series C2) and third (Series C3) test series were conducted in demineralized water for short durations at 90 °C for comparison with the results from Series C1, and for long durations at 90 and 120 °C to track the effect of solution feedback effects and colloid generation. The test matrix is summarized in Table 1. Test specimens were cut from bars of Pu LaBS-B glass that had been provided by SRNL. About 100 specimens were cut as approximately 0.7-mm-thick coupons using a low-speed saw with a diamond wafering blade (with water as a cutting fluid). One coupon was fixed in epoxy and a polished cross-section prepared for examination with a scanning electron microscope (SEM) to determine the distribution of PuO₂ inclusions. The sides and faces of the other coupons were ground successively with 240-grit, 320-grit, 400-grit, and 600-grit SiC paper with water lubrication. The test specimens were ground to have either four or five sides, depending on the general shape of the as-cut coupon. The two faces of each specimen were also successively ground to a 600-grit finish. The dimensions of each specimen were measured using a digital caliper and the geometric surface area was determined.

Series C1 was conducted at 40, 70, and 90 °C in solutions that imposed initial pH values of about 3.3, 4.5, 5.9, 8.7, 10.1, and 11.2. The leachant solution compositions and measured pH values are summarized in Table 2. Although some of these solutions had little or no capacity to buffer the solutions as the glass dissolved, only small changes in the pH occurred as the glass dissolved under the dilute test conditions over the short test durations. The same glass-surface-area-to-solution volume (S/V) ratio was used in each set of tests at the same temperature and pH, but different S/V ratios were used for different test conditions. The S/V ratios were selected so that the solutions generated in the test would be sufficiently concentrated that they could be analyzed reliably, but sufficiently dilute that solution feedback would not affect the dissolution rate significantly. The exact S/V ratios depended on the dimensions of the glass coupons, but tests in the pH 5, 6, 8.5, and 10 solutions were conducted at about 5 m⁻¹, and tests in pH 3.3

Table 1. Test Matrix for Immersion Tests with Pu LaBS-B Glass

Test No.	Target Leachant pH	Duration, days	Test No.	Target Leachant pH	Duration, days	Test No.	Target Leachant pH	Duration, days
Tests at 40 °C								
MLB1-40-1	3.5	1	MLB3-40-1	6.0	1	MLB5-40-1	10	1
MLB1-40-2	3.5	2	MLB3-40-2	6.0	2	MLB5-40-2	10	2
MLB1-40-3	3.5	3	MLB3-40-3	6.0	3	MLB5-40-3	10	3
MLB1-40-4	3.5	4	MLB3-40-4	6.0	4	MLB5-40-4	10	4
MLB1-40-5	3.5	5	MLB3-40-5	6.0	5	MLB5-40-5	10	5
MLB1-40-B1	3.5	5	MLB3-40-B1	6.0	5	MLB5-40-B1	10	5
MLB2-40-1	5.0	1	MLB4-40-1	8.5	1	MLB6-40-1	11	1
MLB2-40-2	5.0	2	MLB4-40-2	8.5	2	MLB6-40-2	11	2
MLB2-40-3	5.0	3	MLB4-40-3	8.5	3	MLB6-40-3	11	3
MLB2-40-4	5.0	4	MLB4-40-4	8.5	4	MLB6-40-4	11	4
MLB2-40-5	5.0	5	MLB4-40-5	8.5	5	MLB6-40-5	11	5
MLB2-40-B1	5.0	5	MLB4-40-B1	8.5	5	MLB6-40-B1	11	5
Tests at 70 °C								
MLB1-70-1	3.5	1	MLB3-70-1	6.0	1	MLB5-70-1	10	1
MLB1-70-2	3.5	2	MLB3-70-2	6.0	2	MLB5-70-2	10	2
MLB1-70-3	3.5	3	MLB3-70-3	6.0	3	MLB5-70-3	10	3
MLB1-70-4	3.5	4	MLB3-70-4	6.0	4	MLB5-70-4	10	4
MLB1-70-5	3.5	5	MLB3-70-5	6.0	5	MLB5-70-5	10	5
MLB1-70-B1	3.5	5	MLB3-70-B1	6.0	5	MLB5-70-B1	10	5
MLB2-70-1	5.0	1	MLB4-70-1	8.5	1	MLB6-70-1	11	1
MLB2-70-2	5.0	2	MLB4-70-2	8.5	2	MLB6-70-2	11	2
MLB2-70-3	5.0	3	MLB4-70-3	8.5	3	MLB6-70-3	11	3
MLB2-70-4	5.0	4	MLB4-70-4	8.5	4	MLB6-70-4	11	4
MLB2-70-5	5.0	5	MLB4-70-5	8.5	5	MLB6-70-5	11	5
MLB2-70-B1	5.0	5	MLB4-70-B1	8.5	5	MLB6-70-B1	11	5
Tests at 90 °C								
MLB1-90-1	3.5	1	MLB3-90-1	6.0	1	MLB5-90-1	10	1
MLB1-90-2	3.5	2	MLB3-90-2	6.0	2	MLB5-90-2	10	2
MLB1-90-3	3.5	3	MLB3-90-3	6.0	3	MLB5-90-3	10	3
MLB1-90-4	3.5	4	MLB3-90-4	6.0	4	MLB5-90-4	10	4
MLB1-90-5	3.5	5	MLB3-90-5	6.0	5	MLB5-90-5	10	5
MLB1-90-B1	3.5	5	MLB3-90-B1	6.0	5	MLB5-90-B1	10	5
MLB2-90-1	5.0	1	MLB4-90-1	8.5	1	MLB6-90-1	11	1
MLB2-90-2	5.0	2	MLB4-90-2	8.5	2	MLB6-90-2	11	2
MLB2-90-3	5.0	3	MLB4-90-3	8.5	3	MLB6-90-3	11	3
MLB2-90-4	5.0	4	MLB4-90-4	8.5	4	MLB6-90-4	11	4
MLB2-90-5	5.0	5	MLB4-90-5	8.5	5	MLB6-90-5	11	5
MLB2-90-B1	5.0	5	MLB4-90-B1	8.5	5	MLB6-90-B1	11	5
Tests at 90 °C in demineralized water								
MLBD-90-1	DIW	1	MLBD-90-4	DIW	4	MLBD-90-6	DIW	28
MLBD-90-2	DIW	2	MLBD-90-5	DIW	5	MLBD-90-7	DIW	56
MLBD-90-3	DIW	3	MLBD-90-B1	DIW	5	MLBD-90-8	DIW	91
Tests at 120 °C in demineralized water and steel vessels								
MLBD-120-1	DIW	28						
MLBD-120-2	DIW	56						

Table 2. Leachant Solution Compositions and Initial pH Values

Leachant number	Target pH	Chemicals	Total with added water, g	Measured pH (at room temperature)
1	3.5	20.40 g potassium hydrogen phthalate + 90.91 g dil. HNO ₃ ^a	2009.1	3.28
2	5	1.9384 g potassium hydrogen phthalate + 0.1177 g LiOH•H ₂ O	1000.09	4.54
3	6	0.7747 g potassium hydrogen phthalate + 0.1395 g LiOH•H ₂ O	1002.20	5.93
4	8.5	72.71 g dil. HNO ₃ ^a + 3.0285 g tris(hydroxymethyl)aminomethane g	1000.30	8.66
5	10	9.95 g dil. HNO ₃ ^a + 0.0596 g LiOH•H ₂ O	1000.06	10.10 ^b
5R	10	0.1067 g conc. HNO ₃ + 0.0611 g LiOH•H ₂ O	1000.02	not measured
6	11	0.4834 g LiCl + 0.2521 g LiOH	2009.3	11.22 ^b

^a Dil. HNO₃ = 1.8184 g concentrated HNO₃ + 182.23 g water.

^b A few drops of conc. HNO₃ were added to lower the pH.

and pH 11 solutions were conducted at an S/V ratio of about 2 m⁻¹. One 5-day blank test was conducted with each leachant solution and at each temperature. Tests were conducted in Teflon vessels having approximately 65- or 120-mL capacities to attain the desired S/V ratios. The concentration measured in the 5-day blank test was used as the background concentration for tests at all durations. After the test solutions were removed from the vessels at the end of the test, the vessels were rinsed 3 times with demineralized water to remove residual test solution, and then filled with an approximately 1% nitric acid solution to dissolve any released glass components that had become fixed to the vessel during the test.

Series C2 was conducted at 90 °C in demineralized water. Short-term tests (through 5 days) were conducted to determine the dissolution rate for comparison with the rates measured at the imposed pH values and long-term tests were conducted to determine when solution feedback effects become significant. Series C3 was conducted at 120 °C in demineralized water to accelerate glass dissolution and increase solubilities. The tests were conducted and analyzed with the same procedures used in Series C1.

The solution pH values were measured at room temperature within a few hours after each set of tests was completed. The test solutions were not filtered prior to analysis, but were acidified with HNO₃. The solutions were analyzed for B, Na, Si, Gd, Hf, and Pu with ICP-MS.

1.2.4 Subtask D: VHTs with Pu LaBS-B and SRL 418 Glasses

Vapor hydration tests (VHTs) were conducted with monolithic specimens of Pu LaBS-B glass and SRL 418 glasses to compare their durabilities under aggressive conditions known to accelerate the corrosion progress (e.g., the formation of alteration phases) of borosilicate glasses. The SRL 418 glass represents the HLW glass in which LaBS glass will be embedded in the can-in-canister waste form. Tests were conducted with specimens of Pu LaBS-B glass and SRL 418 glass that were tied together so they would be in contact and with a separate specimen of Pu LaBS-B glass in the same test vessel. The SRL 418 glass is included to simulate the effect of HLW glass that will surround the Pu LaBS glass in a waste form on the solution contacting the LaBS glass. The HLW glass is a source of alkali metals, the releases of which are expected to significantly increase the pH of the solution, and additional dissolved silica. These are expected to affect both the reactivity of the Pu LaBS-B glass and the assemblage of alteration phases that form as it corrodes. A bar of SRL 418 glass was provided by SRNL for testing. Coupons with sizes similar to the Pu LaBS-B specimens were cut and polished to a final 600-grit finish. Due to the limited amount of glass available, specimens of Pu LaBS-B glass that had been used in immersion tests were repolished to a 600-grit finish and used in the VHTs. Notches were cut in all VHT

specimens to facilitate their being tied with Teflon thread and suspended from a steel rod that was placed in the test vessel.

The VHT test matrix is summarized in Table 3. Tests were conducted at 120 °C and 200 °C for several durations expected to result in different extents of corrosion. Previous VHTs with a LaBS glass having a composition similar to that of Pu LaBS-B showed fairly extensive alteration in 14-day tests at 200 °C, and tests were conducted at 200 °C to provide reasonable assurance that alteration phases would be generated on Pu-LaBS-B glass in a timely manner. However, the highest temperature at which glass could interact with water vapor in the open repository environment is about 120 °C. Tests were conducted at 120 °C, but solids analyses were not completed within the contracted performance period. Scoping tests had been conducted with SRL 418 glass at 150 and 200 °C to gauge the reactivity of that glass for designing the test matrix, and solids analyses of those vapor-reacted specimens are included in this report to describe the alteration phases. It is assumed that the same phases form at 120, 150, and 200 °C.

Table 3. Test Matrix for Vapor Hydration Tests

Test Number	Temperature, °C	Duration, d	Specimen numbers ^a	
			In contact	Separate
VLB-120-1	120	72	B1a and S1	B1b
VLB-120-2	120	72	B2a and S2	B2b
VLB-120-3	120	54	B3a and S3	B3b
VLB-120-4	120	35	B4a and S4	B4b
VLB-120-5	120	21	B5a and S5	B5b
VLB-200-1	200	24	B6a and S6	B6b
VLB-200-2	200	24	B7a and S7	B7b
VLB-200-3	200	24	B8a and S8	B8b
VLB-200-4	200	21	B9a and S9	B9b
VLB-200-5	200	14	B10a and S10	B10b
VBB-120-1	120	65	—	S11 and S12
VBB-120-2	120	35	—	S13 and S14
VBB-200-1	200	14	—	S15 and S16
VBB-200-2	200	24	—	S17 and S18

^a Pu LaBS-B glass indicated by “B” specimens and SRL 418 glass indicated by “S.”

2. TESTING

2.1 PREPARATION OF GLASS TEST SPECIMENS

The monolithic specimens of Pu LaBS-B glass to be used in the immersion tests and VHTs were cut and polished in a glove box. The glass had been provided by SRNL in the form of a bar approximately 4 inches long, 5/8 inch wide, and 1/2 inch deep that had been made by pouring molten glass into a long dish. Additional glass was provided as pieces of a broken bar, but these were too small to cut into test specimens. A coupon was cut from near the center of the bar to characterize the distribution of PuO₂ inclusions in the glass. The cross-section of the bar had a “D” shape, where the rounded edge was arbitrarily referred to as the bottom and the flat side as the top of the as-poured bar. The cross-section was fixed in epoxy and one face was polished to an 800-grit final finish for examination with SEM. The remaining halves of the bar were cut longitudinally to provide nearly equal quarters with the expectation that each quarter had a similar distribution of PuO₂ inclusions, although this was not verified. Several coupons were cut from each quarter of the bar. Figure 1 shows schematic views of how the bar of glass was quartered and then cut into coupons. [Note: We are not certain that what is shown as the top of the bar in Fig. 1 is actually the top of the bar; it may be the bottom of the bar. The orientation is irrelevant to testing.] The perimeter of each coupon was ground to either 4 or 5 flat sides, depending on the shape of the coupon, and all sides and both faces were ground and polished sequentially with 240-, 320-, 400-, and 600-grit SiC paper with water lubrication to generate the test specimens. The polished specimens were ultrasonicated in water and wiped with a paper towel in the glove box, and then transferred to a hood. The specimens were ultrasonicated again in the hood and wiped with a paper towel. The uniformity of the surface finishes were evaluated visually: all specimens had a mirror finish with a small number of visible scratches. The prepared specimens were stored in plastic bags in a slot-front hood. Even light smears of the cleaned specimens resulted in detectable amounts of Pu being removed. It is not clear if fines were being removed or if PuO₂ inclusions were being pulled out of the glass.

The polished cross-section was examined in a scanning electron microscope (SEM) at near-ambient pressure using backscattered electrons. Figure 2 shows a photomicrograph from an area near the (vertical) center of the specimen near one side. The PuO₂ inclusions appear as distinctly brighter regions in the electron backscatter images because the backscattering efficiency of Pu is higher than that of the surrounding glass. The arrow in Figure 2 points to a bright spot near the end of a polishing scratch. Although they are difficult to see, five bright spots were counted in the 400-μm² square drawn in the figure. The contrast between the PuO₂ and the glass is not as high as expected, which may indicate that the PuO₂ inclusions lie just below the polished surface or the Pu content dissolved in the glass is significant. The dark circular spots seen in Figure 2 may be voids where PuO₂ crystallites were pulled from the glass when the cross-section was prepared or cleaned. Regardless, the PuO₂ inclusions that are observed are distributed fairly uniformly in the glass that was examined in the cross-section (as are the voids). The PuO₂ distributions observed near the top and bottom of the specimen were similar to that shown in the figure. Therefore, the distribution of PuO₂ and the Pu concentration in the glass are assumed to be uniform for all test specimens on the scale of the specimen size, although the fractions of Pu in each phase are not known. (The uniformity of the Pu dissolved in the glass is assumed based on the uniformity of the PuO₂ inclusions, which are the sources of the dissolved Pu.)

The dimensions of the specimens to be used in immersion tests were measured with a caliper to determine the length of each side and the thickness of each corner. One diagonal was measured for each 4-sided specimen and two diagonals were measured for each 5-sided specimen. (The dimensions were measured in inches because the gauge blocks used to check the calipers were certified in inches.) The specimens were numbered sequentially as they were dimensioned and put in separate labeled vials. The geometric specimen area of the irregularly shaped specimens was determined as follows. The outline of the

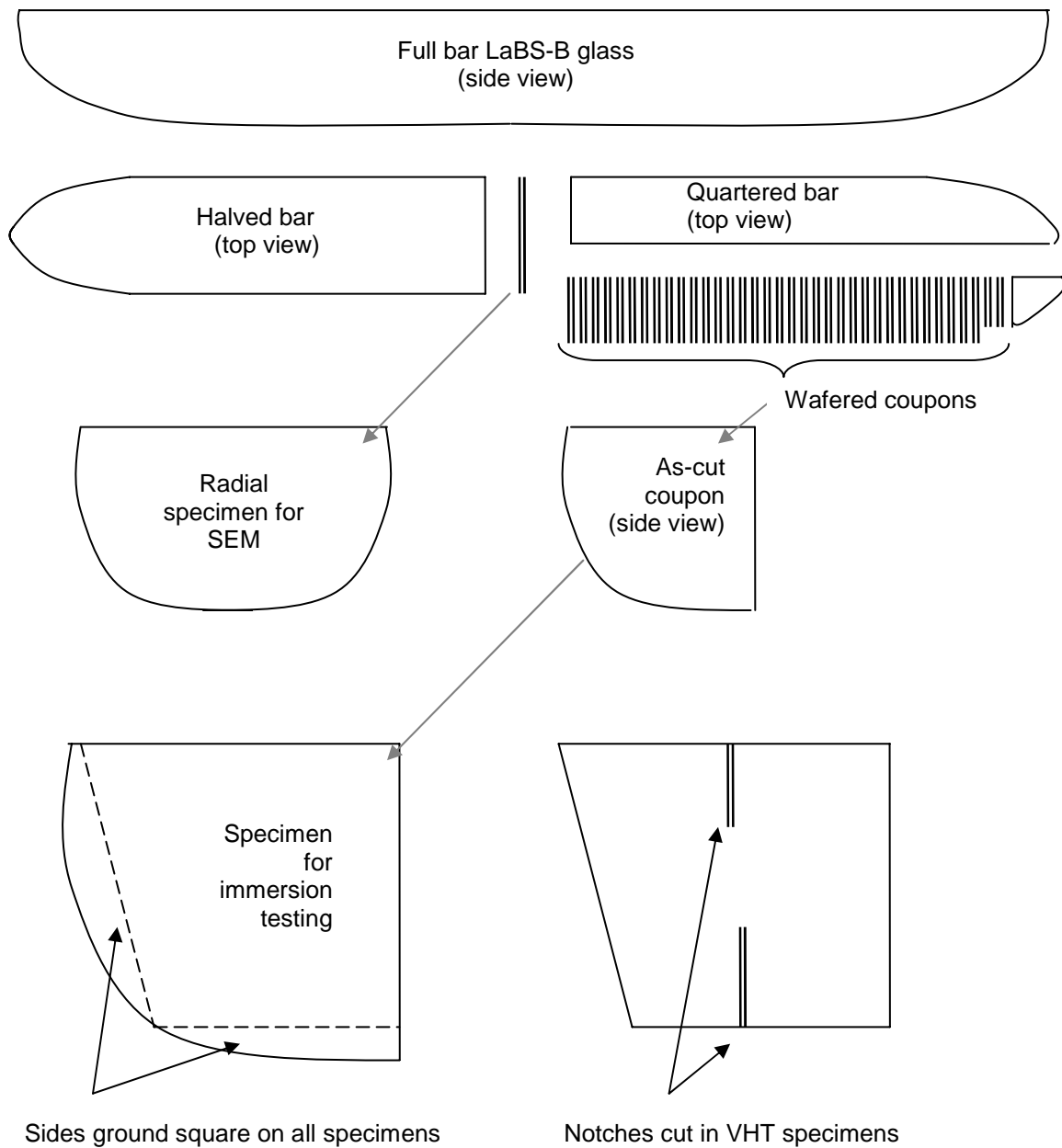


Fig. 1. Schematic Drawing of How Bar of Pu LaBS-B Glass Was Cut into Coupon Specimens for Testing (not to scale).

specimen was drawn on paper based on the measured dimensions using an expanded scale, and the sketch was cut from the paper and weighed. Additional sketches were made as squares with sides having lengths 5×5 , 7×7 and 10×10 arbitrary units (i.e., having 25, 49, and 100 square units) to determine the relationship between area and mass. A plot of the mass against the number of square units was regressed by using the equation

$$mass = 0.00873 + 0.00785 \times \text{square units} \quad (R^2 = 1.000).$$

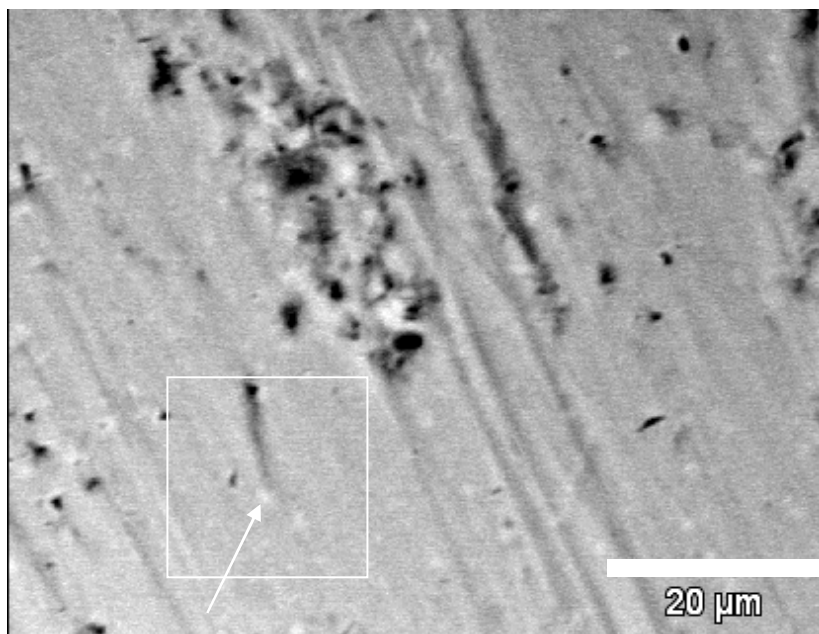


Fig. 2. SEM Photomicrograph of LaBS-B Glass. The arrow points to a bright spot at the bottom end of a polishing gouge thought to be a PuO_2 inclusion.

This was rearranged to calculate the area for each specimen face in terms of arbitrary square units,

$$\text{square units} = (\text{mass} - 0.00873) / 0.00785,$$

which were then converted to cm^2 . The area of each side was calculated from the measured length and average thickness at the two ends (corners). The measured dimensions and calculated areas are summarized in Appendix A, Table A1. Specimens with similar areas were selected for use in each test series. The masses of most specimens were determined by measuring the mass of the storage vial with and without the specimen. The mass was used only to track the movement of ^{239}Pu between laboratories, and was not used to evaluate the dissolution behavior.

The amount of glass provided for testing was not sufficient to conduct all tests with fresh glass. Therefore, 45 specimens were recovered from tests showing the least reactivity (based on solution results) and repolished sequentially with 400- and 600-grit SiC paper and cleaned for reuse in other tests. Twenty of the largest 4-sided repolished specimens were selected for reuse in immersion tests and were assigned specimen numbers 99 – 119. They were dimensioned and the geometric surface areas were determined as previously. Some of these were used to repeat the entire series of tests in the pH 10 leachant (the MLB5 series) because the original batch of leachant (Leachant 5) did not remain stable and the pH of the test solutions varied significantly over time. Repolished and dimensioned specimens were also used in short-term tests in demineralized water. The remaining repolished specimens were used in VHTs; those specimens were not dimensioned because the surface area was not required to interpret the test results.

2.2 GLASS COMPOSITION ANALYSES

Specimens of glass made with Frit X that was provided by SRNL were chemically dissolved and analyzed for composition to (1) establish the dissolution method for chemical analysis of Pu LaBS-B glass and (2) compare the results with those of analyses of Frit X glass conducted at SRNL. Small chips of Frit X glass were collected from various locations of the bar for composition analysis. Three nominally 0.05-g specimens were chemically dissolved in a mixture of 2 mL conc. HCl, 1 mL HNO₃, 0.075 mL HF and about 3 mL demineralized water by heating over night at about 140 °C. The solutions from each analysis contained small amounts of residual solids (presumed to be fluoride salts). The solutions were passed through filter paper (Whatman 42) and the filtrate was diluted to 50 mL with demineralized water. The filter papers were placed in platinum crucibles and then burned in a muffle furnace at about 500 °C for about 2.5 hours. About 1 mL demineralized water and 1 mL 9 M H₂SO₄ were added to the residue in each crucible, which was then heated to fuming on a hot plate. A little more water was added and the solids were dissolved. The solutions were transferred to volumetric flasks and diluted to a final volume of 50.0 mL. The filtrates and dissolved residue were analyzed separately with ICP-MS, then summed. The analytical results are compiled in Appendix A, Table A2, and the glass compositions are summarized in Table 4 on an oxide basis (normalized to 100% total oxides). The results of analyses at SRNL are included in Table 4 for comparison. The results obtained by the two laboratories are in good agreement, except the Argonne results for Hf are about 15% higher than the SRNL results.

Small shards of crushed SRL 418 glass taken from a bar of glass provided by SRNL were dissolved following the same procedure. The glass dissolved completely in the HCl-HNO₃-HF mixture. The analytical results are compiled in Appendix A, Table A3, and the glass composition is summarized in Table 4. The results of analyses at SRNL are included in Table 4 for comparison. Both have been normalized to 100% total oxides. The compositions measured at Argonne and SRNL are in good agreement.

Small shards of Pu LaBS-B glass chipped from various broken pieces of glass were analyzed in duplicate dissolutions following the same procedure used for Frit X glass, including the second dissolution step for residual solids. Aliquots of solutions from the first and second dissolution steps were diluted prior to analysis. The analytical results are compiled in Appendix A, Table A4, and the glass compositions determined from each dissolution and the average are summarized in Table 4. The target composition used at SRNL (see Table 7 in Marra et al. 2006) is included in Table 4 for comparison (the measured composition of the Pu-doped glass was not reported). All compositions have been normalized to 100% total oxides. In the reported target composition, extra HfO₂ is used as a surrogate for PuO₂. It was estimated that the Pu LaBS-B glass that was made had a Pu content of 8.4 mass% Pu (9.5 mass% PuO₂), with a presumed balance of 6.0 mass% HfO₂. Because the analysis of the Pu LaBS-B glass composition was not completed until shortly before this testing activity was completed, the target composition was used in all computations for this report. The results of the two analyses show good agreement in the concentrations of all components. Whereas the Frit B components were expected to be homogeneous, the Pu content was not. This is because the Pu present in inclusions is not expected to be uniformly distributed throughout the glass. The relative amounts of Pu in the inclusions and dissolved in the glass is not known. While the good agreement in the Pu contents measured for these two specimens may be fortuitous, it is consistent with the SEM observations discussed in the preceding section. [Note that the ~50 mg amounts of glass that were dissolved have volumes of about 14 mm³ of glass. A cube of glass with this volume would have a lateral dimension about 30 times larger than the horizontal field of view shown in Fig. 2.] The measured PuO₂ content of the glass is about 30% lower than the target value, and the measured HfO₂ content is about 40% higher than the (presumed) target value. The B₂O₃ content is about 15% lower than the target value. Other components agree with the target within analytical uncertainty of about 10%. The disparity in the HfO₂ content is higher than expected from nonhomogeneity (since Hf is part of the frit). [Note: the ICP-MS analyses were conducted using four

Table 4. Compositions of Pu LaBS-B, Frit X, and SRL 418 Glasses, in Oxide Mass%

Oxide	Pu LaBS-B Glass				Frit X Glass		SRL 418 Glass	
	Run 1	Run 2	average ^a	Target	at ANL ^b	at SRNL ^c	at ANL ^b	at SRNL ^c
Al ₂ O ₃	19.85	20.12	20.0	19.28	8.82	9.55	5.75	5.78
B ₂ O ₃	9.14	9.19	9.17	10.50	12.06	11.9	5.34	5.30
BaO	—	—	— ^d	—	—	—	0.05	0.05
CaO	—	—	—	—	—	—	1.00	1.04
CeO ₂	—	—	—	—	—	0.113	0.071	0.00
Cr ₂ O ₃	—	—	—	—	—	—	0.064	0.082
CuO	—	—	—	—	—	—	0.027	0.030
Fe ₂ O ₃	—	—	—	—	—	—	11.99	11.55
Gd ₂ O ₃	12.25	12.39	12.3	11.58	11.33	12.2	—	—
HfO ₂	7.96	8.52	8.25	6.0 ^e	18.42 ^f	16.0 ^f	—	—
K ₂ O	—	—	—	—	—	—	0.37	0.39
La ₂ O ₃	8.44	7.45	7.93	7.33	16.68	17.1	0.042	0.046
LiO ₂	—	—	—	—	—	—	5.10	5.35
MgO	—	—	—	—	—	—	1.23	1.27
MnO ₂	—	—	—	—	—	—	2.83	3.06
Na ₂ O	—	—	—	—	—	—	11.0	13.0
Nd ₂ O ₃	7.94	7.56	7.74	7.40	13.13	13.3	—	—
NiO	—	—	—	—	—	—	0.613	0.63
P ₂ O ₅	—	—	—	—	—	—	0.059	0.00
PuO ₂	6.66 ^g	6.57 ^h	6.61 ⁱ	9.5 ^e	—	—	—	—
PbO	—	—	—	—	—	—	0.045	0.046
SiO ₂	25.74	25.82	25.78	26.16	17.28	18.02	45.8	52.2
SrO	2.02	2.38	2.21	2.26	2.27	2.22	—	—
TiO ₂	—	—	—	—	—	—	0.024	0.00
ZnO	—	—	—	—	—	—	0.055	0.060
ZrO ₂	—	—	—	—	—	—	0.090	0.10

^aAverage of 2 analyses at Argonne (ANL) normalized to 100% total (see Appendix A).^bAverage of 3 analyses at ANL normalized to 100% total (see Appendix A).^cAverage of 2 analyses at SRNL.^dGlass not analyzed for this component.^eCalculated based on estimated Pu content of 8.4%, with sum HfO₂+PuO₂ = 15.5.^fExcess Hf was used in Frit X glass as a surrogate for Pu.^gSum of 6.22 mass% ²³⁹Pu, 0.40 mass% ²⁴⁰Pu, 0.034 mass% ²⁴¹Pu, and 0.004 mass% ²⁴²Pu.^hSum of 6.14 mass% ²³⁹Pu, 0.39 mass% ²⁴⁰Pu, 0.034 mass% ²⁴¹Pu, and 0.004 mass% ²⁴²Pu.ⁱSum of 6.18 mass% ²³⁹Pu, 0.39 mass% ²⁴⁰Pu, 0.034 mass% ²⁴¹Pu, and 0.004 mass% ²⁴²Pu.

control solutions that in combination contained all of the components in the glass except Pu, and the Pu results are considered semi-quantitative.] The difference in HfO₂ content in the Pu LaBS-B glass analysis is about the same as the difference in the HfO₂ contents measured for Frit X at Argonne and SRNL. This may indicate a systematic error in the Argonne measurement of Hf.

2.3 TESTING EQUIPMENT

The dissolution tests used to determine the pH and temperature dependence of the dissolution rate were conducted in Teflon vessels with Teflon support screens (Saville Corp.). Teflon test vessels and support screens were cleaned prior to use by filling with a NaOH solution and heating overnight at 90 °C, rinsing with distilled and demineralized water, filling with a nitric acid solution and heating overnight at 90 °C, rinsing with distilled and demineralized water, and then air drying. Steel vessels with steel support stands (Parr Instruments Corp.) were used for tests with demineralized water. These were cleaned before use by

filling with a nitric acid solution and heating overnight at 90 °C, rinsing with distilled and demineralized water, and then air drying. The steel vessel lids were fitted with new Teflon gaskets. Vessels selected for use in the VHTs had been used previously. Grooves had been machined in the lids to provide an adequate seal in tests at 200 °C, where the internal pressure is about 15 atm. In previous tests in which Teflon gaskets were used, these vessels had remained sealed (without losing water) for more than a year at that temperature. Those vessels were cleaned by filling with a dilute nitric acid solution and heating overnight, then rinsing several times with distilled water. Teflon and steel vessels are shown in Figure 3.

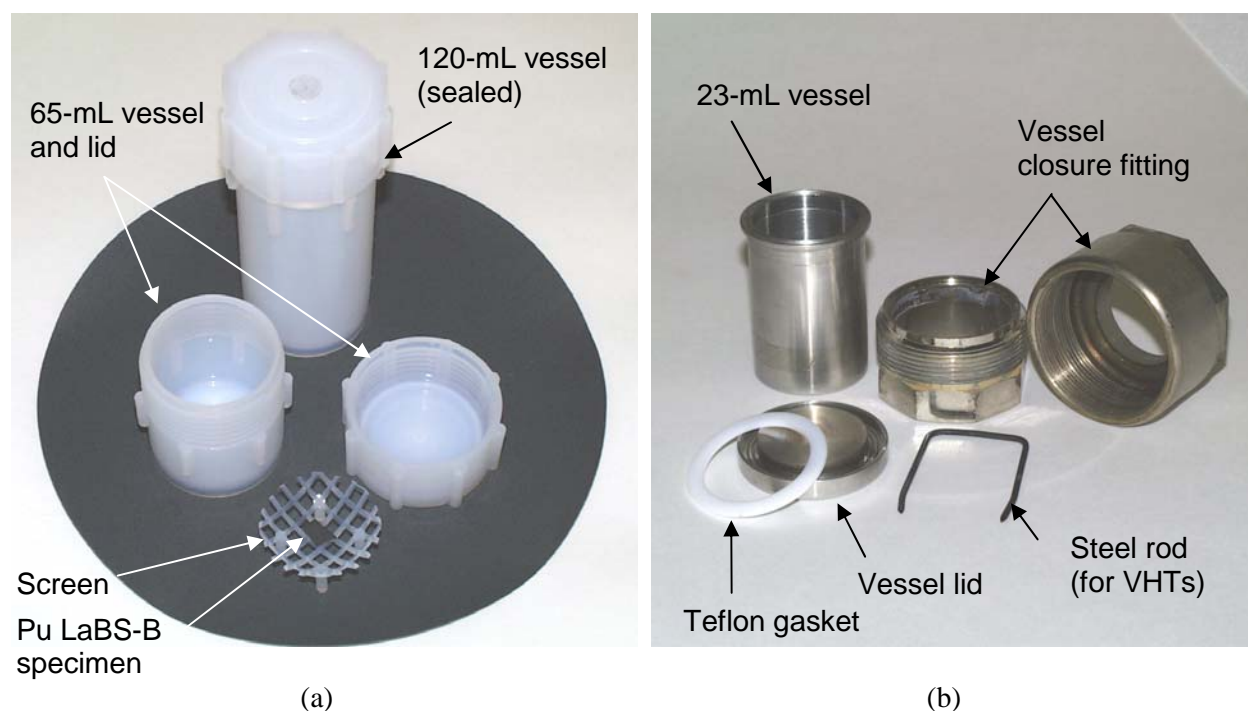


Fig. 3. Photograph of (a) Teflon and (b) Steel Test Vessels and Assemblies for Immersion Tests

Tests were conducted in constant-temperature convection ovens that had been preset and stabilized at the desired temperatures (40, 70, 90, 120, and 200 °C) well before the tests were conducted. The oven temperatures were monitored continuously using Type K thermocouples connected to a data logger that recorded the temperature every 12 hours. The oven temperatures and data logger read-outs were checked with NIST-traceable mercury thermometers prior to use. The oven temperatures measured prior to testing were 41.0 °C, 69.0 °C, 89.0 °C, 120.2 °C, and 199.4 °C. The corresponding data logger readings were 39.3 °C, 69.0 °C, 88.4 °C, 120.1 °C, and 199.2 °C. The data logger readings were checked when the tests were initiated and when terminated to confirm that the oven temperatures remained stable. Except for slight and brief cooling when the oven was opened to add or remove vessels, the data logger temperatures remained within the ranges 39.3 to 39.4 °C, 69.0 to 69.8 °C, 88.3 to 88.4 °C, and 119.8 to 120.2 °C during the tests, which indicated the oven temperatures also remained within the required ranges. The data logger temperature of the 200 °C oven had a ½ day excursion to 197.7 °C, perhaps because the oven door had been opened before the temperature was recorded, but otherwise remained within the range 198.2 to 200.4 °C. This brief excursion does not affect the results of the test.

2.4 TEST EXECUTION

The surface area determined for each specimen of Pu LaBS-B glass was used to calculate the mass of leachant to be included in the test with that specimen to achieve the desired glass-surface-area-to-solution-volume (S/V) ratio. Although it was intended that tests in the pH 3.5 and pH 11 solutions would be conducted at an S/V ratio of about 1.4 m^{-1} and tests in the other leachants would be conducted at a ratio of about 2 m^{-1} , the area of the specimen face was mistakenly used to calculate the mass of water to be used instead of the total area of the specimen. This was discovered after most of the tests had been started. The S/V ratios were recalculated using the correct surface area and the actual amount of leachant used. Therefore, although it was intended that the tests within each series of tests at a particular temperature and pH would be conducted at the same S/V ratio, the actual ratios varied slightly. The S/V ratio used in a static test affects the pH and solution concentrations that are attained as the glass dissolves over time. By using the same S/V ratio, the dissolved concentrations would have been expected to increase with time. Since these tests were conducted in leachant solutions having an imposed pH and the solutions remained dilute under most test conditions, the effect of using slightly different S/V ratios was negligible.

Tests in the 6 leachants were conducted in parallel. The target masses of leachant were added to the cleaned vessels in a non-radiological laboratory. The vessels were sealed and transferred to a radiological laboratory. The appropriate specimens were removed from their storage vials and placed in an open container in the hood. The vessels were opened and held in the slot of the hood front and the specimens were placed in the vessel and the lid replaced. The capped vessel was withdrawn from the hood and sealed. The Teflon vessels were tightened using plastic wrenches that were provided with the vessels. All vessels were sealed as tightly as possible using the wrench (i.e., until the wrench slipped over the ridges on the vessel). Tests in steel vessels were assembled in the same manner. The steel vessels were sealed with separate closure fittings that were torqued to about 120 ft lb (the torque wrench was not calibrated). The assembled test vessels were weighed, and then placed in ovens that had been preset to the appropriate temperature. The time of day that the vessels were placed in the ovens was recorded to the nearest 5 minutes. At the end of the prescribed test duration, the vessels were removed from the oven and allowed to cool to room temperature on the bench top, and then weighed. The time of day that the vessels were removed from the ovens was recorded. The test duration is defined as the time between when the vessels were placed in the oven and when they were removed, even though it is estimated that about 2 hours were required to heat the vessel contents to 90°C and that they cooled back to room temperature within 1 hour. The vessels were opened while being held in the slot-front hood and about 25 mL of the test solution was carefully poured directly into a preweighed and labeled solution bottle; the remaining test solution was discarded. The vessel (with the specimen still in it) was rinsed with a small amount of demineralized water. The specimen was then removed from the vessel and blotted on a paper towel to remove most of the water, and then placed back into the labeled storage vial.

The pH of the test solution was measured with a combination pH electrode that was calibrated with NIST-traceable solutions prior to use. The test solution was then acidified with 5 drops of ultrapure concentrated nitric acid (Optima) and weighed. The solutions were analyzed for B, Si, Sr, La, Nd, Gd, Hf, and Pu with ICP-MS. The test solutions from tests at a given temperature and pH were analyzed in the same batch to minimize the effects of day-to-day variations in the performance of the instrument.

The emptied vessel was rinsed 3 times with demineralized water, and then filled with an amount of demineralized water greater than the volume of test solution. About 0.1 mL of concentrated nitric acid was added to the water and the vessel was resealed and placed in a 70°C oven to soak overnight. The following day, the acid soak solution was poured into a clean preweighed and labeled solution bottle. The solutions were analyzed for Si, Sr, La, Nd, Gd, Hf, and Pu with ICP-MS. Vessels used for blank tests

were not subjected to acid soaks, since the primary objective of the acid soak was to strip Pu from the vessel. The 120-mL Teflon vessels used for blank tests were cleaned and reused in subsequent tests.

It was observed that the pH of the MLB5 series of tests decreased significantly with test duration (between 1 and 5 days) and that the pH of the stock leachant solution had itself drifted. That test series was repeated using test specimens that had been recovered from tests in which little dissolution had occurred (based on the solution results). The specimens were repolished sequentially with 400- and 600-grit SiC paper to remove the reacted surfaces, washed, and dimensioned. No effort was made to track the test in which each specimen had been used previously. The MLB5 series of tests was repeated using a freshly made batch of Leachant 5 (which is referred to as Leachant 5R). The test numbers of the repeated tests are identified with a suffix “R” in the following tables (e.g., the repeat of test MLB5-40-1 is identified as MLB5-40-1R). The results of the original MLB5 test series are included in this report for completeness, but were not used in analyses of the temperature and pH dependences. The vessels from the original MLB5 series were subjected to acid soak, but the vessels from the repeated series were not acid-soaked. The 1- and 2-day tests in demineralized water were conducted using repolished specimens that had been recovered from previous tests, and the other tests in demineralized water were conducted using fresh specimens. The long-term tests were started with the original tests in the pH leachants, and the short-term (1 – 5 days tests) were conducted at the same time as the repeated MLB5 series tests.

The VHTs were conducted with specimens that had been repolished after prior use in immersion tests. The dimensions of the specimens used in the VHTs were not measured. The way the specimens were suspended in the VHTs is illustrated in Figure 4. One end of a short piece of Teflon thread was tied to the VHT specimens and the other was tied to a metal rod to suspend the specimen in the test vessel. For tests conducted with Pu LaBS-B glass in contact with SRL 418 glass, the thread was first tied to a specimen of SRL 418 glass, and then a specimen of Pu LaBS-B glass was tied next to it using the tag end of the same

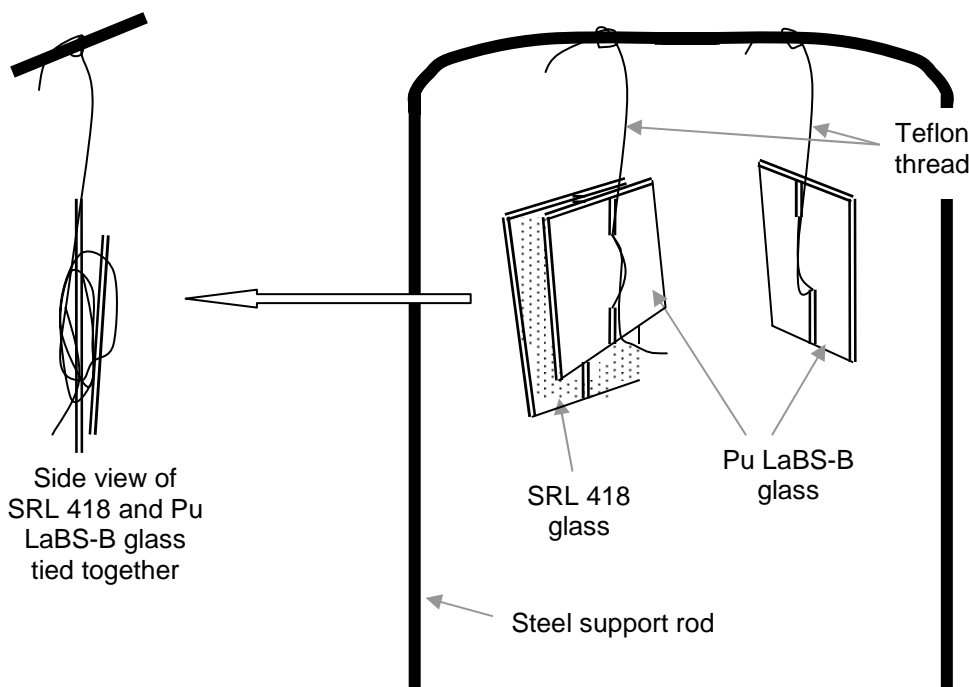


Fig. 4. Schematic Drawing of VHT Specimens Suspended from Support Rod

thread. This resulted in the two glass specimens being separated by the thread rather than in face-to-face contact. This was done to ensure water could collect between the two specimens and form a continuous pathway. Only one edge of each specimen touched the other. (The illustration in Fig. 4 is intended to show that the specimens are separated by the thread near their lateral centers, but exaggerates the distance between them.) The paired Pu LaBS-B and SRL 418 glass specimens and a single specimen of Pu LaBS-B glass were tied to a steel rod and placed into a steel vessel with 0.20 or 0.25 g of demineralized water for tests at 120 and 200 °C, respectively. These amounts of water are sufficient to saturate the vapor at the test temperature and provide water to condense on the specimens, with the intent that water does not drip off during the test. The extent of reaction in VHTs is very sensitive to the amount of water available in the test vessel. Too little water limits the amount of water that condenses on the specimen and could limit the reaction, whereas too much water can establish a reflux cycle in which solution drips from the specimen and fresh vapor condenses. This will moderate increases in the pH and dissolved concentrations as the glass dissolves, and can prevent alteration phases from forming. The amounts of water needed to promote glass corrosion and avoid dripping were not determined. Instead, the same amounts of water commonly used in VHTs with two separated specimens of similar size were used in these tests. This was expected to result in detectable extents of corrosion without dripping.

As was done with the immersion tests, the water was added to the vessels prior to placing the rod with the specimens in the vessel within the slot-front hood. The vessels were sealed, weighed, and then placed in ovens that had been previously set at 120 or 200 °C. The vessels were removed from the ovens and weighed 15 days later to determine if any vessels had leaked water; no significant mass loss had occurred. Tests were terminated by removing the vessels from the oven and setting the vessels in a shallow water bath to cool the vessel bottom and condense the water vapor within the vessel. The vessels were allowed to cool to the touch, and then weighed. The vessel closures were removed carefully, and then the vessel lids were removed while holding the vessels in a slot-front hood. The specimens were removed by lifting the support rod out of the vessel using tweezers and then placing it upright in the hood. The small amount of water remaining in the vessel was discarded and the lid was replaced. Visual observations of the specimens were made and the specimens were left to dry. The Teflon thread was then cut and the specimens were placed in labeled vials. The VHTs conducted with only SRL 418 glass were terminated in a similar way, except the pH of the water in the vessel bottom was measured with pH paper. (The water pH was not measured in VHTs with Pu LaBS-B glass.)

3. IMMERSION TEST RESULTS AND DISCUSSION

Test data and results for the static dissolution tests at 40, 70, and 90 °C are summarized in Appendices B, C, and D: Tables B1, C1, and D1 give the data for test execution; Tables B2, C2, and D2 give the measured concentrations in the test solutions; Tables B3, C3, and D3 give the element masses in the test solutions; Tables B4, C4, and D4 give the measured concentrations in the acid soak solutions; Tables B5, C5, and D5 give the element masses in the acid soak solutions; and Tables B6, C6, and D6 give the normalized element mass losses. The concentrations measured in the 5-day blank tests were used as background concentrations for tests with glass conducted in the same leachant solution and at the same temperature for all durations. (The calculations are discussed in detail in Appendix B.) The mass of each analyte in the test solution and in the acid soak solution was determined and the sum was used to calculate the total mass loss (except for B, which was quantified only in the test solutions). The normalized mass loss based on element i was calculated as

$$NL(i) = \frac{m(i)_{ts} - m^o(i) + m(i)_{as}}{S \times f(i)}, \quad (9)$$

where $NL(i)$ = normalized mass loss of element i , in g/m²,
 $m(i)_{ts}$ = mass element i in test solution, in g,
 $m^o(i)$ = mass element i in equal volume of leachant blank, in g,
 $m(i)_{as}$ = mass element i in acid soak solution, in g,
 S = geometric surface area of specimen, in m², and
 $f(i)$ = mass fraction element i in glass (no units).

The calculated values of $NL(i)$ are given in Appendix B, Table B6, Appendix C, Table C6, and Appendix D, Table D6, for tests at 40, 70, and 90 °C, respectively. The values calculated based on the releases of B, Si, Gd, Hf, and Pu are plotted in Figures 5a – 5f, 6a – 6f, and 7 – 7f. The glass dissolution rates determined by linear regression of the B and Si concentrations are shown in Figures 5 – 7. The rates based on $NL(B)$ are shown by dashed lines and the rates based on $NL(Si)$ are shown by solid lines. The rates are given by the slopes of the fit lines and are referred to as the normalized elemental dissolution rate $NR(i)$. None of the regression lines pass through the origin. The y-intercepts are non-zero due to (1) uncertainty in the background concentrations determined from the blank tests, (2) transient high initial dissolution rates of high-energy sites generated during specimen preparation, which dissolve more quickly than the bulk glass and result in a transient high initial dissolution rate, (3) uncertainty in the surface areas of the set of specimens, and (4) neglect of the affinity term that may become appreciable at longer durations under some test conditions. The first two are the most likely causes for a non-zero intercept in these tests. These affect each test result about the same and are expected to have little effect on the rate that is determined. The third cause is included with the overall testing uncertainty, and the fourth varies with the test conditions. Forcing the regression to pass through the origin is not justified. A few of the test results shown in Figures 5 – 7 were excluded from the regression as either obvious outliers or because they are suspected to have been affected by the chemical affinity term. In all cases, excluding these data resulted in a higher rate and is considered to be conservative with regard to comparison with Defense HLW Glass Degradation Model. That most test results are well represented by linear regression is evidenced by the regression coefficient, R^2 , which is higher than 0.85 for most sets of tests. This indicates that the regression line accounts for more than 85% of the variation in the data. The remaining 15% is expected due to testing uncertainty; a slightly higher level of uncertainty is determined for most tests using the propagation of errors method (see Appendix E). This is because uncertainties in the concentrations of the blank test solutions are included in the propagations, but do not contribute to the uncertainty in the regressed rate because the same background concentration is used for all tests

conducted at the same pH and temperature. The regressions for the results under each test condition are discussed briefly below.

MLB1-40 (Fig. 5a)

The pH values range from 3.69 to 3.71 in this series and a representative pH of 3.70 is used for subsequent analyses. The releases of B and Si are well-fit by linear regressions. The releases of Gd, Hf, and Pu are also fairly linear, with $NL(Gd) > NL(Pu) > NL(Hf)$.

MLB2-40 (Fig. 5b)

The pH values range from 4.85 to 4.89 in this series and a representative pH of 4.89 is used for subsequent analyses. The releases of B and Si are well-fit by linear regressions. The releases of Gd, Hf, and Pu are also fairly linear, with $NL(Gd) > NL(Pu) > NL(Hf)$.

MLB3-40 (Fig. 5c)

The pH values range from 6.06 to 6.09 in this series and a representative pH of 6.09 is used for subsequent analyses. The original analyses of the test solutions were done using a 2-fold dilution and the Si concentrations in the diluted solution were below the detection limit. The test solutions were later re-analyzed for B and Si about 2 months later without dilution. As seen in Table B2, the concentration of B is much higher in the first analysis than in the second analysis. The results of B and Si from the second analysis are plotted with the results of Gd, Hf, and Pu from the first analysis. The releases of B and Si are fairly well-fit by linear regressions, although the 5-day test result lies above the trend set by the shorter-term tests. [Note that the rate of B release determined using the results of the first analysis is $0.00890 \text{ g}/(\text{m}^2\text{d})$, which is in good agreement with the rate determined using the second analysis, even though the concentration in the test solutions differ due to differences in the instrument response.] The releases of Gd, Hf, and Pu increase with time, with $NL(Gd) > NL(Pu) > NL(Hf)$.

MLB4-40 (Fig. 5d)

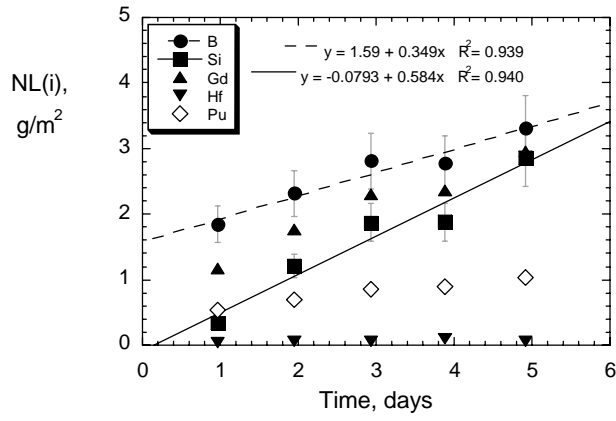
The pH values range from 8.51 to 8.56 in this series and a representative pH of 8.56 is used for subsequent analyses. The release of Si is fairly well-fit by linear regressions, although the 1-day test result lies well above the trend set by the longer-term tests and is excluded as an outlier. The release of B is fairly linear, and this is the only test series in which B is released at a higher rate than Si. The releases of Gd, Hf, and Pu increase with time, with $NL(Gd)$ only slightly higher than $NL(Pu)$ or $NL(Hf)$.

MLB5-40R (Fig. 5e)

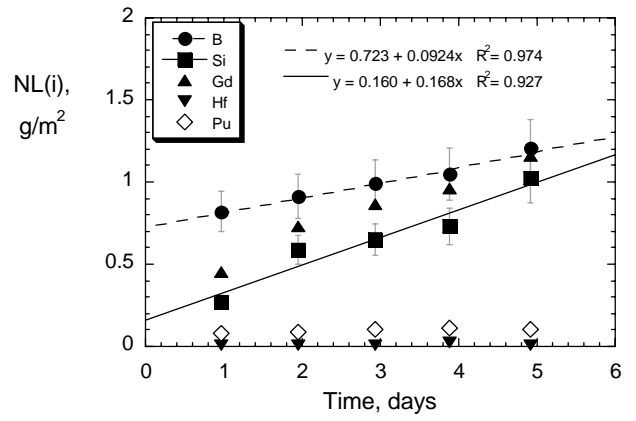
The pH values range from 9.38 to 9.49 in this series and a pH of 9.40 is used for subsequent analyses. The releases of B and Si are fairly well-fit by linear regressions, though the values of $NL(B)$ are low. This is probably due to the use of a background value that is too high. The releases of Gd and Pu do not increase with time and Hf is not detected.

MLB6-40 (Fig. 5f)

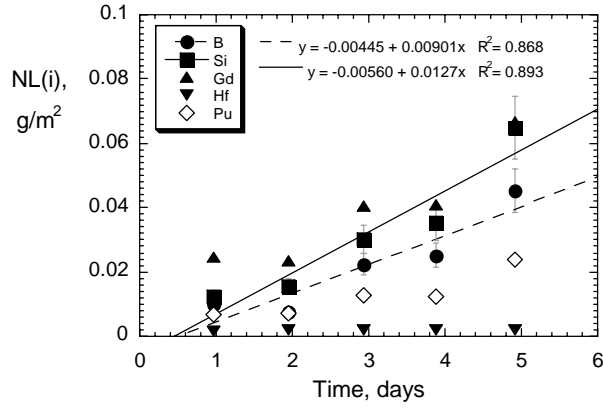
The pH values range from 10.83 to 10.94 in this series and a pH of 10.89 is used for subsequent analyses. The original analyses of the test solutions were done using a 2-fold dilution and the Si concentrations were below the detection limit. The solutions were later re-analyzed for B and Si about 2 months later without dilution. As seen in Table B2, the concentration of B is much higher in the first analysis than in the second analysis. The results of B and Si from the second analysis are plotted with the results of Gd, Hf, and Pu from the first analysis. The releases of B and Si are fairly well-fit by linear regressions, although the 5-day Si result is higher than expected from the trend in the shorter-term tests. The values of $NL(B)$ calculated with the original results yield a fitted line with an unreasonable slope of $-0.316 \text{ g}/(\text{m}^2\text{d})$. The release of Pu increases with time, but releases of Gd and Hf do not.



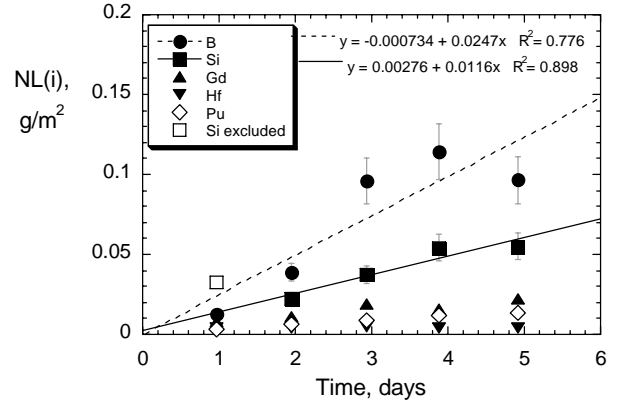
(a)



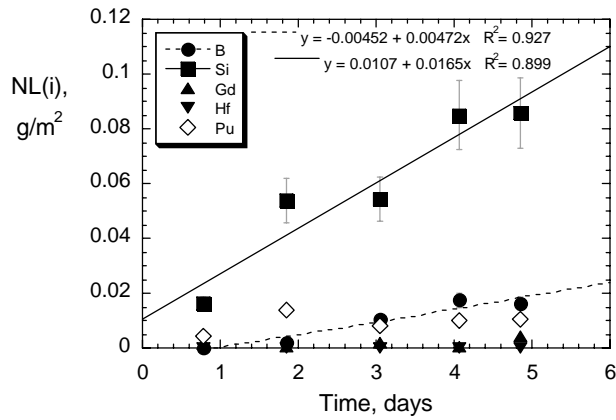
(b)



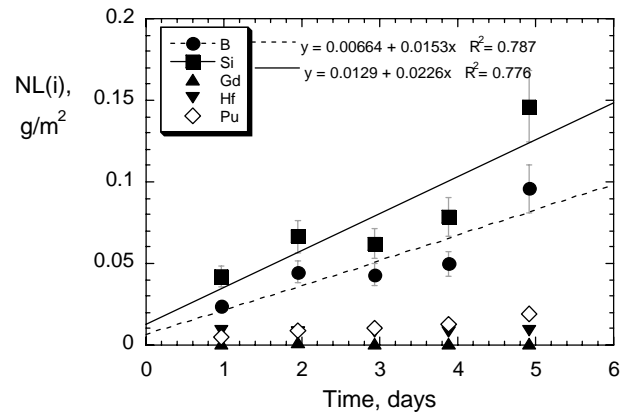
(c)



(d)

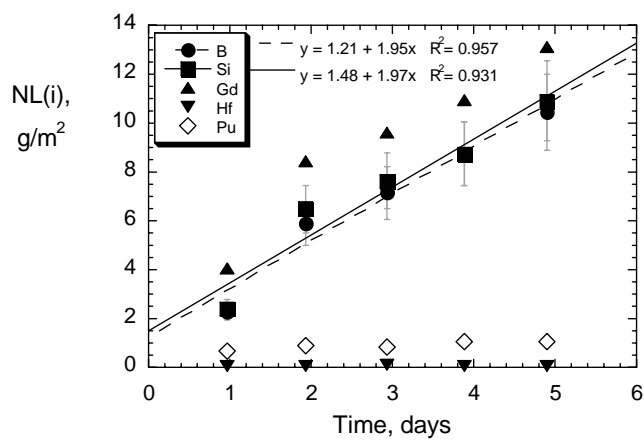


(e)

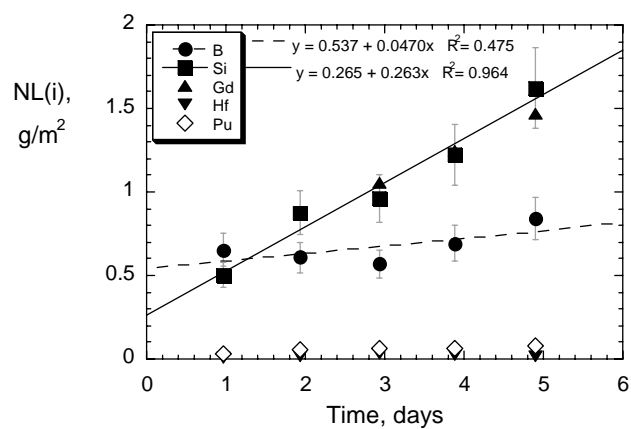


(f)

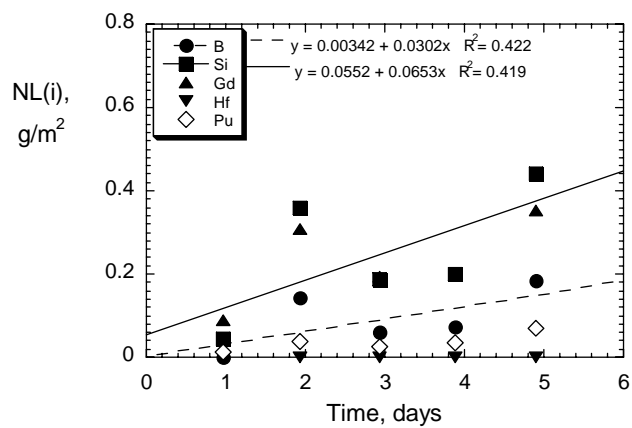
Fig. 5. NL(i) vs. Reaction Time for Tests with Pu LaBS-B Glass at 40 °C and (a) pH 3.70, (b) pH 4.88, (c) pH 6.09, (d) pH 8.56, (e) pH 9.40, and (f) pH 10.89.



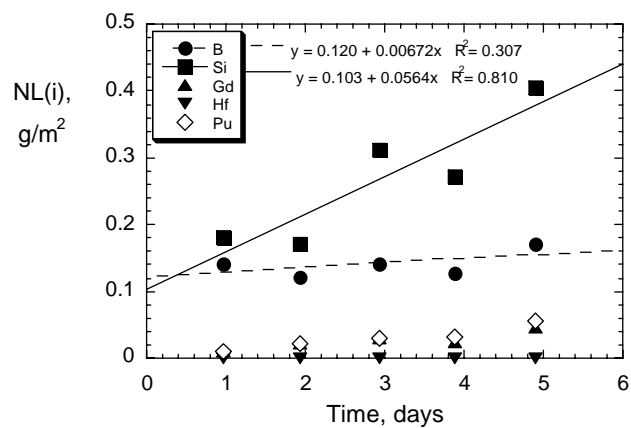
(a)



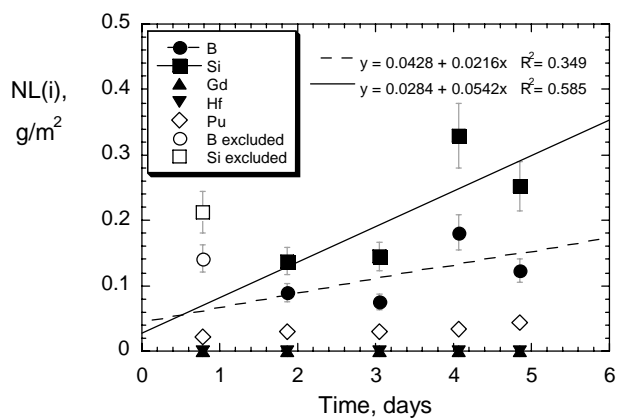
(b)



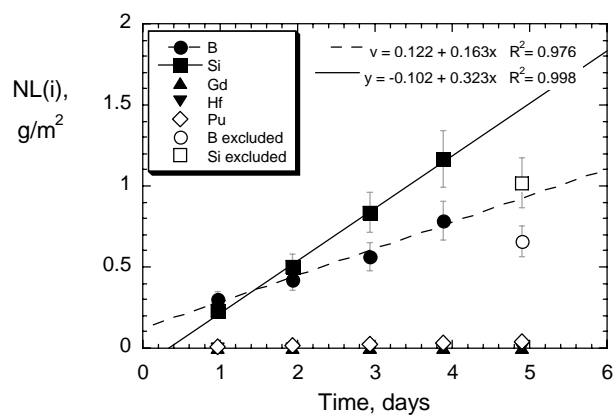
(c)



(d)



(e)



(f)

Fig. 6. NL(i) vs. Reaction Time for Tests with Pu LaBS-B Glass at 70 °C and (a) pH 3.73, (b) pH 4.89, (c) pH 6.10, (d) pH 8.58, (e) pH 9.37, and (f) pH 10.87.

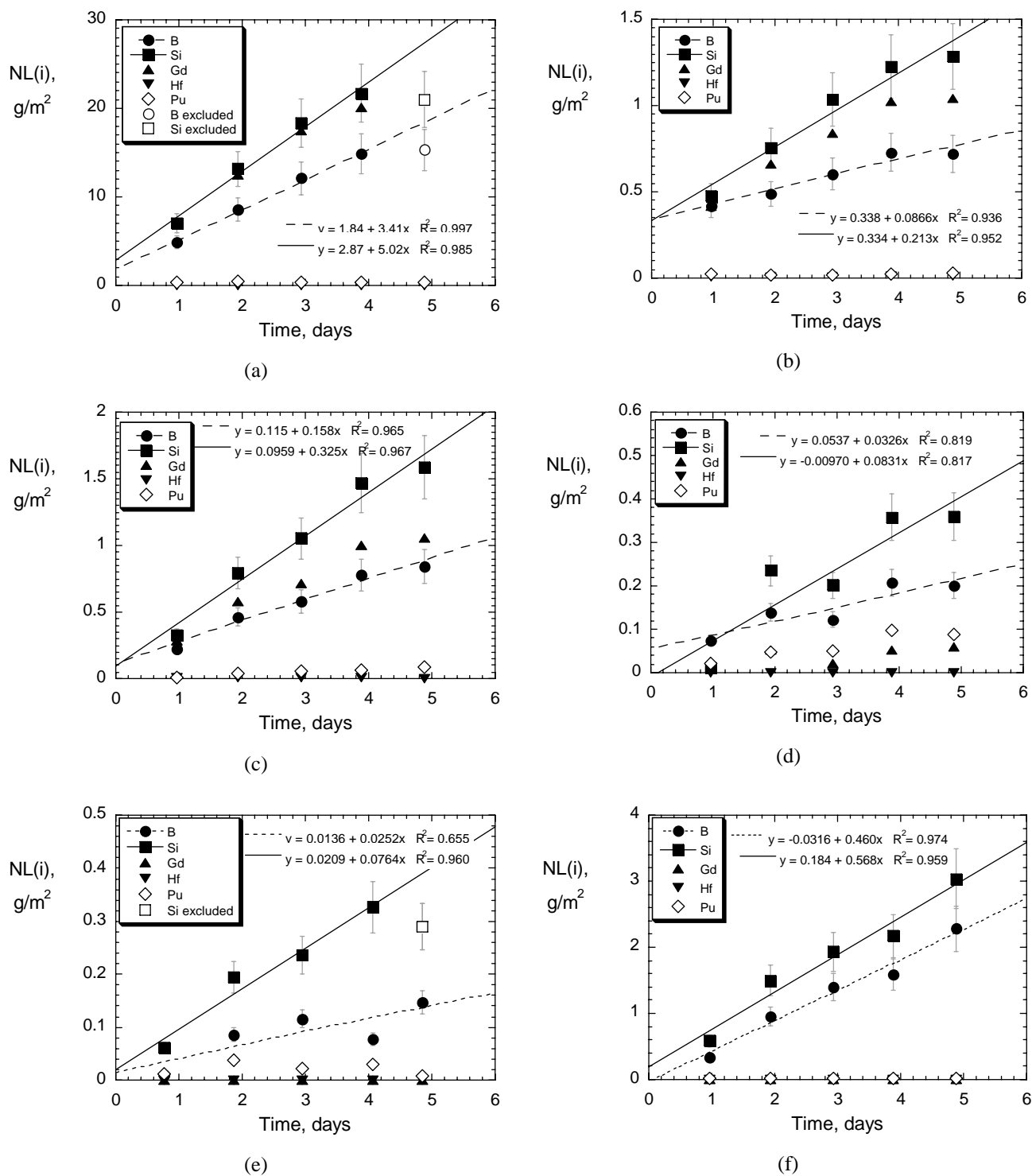


Fig. 7. NL(i) vs. Reaction Time for Tests with Pu LaBS-B Glass at 90 °C and (a) pH 3.74, (b) pH 4.89, (c) pH 6.13, (d) pH 8.60, (e) pH 9.18, and (f) pH 10.87.

MLB1-70 (Fig. 6a)

The pH values range from 3.70 to 3.74 in this series and a representative pH of 3.73 is used for subsequent analyses. The releases of B and Si are well-fit by linear regressions and have about the same slope. The release of Gd is congruent with B and Si, whereas the released amounts of Hf and Pu are nearly constant.

MLB2-70 (Fig. 6b)

The pH values range from 4.86 to 4.90 in this series and a representative pH of 4.90 is used for subsequent analyses. The release of Si is well-fit by a linear regression fit, but the regression to NL(B) is poor. The values of NL(B) in the 1- and 2-day tests appear to be too high, but cannot be excluded. Gd is released congruently with Si, but little Pu or Hf is released.

MLB3-70 (Fig. 6c)

The pH values range from 6.07 to 6.11 in this series and a representative pH of 6.10 is used for subsequent analyses. The releases of both B and Si are poorly fit by linear regressions. The values in the 2-day test appear to be too high but were not excluded. Excluding those points would change the slopes to $NR(B) = 0.0421 \text{ g/(m}^2\text{d)}$ and $NR(Si) = 0.0913 \text{ g/(m}^2\text{d)}$ and improved the fits. Gd is released congruently with Si, but Hf is not detected in either the test solution or the acid soak solution. The release of Pu increases slightly with test duration.

MLB4-70 (Fig. 6d)

The pH values range from 8.56 to 8.58 in this series and a representative pH of 8.58 is used for subsequent analyses. The release of Si is poorly fit by linear regression, but the rate is plausible, and the release of B is low, but fairly well-fit. The values in the 1-day test appear to be too high but were not excluded. The releases of Gd and Pu are similar and both increase slightly with test duration. Hf is only detected in the acid soak solutions of the 1- and 2-day tests.

MLB5-70R (Fig. 6e)

The pH values range from 9.22 to 9.37 in this series and a representative pH of 9.37 is used for subsequent analyses. The releases of B and Si are poorly fit by linear regressions. The values in the 1-day test appear to be too high and were excluded. The releases of Gd and Pu are similar and both fairly invariant with test duration. Hf was not detected in either the test solutions or acid soak solutions.

MLB6-70 (Fig. 6f)

The pH values range from 10.83 to 10.97 in this series and a representative pH of 10.87 is used for subsequent analyses. The releases of B and Si are well-fit by linear regressions. The values in the 5-day test appear to be too low and were excluded. Hf was not detected in either the test solutions or acid soak solutions, and Pu was not detected in the acid soak solutions.

MLB1-90 (Fig. 7a)

The pH values range from 3.70 to 3.75 in this series and a representative pH of 3.74 is used for subsequent analyses. The releases of B and Si are well-fit by linear regressions, though the values in the 5-day test appear to be too low and were excluded. The release of Gd is congruent with Si, whereas the releases of Hf and Pu are nearly constant.

MLB2-90 (Fig. 7b)

The pH values range from 4.86 to 4.89 in this series and a representative pH of 4.89 is used for subsequent analyses. The releases of B and Si are well-fit by linear regressions. The release of Gd is congruent with Si, whereas the releases of Hf and Pu are low and nearly constant.

MLB3-90 (Fig. 7c)

The pH values range from 6.07 to 6.13 in this series and a representative pH of 6.13 is used for subsequent analyses. The release of B and Si are well-fit by linear regressions. The release of Gd is similar to the release of B, whereas the releases of Hf and Pu are low and nearly constant.

MLB4-90 (Fig. 7d)

The pH values range from 8.56 to 8.60 in this series and a representative pH of 8.60 is used for subsequent analyses. The release of B and Si are well-fit by linear regressions. The releases of Gd and Pu increase with the test duration, whereas Hf was not detected.

MLB5-90R (Fig. 7e)

The pH values range from 9.15 to 9.39 in this series and a representative pH of 9.18 is used for subsequent analyses. The release of B and Si are well-fit by linear regressions, though the value of NL(Si) in the 5-day test appeared to be too low and was excluded. The release of Pu is similar at all test durations, whereas the releases of Gd and Hf were very low. The test vessels in the MLB5-90R series were not acid-stripped, but acid strips of the MLB5 series vessels showed small amounts of Gd and Pu, but not Hf.

MLB6-90 (Fig. 7f)

The pH values range from 10.88 to 10.93 in this series and a representative pH of 10.87 is used for subsequent analyses. The releases of B and Si are well-fit by linear regressions. The release of Pu was low at all test durations, and Gd and Hf were not detected in either the test solutions or acid soak solutions.

Although there is scatter in the results, most sets are fairly well-fit by linear regression. Some negative curvature is expected due to the chemical affinity effect, but that effect is within the experimental uncertainty. Therefore, we interpret the rates determined by linear regression to provide adequate estimates of the forward rates for the purpose of determining the pH and temperature dependencies of the dissolution rate. (See Section 3.5 for a discussion of the impact of the affinity term in tests conducted in alkaline solutions.) For convenience, the equations for the Si and B releases given in Figures 5 – 7 are summarized in Tables 5 and 6.

3.1 COMPARISON WITH RATES IN DEFENSE HLW GLASS DEGRADATION MODEL

The linearity of NL(B) and NL(Si) observed in most test solutions indicates that the dissolution rates determined from the test results are good approximations to the forward rates. That is, the results indicate that the value of the chemical affinity term remains very nearly 1. The same approach was taken to estimate the forward rate of a reference HLW glass (referred to as SRL 202G) in the development of the Defense HLW Glass Degradation Model. For the glass used to develop the Model, the acidic leg was determined to have a slope of –0.49 and alkaline leg a slope of 0.49. The equations for the forward dissolution rates in the Model are (see Section 6.5.2.1 in BSC 2004):

$$70^{\circ}\text{C acidic leg:} \quad \log rate_f = 2.34 - 0.49 \times \text{pH} \quad (10a)$$

$$90^{\circ}\text{C acidic leg:} \quad \log rate_f = 2.60 - 0.49 \times \text{pH} \quad (10b)$$

$$70^{\circ}\text{C alkaline leg:} \quad \log rate_f = -5.12 + 0.49 \times \text{pH} \quad (10c)$$

$$90^{\circ}\text{C alkaline leg:} \quad \log rate_f = -4.54 + 0.49 \times \text{pH} \quad (10d)$$

Table 5. Rate Equations for Forward Rates Based on Si Release

Temp., C	Representative pH	Rate Equation (t = reaction time)	Regression coefficient, R^2	Maximum Si concentration, mg/L
40	3.70	$NL(Si) = 0.584 t - 0.0793$	0.940	1.51
	4.88	$NL(Si) = 0.168 t + 0.160$	0.927	0.71
	6.09	$NL(Si) = 0.0127 t - 0.00560$	0.893	0.11
	8.56	$NL(Si) = 0.0116 t + 0.00276$	0.898	0.32
	9.40	$NL(Si) = 0.0165 t + 0.0107$	0.899	0.06
	10.89	$NL(Si) = 0.0226 t + 0.0129$	0.776	0.05
70	3.73	$NL(Si) = 1.97 t + 1.45$	0.935	3.93
	4.89	$NL(Si) = 0.263 t + 0.265$	0.964	1.06
	6.10	$NL(Si) = 0.0653 t - 0.0552$	0.419	0.40
	8.58	$NL(Si) = 0.0564 t + 0.103$	0.810	0.49
	9.37	$NL(Si) = 0.0542 t + 0.0284$	0.585	0.19
	10.87	$NL(Si) = 0.323 t - 0.102$	0.998	0.34
90	3.74	$NL(Si) = 5.02 t + 2.87$	0.985	8.68
	4.89	$NL(Si) = 0.213 t + 0.334$	0.952	1.03
	6.13	$NL(Si) = 0.325 t + 0.0959$	0.967	1.04
	8.60	$NL(Si) = 0.0831 t + 0.0097$	0.817	0.54
	9.18	$NL(Si) = 0.0764 t + 0.0209$	0.960	0.20
	10.87	$NL(Si) = 0.568 t + 0.184$	0.959	0.90

Table 6. Rate Equations for Forward Rates Based on B Release

Temp., C	Representative pH	Rate Equation (t = reaction time)	Regression Coefficient, R^2	Maximum Si concentration, mg/L
40	3.70	$NL(B) = 0.349 t - 1.59$	0.939	1.51
	4.88	$NL(B) = 0.0924 t + 0.723$	0.974	0.71
	6.09	$NL(B) = 0.00901 t - 0.00445$	0.868	0.11
	8.56	$NL(B) = 0.0247 t - 0.000734$	0.776	0.32
	9.40	$NL(B) = 0.00472 t - 0.00425$	0.927	0.06
	10.89	$NL(B) = 0.0153 t + 0.00664$	0.787	0.05
70	3.73	$NL(B) = 1.95 t + 1.21$	0.957	3.93
	4.89	$NL(B) = 0.0470 t + 0.537$	0.475	1.06
	6.10	$NL(B) = 0.0302 t - 0.0342$	0.422	0.40
	8.58	$NL(B) = 0.00672 t + 0.120$	0.307	0.49
	9.37	$NL(B) = 0.0216 t + 0.0428$	0.349	0.19
	10.87	$NL(B) = 0.163 t - 0.122$	0.976	0.34
90	3.74	$NL(B) = 3.41 t + 1.84$	0.997	8.68
	4.89	$NL(B) = 0.0866 t + 0.338$	0.936	1.03
	6.13	$NL(B) = 0.158 t + 0.115$	0.965	1.04
	8.60	$NL(B) = 0.0326 t + 0.0537$	0.819	0.54
	9.18	$NL(B) = 0.0252 t + 0.0136$	0.655	0.20
	10.87	$NL(B) = 0.460 t - 0.0316$	0.974	0.90

From the temperature dependence in the Model, the equations for the rates at 40 °C are:

$$40^{\circ}\text{C acidic leg:} \quad \log \text{rate}_f = 1.887 - 0.49 \times \text{pH} \quad (10\text{e})$$

$$40^{\circ}\text{C alkaline leg:} \quad \log \text{rate}_f = -6.126 + 0.49 \times \text{pH} \quad (10\text{f})$$

These forward rate equations are plotted in Figure 8 along with the dissolution rates measured for Pu LaBS-B glass at specific temperature and pH values. The forward rates used to develop the Defense HLW Glass Degradation Model provide an upper bound to all rates measured for Pu LaBS-B glass.

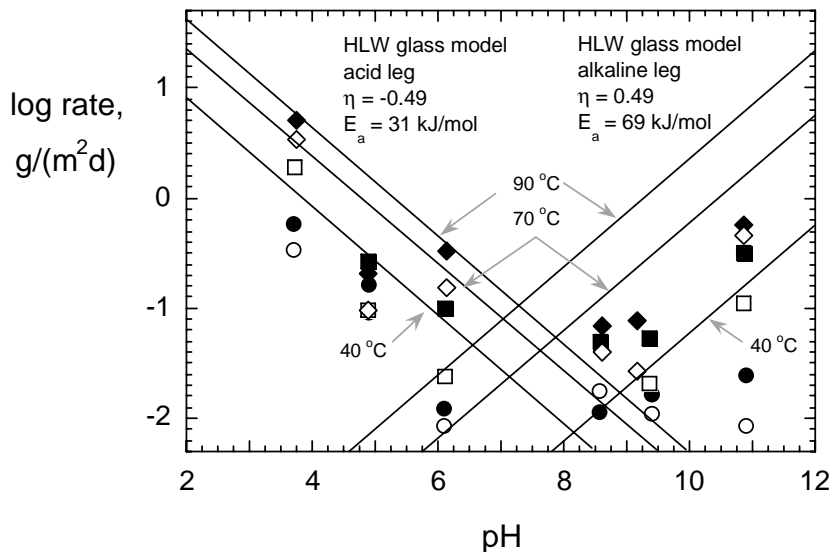


Fig. 8. Comparison of Rates Representing the pH and Temperature Dependence in the Defense HLW Glass Dissolution Model (lines) with Measured Dissolution Rates of Pu LaBS-B Glass in Tests at (●) 40 °C, (■) 70 °C, and (◆) 90 °C. Filled symbols for rates based on Si and open symbols for rates based on B.

3.2 MODEL COEFFICIENTS BASED ON THE RELEASE OF SI

For further comparison of the dissolution behavior of Pu LaBS-B glass with the Defense HLW Glass Degradation Model, the test results were analyzed to determine model coefficient values for Pu LaBS-B glass using the same method that was used for the Model. This involves determining the pH dependence for tests at 70 and 90 °C, determining a single value of η for use at all temperatures (separate values for acidic and alkaline solutions), then determining the temperature dependence.

3.2.1 pH Dependence

To determine the pH dependencies, the rates in tests at 70 and 90 °C were first plotted against the pH to determine values of η for the acid and alkaline legs at each temperature. This is shown in Figure 9a. The results of tests at 40 °C were not used to determine either the pH or temperature dependence; rather, they were reserved for later comparison with predicted rates using the temperature dependence. Note that the rate measured in tests at 90 °C in the pH 5 solution was excluded from the regression used to determine the pH dependence as an outlier.

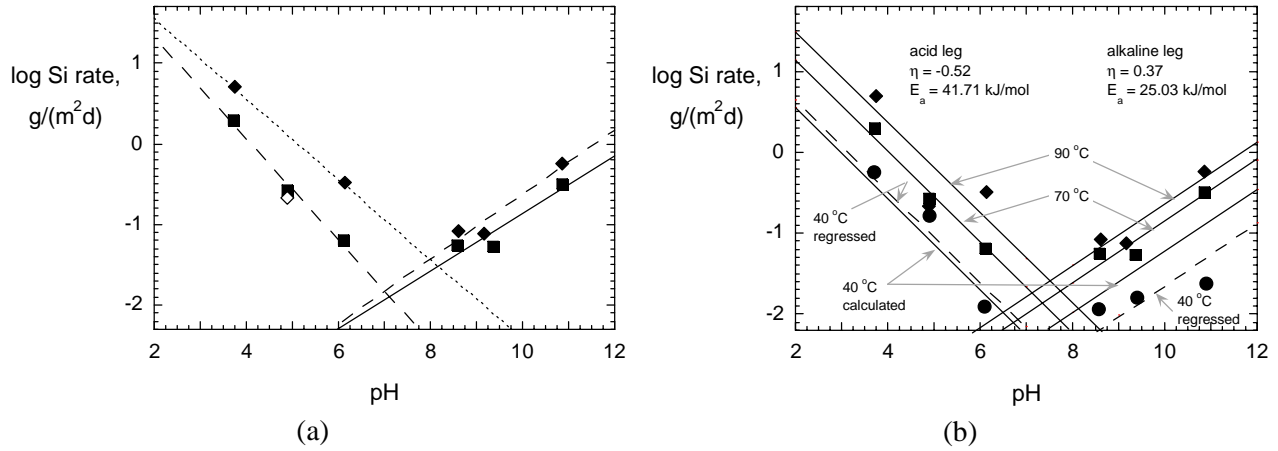


Fig. 9. Regression Fit of NR(Si) Results to Determine Dependence on (a) pH and (b) Temperature at (●) 40 °C, (■) 70 °C and (◆) 90 °C. Open symbols were excluded from regressions.

The regression equations for the acid legs are:

$$\text{at } 70\text{ °C: } \log \text{ rate}_f = 2.57 - 0.624 \times \text{pH} \quad (11a)$$

$$\text{at } 90\text{ °C: } \log \text{ rate}_f = 2.56 - 0.496 \times \text{pH} \quad (11b)$$

Regression equations for the alkaline legs are:

$$\text{at } 70\text{ °C: } \log \text{ rate}_f = 0.355 \times \text{pH} - 4.41 \quad (11c)$$

$$\text{at } 90\text{ °C: } \log \text{ rate}_f = 0.401 \times \text{pH} - 4.64 \quad (11d)$$

By comparison with Equation 6, the constant value in each equation (e.g., the value of 2.57 in Eq. 11a) represents the product of the intrinsic dissolution rate constant (k_0), the chemical affinity term ($I - Q/K$), and the temperature dependence term, and the value that is multiplied by the pH (e.g., the value -0.624 in Eq. 11a) gives the value of η . Single values of η (and E_a) are used in the glass dissolution model for all temperatures (and pH values) in the rate equations for the acidic and alkaline legs. The slopes from the regressed rate equations (Eqs. 11a – 11d) were used to approximate the forward rates at each temperature and pH condition, and the averages of the slopes from tests at 70 and 90 °C were used. Lines with slopes -0.56 and 0.38, respectively, were regressed to the forward rates measured in tests in acidic and alkaline solutions by minimizing the square of the residuals between the measured and calculated rates at each experimentally measured pH, where the residuals (d) were calculated as

$$d = \log \text{ measured rate} - \log \text{ calculated rate} ,$$

using $\eta = -0.56$ for the acidic leg and $\eta = 0.38$ for the alkaline leg with trial values of C . The experimental results and calculated values for the optimum values of C are given in Table 7. The squares of the residuals are given as $\text{sum } d^2$.

Equations of the fitted lines for the acid leg are:

$$\text{at } 40\text{ °C: } \log \text{ rate}_f = 1.77 - 0.56 \times \text{pH} \quad (12a)$$

$$\text{at } 70\text{ °C: } \log \text{ rate}_f = 2.26 - 0.56 \times \text{pH} \quad (12b)$$

$$\text{at } 90\text{ }^{\circ}\text{C: } \log \text{rate}_f = 2.60 - 0.56 \times \text{pH} \quad (12c)$$

and for the alkaline leg are:

$$\text{at } 40\text{ }^{\circ}\text{C: } \log \text{rate}_f = 0.38 \times \text{pH} - 5.43 \quad (12d)$$

$$\text{at } 70\text{ }^{\circ}\text{C: } \log \text{rate}_f = 0.38 \times \text{pH} - 4.65 \quad (12e)$$

$$\text{at } 90\text{ }^{\circ}\text{C: } \log \text{rate}_f = 0.38 \times \text{pH} - 4.44. \quad (12f)$$

These equations are shown as solid lines in Figure 9b; direct regressions of the 40 °C test results to lines with slopes -0.56 at acidic pH values and 0.38 at alkaline pH values are shown as dashed lines.

Table 7. Summary of Experimental Results and Numerical Regression for Si Release

Acid leg	Experimental values			Constant optimized for $\eta = -0.56^a$		
40 °C	pH	rate	log Si rate	1.76	1.77	1.78
	3.70	0.584	-0.2335872	0.006149	0.00468	0.003412
	4.88	0.168	-0.7746907	0.039247	0.035385	0.031723
	6.09	0.0127	-1.8961963	0.060416	0.065432	0.070648
	sum d^2			0.105812	0.105497	0.105783
70 °C	pH	rate	log Si rate	2.25	2.26	2.27
	3.73	1.93	0.2966652	0.018351	0.015742	0.013332
	4.89	0.263	-0.5783961	0.008099	0.009999	0.012099
	6.10	0.0979	-1.1850868	0.000364	0.000846	0.001528
	sum d^2			0.026814	0.026587	0.026959
90 °C	pH	rate	log Si rate	2.59	2.60	2.61
	3.74	5.02	0.7007037	0.042068	0.038065	0.034263
	4.89	0.206	-0.6716204	0.27376	0.284324	0.295088
	6.13	0.325	-0.4854522	0.127697	0.12065	0.113804
	sum d^2			0.443525	0.44304	0.443155
Alkaline leg	Experimental values			Constant optimized for $\eta = 0.38$		
40 °C	pH	rate	log Si rate	5.42	5.43	5.44
	8.56	0.0116	-1.935542	0.053665	0.058399	0.063332
	9.40	0.0165	-1.7825161	0.004288	0.005698	0.007308
	10.89	0.0246	-1.6090649	0.107102	0.100657	0.094412
	sum d^2			0.165056	0.164753	0.165051
70 °C	pH	rate	log Si rate	4.64	4.65	4.66
	8.58	0.0505	-1.2479516	0.017331	0.020064	0.022997
	9.37	0.0542	-1.2660007	0.03482	0.031188	0.027756
	10.87	0.323	-0.4907975	0.000346	0.000818	0.00149
	sum d^2			0.052497	0.05207	0.052243
90 °C	pH	rate	log Si rate	4.43	4.44	4.45
	8.60	0.0688	-1.080399	0.006659	0.008391	0.010323
	9.18	0.0764	-1.1169066	0.030732	0.027326	0.02412
	10.87	0.568	-0.2456517	0.002889	0.004064	0.005439
	sum d^2			0.04028	0.039781	0.039882

^aThe results for the optimum values are given in the center column, with values differing by 0.01 to show the sensitivity.

3.2.2 Activation Energies

The values of the constants in the rate equations (Eqs. 12a – 12f) are the products of the intrinsic rate constant, the affinity term, and temperature dependence terms. Because the intrinsic rate constant depends only on the glass composition and the affinity terms are nearly 1 in all tests, the temperature dependence can be determined **from the rates calculated from the regression equations** (Eqs. 12a – 12f) at a given pH value at two different temperatures. By taking the ratio of the rate expressions at two temperatures, the intrinsic rate constant and affinity term cancel. The activation energy is expressed using the ratio of the Arrhenius expressions for the rates at 70 and 90 °C:

$$\frac{\text{rate } 70^{\circ}\text{C}}{\text{rate } 90^{\circ}\text{C}} = \exp\left(\frac{E_a/R}{1/363 - 1/343}\right) = \exp(-0.01932 E_a). \quad (13a)$$

Taking the natural logarithm of each side and then solving for E_a :

$$E_a = \frac{\ln \text{rate } 90^{\circ}\text{C} - \ln \text{rate } 70^{\circ}\text{C}}{0.01932}. \quad (13b)$$

Using Eqs. 12b and 12c, the calculated rates based on NL(Si) at pH 2 are 13.80 g/(m²d) at 70 °C and 30.20 g/(m²d) and the activation energy is:

$$E_a = \frac{\ln \text{rate } 90^{\circ}\text{C} - \ln \text{rate } 70^{\circ}\text{C}}{0.01932} = \frac{\ln 30.20 - \ln 13.80}{0.01932} = \frac{3.4078 - 2.6249}{0.01932} = 40.52 \text{ kJ/mol}. \quad (14)$$

As a check calculation, the rates at pH 7 are 0.02188 g/(m²d) at 70 °C and 0.04786 g/(m²d) at 90 °C, and the activation energy is:

$$E_a = \frac{-3.0394 + 3.8223}{0.01932} = 40.52 \text{ kJ/mol}. \quad (15)$$

For the alkaline leg, the rates at pH 8 are 0.02455 g/(m²d) at 70 °C and 0.03981 g/(m²d) at 90 °C, and the activation energy is:

$$E_a = \frac{\ln \text{rate } 90^{\circ}\text{C} - \ln \text{rate } 70^{\circ}\text{C}}{0.01932} = \frac{\ln 0.03981 - \ln 0.02455}{0.01932} = \frac{-3.2236 + 3.7072}{0.01932} = 25.03 \text{ kJ/mol}. \quad (16)$$

The rates at pH 12 are 0.8128 g/(m²d) at 70 °C and 1.3183 g/(m²d) at 90 °C, and the activation energy is

$$E_a = \frac{0.2763 + 0.2072}{0.01932} = 25.03 \text{ kJ/mol}. \quad (17)$$

3.2.3 Calculated Rate Expressions at 40 °C

Rate equations at 40 °C were determined using the activation energies determined from results of tests at 70 and 90 °C and the test results are used to verify the calculation. This is similar to the approach taken in developing the Defense HLW Glass Degradation Model, wherein the coefficient values were determined from tests at 70 and 90 °C and the results of 40 °C tests were used to confirm the Model values. The rates

at 40 °C and pH 2 and 7 were calculated using the regression rates at 70 °C and the activation energy (i.e., by rearranging Eq. 7). For the acid leg:

$$rate\ 40\ ^\circ C = rate\ 70\ ^\circ C \times \exp\left(\frac{40.52/R}{1/343 - 1/313}\right). \quad (18)$$

At pH 2, the rate at 70 °C is 13.80 g/(m²d) and the rate at 40 °C is calculated as:

$$rate\ 40\ ^\circ C\ pH\ 2 = 13.80 \times \exp\left(\frac{40.52/0.008314}{1/343 - 1/313}\right) = 3.536\ g/m^2d. \quad (19a)$$

At pH 7, the rate at 70 °C is 0.0219 g/(m²d) and the rate at 40 °C is calculated as:

$$rate\ 40\ ^\circ C\ pH\ 7 = 0.0219 \times \exp\left(\frac{40.52/0.008314}{1/343 - 1/313}\right) = 0.00560\ g/m^2d. \quad (19b)$$

Rearranging Equation 6 to solve for the constant C and substituting the rates from Equations 19a and 19b gives:

$$C = \log 3.536 + 0.56 \times 2 = 1.669 \quad (19c)$$

$$C = \log 0.00560 + 0.56 \times 7 = 1.669 \quad (19d)$$

For the alkaline leg, the Arrhenius expression gives

$$rate\ 40\ ^\circ C = rate\ 70\ ^\circ C \times \exp\left(\frac{25.03/R}{1/343 - 1/313}\right). \quad (20)$$

At pH 8, the rate at 70 °C is 0.02455 g/(m²d) and the rate at 40 °C is calculated to be:

$$rate\ 40\ ^\circ C\ pH\ 8 = 0.02455 \times \exp\left(\frac{25.03/0.008314}{1/343 - 1/313}\right) = 0.009016\ g/m^2d. \quad (21a)$$

At pH 12, the rate at 70 °C is 0.8128 g/(m²d) and the rate at 40 °C is calculated to be:

$$rate\ 40\ ^\circ C\ pH\ 12 = 0.8128 \times \exp\left(\frac{25.03/0.008314}{1/343 - 1/313}\right) = 0.2986\ g/m^2d. \quad (21b)$$

Rearranging Equation 6 to solve for C and substituting the rates calculated in Equations 21a and 21b gives:

$$C = \log 0.009016 - 0.38 \times 8 = 5.015 \quad (22a)$$

and

$$C = \log 0.2986 - 0.38 \times 12 = 5.015. \quad (22b)$$

The calculated rate expressions at 40 °C are:

$$\text{acid leg: } \log \text{rate}_f = 1.67 - 0.56 \times \text{pH} \quad (23a)$$

$$\text{alkaline leg: } \log \text{rate}_f = 0.38 \times \text{pH} - 5.02 \quad (23b)$$

These are identified as “40 °C calculated” in Figure 9b.

3.2.4 Determination of k_+

A lower bounding value of k_0 (referred to as k_+) is estimated by assuming the value of the affinity term is essentially 1 in the 40 °C tests. The expression for the forward rate is

$$\text{rate}_f = k_+ \times 10^{\eta \text{pH}} \times \exp\left(-\frac{E_a}{RT}\right). \quad (24a)$$

Taking the common logarithm and rearranging to solve for $\log k_+$ gives

$$\log k_+ = \log \text{rate}_f + \eta \text{pH} - \frac{E_a}{2.303RT}. \quad (24b)$$

Using the forward rate of 0.5485 g/(m²d) calculated at 40 °C and pH 2 to determine k_+ for the acid leg gives

$$\log k_+ = 0.5485 + 0.56 \times 2.0 - \frac{40.52}{2.303 \times 0.008314 \times 313} = 8.430, \quad (25a)$$

from which $k_{+, \text{acid}} = 2.69 \times 10^8$ g/(m²d). Likewise, using the results for 40 °C and pH 7 gives

$$\log k_+ = -2.2515 + 0.5604 \times 7.0 - \frac{40.52}{2.303 \times 0.008314 \times 313} = 8.430 \quad (25b)$$

and $k_{+, \text{acid}} = 2.69 \times 10^8$ g/(m²d). Using the forward rate of 0.3505 g/(m²d) calculated at 40 °C and pH 12 to determine k_+ for the alkaline leg gives

$$\log k_+ = -0.3505 - 0.38 \times 12.0 - \frac{25.03}{2.303 \times 0.008314 \times 313} = -0.8388, \quad (26a)$$

from which $k_{+, \text{alkaline}} = 0.145$ g/(m²d). The expressions for Pu LaBS-B glass forward dissolution rates in acidic and alkaline solutions based on the **Si release** are

$$\text{rate}_{f_ \text{acid leg}} = 2.69 \times 10^8 \times 10^{-0.56 \text{pH}} \times \exp\left(-\frac{40.52}{RT}\right) \quad (27a)$$

and

$$\text{rate}_{f_ \text{alkaline leg}} = 0.145 \times 10^{0.38 \text{pH}} \times \exp\left(-\frac{25.03}{RT}\right). \quad (27b)$$

3.3 MODEL COEFFICIENTS BASED ON THE RELEASE OF B

The equations for the experimental rates based on the release of B are summarized in Table 6. The rates are plotted against the pH in Figure 10a. The rates measured in the pH 5 solutions at 70 and 90 °C are excluded from the regression as outliers. Regression of $NL(B)$ gives:

$$\text{at } 70^\circ\text{C: } \log \text{ rate}_f = 3.14 - 0.764 \times \text{pH} \quad (28a)$$

$$\text{at } 90^\circ\text{C: } \log \text{ rate}_f = 2.62 - 0.557 \times \text{pH} \quad (28b)$$

and regression equations for alkaline legs are:

$$\text{at } 70^\circ\text{C: } \log \text{ rate}_f = 0.602 \times \text{pH} - 7.32 \quad (28c)$$

$$\text{at } 90^\circ\text{C: } \log \text{ rate}_f = 0.560 \times \text{pH} - 6.49 \quad (28d)$$

The average values for tests at 70 and 90 °C were used for the pH dependence: $\eta = 0.66$ for the acid leg and $\eta = 0.58$ for the alkaline leg. Re-regressing the test results (including the results of tests in the pH 5 solution) gives for the acid leg:

$$\text{at } 40^\circ\text{C: } \log \text{ rate}_f = 1.88 - 0.66 \times \text{pH} \quad (29a)$$

$$\text{at } 70^\circ\text{C: } \log \text{ rate}_f = 2.58 - 0.66 \times \text{pH} \quad (29b)$$

$$\text{at } 90^\circ\text{C: } \log \text{ rate}_f = 3.02 - 0.66 \times \text{pH} \quad (29c)$$

and for the alkaline leg:

$$\text{at } 40^\circ\text{C: } \log \text{ rate}_f = 0.58 \times \text{pH} - 7.94 \quad (30a)$$

$$\text{at } 70^\circ\text{C: } \log \text{ rate}_f = 0.58 \times \text{pH} - 7.10 \quad (30b)$$

$$\text{at } 90^\circ\text{C: } \log \text{ rate}_f = 0.58 \times \text{pH} - 6.68 \quad (30c)$$

These fitted lines are plotted with the measured rates in Figure 10b.

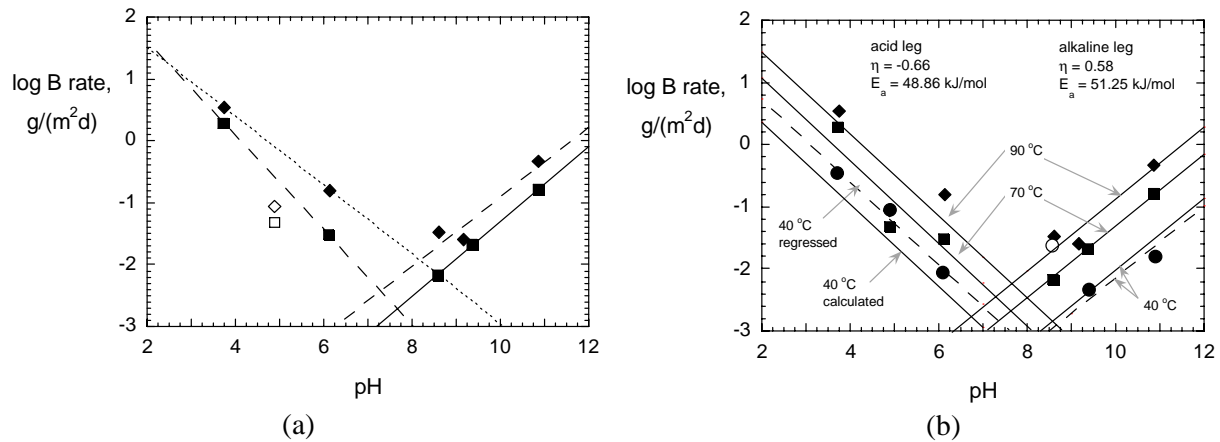


Fig. 10. Regression Fit of NR(B) Results to Determine Dependence on (a) pH and (b) Temperature at (●) 40 °C, (■) 70 °C and (◆) 90 °C. Open symbols were excluded from regressions.

Following the same methods as in Equations 13 - 17, the activation energies determined from the B results are 48.86 kJ/mol for the acid leg and 51.25 kJ/mol for the alkaline leg. Lower bounds to the forward rate constants are $k_+ = 6.76 \times 10^9 \text{ g}/(\text{m}^2\text{d})$ and $2.14 \text{ g}/(\text{m}^2\text{d})$ for the acid and alkaline legs, respectively. The expressions for Pu LaBS-B glass forward dissolution rates **based on the B** release are

$$rate_{f_acid\ leg} = 6.76 \times 10^9 \times 10^{-0.66\text{pH}} \times \exp\left(-48.86/RT\right) \quad (31a)$$

and

$$rate_{f_alkaline\ leg} = 2.14 \times 10^{0.58\text{pH}} \times \exp\left(-51.25/RT\right). \quad (31b)$$

The forward rates based on the releases of B and Si are plotted in Figure 11, where the forward rate based on Si is calculated as the sum of Equations 27a and 27b, and the forward rate based on B is calculated as the sum of Equations 31a and 31b. Both are extrapolated beyond the range of the experimental results (which are about pH 3.7 to pH 10.9). The forward rate based on the release of B lies below the forward rate based on the release of Si between the range pH 2.00 to pH 13.02; this exceeds the range of interest in TSPA calculations. When calculating rates, it is important to use the parameter values as a set rather than individually. That is, while the values of η , E_a , and k_0 (and also k_+ and k_E) differ significantly in the equations based on the Si and B releases, the rates for Pu LaBS-B glass dissolution calculated with the two equations are similar.

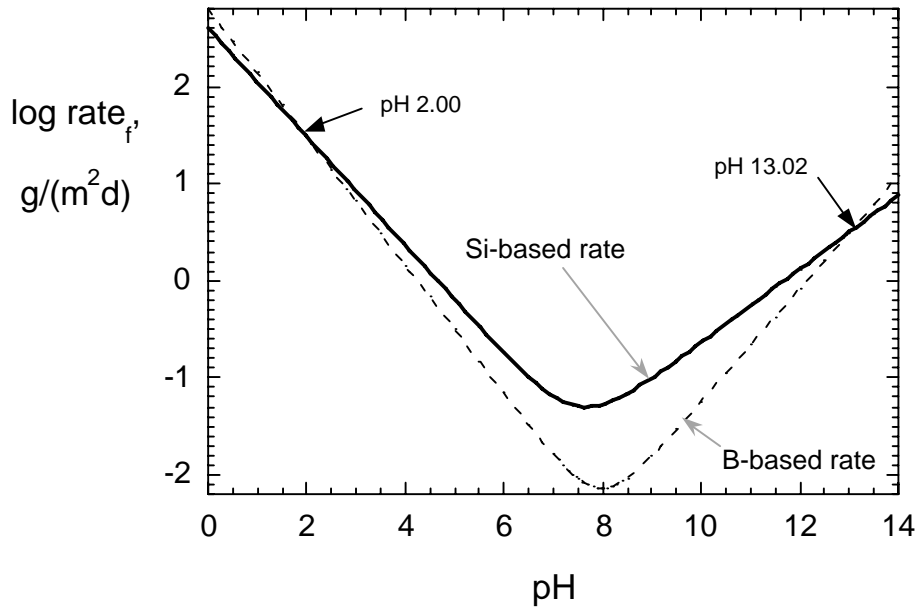


Fig. 11. Comparison of Forward Dissolution Rate Models for Pu LaBS-B Glass Based on Releases of Si and B at 90 °C.

3.4 COMPARISON WITH THE SIMPLIFIED RATE EXPRESSION USED IN DEFENSE HLW GLASS DEGRADATION MODEL

As given in Equation 2, the dissolution rate is the product of the forward rate and the affinity term. In the preceding analyses, it was assumed that the value of the affinity term was 1 to calculate lower bounds to

the forward rate. However, the value of the affinity term will change with time as glass dissolves and dissolved silica accumulates in the solution. Because the silica concentration is not tracked in TSPA calculations, the affinity term cannot be modeled directly. In the development of the HLW glass model, the affinity term was combined with the forward rate constant in the parameter k_E , and bounding values of k_E were determined from experiments conducted under a range of repository-relevant conditions. Maximum and minimum values of k_E were determined from test in dripping water, in water vapor, and in aqueous solutions. The maximum rates are used for the present comparison of Pu LaBS-B glass dissolution with the model. The maximum rate from the Defense HLW Glass Degradation Model is

$$rate_G = 1.15 \times 10^7 \times 10^{-0.49 pH} \times \exp\left(-\frac{31}{RT}\right) + 3.47 \times 10^4 \times 10^{0.37 pH} \times \exp\left(-\frac{69}{RT}\right). \quad (32)$$

Maximum values of the model parameters can be determined for Pu LaBS-B glass for comparison with the Model. The value of k_0 is used directly as the maximum value of k_E for the acid leg. The maximum value of k_E for the alkaline leg is determined from the results of 7-day PCT as

$$rate_{PCT} = \frac{NL(B)}{7} = k_E \times 10^{\eta pH} \times \exp\left(-\frac{E_a}{RT}\right), \quad (33)$$

where $rate_{PCT}$ is the average rate in a 7-day PCT,
 $NL(B)$ is the normalized boron mass loss after 7 days,
 k_E is the effective rate constant, and
 pH is the room temperature-pH of the test solution after 7 days.

From 7-day PCTs conducted at SRNL, $NL(B) = 0.012 \text{ g/m}^2$ and $pH = 7.2$. Using the parameter values for the pH and temperature dependencies **based on Si**, the value of k_E for the alkaline leg is:

$$k_E = \frac{\left(0.012 \text{ g/m}^2 / 7 \text{ days}\right)}{10^{0.38 \times 7.2} \times \exp\left(-\frac{25.03}{0.008314 \times 363}\right)} = 0.01259 \frac{\text{g}}{\text{m}^2 \text{d}}. \quad (34a)$$

Using the parameter values **based on B** in the rate expression:

$$k_E = \frac{\left(0.012 \text{ g/m}^2 / 7 \text{ days}\right)}{10^{0.58 \times 7.2} \times \exp\left(-\frac{52.44}{0.008314 \times 363}\right)} = 1.2279 \frac{\text{g}}{\text{m}^2 \text{d}}. \quad (34b)$$

Similar to the Defense HLW Glass Degradation model, the values of k_E are lower than the values of k_0 due to solution feedback effects. As is done in the Defense HLW Glass Degradation Model, using the value of k_0 for the acid leg and the values of k_E for the alkaline leg, the model rate expression **based on the Si** release is:

$$rate_G = 2.69 \times 10^8 \times 10^{-0.56 pH} \times \exp\left(-\frac{40.52}{RT}\right) + 0.0126 \times 10^{0.38 pH} \times \exp\left(-\frac{25.03}{RT}\right) \quad (35)$$

and the rate expression **based on the B** release is

$$rate_G = 6.75 \times 10^9 \times 10^{-0.66 pH} \times \exp\left(-\frac{48.86}{RT}\right) + 1.23 \times 10^{0.58 pH} \times \exp\left(-\frac{51.25}{RT}\right). \quad (36)$$

The rates calculated at 90 °C with Eqs. 32, 35, and 36 are shown in Figure 12. The Defense HLW Glass Dissolution Model provides an upper bound to the Pu LaBS-B glass dissolution rates based on the release of Si at all pH values, and to the Pu LaBS-B glass dissolution rates calculated based on the release of B at pH values higher than pH 1.17.

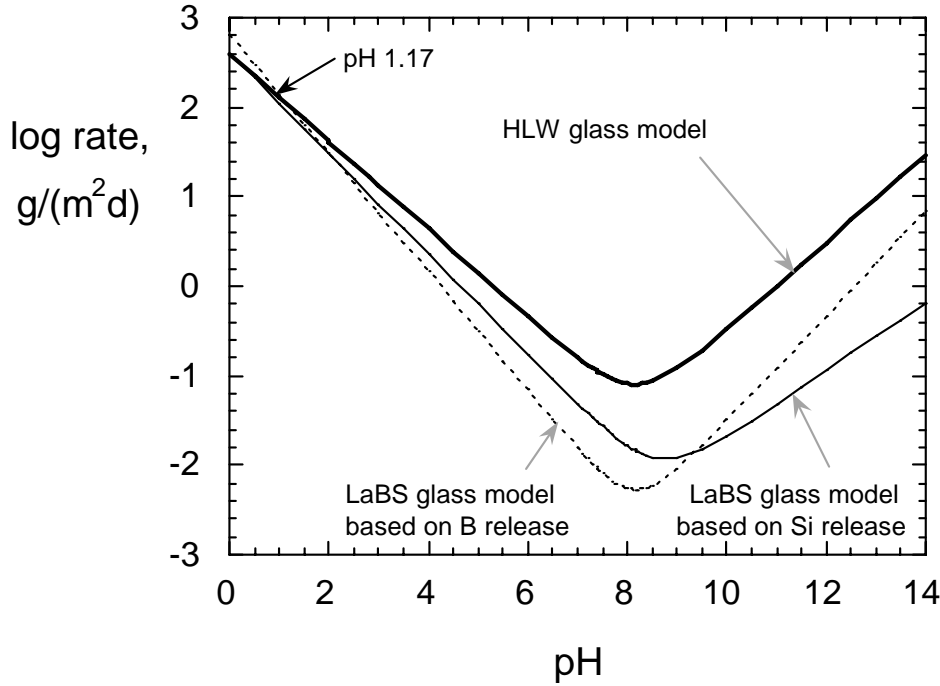


Fig. 12. Comparison of Defense HLW Glass Model (Eq. 32) with Analogous Rate Equations for Pu LaBS-B Glass Based on Releases of Si (Eq. 35) and B (Eq. 36) at 90 °C

3.5 FITTING TEST RESULTS WITH RATE EQUATION

Using the values of η and E_a determined above, the test results can be fitted with the rate expression given in Equation 4 to solve for k_0 using an assumed value of K :

$$rate_G = k_0 \cdot 10^{\eta \cdot pH} \cdot \exp\left(\frac{-E_a}{RT}\right) \cdot \left(1 - \frac{Q}{K}\right). \quad (4)$$

This was done for the rates measured tests conducted in alkaline solutions at 70 and 90 °C using coefficient values $\eta = 0.38$ and $E_a = 25.03$ kJ/mol. The values of K were selected based on values typically used to model borosilicate waste glass dissolution at 90 °C, which are typically between 28 and 36 mg/L (usually expressed as $10^{-3.0}$ to $10^{-2.9}$ M). It is expected that values of K for Pu LaBS-B glass can be estimated from the results of long-term PCTs in which a maximum Si concentration is approached. The Si concentrations in recent PCTs conducted at SRNL at 90 °C and about 20,600 m⁻¹ increase nearly linearly in tests between 7 and 56 days up to about 26 mg/L (see Section 3.6). This is probably near the solubility limit for Pu LaBS glass.

Tests conducted for longer durations (and/or at higher S/V ratios) are needed to measure the apparent saturation concentration and estimate the value of K for Pu LaBS-B glass. For the present analysis, we note that the values of k_0 in the regressions are not very sensitive to the value of K over a significant range. For example, the optimum values of k_0 for tests at pH 10.87 at 90 °C are 1.23 g/(m²d) using $K = 10$ mg/L and 1.15 g/(m²d) using $K = 50$ mg/L. The present calculations were conducted using $K = 30$ mg/L for tests at 90 °C and $K = 23$ mg/L for tests at 70 °C. The lower value of K used at 70 °C reflects a presumed lower solubility of Pu LaBS-B glass at lower temperatures analogous to the lower solubilities of silicate minerals. The experimentally measured dissolved Si concentration was used for Q . Values of $rate_G$ were calculated with trial values of k_0 at the pH measured at each test duration and then multiplied by the test duration to calculate the extent of reaction in terms of g/m², which is referred to as the calculated value of NL(Si). Those calculated values were then compared with the measured values of NL(Si) under each set of pH-temperature conditions. Separate values of k_0 that minimized the difference between the measured and calculated values of NL(Si) were determined from the results of tests in the pH 10.87 solutions: $k_0 = 0.952$ g/(m²d) at 70 °C and $k_0 = 1.17$ g/(m²d) at 90 °C. The small difference probably reflects uncertainty in the regressed temperature dependence. In Figure 13, the measured values of NL(Si) are plotted with the linear regressions that were used to determine the pH dependence (squares and dashed lines), and the calculated values of NL(Si) are plotted with an empirical curve to guide the eye (circles and solid lines). The increases in the measured and calculated values of NL(Si) are in good agreement, and indicate that the values of k_0 are reasonable. The y intercepts differ, probably due to error in the background values used for the measured NL(Si).

Note that these values of k_0 are higher than the lower bounding values that were estimated earlier with the derived forward rate equations for the alkaline leg. For example, $k_0 = 1.17$ g/(m²d) from the above regression of the test results at each temperature and pH is greater than $k_+ = 0.145$ g/(m²d) from Equation 26a using the average of the combined results. Part of the difference is because the slowing effect of the affinity term was implicitly included in the value of k_+ determined in Equation 26a, but has been deconvoluted from the value of $k_0 = 1.17$ g/(m²d) used for the regression in Figure 13. The difference between k_+ and k_0 suggests that the (average) value of the affinity term in the dissolution tests is about 0.124. This value is unreasonably small. For example, the maximum Si concentration in the test at 90 °C in the pH 10.87 solution was 0.9 mg/L, which yields a calculated value of $(1 - 0.9/30) = 0.97$ for the affinity term. Most of the difference between k_+ and k_0 must be due to fitting the set of test results to single values of η and E_a when determining the value of k_+ , whereas the value of k_0 was determined directly from the results of tests at 90 °C and pH 10.87. The experimental results are not sufficiently precise to distinguish between the linear fit and the fit to the rate equation. This is expected because the tests were designed to maintain solutions dilute enough that the value of the affinity term remained nearly 1 and glass dissolution would be nearly linear in time. Consistent with the data, the fits by the rate equations have very slight negative curvatures. Longer-term tests in which Si builds up to higher concentrations are needed to better determine the values of k_0 and K .

The mechanistic rate expression is:

$$rate_G = k_{0_acid} \times 10^{\eta pH} \times \exp\left(-\frac{E_a}{RT}\right) + k_{0_alkaline} \times 10^{\eta pH} \times \exp\left(-\frac{E_a}{RT}\right) \times \left(1 - \frac{Q}{K}\right), \quad (37)$$

where the chemical affinity term for acidic solutions is presumed to be 1. Based on the Si release, the rate expression for Pu LaBS-B glass is:

$$rate_G = 2.69 \times 10^8 \times 10^{-0.56 pH} \times \exp\left(-\frac{40.52}{RT}\right) + 0.126 \times 10^{0.38 pH} \times \exp\left(-\frac{25.03}{RT}\right) \times \left(1 - \frac{[Si]}{30}\right), \quad (38)$$

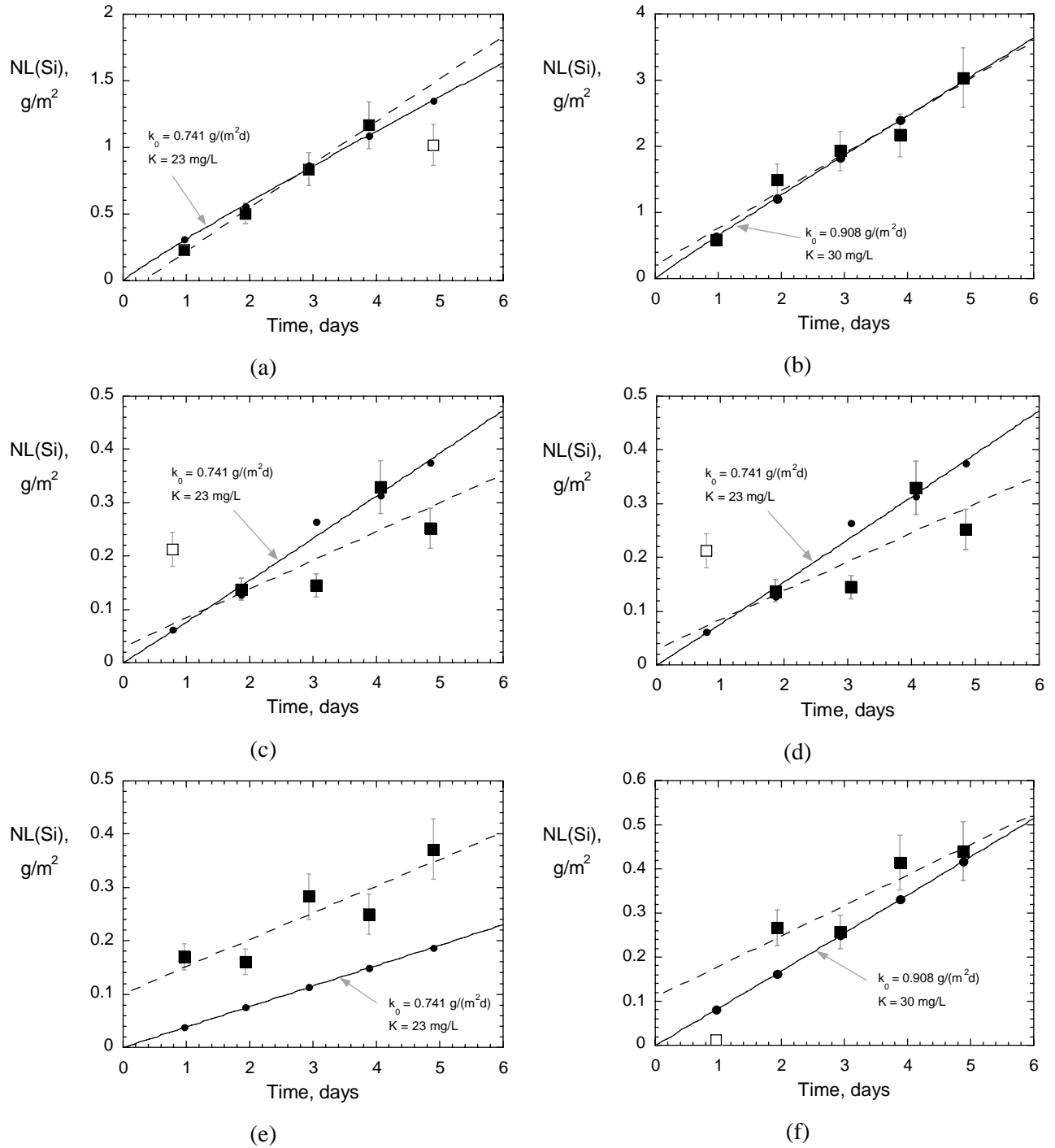


Fig. 13. NL(Si) Results Fitted by Linear Regression (■ and dashed lines) and by Regression to Glass Dissolution Equations (● and solid curves) for Tests at (a) 70 °C in pH 10.87 Solution, (b) 90 °C in pH 10.87 Solution, (c) 70 °C in pH 9.37 Solution, (d) 90 °C in pH 9.18 Solution, (e) 70 °C in pH 8.58 Solution, and (f) 90 °C in pH 8.60 Solution. Open squares were excluded from linear regressions.

where pH is the pH at room temperature and $[Si]$ is the silicon concentration in mg/L. Although a constant value of $K = 30$ mg Si/L is used in Equation 38, the value of K is probably temperature-dependent. The use of a too-high value of K will yield a conservatively high calculated dissolution rate.

3.6 TESTS IN DEMINERALIZED WATER AT 90 AND 120 °C

In the tests conducted in demineralized water, the pH was allowed to drift as the glass dissolved. Due to the lack of alkali metals and the low ionic strengths, the test solutions remained slightly acidic, probably due to the uptake of CO_2 . Figures 14a and 14b show the results of the short-term and long-term tests, respectively. (In Fig. 14b, the results for tests at 120 °C after 28 and 56 days are off-set on the x-axis to distinguish them from the results of tests conducted at 90 °C for the same duration.) The Si concentration measured in the blank test MLBD-90-B was 171 $\mu g/L$, which is surprisingly high for demineralized water. This was used as the background for all tests in demineralized water. As mentioned earlier, this will shift all test concentrations the same amount and will not affect the dissolution rate determined from the data set (if the origin is excluded).

The releases of B and Si increase linearly with time during the first 5 days with rates $NR(Si) = 0.120$ g/(m²d) and $NR(B) = 0.0771$ g/(m²d). These rates are about 3X and 2X lower than those measured in the pH 6.13 leachant, and both Si and B show significantly more rollover with reaction time in tests conducted in demineralized water than in tests in the pH 6.13 leachant. The slightly higher pH values attained in the test in demineralized water (pH 6.6 vs pH 6.13 after 5 days) is predicted to increase the rate, but the higher Si concentrations (1.16 mg/L vs. 1.04 mg/L after 5 days) is predicted to lower the rate. However, note that the pH of the test solutions in demineralized water were not stable due to the very low ionic strength and were probably affected by the uptake of CO_2 during the measurement. The comparison with the pH 6.13 leachant is only approximate.

Figure 14b includes the results of long-term tests in demineralized water; the dotted line shows the linear fit to $NL(Si)$ values over the first 5 days. The long-term tests become affected by the buildup of dissolved silicon in the solution (and perhaps by the buildup of other components) through the affinity term. The effect of temperature on the dissolution rate is shown qualitatively by the higher $NL(i)$ values for tests run

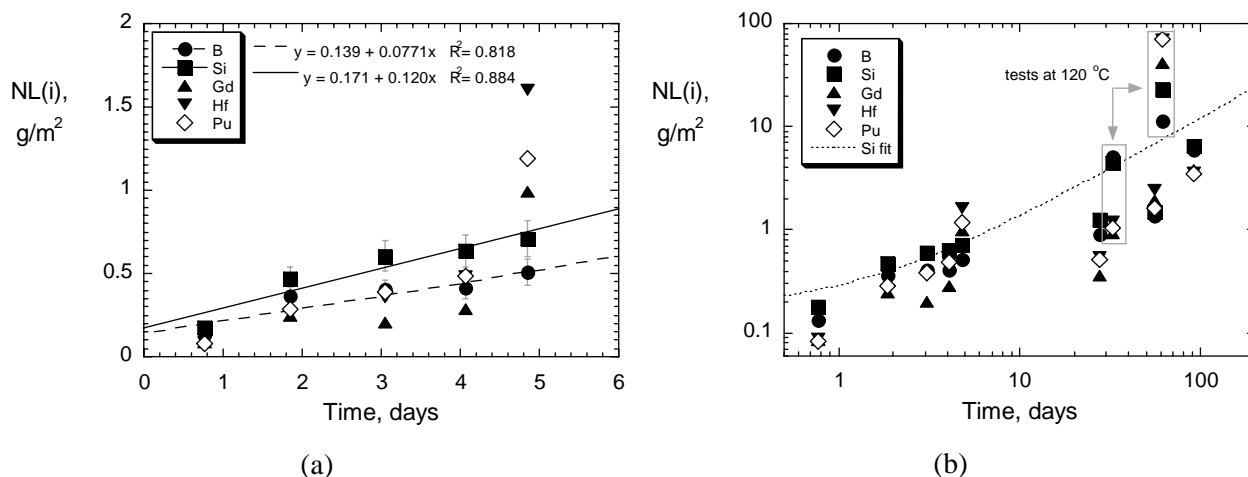


Fig. 14. Results of Tests Conducted in Demineralized Water (a) through 5 Days and (b) through 91 Days. Dotted curve in (b) gives values of $NL(i)$ calculated by extrapolation of short-term rates at 90 °C based on $NL(Si)$.

at 120 °C for 28 and 56 days. The 28-, 56-, and 91-day tests at 90 °C attain Si concentrations of 2.0, 2.3, and 9.7 mg/L, respectively, which are all less than 30% of the assumed saturation concentration of 30 mg/L.

Figure 15 shows the results of long-term product consistency tests (PCTs) at 90 °C and about 21,000 m⁻¹ that were conducted at SRNL. Power-law fits are drawn to guide the eye. Both NL(Si) and NL(B) increase nearly linearly between 7 and 56 days: $NR(Si) = 1.4 \times 10^{-4} \text{ g/(m}^2\text{d)}$ and $NR(B) = 2.8 \times 10^{-4} \text{ g/(m}^2\text{d)}$. The solution pH values were measured to be about 8 with pH paper. These rates are much lower than the forward rates measured in the immersion tests due to the (relatively) higher Si concentrations that were attained in the PCTs. It is expected that highly concentrated solutions will be generated after short test durations at high S/V ratios and that the dissolution rate will decrease with time. The Si concentration calculated from data in Tables 7 and 14 of Marra et al. 2006 is about 26 mg/L after 56 days, which is only slightly below the expected saturation concentration of about 30 mg/L. Note that values of NL(B) are higher than values of NL(Si) in all PCTs, whereas NL(Si) values were higher than NL(B) values for all immersion tests. This indicates that the release of Si was slowed by solution feedback effects in the PCTs, but was not slowed significantly in the immersion tests. The release of B is affected by solution feedback only as a consequence of the effect on Si. Boron continues to be released at a high rate after the release of Si is slowed by solution feedback effects, although the rate will eventually decrease due to diffusion constraints.

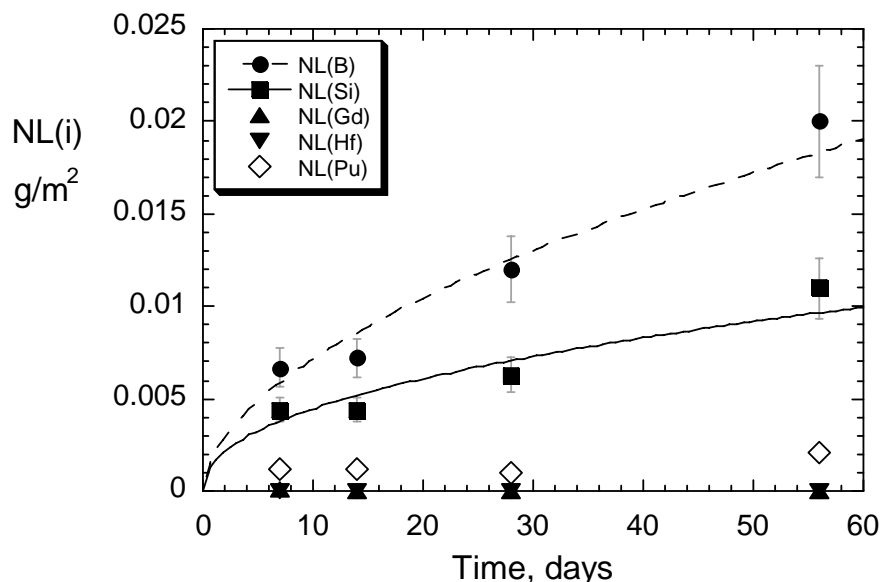


Fig. 15. Results of PCTs Conducted at SRNL with Pu LaBS-B Glass at 90 °C and 21,000 m⁻¹.

3.7 CONCENTRATIONS OF PU, GD, AND HF IN TEST SOLUTIONS

The molar concentrations of Pu, Gd, and Hf in the test solutions were calculated from the measured mass concentrations. The resulting values are plotted in Figures 16a - 16c for all tests at 40, 70, and 90 °C, respectively, against the measured pH. The Gd concentrations are higher than the Pu concentrations in acidic solutions, but the Pu concentrations are higher than the Gd or Hf concentrations in alkaline solutions. The (overall) concentrations **in the glass** are 3.10 moles Pu, 2.87 moles Hf, and 5.80 moles Gd per 100 g glass. Examination of the glass indicated that some of the Pu was contained in approximately 2-μm-sized PuO₂ inclusion phases. (The relative amounts of Pu in the inclusions and dissolved in the

glass are not known.) These are presumed to be residual undissolved crystallites that were added when the glass was made, and are presumed not to contain Hf or Gd. All of the Hf and Gd is presumed to be dissolved in the glass. The fraction of Pu that is dissolved in the glass is not known. Note that the mass fractions of Pu used to calculate the normalized mass losses that were plotted in Figures 5 – 7 did not distinguish between Pu dissolved in the glass and Pu in PuO₂ inclusions. The calculated values of NL(Pu) were based on the total concentrations in the glass.

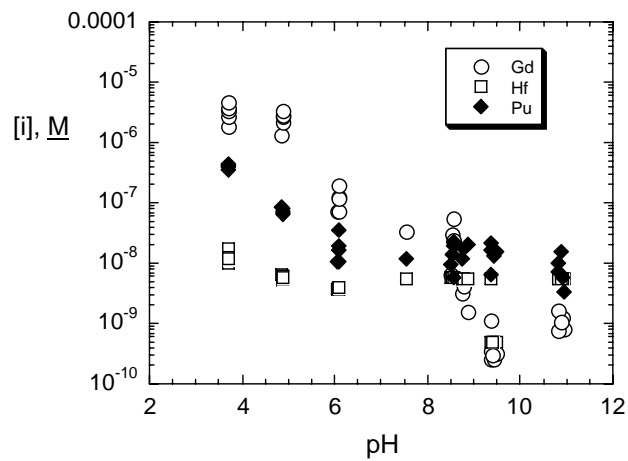
The amount of glass that has dissolved can be estimated from the normalized mass loss and the density of glass, which is 3.57 g/cm³ (Marra et al. 2006). The depth to which the glass dissolved in a test can be estimated as

$$\text{dissolution depth, } \mu\text{m} = \frac{NL(\text{Si}), \frac{\text{g}}{\text{m}^2}}{\rho, \frac{\text{g}}{\mu\text{m} \cdot \text{m}^2}}. \quad (39)$$

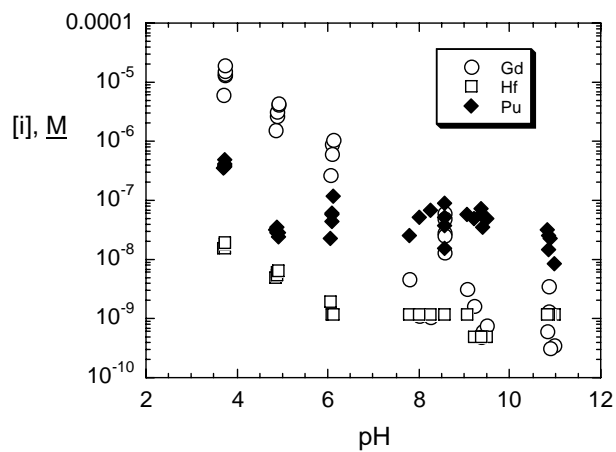
In the 56-day PCT conducted at SRNL, NL(Si) = 0.011 g/m² and the estimated dissolution depth is 0.003 μm. More glass dissolves in tests conducted with monolith specimens at lower S/V ratios than in the PCTs: the highest values of NL(Si) were 21.1 g/m² in the test conducted at 90 °C at pH 3.75 and 22.7 g/m² in the test conducted at 120 °C for 56 days in demineralized water. The estimated dissolution depths in those tests are 5.6 and 6.4 μm.

Figure 14b showed NL(Pu) to be significantly higher than NL(Si) in the test conducted at 120 °C for 56 days (MLBD-120-2). Enough glass dissolved in these tests that PuO₂ inclusions at the surface could have been released as colloids. The test solutions were not filtered or otherwise analyzed for the presence of colloids. The values of NL(Gd), NL(Hf), and NL(Pu) relative to NL(Si) indicate whether these elements are released congruently with Si, which is taken to represent dissolution of the glass phase. The ratios for test series conducted at 90 °C in the different leachants are shown in Figure 17. The release of Gd is congruent with Si in acidic solutions (i.e., the ratios are near 1), but not in alkaline solutions. The three ratios are all anomalously high in the 1-day test in the pH 8.5 solution. This is because NL(Si) is anomalously low (see Fig. 7d). The release of Pu is greater than the releases of Gd and Hf in alkaline solutions.

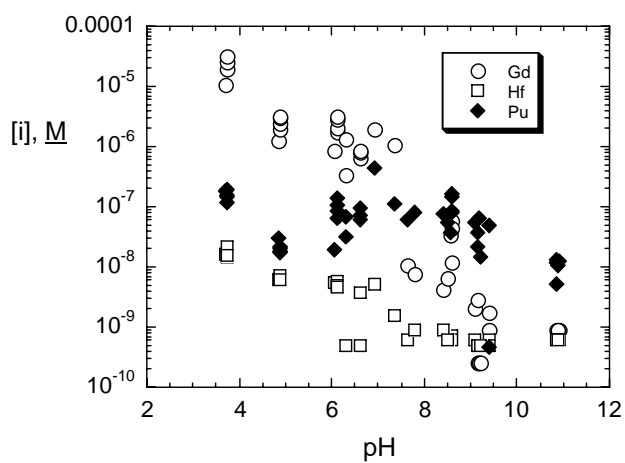
Figure 18 shows the distributions of Gd, Hf, and Pu between the test solutions and the acid soak solutions. (Note that acid soak solutions were not analyzed for the rerun MLB5 test series). The Gd is present almost entirely in the test solution in tests in Teflon vessels, but is present mostly in the acid soak solutions in the tests conducted in steel vessels. For tests in Teflon vessels, about half of the released Hf and Pu is present in the acid soak solutions in the pH 3.7 and pH 4.9 tests, and smaller fractions are in the acid soak solutions at higher pHs. Essentially all of the Hf and Pu released in tests conducted in steel vessels is present in the acid soak solutions. The ratios for tests in demineralized water are shown in Figure 19. The results of 28- and 56-day tests at 120 °C are off-set on the time axis for clarity and are enclosed in boxes. The ratios are similar and close to 1 in all tests. This behavior is different than seen in tests in the pH 6.13 solution conducted in Teflon vessels, and is probably due to interactions with the steel vessel. Almost all of the Gd, Hf, and Pu released in tests in the steel vessels were present in the acid soak solutions, whereas most of the released elements were present in the test solution in tests in Teflon vessels. Clearly, sorption on steels in the waste package will impact the release and physical separation of Gd and Hf from Pu in the disposal system.



(a)



(b)



(c)

Fig. 16. Concentrations of Gd, Hf, and Pu in the Test Solutions at (a) 40 °C, (b) 70 °C, and (c) 90 °C.

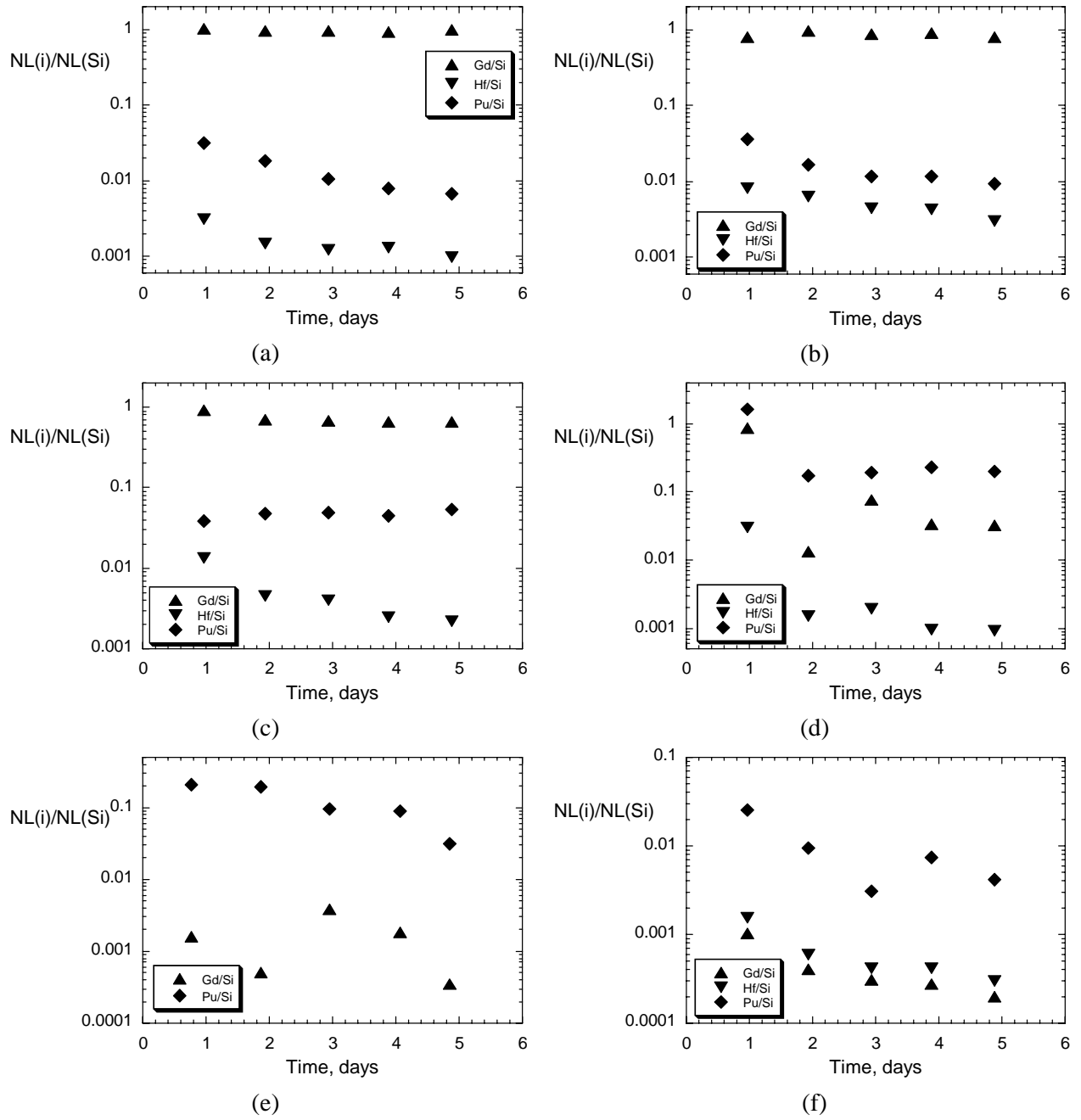


Fig. 17. Ratios (▲) $NL(Gd)/NL(Si)$, (▼) $NL(Hf)/NL(Si)$, and (◆) $NL(Pu)/NL(Si)$ for Test Series (a) MLB1-90, (b) MLB2-90, (c) MLB3-90, (d) MLB4-90, (e) MLB5-90R, and (f) MLB6-90

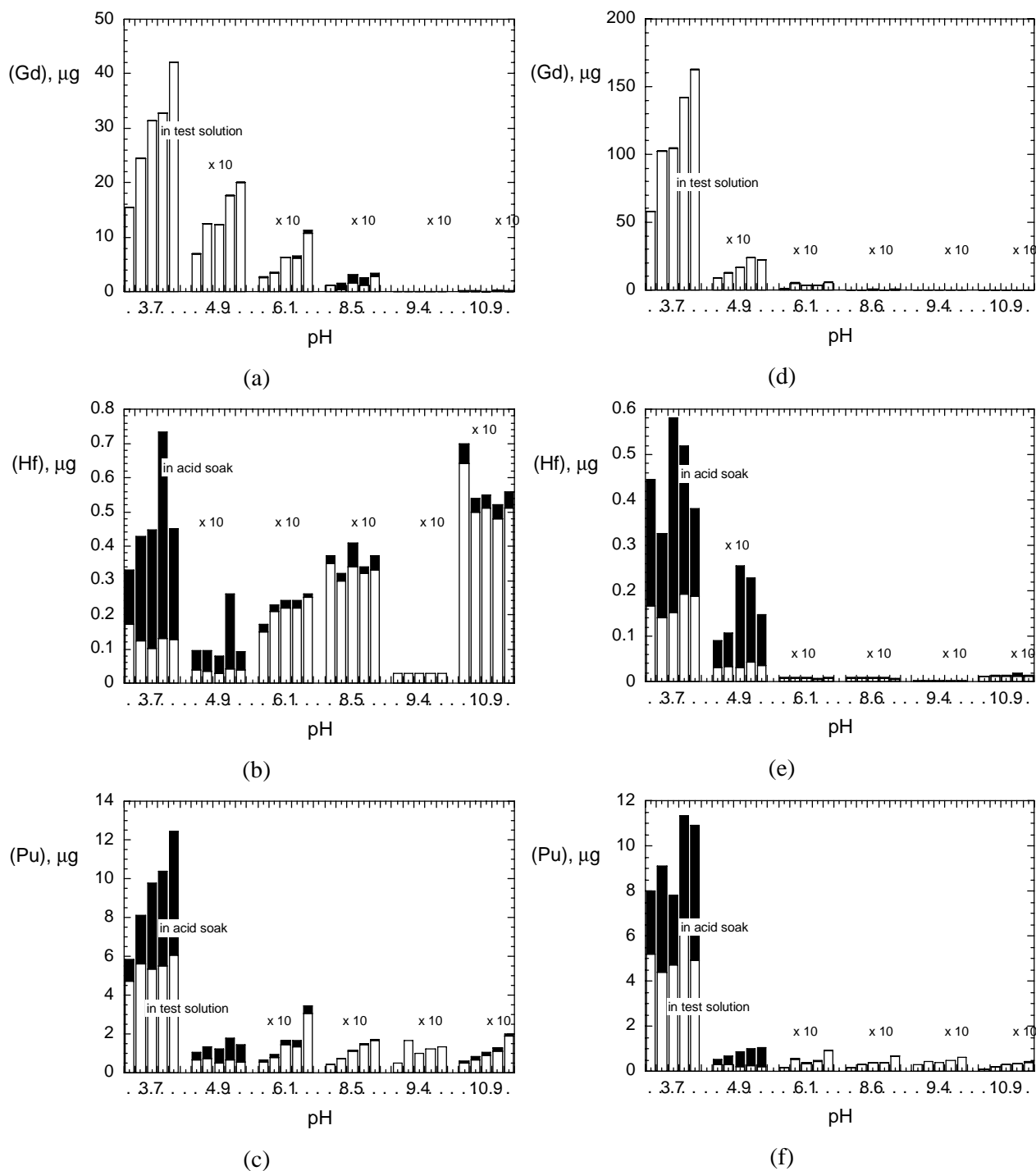
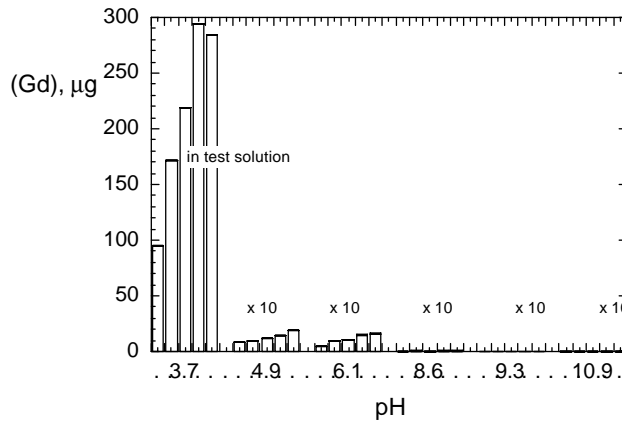
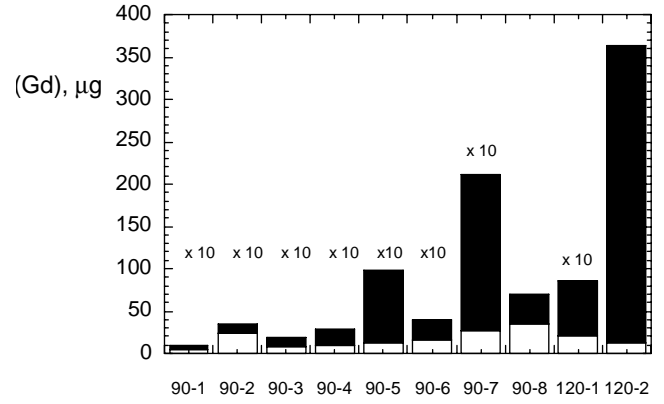


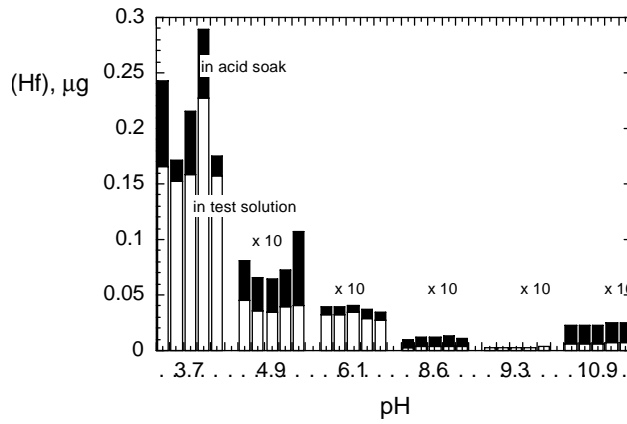
Fig. 18. Distributions of Gd, Hf, and Pu Between Test Solutions (open bars) and Acid Soak Solutions (filled bars): (a) Gd, (b) Hf, and (c) Pu in tests at 40 °C, (d) Gd, (e) Hf, and (f) Pu in tests at 70 °C, and (g) Gd, (h) Hf, and (i) Pu in tests at 90 °C, and (j) Gd, (k) Hf, and (l) Pu in tests at 90 °C in demineralized water. Results for 1-, 2-, 3-, 4-, and 5-day tests grouped sequentially by pH. The elements in some groups are plotted as 10X the measured mass.



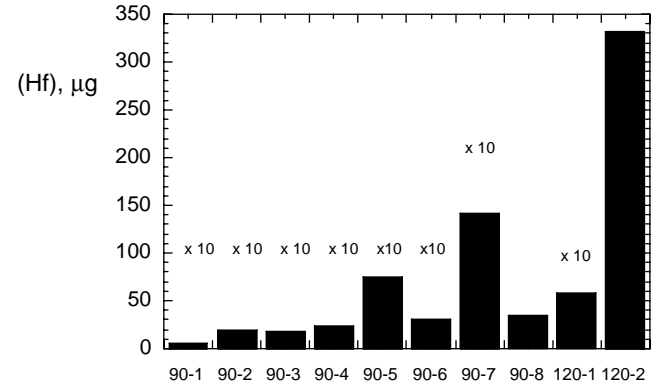
(g)



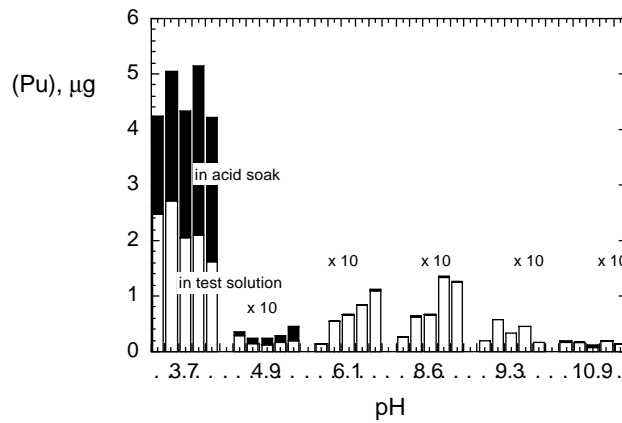
(j)



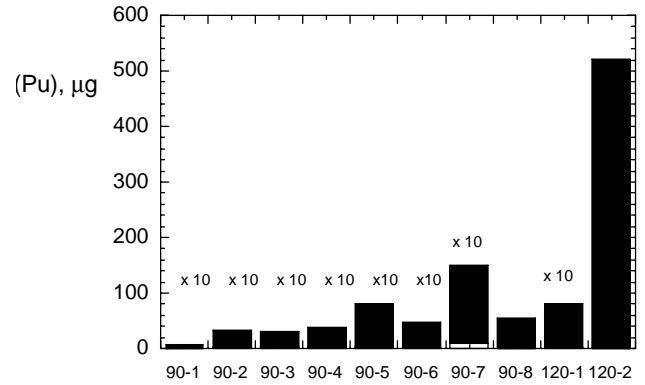
(h)



(k)



(i)



(l)

Fig. 18. (cont.)

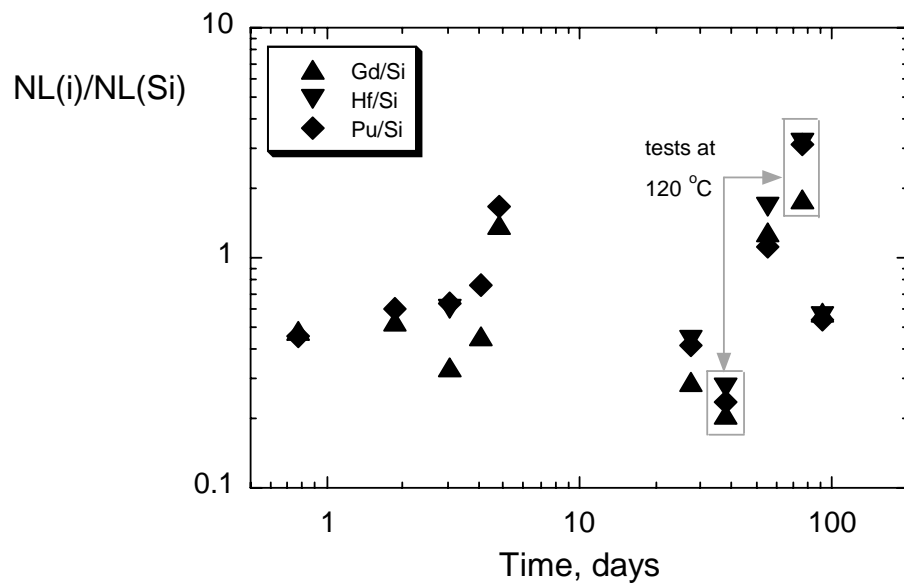


Fig. 19. Ratios (\blacktriangle) $NL(Gd)/NL(Si)$, (\blacktriangledown) $NL(Hf)/NL(Si)$, and (\blacklozenge) $NL(Pu)/NL(Si)$ for Tests Conducted in Demineralized Water at 90 and 120 °C

4. VAPOR HYDRATON TEST RESULTS AND DISCUSSION

A small number of VHTs were conducted as scoping tests to study the behavior of Pu LaBS glass when contacted by solutions with high concentrations of dissolved glass components and high pH, which is the expected environment in a breached and fractured waste package under disposal conditions. Since LaBS glass will be encapsulated in a large volume of HLW glass in the waste form, any water that contacts LaBS glass will have previously contacted and reacted with the HLW glass. Dissolution of the HLW glass will have caused a significant pH rise and contributed dissolved alkali metals and silicon. Corrosion of the HLW glass may also result in the formation of secondary phases, including clays and zeolites. The consumption of Al and Si by the formation of zeolites is known to cause an increase in the glass dissolution rate. Although zeolites will not form when LaBS glass dissolves in isolation due to the absence of alkali metals, they may be present in the waste package due to corrosion of HLW glass and control the solution that contacts the LaBS glass. The intent of the VHTs was to determine if corroding HLW glass affects the corrosion behavior of Pu LaBS-B glass.

Two series of VHTs were conducted. One series of tests was conducted with SRL 418 glass to gauge the reactivity of that glass at 120 and 200 °C and catalogue the secondary phases that formed. The other series was conducted with specimens of Pu LaBS-B and SRL 418 glasses in physical contact and with a separate specimen of Pu LaBS-B glass in the same test vessel (a schematic drawing of the test setup was shown in Fig. 4). The test execution data are compiled in Appendix F. A photograph of Pu LaBS-B and SRL 418 glasses reacted in two VHTs conducted for 72 days at 120 °C is shown in Figure 20; the specimens from test VLB-120-1 are on the support rod to the left and the specimens from test VLB-120-2 are on the support rod to the right. Note the close proximity of the two specimens that are tied together with Teflon thread (on the left side of each rod). Alteration phases are visible on the entire surfaces of the SRL 418 glass specimens. A small number of phases are visible at some locations of the Pu LaBS-B specimens (for example, near the top of the separated specimen in Fig. 20). Figure 21 shows two vapor-reacted specimens in a VHT conducted for 65 days at 120 °C with only SRL 418 glass. Alteration phases completely cover the surfaces of the SRL 418 glass specimens.

The SRL 418 glass was completely corroded within several days in VHTs conducted at 200 °C, and was converted to alteration phases. The alteration was slower in tests at 120 °C. The specimens from tests at 120 °C were not examined in detail, but it appears that the same suite of phases is formed at both temperatures. The surface of a specimen of SRL 418 glass reacted in scoping tests at 150 °C was examined to gain insight into the phases that form. The most abundant alteration phases were clay, analcime ($\text{NaAlSi}_3\text{O}_8 \cdot \text{H}_2\text{O}$), and unidentified sodium-silicate phases, which are shown in the photomicrographs in Figure 22. Figure 22a shows several analcime crystals embedded in a layer of clay, and Figure 22b shows high magnification image of the clay with the familiar “honey-comb-like” texture of smectite clays. The dimpled tops of the crystals probably indicate that crystal growth normal to the surface was limited by the depth of the water layer, i.e., that the crystals were not completely submerged in water. Figures 22c and 22d show several silicates having “lath-like” or “needle-like” morphologies—possibly phillipsite, $\text{Na}(\text{AlSi})_8\text{O}_{16}$. The approximate compositions of these phases were measured with energy dispersive x-ray fluorescence spectroscopy (EDS), and the results are summarized in Table 8 (see Figs. 22a – 22c to orient spectrum numbers). The reported compositions are qualitative.

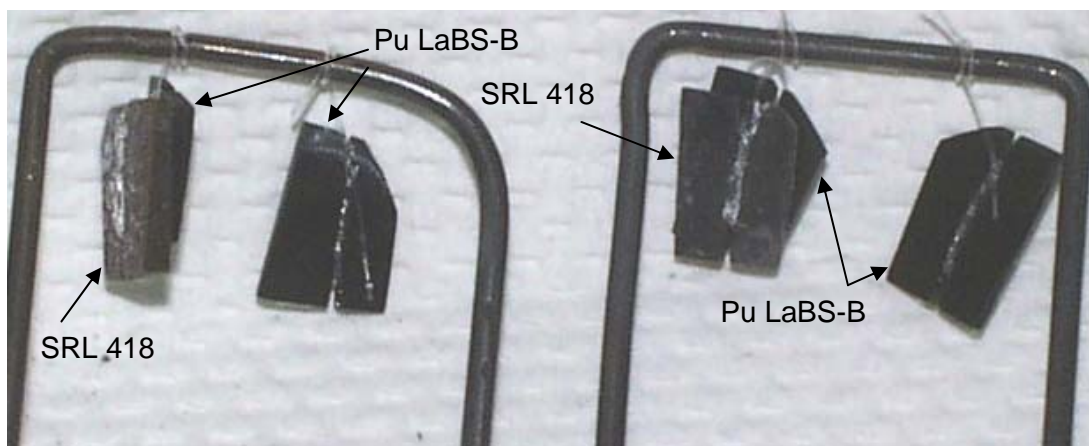
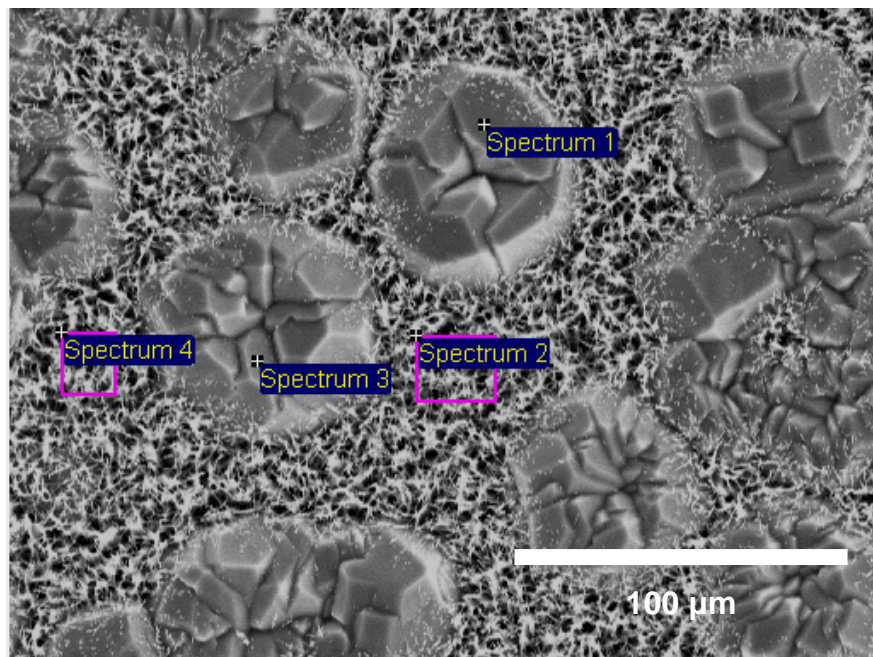


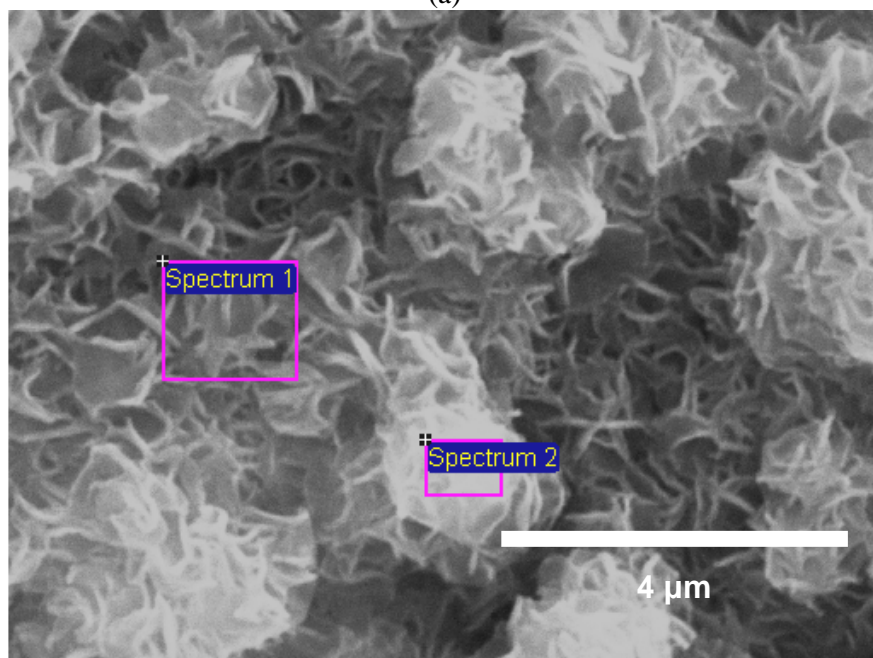
Fig. 20. Vapor-Reacted Pu-LaBS-B Glass Contacting SRL 418 Glass (left), and Separated (right).



Fig. 21. Vapor-Reacted SRL 418 Glass.

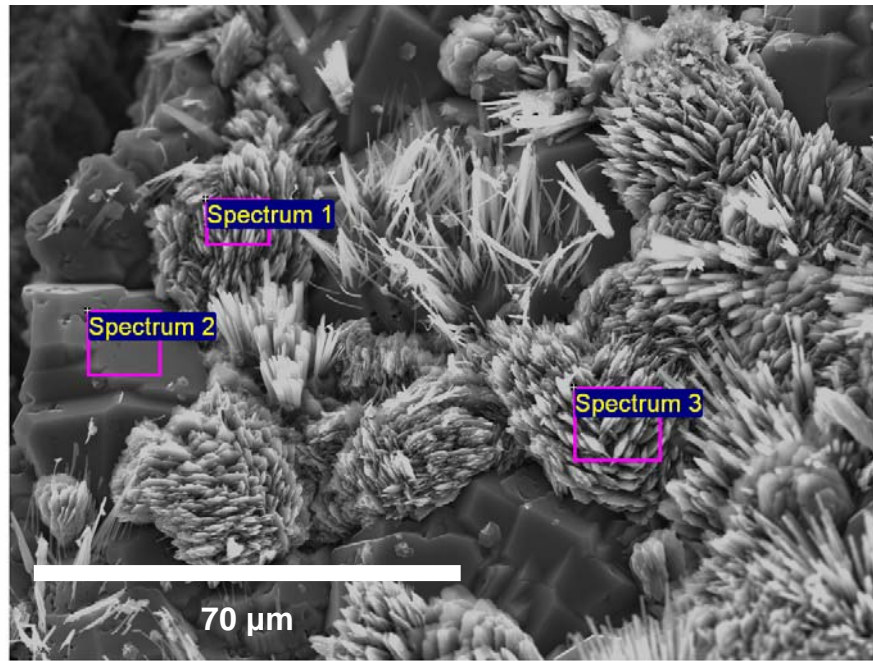


(a)



(b)

Fig. 22. SEM Photomicrographs of Alteration Phases Formed on Surface of Vapor-Hydrated SRL 418 Glass: (a) analcime crystals embedded in clay, (b) high magnification image of clay, and (c) unidentified sodium silicate phases intergrown with analcime



(c)

Fig. 22 (cont.)

Table 8. EDS Compositions of Phases on Surface of Vapor-Hydrated SRL 418 Glass, atomic %

Element	Figure 22a				Figure 22b		Figure 22c		
	Spectrum 1	Spectrum 2	Spectrum 3	Spectrum 4	Spectrum 1	Spectrum 2	Spectrum 1	Spectrum 2	Spectrum 3
O	73.3	72.7	74.6	73.7	71.7	79.9	81.4	75.5	80.9
Na	5.3	13	5.3	13	2.3	2.2	0.53	7.3	0.49
Mg	—	—	—	—	0.74	0.68	—	—	—
Al	6.5	0.08	6.2	0.11	2.3	2.0	0.11	5.3	0.08
Si	15	10	14	9.8	18	13	18	12	18
K	0	0.18	0	0.15	0.11	0.03	—	—	—
Ca	0	3.7	0	3.1	0.10	0.03	0.08	0.07	0.03
Mn	—	—	—	—	0.90	0.51	—	—	—
Fe	0.11	0.065	0.88	0	3.6	1.8	0.08	0.15	0.05
Ni	—	—	—	—	0.22	0.093	—	—	—
ID	analcime	clay	analcime	clay	clay	clay	?	analcime	?

One of the highly corroded specimens recovered from a scoping test conducted with only SRL 418 glass was fixed in epoxy and a polished cross-section was examined with an SEM to characterize the structure and compositions of the alteration phases. A low-magnification SEM image of a cross-sectioned completely reacted specimen of SRL 418 glass is shown in Figure 23. The glass has been completely converted to a complex mixture of alteration phases, with several distinct layers overlying the altered interior. Several of the layers separated during the test (or when the specimen dried) and are detached in the cross-sectioned specimen. These layers probably formed by *in-situ* alteration of the glass, although phases formed on the outermost layer probably precipitated from the film of water covering the surface during the test. The 4 outermost layers are shown at higher magnification in Figures 24a and 24b, and the EDS compositions of these layers are summarized in Table 9. These are not quantitative measurements,

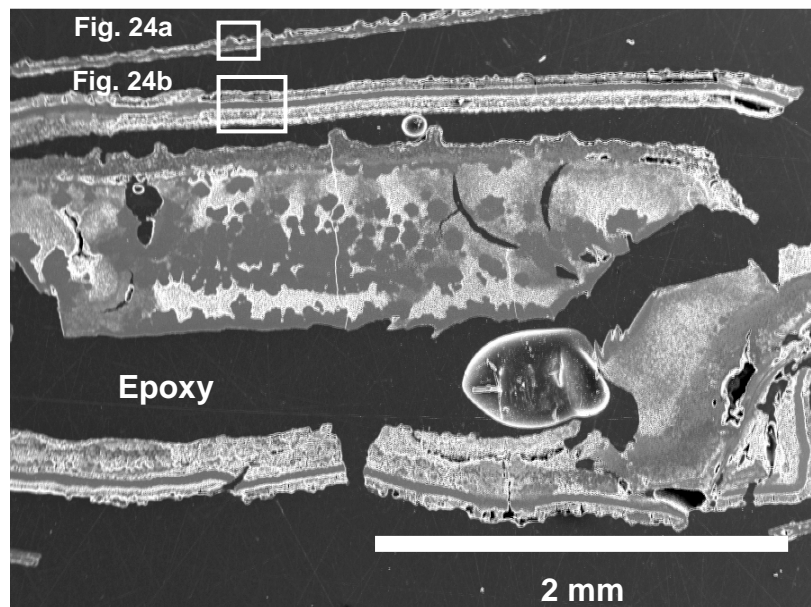
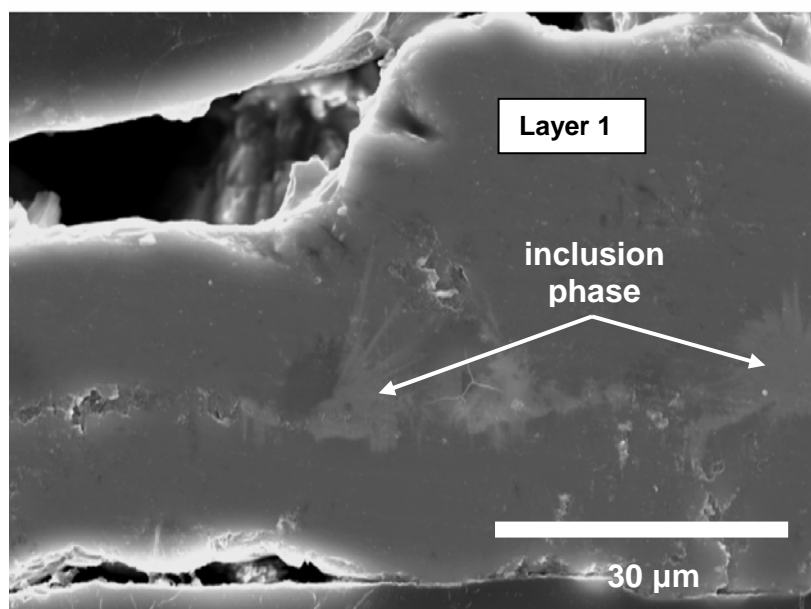


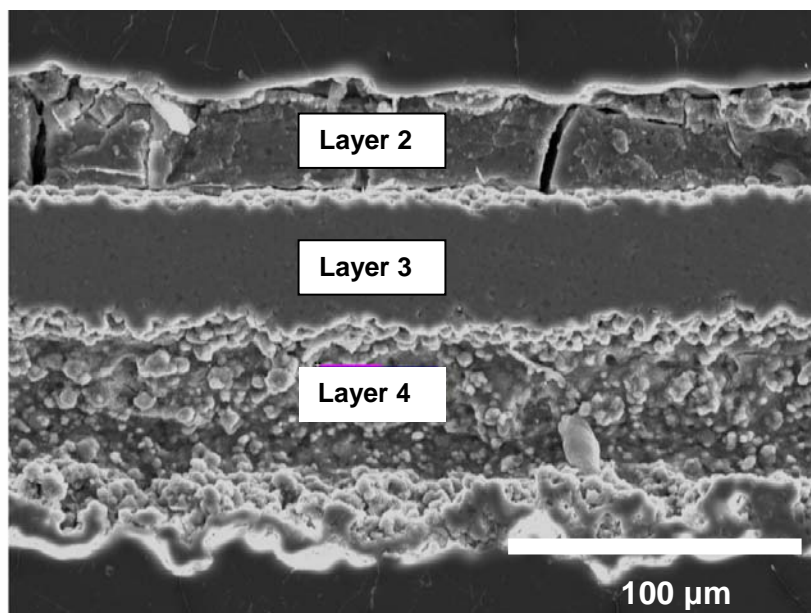
Fig. 23. SEM Photomicrograph of Vapor-Reacted SRL 418 Glass

but provide insight into the relative compositions of the different layers; the measured composition of unreacted SRL 418 glass measured from another specimen is included in the table for comparison to show relative enrichments or depletions of particular elements in the different layers. The EDS-measured composition of the glass is consistent with the bulk glass composition given in Table 1. The composition of the outermost layer is similar to analcime, which is a commonly formed alteration product of laboratory-reacted HLW glasses. Analcime was likely formed by precipitation from the solution onto the outer surface of the specimen initially, and then also formed elsewhere in the specimen (including spaces between separated layers) as corrosion continued. From the photomicrograph in Figure 23a, a small amount of a Ca-rich phase is encapsulated as an inclusion within the layer of analcime. Layers 2, 3, and 4 have distinct compositions and morphologies. Layer 4 is enriched in Fe and Mn relative to the other layers and to the initial glass. Layer 2 is fractured into blocky pieces, similar to the partially dehydrated smectite clay layers that have been seen in tests with similar glasses. The fracturing probably occurred when the specimen was dried, and suggests that Layer 2 had a higher water content than Layer 3, which did not crack. The interior of the altered specimen is comprised of several intermingled phases and was not analyzed in detail.

Other specimens of corroded SRL 418 glass (specimens S17 and S18) were finely crushed and analyzed with powder XRD to identify crystalline alteration phases. The XRD results are summarized in Table 10. Consistent with the SEM results, analcime is the predominant crystalline phase, and peaks corresponding to 3 natural samples (and a distorted tetragonal form of analcime) are observed. Several significant peaks are detected that cannot be indexed to analcime or other commonly formed zeolite. One exception is the peak with a d-spacing of about 2.31 Å, which is consistent with phillipsite, $\text{Na}(\text{AlSi})_8\text{O}_{16}$, which is a commonly formed alteration phase in laboratory corrosion tests with borosilicate waste glasses. That peak is also consistent with Li_2SiO_3 . However, the XRD results do not include the strongest peaks of clays such as smectite (4.45 Å), illite (4.43 Å), and nontronite (4.56 Å) that are common alteration products of weathered glasses.



(a)



(b)

Fig. 24. SEM Photomicrographs of (a) Outermost and (b) Interior Alteration Layers Formed on Vapor-Reacted SRL 418 Glass

Table 9. EDS Compositions of Phases in Outer Layers of Vapor-Hydrated SRL 418 Glass, atomic %

Element	Figure 24a		Figure 24b			Glass ^a
	Layer 1	inclusion phase	Layer 2	Layer 3	Layer 4	
O	66.36	65.72	56.66	66.58	36.12	63.2
Na	4.79	6.20	2.99	6.26	1.98	8.81
Mg	0.00	0.14	1.39	0.44	0.51	0.71
Al	8.04	0.14	0.96	0.20	0.26	2.45
Si	20.34	18.50	12.54	15.35	6.24	19.9
K	—	—	0.20	0.12	0.19	0.16
Ca	0.04	8.48	1.04	1.11	0.83	0.44
Mn	0.00	0.12	1.76	0.59	3.57	0.79
Fe	0.42	0.69	3.90	3.90	25.10	3.35
Ni	—	—	0.38	0.14	1.01	0.19

^a Average of 4 measurements.

In the VHTs conducted with specimens of SRL 418 and Pu LaBS-B glass in contact, the SRL 418 glass was corroded to various degrees, whereas the Pu LaBS-B glasses recovered from all tests appeared visually to be unreacted. Separated specimen B7b and contacting specimens B7a and S7 from a test in which the SRL 418 glass was highly reacted were fixed in epoxy and cross-sectioned for examination with SEM. The specimens were examined to determine whether any alteration of the Pu LaBS-B glass specimens (B7a and B7b) occurred and whether Pu (or other components of the Pu LaBS-B glass) was incorporated in the alteration phases formed as SRL 418 glass specimen (S7) corroded. Figure 25 shows several backscattered electron images of the near-surface region of Pu LaBS-B specimen B7a that were examined. The numbers on the photomicrographs locate regions that were analyzed with EDS. [Note that the window to the EDS detector was covered with a piece of capton tape to protect it from high radiation doses. This effectively attenuated x-rays below about 3 keV, so glass matrix components such as Na, Mg, Al, and Si were not detected. The objective of the EDS analyses was to detect, qualitatively, the presence of Gd, Hf, and Pu in alteration phases. A few spectra were collected after the capton tape was removed.] The EDS results are summarized in Table 11 in terms of the relative peak intensities of the spectra. Figure 25a shows a relatively low magnification view of the cross-sectioned Pu LaBS-B glass specimen, which appears bright in the backscattered electron image. The entire perimeter of the Pu LaBS-B glass specimen was covered with a fairly uniform layer of alteration material about 10 μm thick. The layer is not as bright as the glass in the backscattered electron image, which indicates that it does not contain high atomic weight components. A piece of altered SRL 418 glass specimen S7 is seen in the bottom right corner of Figure 25a (compare with the delaminated top layer in Fig. 23). Neither La, Gd, Hf, nor Pu was detected in this layer (location 2).

The layer around the perimeter of the glass is interrupted by other alteration phases that have distinct morphology; one cluster of phases is located in the box drawn in Figure 25a, and a high-magnification image of the cluster is shown in Figure 25b. The cluster is composed of needle- or lath-like features radiating from a central core. Note that the larger cluster appears to have nucleated on the surface of the Pu LaBS-B glass and became surrounded by the phase that forms the layer. The EDS analyses indicate that the core of the cluster (location 3) contains La and Gd, and the outer regions contain these elements and also Pu. Small amounts of Gd and Hf were detected in the layer (location 4).

Figure 25c shows an area where the Pu LaBS-B glass and the SRL 418 glass were in close proximity and appear to be nearly bridged by alteration phases. A trace of Pu was detected in the bulk of one of the bridging phases (location 6). The material in location 6 was analyzed again after the capton tape covering the detector window had been removed. It contained Na, Al, and Si in ratios that suggested the material is analcime. Note that the material appears much more porous than the cross-sectioned analcime shown in

Table 10. Results of XRD Analyses of Vapor-Reacted SRL 418 Glass

SRL418-150S1		SRL418-200S1		SRL418-200S2		Analcime O PDF#19-1180		Analcime C PDF#41-1478		Analcime P PDF#43-0136	
d-spacing	I%	d-spacing	I%	d-spacing	I%	d-spacing	I%	d-spacing	I%	d-spacing	I%
5.6215	30.9	5.6754	32.1	5.6751	45.9						
5.5937	53.8	5.6029	81.9			5.6000	60.0	5.5901	60.0	5.6048	92.3
5.4341	19.4	5.4182	40.5								
4.8439	14.4							4.8438	11.0		
4.6553	30.1	4.6648	30.3								
4.5607	4.9										
3.4410	26.4										
3.4242	100.0			3.4399	55.2	3.4300	100.0	3.4254	100.0	3.4323	100.0
3.4059	35.3										
3.2772	49.0	3.2786	66.8	3.2758	34.0						
3.0654	2.3			3.0825	8.5					3.0699	0.8
2.9303	27.5			2.9742	11.1						
2.9205	80.5	2.9217	100.0	2.9223	100.0	2.9270	50.0	2.9205	40.0		
		2.7997	7.1	2.7967	15.1						
2.7037	31.5										
2.6890	53.3	2.6906	73.3	2.6880	44.1	2.6930	16.0	2.6875	12.0	2.6925	14.9
2.6789	14.6	2.6792	9.5								
				2.5392	8.1						
2.5027	13.1	2.5040	22.8					2.5007	11.0		
2.3081	55.5	2.3086	77.7	2.3068	43.5						
		2.2934	4.6	2.2354	3.8						
2.2236	8.7			2.2236	16.0			2.2223	9.0	2.2271	5.7
2.1643	1.1					2.1690	2.0				
2.0764	3.6	2.0715	7.0	2.0665	3.7						
				2.0202	3.1						
1.9010	18.0			1.9005	17.2			1.9012	10.0		
1.8099	48.3	1.8094	31.0								
1.8074	72.3	1.8021	33.8	1.8369	10.2					1.8027	0.1
1.7558	24.2										
1.7415	46.4	1.7417	54.2	1.7407	25.5			1.7406	20.0		
1.6455	3.9	1.6459	8.1	1.6618	4.1						
				1.5928	10.3						
1.5529	13.5	1.5530	18.1	1.5521	1.5					1.5545	0.1
		1.4613	11.1	1.5176	13.6					1.4472	1.4
1.4141	10.0	1.4142	13.0	1.4135	10.7			1.4137	5.0		
1.3372	12.6	1.3349	19.3	1.3571	15.6					1.3335	0.1
1.2902	13.5	1.2911	17.7	1.3069	6.6	1.2893	2.0				
1.2846	19.8	1.2848	26.4	1.2841	8.3	1.2855	4.0				
		1.2449	5.5	1.2618	4.0						
1.2215	10.6	1.2215	18.5	1.2211	13.3			1.2290	6.0		
1.1669	5.7	1.1669	5.4	1.1664	3.2			1.1667	2.0		
1.1197	3.6	1.1664	3.2	1.1192	5.3			1.1194	2.0	1.1285	0.3

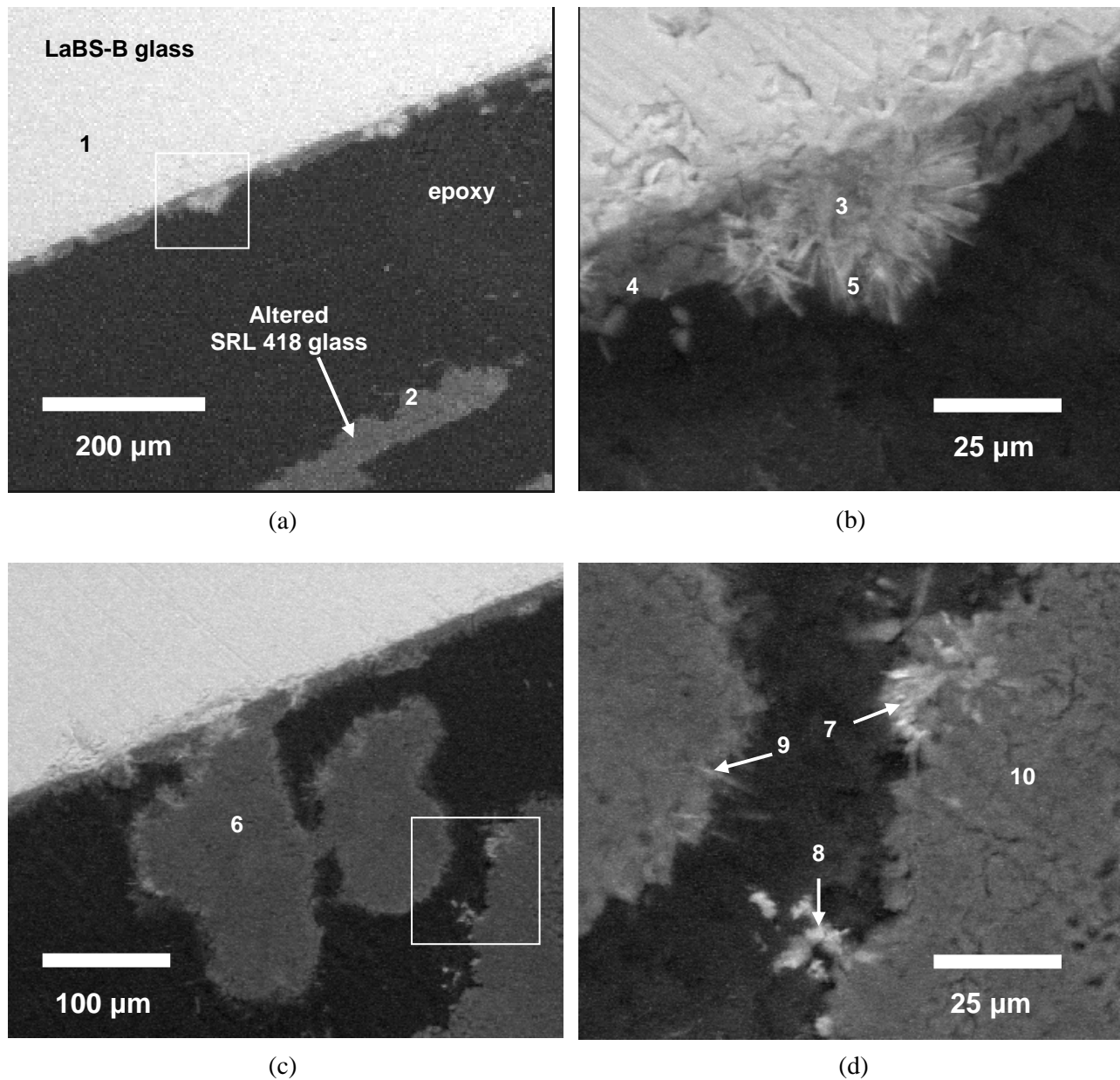


Fig. 25. SEM Photomicrographs of Alteration Phases Formed on Pu LaBS-B Glass Contacted with SRL 418 Glass in VHT at 200 °C: (a) and (b) phases on surface of Pu LaBS-B glass near SRL 418 glass, (c) and (d) phases on surface of altered SRL 418 glass, (e) and (f) phases on back surface of Pu LaBS-B glass contacting SRL 418 glass.

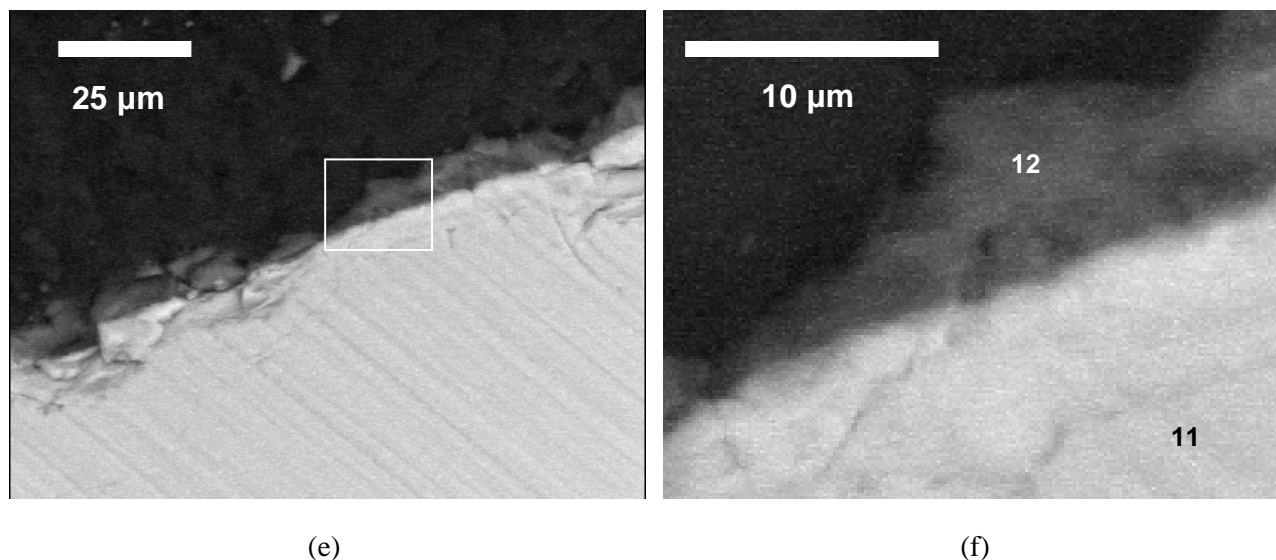


Fig. 25. (cont.)

Figure 24a. The photomicrographs show bright features decorating the perimeters of the bridging phases, which is an indication that the phases contain high atomic weight components. The features in the box drawn in Figure 25c are shown at high magnification in Figure 25d. Small amounts of Gd and Hf (and probably Pu) were detected at locations 7, 8, and 9 in EDS analyses. A trace amount of Pu was detected in the bulk of the alteration phase in location 10. Figures 25e and 25f show the side of the Pu LaBS-B glass specimen B7a that was not contacting the SRL 418 glass. A similar amount of the layer material, but only a few of the bright clusters similar to that shown in Figure 25b, were detected on the side away from the SRL 418 glass. Similar to other locations, La, Gd, and Hf were detected in the layer material on this side of the specimen (location 12). The thickness of the layer is similar on both sides of specimen B7a, which suggests that the amount and composition of the solution was similar on both sides of the specimen. The smaller amounts of bright clusters suggests that the migration of component species released from SRL 418 to the far side of the Pu LaBS-B glass limited the amounts of some phases that formed. The similarity in the amounts of layer on both sides of the specimen suggests that it is formed *in-situ* rather than by precipitation.

Photomicrographs of Pu LaBS-B glass specimen B7b, which was not contacted by SRL 418 glass in the VHT, are shown in Figure 26. [Note that specimen B7b tipped when it was embedded in expoy and was cross-sectioned at an angle of about 60° rather than perpendicular to the surface. This may have obscured the view of the layer on one side of the specimen and enhanced the thickness of the layer on the other side.] Alteration layer was not observed around most of the perimeter (Fig. 26a shows one side of the specimen and Fig. 26b shows the other side), but layer was seen at the end of one side (Fig. 26c) near what was the bottom of the specimen when it hung in the vessel during the test. A few small inclusions that were compositionally similar to the glass were detected in a few locations of the layer (e.g., location 13 in Fig. 26c). These are probably pieces of glass that were displaced during polishing; they are not PuO₂ inclusions. (High magnification images of the glass in the interior of specimen B7b showed a few bright spots similar to what was identified as PuO₂ in Fig. 2.) A relatively large semi-spherical alteration phase was seen in one location of the perimeter of the specimen (Fig. 26d). The composition of the large alteration phase shown in Fig. 26d (location 15) measured with EDS is indistinguishable from that of the underlying glass (location 16), but the contrast in the backscattered electron image indicates that it has a lower average atomic number than the glass. The alteration material appears to continue on the surface,

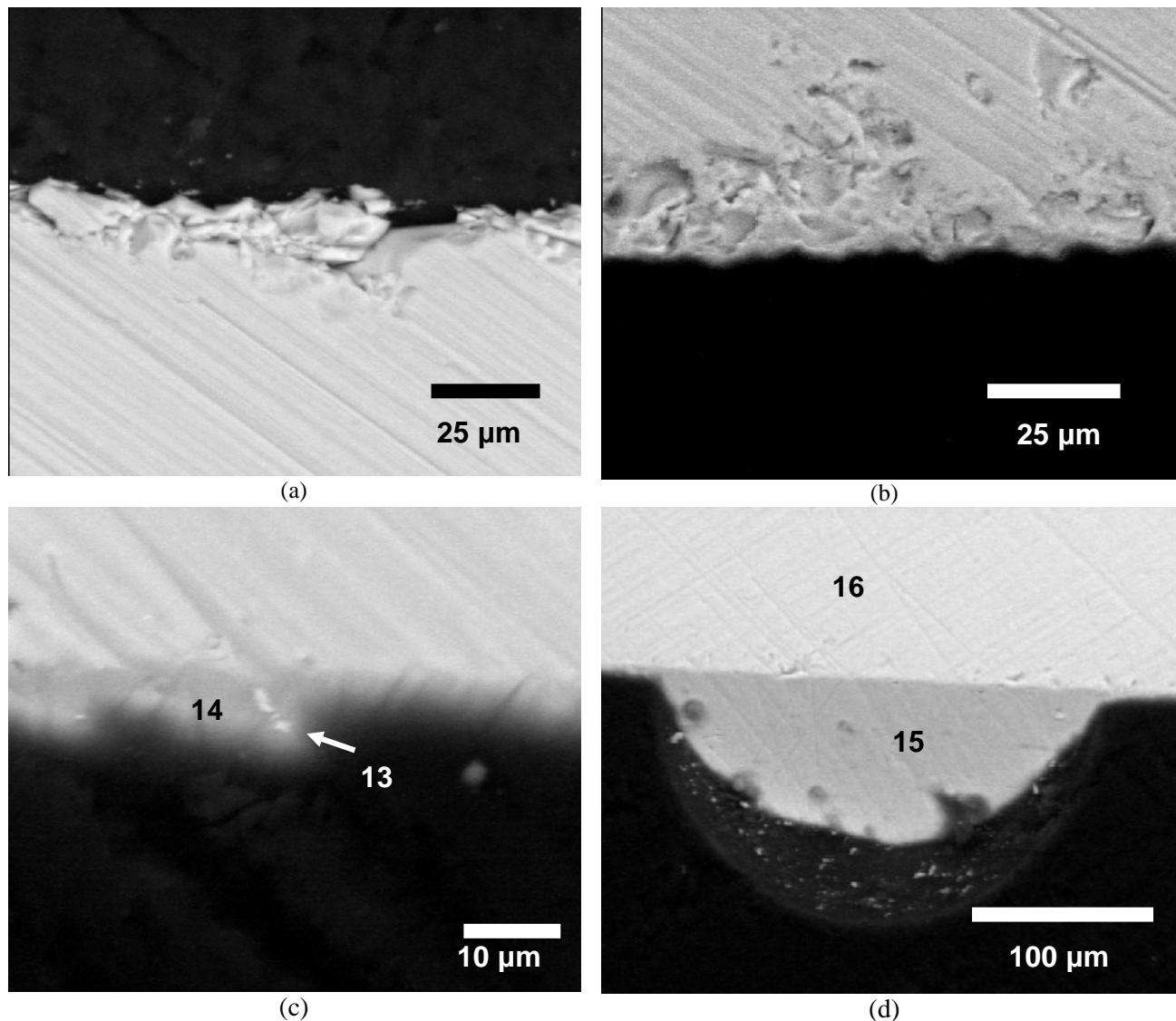


Fig. 26. SEM Photomicrographs of Alteration Phases Formed on Pu LaBS-B Glass Specimen B7b (a) and (b) Regions with No Detectable Layer, (c) Region with Detectable Layer, and (d) Large Alteration Phase.

forming a thin layer on both sides. The origin of the feature in Figure 26d is uncertain. Its composition suggests that it is depleted glass but its size and shape suggest it was precipitated from solution, since the specimen faces had been polished flat prior to testing. The smooth interface between this feature and the underlying glass suggests that it is not a reacted fine left on the specimen.

These results indicate that the presence of Pu LaBS glass and HLW glass in the same system will affect the corrosion behavior of both glasses and will result in commingling of released components in the alteration phases. Degradation of the much less durable SRL 418 glass (1) generated a high pH environment (probably pH 11 or higher) that promoted the dissolution of Pu LaBS-B glass and (2) led to the formation of alteration phases that either incorporated Gd, Hf, and/or Pu into their structure (phases that form during degradation of SRL 418 glass itself) or provided a solution chemistry that was conducive

Table 11. Summary of EDS Results, in relative peak intensity

Spectrum No.	Ca ^a	Fe ^a	La	Gd	Hf	Pu
1 ^b		trace	major	major	major	minor
2		trace				
3	major	trace	minor	minor		
4		trace		minor	trace	
5	minor		minor	minor		trace
6						trace
7		trace			trace	
8		trace			trace	
9	minor			trace	trace	
10	minor					
11 ^b		trace	major	major	major	minor
12			minor	minor	minor	
13						
14						
15		trace	major	major	major	minor

^aReleased from SRL 418 glass.

^bSpectrum of unreacted Pu LaBS-B glass.

to the formation of other phases bearing those elements. It is not clear whether the uniform layer observed on Pu LaBS-B glass surface was formed *in situ* as the glass degraded or is material from dissolved SRL 418 glass that precipitated from solution onto the LaBS glass. The orientation of the clusters adjacent to the Pu LaBS-B glass and their being surrounded by the layer (e.g., as shown in Fig. 25b) suggests that the layer and cluster grew simultaneously and that the layer was not precipitated—that is, layer material is not seen overlaying the cluster. The relative abundance of Gd, Hf, and Pu detected in alteration phases (both in clusters on the Pu LaBS-B glass and in phases decorating altered SRL 418 phases) suggests that a significant amount of Pu LaBS-B glass has dissolved (enough to form an approximately 10- μ m-thick residual layer). However, it is expected that if the observed layer is altered Pu LaBS-B glass, some residual PuO₂ inclusion phases would be observed; none were observed in the layer. It is important to note that, although the SEM examination was not exhaustively thorough, no features resembling PuO₂ crystallites were detected within or among the alteration phases. All of the Pu that was detected was incorporated in other phases.

Finally, in an earlier discussion relating the solution results to the estimated reaction depth (Eq. 39), it was estimated that the immersion test at 120 °C resulted in the formation of a layer about 6.4 μ m thick after 56 days. This was in a fairly dilute solution in which the value of the affinity term was probably fairly high. Considering that the higher temperature and pH in the VHT will accelerate the dissolution while the much more concentrated solution (much lower value of the affinity term) will slow the dissolution, the formation of a layer about 10 μ m thick in a VHT conducted at 200 °C for 24 days is reasonable. More detailed analysis of the layer (e.g., determination of the layer composition) would provide needed insight to better understand the origin of the layer and other alteration phases. Nevertheless, the examinations completed within the time constraints of this activity clearly show the importance of studying the impact of a HLW glass on the corrosion behavior of LaBS glass and the disposition of released Gd, Hf, and Pu.

5. ADDITIONAL COMMENTS

5.1 HOMOGENEITY OF PU LABS-B GLASS

The presence of PuO_2 inclusions can lead to additional uncertainties in the interpretation of the test results. A nonuniform distribution in the glass will lead to different amounts of PuO_2 and glass in aliquots dissolved to measure the glass composition and different amounts exposed at the surface of the test specimens. Analyses of Pu LaBS-B glass made in crucibles at SRNL showed the PuO_2 inclusions to be highly localized in clusters. Similar clustering was not observed in the glass provided to Argonne (although only a few samples were examined). This may be due to additional mixing that occurred when the molten glass was poured from a crucible into the mold used to form the bar. Coupons were cut from the bar to be as consistent as possible with regard to the regions of glass included in each specimen. That is, the bar was cut longitudinally from top to bottom (or bottom to top) and then wafered so that all specimens would contain glass from the bottom of the bar where the PuO_2 inclusions may have accumulated, the top where it may be depleted, and one side. This was done so that the geometric surface area would be proportional to the fraction of inclusions exposed at the surface, and would be nearly the same for all specimens. This was important with regard to assuming that the releases of B and Si are representative of the glass, as are the releases of Gd, Hf, and Pu. That is, differences in the amounts released due to differences in how much glass is exposed at the surface of the specimen could be misconstrued as difference in dissolution rate. While the heterogeneity of the glass probably adds to the scatter in the data, it is presumed not to be significant based on the observed uniformity of the glass that was examined.

5.2 LEACHANT SOLUTIONS

The Si concentrations in some of the leachant solutions used in these tests were too high. It is not known if this is due to Si in the chemicals used to make the leachant solutions or possible external contamination. This did not affect the reliability of the dissolution rates that were extracted from each set of tests (i.e., at a particular temperature and pH) since the same background concentration was used for all tests. However, it may have added uncertainty to the temperature dependence since the Si concentrations measured in the same leachant solution in tests conducted at different temperatures were different. (This suggests external contamination in those cases.) The background Si concentrations are summarized in Table 12. The variation with temperature is most significant in the acidic leachants. Another contributor to the scatter in the background concentrations is small variations in the day-to-day performance of the ICP-MS, even though the same standard solutions were used to calibrate the instrument every day. It was for this reason that the solutions from each test series were analyzed in the same batch of specimens, with the instrument in the same calibration setting. The limits of quantitation for each analyte (expressed as the detection limit in the tables) are determined when the instrument is calibrated before each set of specimen from replicate analyses of demineralized water that has been acidified and spiked with internal standards like the test solutions. As seen for Leachant 6 in Table 12, the variation in the limit of quantitation is small, but significant in the present tests when the extent of dissolution is determined as the small difference between two large numbers.

The leachant solution compositions used to impose the initial pH were selected from mixtures cited in literature publications. While most solutions appeared to remain stable, Leachant 5 (target pH 10) was noticeably unstable in the first series of tests. It was acceptably stable in the repeated series (MLB5R), in which case the tests were conducted within a few days after the leachant was prepared. The stability of the leachant solutions should be checked before tests are started, and an additional short-term blank test should be conducted in parallel with the tests with glass.

Table 12. Si Concentrations Measured in Blank Tests Conducted at Different Temperatures, in $\mu\text{g/L}$

Test Temp., $^{\circ}\text{C}$	Leachant Number					
	1	2	3	4	5	6
40	669	124	76.8 ^a	285 ^a	<9	21.3 ^a
70	850	106	141	252	<9	<17
90	2200	280	127	326	<9	<9

^aFrom reanalysis of the blank test solution without dilution.

5.3 DISSOLUTION RATES COMPARED WITH DEFENSE HLW GLASS DEGRADATION MODEL

The dissolution rates were estimated by linear regression of the test results (essentially the Si concentration) over the test duration with the purpose of determining the pH and temperature dependences, even though the dissolution rates slowed slightly with time as the Si concentration increases. This approach presumes that the effect of the affinity term is negligible compared with the uncertainties in the pH and temperature dependencies (and the measured Si concentrations), and the test conditions of low S/V ratios and short test durations were selected with this intended purpose. The verification of this assumption is addressed in Section 3.5 by comparing the extents of reaction measured under particular test conditions with the extents predicted based on the extracted pH and temperature dependencies. With the current lack of knowledge regarding the value of K in the affinity term, we believe this approach is adequate for the present purpose of comparing Pu LaBS-B glass dissolution with the Defense HLW Glass Degradation Model. Further testing is needed to determine the value of K for Pu LaBS-B glass.

Direct comparison of the measured dissolution rates of Pu LaBS-B glass with the forward rates calculated in the development of the Defense HLW Glass Degradation Model at the same temperature and pH (see Fig. 8) shows that the forward rates used to develop the Model provide an upper bound to each of the rates measured for Pu LaBS-B glass. We emphasize that the forward rates used to determine the pH and temperature dependence used in the Model and used for the present comparison were determined from immersion tests with SRL 202G glass conducted under very similar conditions to those used in this work with Pu LaBS-B glass. The testing and analysis uncertainties are similar in both sets of tests. The results of tests with Pu LaBS-B glass are expected to be less affected by the Si that dissolved during the tests than those with SRL 202G glass, so the rates are expected to be closer to the forward rates.

The Defense HLW Glass Degradation Model provides a rate for use in TSPA calculations predicted to occur under anticipated repository conditions, including a significant impact of the affinity term. The maximum slowing effect of the affinity term is estimated to be the same as the integrated effect over a 7-day PCT at 90 $^{\circ}\text{C}$. In that test, glass is contacted initially by demineralized water so the value of the affinity term is initially 1. The solution pH changes (it usually increases) as the glass dissolves and the value of the affinity term decreases as dissolved components accumulate in the solution. Because the affinity term affects the release of Si more than the release of B initially, the Model uses the release of B to represent the extent of HLW glass dissolution in the PCT. As the affinity term becomes more significant, the release of B from Pu LaBS-B glass also occurs faster than the release of Si; this is seen in the results of the PCTs (see Fig. 15).

In the immersion tests, the dissolution rates based on the release of Si are consistently higher than the rates based on the release of B. This provides added confidence that the dissolution is not being slowed significantly by the affinity term.

5.4 MODEL COEFFICIENT VALUES

The model coefficient values η and E_a determined for Pu LaBS-B glass are compared with the values in the Defense HLW Glass Degradation Model and with values determined for other glasses in Table 13. Notice first the sizeable ranges in both η and E_a for different glass compositions. As alluded to earlier, the values η and E_a must be used together because they capture uncertainties in the regression and possible cross terms (i.e., some of the effect of temperature may be contained in the value of η and visa versa). The value of E_a for the alkaline leg of Pu LaBS-B glass determined from the Si release is much lower than the values for other glasses. Since the same reaction step is thought to lead to the release of Si from all glasses (see Section 1.1), the activation energies are expected to be similar.

Table 13. Comparison of Model Coefficient Values η and E_a Measured for Various Glasses

Glass	Element	Temperature, °C	η	E_a , kJ/mol	Reference
Acidic Solutions					
SRL 202G ^a	B	40, 70, 90	-0.49	31	BSC 2004
CSG ^b	Si	25, 50, 70	-0.70	60	Knauss et al. 1990
MW ^c	Si	30, 50, 70, 90	-0.43	32	Abratis et al. 2000
Binder Glass ^d	Si	40, 70, 90	-0.36	72	Fanning et al. 2003
Pu LaBS-B glass	Si	40, 70, 90	-0.56	40.5	This work
Pu LaBS-B glass	B	40, 70, 90	-0.66	48.9	This work
Alkaline Solutions					
SRL 202G ^a	B	40, 70, 90	0.49	69	BSC 2004
CSG ^b	Si	25, 50, 70	0.49	85	Knauss et al. 1990
MW ^c	Si	30, 50, 70, 90	0.43	56	Abratis et al. 2000
Binder Glass ^d	Si	40, 70, 90	0.64	83	Fanning et al. 2003
LD6-5412 ^e	Si	20, 40, 70, 90	0.40	75	McGrail et al. 1997
R7T7 ^f	B	90	—	59	Delage and Dussossoy 1991
R7T7 ^f	B	90	0.39	—	Gin et al. 1994
Pu LaBS-B glass	Si	40, 70, 90	0.38	25.0	This work
Pu LaBS-B glass	B	40, 70, 90	0.58	51.2	This work

^aGlass used to determine the values of η and E_a used in the Defense HLW Glass Degradation Model.

^bSimple 5-component glass used to simulate HLW glass.

^cGlass developed for Magnox waste.

^dGlass used to microencapsulate sodalite in glass-bonded ceramic waste form.

^eSurrogate waste glass for Hanford low-activity waste.

^fSurrogate waste form for French HLW.

The pH dependencies are expected to be more sensitive to the glass composition. The pH dependence of the glass dissolution rate is not understood mechanistically. Qualitatively, the reaction in Equation 1a can be written with hydroxide as the nucleophile rather than water to yield a dissociated surface hydroxyl group (the surface hydroxide is more acidic than orthosilicic acid). The pH will also affect other reactions that occur simultaneously with the hydrolysis of Si–O bonds, such as ion-exchange reactions to release alkali metals and alkaline earth elements. These other reactions will have a secondary effect on the degradation of the silicate matrix.

The deconvolution of the measured rates into terms to represent the pH and temperature dependencies is affected by the uncertainty in the test data. From the method used in this report (see Section 3.2), the value of E_a used to model the temperature dependence is strongly affected by the value of η that is determined from the pH dependence of the test results. Error in the value of η that is extracted due to

uncertainty in the experimentally measured rates will lead to error in the value of E_a . However, the errors in η and E_a effectively cancel when the rate is calculated, and the range of calculated rates reflects the uncertainty in the test results. Therefore, some of the variance in the values of η and E_a for different glasses in Table 13 is due to errors introduced during the deconvolution, and direct comparison of the individual values η and E_a should be done with that understanding.

5.5 EFFECT OF HLW GLASS ON LABS GLASS DISSOLUTION

The SRL 418 glass was intended to represent the effects of HLW glass dissolution on the dissolution behavior of LaBS glass and simulate the solution chemistry of groundwater in a breached waste package. Contact with SRL 418 glass in the VHTs had little visible effect on the extent of Pu LaBS-B glass corrosion, but did affect the alteration phases that were formed. The pH values of the solutions contacting the Pu LaBS-B glass were not measured, but probably attained pH values similar to the solutions generated in VHTs conducted with only SRL 418 glass, which was about pH 11. The durability of the Pu LaBS-B glass contacted by these highly alkaline solutions is consistent with the much lower dissolution rate predicted for Pu LaBS-B glass compared with the HLW glass degradation model (see Fig. 12). The VHTs show that the SRL 418 glass composition is highly susceptible to accelerated dissolution after alteration phases form (since the glass is completely altered within a few weeks in VHTs at 200 °C). It is believed that the formation of analcime (and perhaps other phases) provides a demand for Na, Al, and Si that promotes dissolution of the SRL 418 glass. However, the formation of analcime does not result in and enhancement in the dissolution of Pu LaBS-B glass to the same extent. This is because the maximum possible dissolution rate of the Pu LaBS-B glass (i.e., the forward rate measured in the immersion tests) is significantly lower than that of SRL 418 glass. For example, the forward rate of Pu LaBS-B glass was measured to be about 0.568 g/(m²d) at pH 10.87 and 90 °C (from Table 5), whereas the forward rate of HLW glasses used in the Defense HLW Glass Degradation Model (and probably SRL 418) is calculated to be 16.8 g/(m²d) at pH 10.87 (using Eq. 10d). A similar difference is expected at 200 °C.

The results of the 7-day PCT with Pu LaBS-B glass provides added insight when compared with the results of PCT conducted with HLW glasses. In 7-day PCT, surrogate HLW glasses typically drive the solution pH to pH 10 or higher, and attain NL(B) values near 0.3 g/m². The 7-day PCT with Pu LaBS-B glass conducted at SRNL gave a pH of 7.2 and NL(B) = 0.012 g/m². The lack of alkali metals in the Pu LaBS-B glass prevents the pH rise seen in PCTs with other HLW glasses, and is one reason why the dissolution rate in the PCT is lower than that of other HLW glasses. For example, a pH dependence of $\eta = 0.5$ with an increase of 3 pH units gives a predicted increase in the dissolution rate of about 30X, which is similar to the observed difference in the 7-day PCT average dissolution rates. Even with the smaller pH dependence of $\eta = 0.38$ determined from the Si release, an increase of 3 pH units corresponds to an increase of about 15X in the dissolution rate. This implies that the intrinsic dissolution rate of Pu LaBS-B glass is about 15X lower than HLW glasses. This is consistent with the different durabilities observed in the VHTs of Pu LaBS-B glass and SRL 418 glass, which also supports the weaker pH dependence of the Pu LaBS-B glass dissolution rate compared with HLW glasses.

From the VHTs conducted with Pu LaBS-B glass and SRL 418 glass in contact, the most significant difference is the formation of Pu-bearing alteration phases that decorate the surfaces of alteration phases formed by SRL 418 glass degradation. Although more analyses are needed to identify the phases that form, the Pu-bearing phases appear to be composed primarily of components released from the SRL 418 glass (e.g., Ca and Si) and cover the surfaces of what appear to be analcime and clay phases formed during the degradation of the SRL 418 glass. It appears that, in the VHTs, the SRL 418 glass is rapidly converted to alteration phases that control the chemistry of the solution contacting the Pu LaBS-B glass, and that (1) phases that sequester Pu, Gd, and Hf can precipitate from that solution and (2) dissolved Pu, Gd, and Hf can sorb onto phases that form as SRL 418 corrodes. In summary, the corrosion behavior of Pu LaBS

glass should be measured in the presence of the HLW glass that will be used to encapsulate it to provide repository-relevant solution chemistries and assemblages of alteration phases.

5.6 RECOMMENDATIONS FOR FURTHER WORK

It is expected that a similar suite of tests will be conducted with a Pu-bearing glass made with Frit X, which was developed to better accommodate Pu (to dissolve more Pu in the glass and have fewer residual PuO₂ inclusions). Insights gained from the present study with Pu LaBS-B glass should be addressed in the test plan for Pu LaBS-X glass to provide a more complete data base to evaluate the suitability of this waste form for disposal.

To the extent possible, glass(es) made for testing should be subjected to the thermal conditions expected during production of the can-in-canister waste form. A thorough examination of the resulting glass is needed to determine (1) the spatial distribution of inclusion phases that may form, including PuO₂, and (2) the relative amounts of Pu in the inclusion phases and dissolved in the glass. The glass(es) should be mixed as well as possible to provide a uniform spatial distribution of inclusion phases (if any are present), at least on the scale of the test sample size. The glass composition should be based on analyses of several samples of glass (5 samples are recommended) because the distribution of Pu-bearing inclusions may not be homogeneous on the scale of the analyzed sample (e.g., typically 50 – 100 mg). Variance in the relative amounts of inclusions will affect the determinations of other component concentrations, including those used to determine the glass dissolution rate (usually B and Si).

The test matrix used to determine the pH and temperature dependence of a Pu LaBS-X glass should include tests for longer durations, particularly at 40 °C. The Pu LaBS-B glass was about 10X more durable than HLW glasses in alkaline solutions, so higher Si solution concentrations could have been reached before feedback effects became significant. Additional long-term tests at 90 °C would allow a better estimate of the Si saturation concentration (which is used as the value of K in the affinity term) to be determined from the rollover in NL(Si) with increasing test duration.

In the present study, tests were conducted at only 3 pH values to estimate the pH dependence in acid and alkaline solutions. Although these were sufficient to show the dissolution of Pu LaBS-B glass to be consistent with the V-shape pH dependence and Arrhenius temperature dependence in the Defense HLW Glass Degradation Model, tests at more pH and temperature values will provide more reliable values of η and E_a .

Long-term PCTs should be conducted at 40, 70, and 90 °C to measure the apparent Si solubility limits and provide data that could be used to determine values of K in the affinity term. This would allow more complete analysis of the reaction progress in the immersion tests. Tests should be conducted at 2 different S/V ratios to measure the effect of test conditions on the test results. Because the Pu LaBS-B glass was very slow to dissolve and the Pu LaBS-X glass is expected to have a similar chemical durability, tests should be conducted at very high S/V ratios to minimize the amount of glass that has to dissolve to saturate the solution.

The VHTs conducted in this activity showed the importance of studying the corrosion of Pu LaBS glass in solutions generated during the dissolution of the HLW glass that encapsulates it. Similar VHTs should be conducted with Pu LaBS-X glass and SRL 418 glass with the intent of more thorough examinations of the alteration phases than was possible within the time frame of this activity. Particular attention should be given to the fate of PuO₂ inclusions (if they are present in Pu LaBS-X glass) as the glass corrodes. The transport modes for released Pu are expected to be important in the acceptance of LaBS glass waste forms. Other test methods would complement the VHTs in providing insight into glass interactions. For example, a hybrid test with crushed SRL 418 glass and a monolithic specimen of Pu LaBS-X glass would

provide a solution dominated by dissolved SRL 418 and a retrievable specimen of reacted Pu LaBS-X glass for examination. A modified SRL 418 glass could be made without B so that dissolution of the Pu LaBS-X glass could be tracked through solution analyses. This would provide data needed to model glass corrosion corresponding with the observed model of Pu release.

5.7 ESTIMATED IMPACT OF PU LABS GLASS ON HLW INVENTORY USED IN TSPA CALCULATIONS

For TSPA-LA calculations, the radionuclide inventories in various HLW waste forms are averaged to provide a mass per waste package value, based on a total of 3412 co-disposal waste packages (BSC 2005, Table 7-1). The impact of Pu LaBS glass on the inventory used in the calculations is estimated from the total amounts of each isotope in average HLW packages and average packages with Pu LaBS glass. For example, the average ^{239}Pu content of HLW in a co-disposal waste package is 606 g. (Note that co-disposal packages may contain 2, 3, or 5 canisters of HLW glass with 1 or 2 units of DOE spent nuclear fuel.) The total ^{239}Pu content is $606 \text{ g} \times 3412 \text{ co-disposal packages} = 128 \text{ kg}$. The curie content of a waste package with 5 canisters of Pu LaBS glass is estimated to be 4380 or 4530 Ci for immobilization of 7 MT or 13 MT of excess weapons plutonium (Marra and Ebert 2003, Table 9). (This excludes the HLW glass used to encapsulate the Pu LaBS glass, which is taken into account in the HLW glass inventory.) Calculations were done using the LaBS glass inventories for immobilization of 13 MT. Because the radionuclide contents and total number of canisters have not been established; these calculations are intended to provide a qualitative estimation of the impact of Pu LaBS glass on the TSPA-LA inventory. Because approximately 800 canisters of HLW with embedded Pu LaBS glass could be made, these calculations assume 160 waste packages contain Pu LaBS glass. The total ^{239}Pu content of the Pu LaBS glass is 725 kCi, which is more than 5X the amount in all of the other HLW waste forms. The revised average ^{239}Pu content for all HLW in the repository would be the sum of the content in HLW (from BSC 2005) plus that in Pu LaBS glass, divided by 3570 total packages; this is 3850 g/package. The amounts of other plutonium isotopes in Pu LaBS glass are compared with the total amounts assumed to be present in other HLW waste forms for TSPA-LA calculations in Table 14. As seen in the table, the Pu LaBS glass will increase the inventories of Pu isotopes that should be used in TSPA calculations by as much as a factor of 2. Further discussion regarding the impact of Pu LaBS glass is provided elsewhere (Marra et al. 2005).

Table 14. Impact of the Estimated Plutonium Content in Pu LaBS Glass on TSPA-LA Inventory

	HLW			LaBS Glass		Revised Total HLW	
	g/package	Ci/package	Ci in 3412 packages	Ci/package	Ci in 160 packages	g/package	% increase
Pu-238	4.24E+01	7.26E+02	2.48E+06	1.23E+03	1.97E+05	4.37E+01	3.0%
Pu-239	6.06E+02	3.76E+01	1.28E+05	4.53E+03	7.25E+05	3.85E+03	84%
Pu-240	5.01E-01	1.14E+01	3.88E+04	1.48E+03	2.37E+05	3.40E+02	100%
Pu-241	1.32E+00	1.36E+02	4.64E+05	2.72E+04	4.35E+06	1.31E+01	90%
Pu-242	4.22E+00	1.66E-02	5.66E+01	5.04E-01	8.06E+01	9.77E+00	57%

6. CONCLUSIONS

- The short-term immersion tests provided an adequate measure of the forward dissolution rate to determine the pH and temperature dependence of Pu LaBS-B glass dissolution rate.
- Direct comparison of the forward dissolution rates of Pu LaBS-B glass over the range of temperatures and pH values relevant to disposal are bounded by the forward rates used to develop the Defense HLW Glass Degradation Model for TSPA calculations.
- The parameter values determined for Pu LaBS-B glass using the immersion test results give predicted dissolution rates that are bounded by the Defense HLW Glass Degradation Model. The equation for the maximum dissolution rate of Pu LaBS-B glass (based on the release of Si) is

$$rate_G = 2.69 \times 10^8 \times 10^{-0.56 pH} \times \exp\left(-40.52/RT\right) + 0.126 \times 10^{0.38 pH} \times \exp\left(-25.03/RT\right) \times \left(1 - [Si]/30\right),$$

where pH is the solution pH measured at room temperature, R is the gas constant, and T is the temperature, in Kelvin.

- The maximum rate of Pu LaBS-B glass dissolution predicted from the above rate equation is bounded by the equation for the maximum rate of HLW glass dissolution used in the Defense HLW Glass Degradation Model over the range of interest.
- Dissolution of Pu LaBS-B glass results in the release of Pu, Gd, and Hf to solution. The relative releases in acidic solutions are Gd > Pu > Hf, and the relative releases in neutral and alkaline solutions are (generally) Pu > Gd ≈ Hf.
- Almost all of the Gd, Hf, and Pu that is released from the glass as it dissolves becomes fixed to steel vessels during the test; only small amounts of Hf and Pu become fixed to Teflon vessels.
- The presence of SRL 418 (a surrogate HLW glass) in VHTs at 120 and 200 °C does not accelerate the degradation of Pu LaBS-B glass to a rate similar to the degradation rate of SRL 418 glass.
- The presence of SRL 418 does promote the formation of Pu-bearing alteration phases (as well as Gd- and Hf-bearing alteration phases).

REFERENCES*

P. Aagaard and H. C. Helgeson, "Thermodynamics and Kinetic Constraints on Reaction Rates Among Minerals and Aqueous Solutions. I. Theoretical Considerations," *American Journal of Science* **282**, 237-285 (1982) TIC: 225516.

P. K. Abraitis, F. R. Livens, J. E. Monteith, J. S., Small, D. P. Trivedi, D. J. Vaughan, and R. A. Wogelius, "The Kinetics and Mechanisms of Simulated British Magnox Waste Glass Dissolution as a Function of pH, Silicic Acid Activity, and Time in Low Temperature Aqueous Systems," *Applied Geochemistry* **15**, 1399-1416 (2000) TIC: 254333.

BSC, "Defense HLW Glass Degradation Model," Bechtel SAIC Company report ANL-EBS-MD-000016, Rev 02 (2004).

BSC 2005, "Initial Radionuclide Inventories," Bechtel SAIC Company report ANL-WIS-MD-000020, Rev. 01 (issue date September 2004 with ACN-001 dated 09/27/2005) (2005).

F. Delage and J. L. Dussossoy, "R7T7 Glass Initial Dissolution Rate Measurements Using a High-Temperature Soxhlet Device," *Material Research Society Symposium Proceedings* **212**, 41-47 (1991) TIC: 203656.

T. H. Fanning, W. L. Ebert, S. M. Frank, M. C. Hash, E. E. Morris, L. R. Morss, T. P. O'Holleran, and R. A. Wigeland, "Status of Ceramic Waste Form Degradation and Radionuclide Release Modeling," Argonne National Laboratory report ANL-03/8 (2003). TIC: 254324.

S. Gin, N. Godon, J. P. Mestre, E. Y. Vernaz, and D. Beaufort, "Experimental Investigation of Aqueous Corrosion of R7T7 Nuclear Glass at 90C in the Presence of Organic Species," *Applied Geochemistry* **9**, 255-269 (1994) TIC: 254470.

B. Grambow, "A General Rate Equation for Nuclear Waste Glass Corrosion," *Material Research Society Symposium Proceedings* **44**, 15-24 (1985) TIC: 203665.

K. G. Knauss, W. L. Bourcier, K. D. McKeegan, C. I. Merzbacher, S. N. Nguyen, F. J. Ryerson, D. K. Smith, and H. C. Weed, H.C. 1990. "Dissolution Kinetics of a Simple Analogue Nuclear Waste Glass as a Function of pH, Time, and Temperature," *Material Research Society Symposium Proceedings* **176**, 371-381 (1990) TIC: 203658.

A. C. Lasaga and G. V. Gibbs, "*Ab-Initio* Quantum Mechanical Calculations of Water-Rock Interactions: Adsorption and Hydrolysis Reactions," *American Journal of Science* **290**, 263-295 (1990) TIC: 236214.

J. C. Marra and W. L. Ebert, "Accounting for a Vitrified Plutonium Waste Form in the Yucca Mountain Repository Total System Performance Assessment (TSPA)," Savannah River National Laboratory report WSRC-TR-2003-00530 (2003).

J. C. Marra, M. K. Hackney, and R. E. Claxton, "Vitrified Plutonium Waste Form Data for Yucca Mountain License Application," Savannah River National Laboratory report WSRC-TR-00125 (2005).

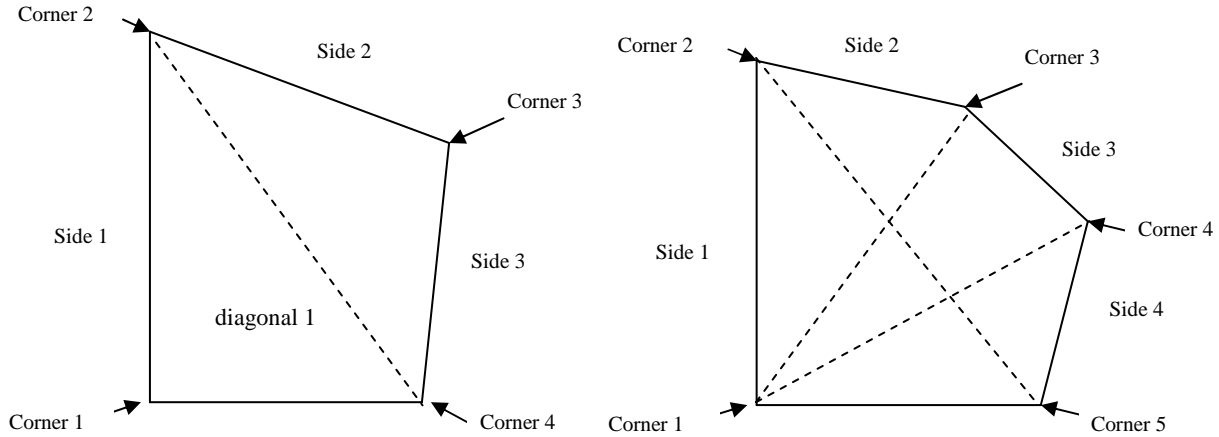
*The TIC number provided at the end of some references refers to the entry number for that publication in the BSC technical information data base.

J. C. Marra, C. L. Crawford, and N. E. Bibler, "Glass Fabrication and Product Consistency Testing of Lanthanide Borosilicate Frit B Composition for Plutonium Disposition," Savannah River National Laboratory report WSRC-TR-00033 (2006).

B.P. McGrail, W. L. Ebert, A. J. Bakel, and D. K. Peeler, "Measurement of Kinetic Rate Law Parameters on a Na-Ca-Al Borosilicate Glass for Low-Activity Waste," Journal of Nuclear Material **249**, 175-189 (1997) TIC: 246080.

APPENDIX A: GLASS TEST SPECIMENS

The dimensions of the Pu LaBS-B glass test specimens used in immersion tests were measured with a caliper that was calibrated in inches. The layouts of the 4- and 5-sided specimens are shown below. The thicknesses were measured at all corners of the 4- or 5-sided specimens, and the lengths of all the sides and 1 or 2 diagonals were measured. The diagonals between corners 2 and 4 were measured for all 4-sided specimens and the diagonals between corners 2 and 5 were measured for 5-sided specimens. These are listed in Table A1 under the column *Length diagonal 1*. The diagonals between corners 1 and 2 or between corners 2 and 5 were also measured for all 5-sided specimens, depending on the shape of the specimen. These are listed in Table A1 under the column *Length diagonal 2*.



The area of side 1 is calculated as

$$area\ side\ 1 = length\ side\ 1 \times \left(\frac{thickness\ corner\ 1 - thickness\ corner\ 2}{2} \right). \quad (A-1)$$

Likewise, the area of side 2 is calculated as the length of side 2 times the average of the thicknesses of corners 2 and 3. The total area of the side is simply the sum of the areas for the 4 or 5 sides. The area in $in.^2$ is multiplied by $(2.54\ cm/in.)^2$ to convert to area in cm^2 .

The area of the face was determined by weighing a scaled drawing of the measured specimen dimensions and converting the mass to area using the relationship

$$scaled\ area = \frac{(mass + 0.00873)}{0.00785}.$$

To convert to cm^2 , the scaled area was multiplied by the factor

$$(2.54\ cm/inch \div 20\ scaled\ units/inch)^2 = 0.01613\ cm^2/scaled\ unit^2.$$

The total area was calculated as the sum of the areas of the 4 or 5 sides and 2 times the area of the face. The measured dimensions and masses and the calculated areas for the specimens used in immersion tests are compiled in Table A1.

The results of glass composition analyses are compiled in Table A2 for Frit X glass, Table A3 for SRL 418 glass, and Table A4 for Pu LaBS-B glass. Three samples of the Frit X and SRL 418 glasses and 2 samples of the Pu LaBS-B glass were dissolved and analyzed. The concentrations of each analyte measured with ICP-MS are given in units of g/L (parts per billion, ppb). The mass percent of that element in the glass is calculated as

$$\text{mass \%} = \text{measured solution concentration, } \mu\text{g} / \text{L} \times \left(\frac{\text{solution volume, mL}}{\text{glass mass, } \mu\text{g}} \right),$$

where the measured solution concentration is multiplied by the quotient of the dissolved sample volume and the mass dissolved. The oxide mass% is calculated by dividing the elemental mass% by the mass fraction of the element in its oxide (Fe as Fe₂O₃). For example,

$$\text{mass\% } Al_2O_3 = \text{mass\% } Al \times \left(\frac{101.96 \text{ g } Al_2O_3}{53.96 \text{ g } Al} \right).$$

The oxide mass% is normalized to 100% by multiplying the

$$\text{normalized oxide mass\%} = \text{measured oxide mass\%} \times \left(\frac{100}{\text{total measured oxide mass\%}} \right).$$

The normalized elemental mass% is calculated by multiplying the normalized oxide mass% by the mass fraction for each element in its oxide.

Table A1. Measured Dimensions of Monolithic Pu-LaBS-B Glass Test Specimens

Specimen Number	Thickness corner 1, inches	Thickness corner 2, inches	Thickness corner 3, inches	Thickness corner 4, inches	Thickness corner 5, inches	Length side 1, inches	Length side 2, inches	Length side 3, inches	Length side 4, inches	Length side 5, inches
1	0.0285	0.0335	0.0315	0.0270	—	0.4470	0.3105	0.4140	0.2360	—
2	0.0265	0.0305	0.0285	0.0275	—	0.4520	0.2985	0.3935	0.2425	—
3	0.0285	0.0265	0.0280	0.0315	—	0.3700	0.2810	0.3330	0.2545	—
4	0.0255	0.0315	0.0330	0.0275	—	0.4520	0.3335	0.3890	0.2565	—
5	0.0245	0.0300	0.0270	0.0260	—	0.4470	0.3275	0.3395	0.2685	—
6	0.0335	0.0290	0.0300	0.0320	—	0.2970	0.2935	0.3110	0.2510	—
7	0.0270	0.0315	0.0300	0.0270	—	0.4505	0.3150	0.4050	0.2330	—
8	0.0335	0.0290	0.0305	0.0340	0.0315	0.3980	0.1370	0.2295	0.2325	0.2530
9	0.0300	0.0345	0.0345	0.0315	—	0.3705	0.3315	0.3215	0.2445	—
10	0.0455	0.0575	0.0510	0.0420	—	0.4140	0.3255	0.3545	0.2820	—
11	0.0135	0.0220	0.0165	0.0165	—	0.4070	0.2905	0.2535	0.2460	—
12	0.0285	0.0320	0.0335	0.0325	0.0315	0.4300	0.1815	0.1645	0.2470	0.2690
13	0.0255	0.0230	0.0295	0.0315	0.0305	0.3785	0.1020	0.2470	0.2270	0.2455
14	0.0245	0.0230	0.0235	0.0230	—	0.3975	0.3475	0.2215	0.2765	—
15	0.0250	0.0130	0.0150	0.0160	—	0.3670	0.2315	0.2355	0.3335	—
16	0.0220	0.0180	0.0150	0.0165	—	0.4075	0.3100	0.1865	0.2730	—
17	0.0335	0.0390	0.0380	0.0330	—	0.3695	0.2850	0.2295	0.2345	—
18	0.0275	0.0250	0.0240	0.0245	—	0.3585	0.2705	0.2760	0.2760	—
19	0.0300	0.0410	0.0380	0.0350	—	0.4335	0.3195	0.3955	0.2745	—
20	0.0255	0.0240	0.0280	0.0270	0.0260	0.4057	0.2685	0.0760	0.2345	0.2760
21	0.0315	0.0285	0.0315	0.0300	—	0.3330	0.2800	0.3115	0.3060	—
22	0.0180	0.0225	0.0230	0.0170	—	0.3875	0.3200	0.2480	0.2830	—
23	0.0115	0.0205	0.0250	0.0245	0.0215	0.4355	0.1590	0.2320	0.2055	0.2180
24	0.0295	0.0355	0.0315	0.0315	—	0.4250	0.3245	0.3700	0.2685	—
25	0.0285	0.0285	0.0290	0.0285	—	0.2835	0.1525	0.3290	0.4120	—
26	0.0255	0.0235	0.0270	0.0250	0.0245	0.1390	0.2665	0.2290	0.1400	0.4090
27	0.0360	0.0370	0.0320	0.0325	—	0.4055	0.3150	0.2895	0.2465	—
28	0.0295	0.0345	0.0290	0.0320	—	0.4340	0.2735	0.3940	0.2230	—
29	0.0295	0.0260	0.0240	0.0250	0.0260	0.4035	0.0965	0.2465	0.2025	0.2645
30	0.0260	0.0270	0.0325	0.0320	0.0315	0.3880	0.1640	0.1880	0.2960	0.2475
31	0.0260	0.0310	0.0295	0.0255	—	0.4405	0.2960	0.3740	0.2655	—
32	0.0220	0.0305	0.0305	0.0285	—	0.3600	0.2670	0.2325	0.2490	—
33	0.0295	0.0325	0.0345	0.0320	0.0310	0.4270	0.1950	0.1425	0.3185	0.2660
34	0.0285	0.0300	0.0335	0.0325	—	0.3525	0.2625	0.2405	0.2720	—
35	0.0220	0.0180	0.0205	0.0210	—	0.3650	0.2805	0.2680	0.2805	—
36	0.0350	0.0330	0.0310	0.0310	—	0.4205	0.3055	0.3530	0.2435	—
37	0.0325	0.0325	0.0335	0.0300	—	0.4140	0.2870	0.3035	0.2520	—
38	0.0340	0.0415	0.0440	0.0455	0.0395	0.3995	0.1585	0.1520	0.2410	0.2825
39	0.0285	0.0240	0.0290	0.0325	—	0.4140	0.2935	0.2165	0.2455	—
40	0.0240	0.0245	0.0230	0.0240	—	0.4260	0.2035	0.3350	0.2150	—
41	0.0295	0.0320	0.0310	0.0290	—	0.4350	0.3110	0.2940	0.2600	—
42	0.0260	0.0205	0.0205	0.0235	—	0.3890	0.3360	0.2530	0.2565	—
43	0.0285	0.0295	0.0315	0.0310	0.0305	0.4140	0.1860	0.1445	0.3265	0.2505
44	0.0230	0.0250	0.0250	0.0245	—	0.4200	0.3000	0.4060	0.2130	—
45	0.0195	0.0175	0.0195	0.0240	—	0.3470	0.1675	0.3020	0.2325	—
46	0.0255	0.0285	0.0260	0.0250	0.0250	0.4000	0.2650	0.2495	0.0655	0.2785
47	0.0235	0.0325	0.0315	0.0250	—	0.4020	0.2915	0.3375	0.2580	—
48	0.0260	0.0345	0.0360	0.0345	—	0.4390	0.0665	0.2480	0.2985	—
49	0.0230	0.0215	0.0175	0.0185	—	0.4085	0.2980	0.3410	0.1815	—
50	0.0240	0.0250	0.0305	0.0290	—	0.4175	0.3040	0.2980	0.2370	—
51	0.0175	0.0240	0.0235	0.0200	—	0.3710	0.2945	0.2515	0.2605	—
52	0.0295	0.0325	0.0330	0.0325	0.0265	0.4105	0.1780	0.2180	0.1970	0.3030
53	0.0290	0.0340	0.0345	0.0270	—	0.4280	0.3130	0.3120	0.2675	—
54	0.0255	0.0215	0.0190	0.0190	—	0.2965	0.2785	0.2380	0.2875	—
55	0.0240	0.0240	0.0340	0.0320	—	0.3515	0.2950	0.2725	0.2850	—
56	0.0305	0.0320	0.0310	0.0305	—	0.4115	0.3105	0.3225	0.2555	—
57	0.0270	0.0300	0.0345	0.0320	0.0310	0.4060	0.1230	0.2140	0.2155	0.2905
58	0.0295	0.0325	0.0340	0.0345	0.0305	0.4305	0.1910	0.2030	0.2355	0.2285
59	0.0315	0.0330	0.0335	0.0315	—	0.4040	0.3105	0.2445	0.2565	—
60	0.0290	0.0325	0.0345	0.0345	—	0.4085	0.2090	0.1585	0.2485	—
61	0.0315	0.0330	0.0315	0.0325	0.0325	0.3915	0.2330	0.1305	0.2285	0.2525

Table A1. (cont.)

Specimen Number	Thickness corner 1, inches	Thickness corner 2, inches	Thickness corner 3, inches	Thickness corner 4, inches	Thickness corner 5, inches	Length side 1, inches	Length side 2, inches	Length side 3, inches	Length side 4, inches	Length side 5, inches
62	0.0290	0.0335	0.0325	0.0335	0.0295	0.3285	0.1665	0.1730	0.2795	0.2600
63	0.0290	0.0320	0.0325	0.0290	—	0.4065	0.2945	0.3315	0.2565	—
64	0.0320	0.0305	0.0295	0.0295	—	0.4035	0.2925	0.3285	0.2585	—
65	0.0360	0.0310	0.0230	0.0315	—	0.4020	0.2895	0.3335	0.2525	—
66	0.0350	0.0340	0.0390	0.0405	—	0.4360	0.2860	0.3640	0.2330	—
67	0.0250	0.0335	0.0350	0.0290	—	0.4335	0.2990	0.3690	0.2315	—
68	0.0295	0.0305	0.0305	0.0285	—	0.4375	0.3020	0.3675	0.2470	—
69	0.0285	0.0310	0.0290	0.0290	—	0.4530	0.3060	0.4110	0.2195	—
70	0.0310	0.0270	0.0285	0.0275	—	0.3980	0.2925	0.3320	0.2555	—
71	0.0375	0.0335	0.0305	0.0360	—	0.4430	0.3165	0.4000	0.2600	—
72	0.0320	0.0285	0.0300	0.0315	—	0.4020	0.2965	0.3295	0.2545	—
73	0.0230	0.0280	0.0240	0.0250	—	0.4430	0.3130	0.3740	0.2375	—
74	0.0280	0.0305	0.0295	0.0305	—	0.4490	0.3345	0.3845	0.2370	—
75	0.0290	0.0320	0.0305	0.0300	—	0.4410	0.3110	0.3745	0.2315	—
76	0.0250	0.0250	0.0230	0.0255	—	0.4490	0.3215	0.4080	0.2360	—
77	0.0330	0.0325	0.0285	0.0315	—	0.4430	0.3165	0.3960	0.2630	—
78	0.0300	0.0275	0.0280	0.0300	—	0.4155	0.3080	0.3000	0.2405	—
79	0.0225	0.0300	0.0215	0.0295	—	0.4470	0.3025	0.3945	0.2560	—
80	0.0270	0.0270	0.0275	0.0305	—	0.3670	0.2705	0.3325	0.2545	—
81	0.0265	0.0270	0.0295	0.0300	—	0.4400	0.2990	0.3730	0.2300	—
82	0.0210	0.0305	0.0305	0.0295	—	0.4030	0.2970	0.3160	0.2550	—
83	0.0375	0.0335	0.0360	0.0315	—	0.3500	0.3065	0.2685	0.2855	—
84	0.0335	0.0280	0.0295	0.0300	—	0.3720	0.2880	0.3220	0.2535	—
85	0.0280	0.0310	0.0305	0.0285	—	0.4445	0.3165	0.3895	0.2370	—
86	0.0335	0.0305	0.0280	0.0285	—	0.4525	0.2960	0.4135	0.2095	—
87	0.0305	0.0350	0.0335	0.0315	—	0.4465	0.3230	0.3705	0.2525	—
88	0.0285	0.0285	0.0295	0.0290	—	0.4420	0.3150	0.3875	0.2360	—
89	0.0285	0.0305	0.0280	0.0275	—	0.4465	0.3215	0.3930	0.2550	—
90	0.0220	0.0285	0.0275	0.0225	—	0.3380	0.2950	0.2775	0.2580	—
91	0.0290	0.0305	0.0330	0.0305	0.0290	0.3755	0.1770	0.1770	0.2490	0.2430
92	0.0245	0.0200	0.0190	0.0175	—	0.3600	0.2215	0.2115	0.3050	—
93	0.0210	0.0225	0.0290	0.0230	0.0230	0.3005	0.2215	0.2465	0.0570	0.2715
94	0.0220	0.0230	0.0230	0.0185	—	0.3315	0.3280	0.1615	0.2085	—
95	0.0195	0.0215	0.0240	0.0230	—	0.3580	0.2720	0.1530	0.2715	—
96	0.0185	0.0205	0.0195	0.0250	0.0220	0.1925	0.1590	0.2305	0.1435	0.2545
97	0.0230	0.0240	0.0250	0.0240	0.0230	0.2900	0.2290	0.2295	0.0755	0.2550
98	0.0330	0.0360	0.0310	0.0325	—	0.3280	0.3120	0.2585	0.2815	—
Repolished Specimens										
99	0.0280	0.0325	0.0295	0.0265	—	0.4040	0.3100	0.2845	0.2380	—
100	0.0235	0.0315	0.0335	0.0270	—	0.4355	0.2900	0.3490	0.2300	—
101	0.0245	0.0305	0.0285	0.0250	—	0.4045	0.2910	0.3465	0.2540	—
102	0.0325	0.0305	0.0300	0.0315	—	0.4045	0.2965	0.3260	0.2530	—
103	0.0310	0.0315	0.0260	0.0295	—	0.4445	0.3185	0.3935	0.2630	—
104	0.0295	0.0295	0.0260	0.0270	—	0.4085	0.2945	0.3285	0.2560	—
105	0.0270	0.0285	0.0285	0.0280	—	0.4470	0.3165	0.3880	0.2340	—
106	0.0260	0.0315	0.0295	0.0260	—	0.4345	0.3290	0.2950	0.2535	—
107	0.0195	0.0290	0.0320	0.0275	—	0.3590	0.2805	0.2470	0.2535	—
108	0.0285	0.0325	0.0285	0.0295	—	0.4050	0.3000	0.3155	0.2550	—
109	0.0280	0.0300	0.0290	0.0270	—	0.4540	0.3070	0.4050	0.2315	—
110	0.0295	0.0295	0.0295	0.0300	—	0.4110	0.3010	0.3260	0.2535	—
111	0.0315	0.0355	0.0335	0.0300	—	0.4480	0.3265	0.3730	0.2475	—
112	0.0250	0.0280	0.0320	0.0270	—	0.4440	0.3340	0.3900	0.2565	—
113	0.0240	0.0235	0.0250	0.0260	—	0.4520	0.3205	0.4040	0.2415	—
114	0.0320	0.0310	0.0285	0.0285	—	0.4135	0.2990	0.3405	0.2380	—
115	0.0260	0.0250	0.0290	0.0270	—	0.4390	0.2970	0.3740	0.2330	—
116	0.0275	0.0295	0.0280	0.0280	—	0.4515	0.3015	0.4165	0.2065	—
117	0.0270	0.0285	0.0300	0.2900	—	0.4400	0.3150	0.3795	0.2340	—
118	0.0290	0.0300	0.0295	0.0255	—	0.4415	0.3035	0.3815	0.2405	—
119	0.0220	0.0220	0.0240	0.0225	—	0.4160	0.2990	0.4035	0.2155	—
99R	0.0280	0.0325	0.0340	0.0280	—	0.4040	0.3100	0.2840	0.2470	—

Table A1. (cont.)

Specimen Number	Length diagonal 1, inches	Length diagonal 2, inches	area side 1, inch ²	area side 2, inch ²	area side 3, inch ²	area side 4, inch ²	area side 5, inch ²	Mass paper cut-out, g	area of 1 face, cm ²	Total area, cm ²
1	0.4670	—	0.01386	0.01009	0.01211	0.00655	—	0.3019	0.6382	1.55
2	0.4890	—	0.01288	0.00881	0.01102	0.00655	—	0.3461	0.7291	1.71
3	0.4450	—	0.01018	0.00766	0.00991	0.00764	—	0.2834	0.6002	1.43
4	0.4970	—	0.01288	0.01076	0.01177	0.00680	—	0.3695	0.7771	1.83
5	0.4785	—	0.01218	0.00933	0.00900	0.00678	—	0.3531	0.7434	1.73
6	0.4150	—	0.00928	0.00866	0.00964	0.00822	—	0.2514	0.5345	1.30
7	0.4880	—	0.01318	0.00969	0.01154	0.00629	—	0.3469	0.7307	1.72
8	0.4720	0.3845	0.01244	0.00408	0.00740	0.00761	0.00822	0.2879	0.6095	1.48
9	0.4665	—	0.01195	0.01144	0.01061	0.00752	—	0.3055	0.6456	1.56
10	0.4880	—	0.02132	0.01766	0.01648	0.01234	—	0.3537	0.7447	1.93
11	0.4370	—	0.00722	0.00559	0.00418	0.00369	—	0.2468	0.5250	1.18
12	0.4870	0.4565	0.01301	0.00594	0.00543	0.00790	0.00807	0.2984	0.6310	1.52
13	0.4430	0.3835	0.00918	0.00268	0.00753	0.00704	0.00687	0.2758	0.5846	1.38
14	0.4585	—	0.00944	0.00808	0.00515	0.00657	—	0.2747	0.5823	1.35
15	0.4245	—	0.00697	0.00324	0.00365	0.00684	—	0.2389	0.5088	1.15
16	0.4260	—	0.00815	0.00512	0.00294	0.00526	—	0.2441	0.5195	1.18
17	0.4245	—	0.01339	0.01097	0.00815	0.00780	—	0.2260	0.4823	1.22
18	0.4655	—	0.00941	0.00663	0.00669	0.00718	—	0.2458	0.5230	1.24
19	0.4910	—	0.01539	0.01262	0.01444	0.00892	—	0.3638	0.7654	1.86
20	0.4550	0.3990	0.01004	0.00698	0.00209	0.00621	0.00711	0.2944	0.6228	1.45
21	0.4860	—	0.00999	0.00840	0.00958	0.00941	—	0.2784	0.5900	1.42
22	0.4500	—	0.00785	0.00728	0.00496	0.00495	—	0.2882	0.6101	1.38
23	0.4545	0.4075	0.00697	0.00362	0.00574	0.00473	0.00360	0.2919	0.6177	1.39
24	0.5035	—	0.01381	0.01087	0.01166	0.00819	—	0.3595	0.7566	1.80
25	0.4040	—	0.00808	0.00439	0.00946	0.01174	—	0.2364	0.5037	1.22
26	0.4190	0.4180	0.00341	0.00673	0.00595	0.00347	0.01023	0.2661	0.5647	1.32
27	0.4425	—	0.01480	0.01087	0.00934	0.00844	—	0.2854	0.6043	1.49
28	0.4745	—	0.01389	0.00868	0.01202	0.00686	—	0.3076	0.6499	1.57
29	0.4575	0.4060	0.01120	0.00241	0.00604	0.00516	0.00734	0.2708	0.5743	1.36
30	0.4525	0.4190	0.01028	0.00488	0.00606	0.00940	0.00712	0.3192	0.6738	1.59
31	0.5035	—	0.01255	0.00895	0.01029	0.00684	—	0.3405	0.7175	1.68
32	0.4450	—	0.00945	0.00814	0.00686	0.00629	—	0.2143	0.4582	1.11
33	0.4865	0.4515	0.01324	0.00653	0.00474	0.01003	0.00805	0.3426	0.7219	1.72
34	0.4240	—	0.01031	0.00833	0.00794	0.00830	—	0.2387	0.5084	1.24
35	0.4635	—	0.00730	0.00540	0.00556	0.00603	—	0.2570	0.5460	1.25
36	0.4805	—	0.01430	0.00978	0.01094	0.00804	—	0.3180	0.6713	1.62
37	0.4815	—	0.01346	0.00947	0.00964	0.00788	—	0.2806	0.5945	1.45
38	0.4520	0.4145	0.01508	0.00678	0.00680	0.01024	0.01038	0.2875	0.6086	1.54
39	0.4830	—	0.01087	0.00778	0.00666	0.00749	—	0.2091	0.4476	1.11
40	0.4665	—	0.01033	0.00514	0.00838	0.00516	—	0.2374	0.5057	1.19
41	0.5010	—	0.01338	0.00980	0.00882	0.00761	—	0.3055	0.6456	1.55
42	0.4515	—	0.00904	0.00689	0.00557	0.00635	—	0.3145	0.6641	1.51
43	0.4805	0.4460	0.01201	0.00567	0.00452	0.01004	0.00739	0.3435	0.7237	1.70
44	0.5005	—	0.01008	0.00750	0.01005	0.00506	—	0.3142	0.6635	1.54
45	0.4130	—	0.00642	0.00310	0.00657	0.00506	—	0.1828	0.3935	0.923
46	0.4465	0.3105	0.01080	0.00722	0.00636	0.00090	0.00390	0.3096	0.6541	1.52
47	0.4740	—	0.01126	0.00933	0.00953	0.00626	—	0.3116	0.6582	1.55
48	0.4995	0.4610	0.01328	0.00234	0.00874	0.00978	0.00757	0.3147	0.6645	1.60
49	0.4345	—	0.00909	0.00581	0.00614	0.00377	—	0.2664	0.5653	1.29
50	0.4390	—	0.01023	0.00844	0.00887	0.00628	—	0.2836	0.6006	1.42
51	0.4360	—	0.00770	0.00699	0.00547	0.00488	—	0.2504	0.5324	1.23
52	0.4600	0.4325	0.01273	0.00583	0.00714	0.00581	0.00848	0.2519	0.5355	1.33
53	0.4905	—	0.01348	0.01072	0.00959	0.00749	—	0.3174	0.6701	1.61
54	0.4165	—	0.00697	0.00564	0.00452	0.00640	—	0.2185	0.4669	1.09
55	0.4505	—	0.00844	0.00856	0.00899	0.00798	—	0.2668	0.5661	1.35
56	0.4595	—	0.01286	0.00978	0.00992	0.00779	—	0.3039	0.6423	1.55
57	0.4575	0.4165	0.01157	0.00397	0.00712	0.00679	0.00842	0.2974	0.6290	1.50
58	0.4735	0.4345	0.01335	0.00635	0.00695	0.00765	0.00686	0.3082	0.6512	1.57
59	0.4305	—	0.01303	0.01032	0.00795	0.00808	—	0.2659	0.5643	1.38
60	0.4545	0.4225	0.01256	0.00700	0.00547	0.00820	0.00740	0.3082	0.6512	1.56
61	0.4510	0.4035	0.01263	0.00751	0.00418	0.00743	0.00808	0.2950	0.6241	1.51

Table A1. (cont.)

Specimen Number	Length diagonal 1, inches	Length diagonal 2, inches	area side 1, inch ²	area side 2, inch ²	area side 3, inch ²	area side 4, inch ²	area side 5, inch ²	Mass paper cut-out, g	area of 1 face, cm ²	Total area, cm ²
62	0.4545	0.3515	0.01027	0.00549	0.00571	0.00880	0.00761	0.2785	0.5902	1.42
63	0.4705	—	0.01240	0.00950	0.01019	0.00744	—	0.2990	0.6323	1.52
64	0.4730	—	0.01261	0.00878	0.00969	0.00795	—	0.2918	0.6175	1.49
65	0.4635	—	0.01347	0.00782	0.00909	0.00852	—	0.2891	0.6119	1.47
66	0.4600	—	0.01504	0.01044	0.01447	0.00880	—	0.3072	0.6491	1.61
67	0.4730	—	0.01268	0.01024	0.01181	0.00625	—	0.3210	0.6775	1.62
68	0.4890	—	0.01313	0.00921	0.01084	0.00716	—	0.3230	0.6816	1.62
69	0.4970	—	0.01348	0.00918	0.01192	0.00631	—	0.3386	0.7136	1.69
70	0.4615	—	0.01154	0.00812	0.00930	0.00747	—	0.3012	0.6368	1.51
71	0.5035	—	0.01573	0.01013	0.01330	0.00956	—	0.3637	0.7652	1.84
72	0.4675	—	0.01216	0.00867	0.01013	0.00808	—	0.3017	0.6378	1.53
73	0.4845	—	0.01130	0.00814	0.00916	0.00570	—	0.3028	0.6401	1.50
74	0.5020	—	0.01313	0.01004	0.01154	0.00693	—	0.3422	0.7210	1.71
75	0.4835	—	0.01345	0.00972	0.01133	0.00683	—	0.3166	0.6684	1.60
76	0.5000	—	0.01123	0.00772	0.00989	0.00596	—	0.3514	0.7399	1.70
77	0.5055	—	0.01451	0.00965	0.01188	0.00848	—	0.3627	0.7632	1.81
78	0.4535	—	0.01195	0.00855	0.00870	0.00722	—	0.2769	0.5869	1.41
79	0.5040	—	0.01173	0.00779	0.01006	0.00666	—	0.3468	0.7305	1.69
80	0.4370	—	0.00991	0.00737	0.00964	0.00732	—	0.2722	0.5772	1.38
81	0.4820	—	0.01177	0.00845	0.01110	0.00650	—	0.3163	0.6678	1.58
82	0.4640	—	0.01038	0.00906	0.00948	0.00644	—	0.2961	0.6263	1.48
83	0.4795	—	0.01243	0.01065	0.00906	0.00985	—	0.2677	0.5680	1.41
84	0.4375	—	0.01125	0.00828	0.00958	0.00792	—	0.2792	0.5916	1.42
85	0.4925	—	0.01311	0.00973	0.01149	0.00670	—	0.3440	0.7247	1.71
86	0.4925	—	0.01448	0.00866	0.01168	0.00649	—	0.3243	0.6843	1.64
87	0.4860	—	0.01462	0.01106	0.01204	0.00720	—	0.3280	0.6919	1.68
88	0.4895	—	0.01260	0.00914	0.01133	0.00679	—	0.3360	0.7083	1.67
89	0.5005	—	0.01317	0.00940	0.01091	0.00714	—	0.3516	0.7404	1.74
90	0.4590	—	0.00853	0.00826	0.00694	0.00574	—	0.2443	0.5199	1.23
91	0.4360	0.3880	0.01117	0.00562	0.00562	0.00741	0.00705	0.2829	0.5992	1.44
92	0.3900	—	0.00801	0.00432	0.00386	0.00641	—	0.2143	0.4582	1.06
93	0.2840	0.2720	0.00654	0.00570	0.00641	0.00131	0.00597	0.2146	0.4589	1.09
94	0.4165	—	0.00746	0.00754	0.00335	0.00422	—	0.1715	0.3703	0.886
95	0.3705	—	0.00734	0.00619	0.00360	0.00577	—	0.1904	0.4091	0.966
96	0.3090	0.3185	0.00375	0.00318	0.00513	0.00337	0.00515	0.1921	0.4126	0.958
97	0.4235	not det.	0.00682	0.00561	0.00562	0.00177	0.00587	0.2186	0.4671	1.10
98	0.4050	—	0.01132	0.01045	0.00821	0.00922	—	0.2500	0.5316	1.32
Repolished Specimens										
99	0.4415	—	0.01222	0.00961	0.00797	0.00649	—	0.2730	0.5789	1.39
100	0.4725	—	0.01198	0.00943	0.01056	0.00581	—	0.2977	0.6296	1.50
101	0.4720	—	0.01114	0.00858	0.00927	0.00629	—	0.3020	0.6384	1.50
102	0.4690	—	0.01274	0.00897	0.01002	0.00810	—	0.3005	0.6354	1.53
103	0.5045	—	0.01389	0.00916	0.01092	0.00796	—	0.3683	0.7747	1.82
104	0.4760	—	0.01205	0.00817	0.00871	0.00723	—	0.3027	0.6399	1.51
105	0.4925	—	0.01240	0.00902	0.01096	0.00644	—	0.3405	0.7175	1.69
106	0.4880	—	0.01249	0.01003	0.00819	0.00659	—	0.3263	0.6884	1.62
107	0.4430	—	0.00871	0.00856	0.00735	0.00596	—	0.2304	0.4913	1.18
108	0.4645	—	0.01235	0.00915	0.00915	0.00740	—	0.2936	0.6212	1.49
109	0.4915	—	0.01317	0.00906	0.01134	0.00637	—	0.3438	0.7243	1.71
110	0.4635	—	0.01212	0.00888	0.00970	0.00754	—	0.3200	0.6754	1.60
111	0.4855	—	0.01501	0.01126	0.01184	0.00761	—	0.3466	0.7301	1.76
112	0.5035	—	0.01177	0.01002	0.01151	0.00667	—	0.3634	0.7646	1.79
113	0.4995	—	0.01074	0.00777	0.01030	0.00604	—	0.3551	0.7475	1.72
114	0.4795	—	0.01303	0.00890	0.00970	0.00720	—	0.3011	0.6366	1.52
115	0.4805	—	0.01119	0.00802	0.01047	0.00617	—	0.3150	0.6652	1.56
116	0.4915	—	0.01287	0.00867	0.01166	0.00573	—	0.3263	0.6884	1.63
117	0.4905	—	0.01221	0.00921	0.06072	0.03709	—	0.3274	0.6906	2.15
118	0.4835	—	0.01302	0.00903	0.01049	0.00655	—	0.3271	0.6900	1.63
119	0.4970	—	0.00915	0.00688	0.00938	0.00479	—	0.3108	0.6565	1.51
99R	0.4415	—	0.01222	0.01031	0.00880	0.00692	—	0.2747	0.5823	1.41

Table A2. Measured Composition of Frit X Glass^a

	Frit X-A		Frit X-B		Frit X-C		Average		Normalized	
	µg/L	mass%	µg/L	mass%	µg/L	mass%	mass%	oxide mass%	oxide mass%	element mass%
Initially dissolved fraction										
Al	45.9	4.573	47.2	4.630	47.8	4.641				
B	36.7	3.656	37.4	3.669	37.6	3.650				
Gd	80.5	8.020	87	8.534	96.6	9.379				
Hf	125	12.453	129	12.655	134	13.010				
La	54.9	5.469	65.7	6.445	91.6	8.893				
Nd	72.2	7.193	80.7	7.916	95.4	9.262				
Si	87.25	8.692	88.78	8.709	89.93	8.731				
Sr	14.4	1.435	15.4	1.511	16.7	1.621				
Re-dissolved fraction										
Al	0.641	0.064	0.519	0.051	0.364	0.035				
B		0.000		0.000		0.000				
Gd	21	2.092	19.2	1.883	12	1.165				
Hf	8.91	0.888	8.13	0.798	4.72	0.458				
La	77.7	7.741	78.6	7.710	55.5	5.388				
Nd	36.3	3.616	34.7	3.404	22.9	2.223				
Si		0.000		0.000		0.000				
Sr	2.66	0.265	2.4	0.235	1.48	0.144				
Total										
Al		4.636		4.681		4.676	4.665	8.814	8.958	4.741
B		3.656		3.669		3.650	3.658	11.764	11.957	3.718
Gd		10.112		10.418		10.544	10.358	11.938	12.134	10.528
Hf		13.340		13.452		13.468	13.420	15.826	16.085	13.640
La		13.210		14.155		14.282	13.882	16.284	16.551	14.110
Nd		10.809		11.320		11.485	11.205	13.070	13.284	11.389
Si		8.692		8.709		8.731	8.711	18.636	18.942	8.854
Sr		1.700		1.746		1.765	1.737	2.054	2.088	1.765
Total		66.165		68.151		68.601	67.636	98.386	100	68.745

^aDissolved samples for analysis:

Sample Frit X-A: 50.19 mg glass/50.00 mL.

Sample Frit X-B: 50.97 mg glass/50.00 mL.

Sample Frit X-C: 51.50 mg glass/50.00 mL.

Table A3. Measured Composition of SRL 418 Glass^a

	SRL 418-A		SRL 418-B		SRL 418-C		Average		Normalized	
	µg/L	mass%	µg/L	mass%	µg/L	mass%	mass%	oxide mass%	oxide mass%	element mass%
Al	37600	3.052	31600	3.090	30200	2.988	3.043	5.752	6.283	3.324
B	20000	1.624	17300	1.692	16800	1.662	1.659	5.342	5.835	1.812
Ba	548	0.044	460	0.045	452	0.045	0.045	0.050	0.055	0.049
Ca	8660	0.703	7360	0.720	7380	0.730	0.718	1.005	1.097	0.784
Ce	711	0.058	602	0.059	575	0.057	0.058	0.071	0.078	0.063
Cr	559	0.045	465	0.045	412	0.041	0.044	0.064	0.070	0.048
Cu	270	0.022	224	0.022	208	0.021	0.021	0.027	0.029	0.023
Fe	100000	8.118	87700	8.576	85500	8.459	8.384	11.990	13.095	9.158
K	3590	0.291	3150	0.308	3220	0.319	0.306	0.367	0.401	0.334
La	410	0.033	392	0.038	352	0.035	0.035	0.042	0.045	0.039
Li	28700	2.330	24500	2.396	24200	2.394	2.373	5.103	5.573	2.592
Mg	9240	0.750	7790	0.762	7280	0.720	0.744	1.234	1.347	0.813
Mn	21800	1.770	18500	1.809	18200	1.801	1.793	2.833	3.094	1.959
Na	92500	7.509	86400	8.449	86300	8.538	8.165	11.023	12.040	8.918
Ni	5990	0.486	5140	0.503	4640	0.459	0.483	0.613	0.669	0.527
P	276	0.022	276	0.027	276	0.027	0.026	0.059	0.064	0.028
Pb	515	0.042	420	0.041	425	0.042	0.042	0.045	0.049	0.045
Si	256000	20.783	218000	21.318	223000	22.062	21.388	45.769	49.990	23.360
Ti	193	0.016	156	0.015	123	0.012	0.014	0.024	0.026	0.016
Zn	547	0.044	454	0.044	437	0.043	0.044	0.055	0.060	0.048
Zr	838	0.068	672	0.066	676	0.067	0.067	0.090	0.099	0.073
Total		47.812		50.026		50.520	49.452	91.557	100	54.013

^aDissolved samples for analysis:

Sample SRL 418A: 61.59 mg glass/50.00 mL.

Sample SRL 418B: 51.13 mg glass/50.00 mL.

Sample SRL 418C: 50.54 mg glass/50.00 mL.

Table A4. Measured Composition of Pu LaBS-B Glass^a

Element	Dissolved		Residue		Total mass%
	µg/L	mass%	µg/L	mass%	
LaBS-B-1					
Al	9700	9.08	51.1	0.05	9.13
B	2540	2.38	86	0.09	2.47
Gd	5710	5.34	3750	3.90	9.24
Hf	5110	4.78	302	0.31	5.10
La	496	0.46	5590	5.81	6.27
Nd	2060	1.93	3820	3.97	5.90
²³⁹ Pu	2600	2.43	2250	2.34	4.77
²⁴⁰ Pu	173	0.1619	136	0.1413	0.3032
²⁴¹ Pu	20.6	0.0193	5.93	0.0062	0.0254
²⁴² Pu	1.82	0.0017	1.59	0.0017	0.0034
Si	11100	10.39	63.8	0.07	10.45
Sr	1430	1.34	145	0.15	1.49
LaBS-B-2					
Al	10700	10.05	46.9	0.05	10.10
B	2810	2.64	69.6	0.07	2.71
Gd	7750	7.28	2930	2.92	10.20
Hf	6130	5.76	191	0.19	5.95
La	898	0.84	5220	5.20	6.04
Nd	3070	2.88	3260	3.25	6.13
²³⁹ Pu	3690	3.47	1680	1.67	5.14
²⁴⁰ Pu	234	0.2198	108	0.1076	0.3274
²⁴¹ Pu	25.6	0.0241	4.56	0.0045	0.0286
²⁴² Pu	2.44	0.0023	1.24	0.0012	0.0035
Si	12100	11.37	79.1	0.08	11.45
Sr	1860	1.75	164	0.16	1.91
Average					
	Elemental mass%	Oxide basis	Average oxide mass%	Normalized oxide mass%	Normalized element mass%
Al	9.62	Al ₂ O ₃	18.17	19.99	10.58
B	2.59	B ₂ O ₃	8.33	9.17	2.85
Gd	9.72	Gd ₂ O ₃	11.20	12.33	10.69
Hf	5.52	HfO ₂	7.50	8.25	6.08
La	6.16	La ₂ O ₃	7.20	7.93	6.77
Nd	6.01	Nd ₂ O ₃	7.04	7.74	6.62
²³⁹ Pu	4.96	²³⁹ PuO ₂	5.62	6.18	5.45
²⁴⁰ Pu	0.3153	²⁴⁰ PuO ₂	0.357	0.3931	0.3469
²⁴¹ Pu	0.0270	²⁴¹ PuO ₂	0.031	0.0337	0.0297
²⁴² Pu	0.0034	²⁴² PuO ₂	0.004	0.0043	0.0038
Si	10.95	SiO ₂	23.4	25.78	12.05
Sr	1.70	SrO	2.01	2.21	1.87
Total			90.90		

^aMasses dissolved for analysis:

	LaBS-B-1		LaBS-B-2	
	Dissolved	Residue	Dissolved	Residue
Dissolved mass, g	0.0487	0.0487	0.0579	0.0579
Mass 1st dilution, g	15.8841	15.881	17.9764	16.1669
Aliquot from 1st dilution, g	0.4192	0.4343	0.4983	0.3528
Mass 2nd dilution, g	12.0282	13.839	15.0786	12.5852
Dilution Factor	9358.65	10391.15	9394.95	9960.47

APPENDIX B: DATA AND RESULTS FOR IMMERSION TESTS AT 40 °C

The tests data for the initiation and termination of tests at 40 °C are summarized in Table B1. The data given in each column are summarized below

Test Number	Test number from test matrix
Specimen Number	Specimen number of monolith used in test
Specimen Area	Surface area of monolith specimen, in cm ²
Leachant Mass	Mass leachant solution used in test, in g
S/V	Specimen surface-area-to-solution volume (S/V) ratio, in m ⁻¹ , calculated as $S / V = \frac{\text{Sample Area, cm}^2}{\text{Leachant mass, g}} \times \frac{1 \text{ g solution}}{1 \text{ cm}^3 \text{ solution}} \times \frac{100 \text{ cm}}{m}$
Vessel No.	Number assigned to test vessel
Vessel Mass	
Initial	Total mass of vessel + leachant + specimen at beginning of test, in g
Final	Total mass of vessel + leachant + specimen at end of test, in g
Change	Change in vessel mass, in g, calculated as <i>Change, g = Final Vessel Mass – Initial Vessel Mass</i>
Adjusted	Change in leachant mass due to change in vessel mass
Leachant Mass	(only calculated if change in vessel mass > 0.02 g)
Effective S/V	S/V ratio calculated with adjusted leachant mass
Date and Time into Oven	Calendar date and time vessel placed into oven
Date and Time out of oven	Calendar date and time vessel placed removed from oven
Test Time	Test duration calculated in hours as <i>Test Time = Date and Time out of oven – Date and Time into oven</i>
Test Time, days	Test time, hours divided by 24 hours per day
pH	pH of test solution measured at room temperature
Solution Bottle	Mass empty 30-mL polyethylene solution bottle, g
Bottle + solution + HNO ₃	Total mass solution bottle, test solution, and 5 drops concentrated HNO ₃ . (Note: the small volume dilution due to addition of HNO ₃ is ignored in calculations.)
Mass solution	Mass test solution, in g, calculated as <i>mass solution = (mass with solution + HNO₃) – Solution bottle tare</i>
Total mass acid soak solution	Mass demineralized water and HNO ₃ added to vessel after specimen and test solution were removed, in g. (Note. Measured directly.)

The concentrations measured in the test solutions are summarized in Table B2. The concentrations are given in $\mu\text{g/L}$ (parts per billion, ppb). Dashes in the field indicate the solution was not analyzed for that element. Note that sample of the test solutions were diluted 2X prior to analysis. Solutions from test series MLB3-40, MLB4-40, and MLB6-40 were reanalyzed without dilution.

The calculated masses of elements in the test solutions are summarized in Table B3, in μg . The masses are calculated as the product of the leachant mass, in g, given in Table B1, and the concentrations given in Table B2 as

$$\text{mass } i \text{ in test solution, } \mu\text{g} = \text{leachant, g} \times \frac{1 \text{ mL leachant}}{\text{g leachant}} \times \text{concentration } i, \mu\text{g/L} \times \frac{1 \text{ L}}{1000 \text{ mL}}.$$

The concentrations measured in the acid soak solutions are summarized in Table B4. The concentrations are given in $\mu\text{g/L}$ (parts per billion, ppb). Dashes in the field indicate the solution was not analyzed for that element.

The calculated masses of elements in the acid soak solutions are summarized in Table B5, in μg . The masses are calculated as the product of the mass acid soak solution, in g, from Table B1 and the concentrations given in Table B4 as

$$\text{mass } i \text{ in acid soak solution, } \mu\text{g} = \text{mass acid soak, g} \times \frac{1 \text{ mL solution}}{\text{g solution}} \times \text{concentration } i, \mu\text{g/L} \times \frac{1 \text{ L}}{1000 \text{ mL}}.$$

Entries of "not det." indicate that the acid soak was not performed for that test.

The normalized elemental mass losses are summarized in Table B6, in g/m^2 . The normalized elemental mass loss was calculated as

$$NL(i) = \frac{\text{mass in test solution} - \text{mass in blank} \left(\frac{\text{blank solution}}{\text{test solution}} \right) + \text{mass in acid soak solution}}{\text{Sample Area} \times \text{Mass fraction in glass}}.$$

The mass measured in the blank test was scaled by the amounts of solution used in the test and the blank test because those amounts differed significantly in some cases.

The mass fractions of elements in the Pu LaBS-B glass used in the calculations are:

B = 0.0326
Al = 0.1020
Si = 0.1222
Sr = 0.0192
La = 0.0626
Nd = 0.0636
Gd = 0.1005
Hf = 0.0526
Pu = 0.0840

Negative values indicate that the concentration in the blank test exceeded the sum of the concentrations in the test solution and acid soak solutions. Less-than values indicate that the analyzed concentration in the test solution, the acid soak solution, or both, were below the detection limit, and the values of NL provide

upper bounds. Values shown as strike-outs were not used in analyses, and were replaced by re-run tests or re-analyses of solutions. Calculated values are given to the four decimal place or 3 significant figures.

Table B1. Test Data for Tests at 40 °C

Test Number	Specimen Number	Specimen Area, cm ²	Leachant mass, g	S/V, m ⁻¹	Vessel No.	Vessel Mass			Adjusted leachant mass, g	Effective S/V, m ⁻¹
						Initial, g	Final, g	Change, g		
MLB1-40-1	6	1.30	54.62	2.38	123	244.10	244.09	-0.01	54.62	2.38
MLB1-40-2	13	1.38	58.46	2.36	106	250.25	250.26	0.01	58.46	2.36
MLB1-40-3	14	1.35	58.23	2.32	101	246.72	246.72	0.00	58.23	2.32
MLB1-40-4	59	1.38	56.43	2.45	118	246.72	246.73	0.01	56.43	2.45
MLB1-40-5	62	1.42	59.02	2.41	119	249.96	249.95	-0.01	59.02	2.41
MLB1-40-B1	—	—	59.41	—	120	250.35	250.37	0.02	59.41	—
MLB2-40-1	1	1.55	32.98	4.70	68	164.46	164.46	0.00	32.98	4.70
MLB2-40-2	2	1.71	36.45	4.69	43	166.94	166.93	-0.01	36.45	4.69
MLB2-40-3	3	1.43	30.01	4.76	45	157.97	157.96	-0.01	30.01	4.76
MLB2-40-4	4	1.83	38.86	4.70	7	169.52	169.49	-0.03	38.83	4.70
MLB2-40-5	5	1.73	37.17	4.65	8	165.06	165.04	-0.02	37.17	4.65
MLB2-40-B1	—	—	31.79	—	9	160.57	160.57	0.00	31.79	—
MLB3-40-1	32	1.11	23.62	4.70	71	151.26	151.25	-0.01	23.62	4.70
MLB3-40-2	27	1.49	30.22	4.93	50	160.00	159.99	-0.01	30.22	4.93
MLB3-40-3	28	1.57	32.50	4.82	51	162.52	162.51	-0.01	32.50	4.82
MLB3-40-4	30	1.59	33.69	4.72	16	161.42	161.27	-0.15	33.54	4.74
MLB3-40-5	31	1.68	35.88	4.69	17	162.30	162.30	0.00	35.88	4.69
MLB3-40-B1	—	—	30.71	—	18	157.78	157.78	0.00	30.71	—
MLB4-40-1	48	1.60	33.23	4.81	74	161.54	161.56	0.02	33.23	4.81
MLB4-40-2	50	1.42	30.03	4.73	56	160.85	160.85	0.00	30.03	4.73
MLB4-40-3	53	1.61	33.50	4.81	57	162.88	162.88	0.00	33.50	4.81
MLB4-40-4	56	1.55	32.12	4.83	25	162.37	162.36	-0.01	32.12	4.83
MLB4-40-5	57	1.50	31.45	4.77	26	158.91	158.90	-0.01	31.45	4.77
MLB4-40-B1	—	—	29.48	—	27	159.95	159.94	-0.01	29.48	—
MLB5-40-1	70	1.51	31.84	4.74	77	160.89	160.88	-0.01	31.84	4.74
MLB5-40-2	72	1.53	31.89	4.79	62	162.43	162.41	-0.02	31.89	4.79
MLB5-40-3	73	1.50	32.00	4.69	63	160.13	160.14	0.01	32.00	4.69
MLB5-40-4	74	1.71	36.05	4.75	34	163.44	163.42	-0.02	36.05	4.75
MLB5-40-5	75	1.60	33.42	4.80	35	158.29	158.29	0.00	33.42	4.80
MLB5-40-B1	—	—	30.36	—	42	161.10	161.10	0.00	30.36	—
MLB5-40-1R	104	1.51	32.19	4.70	85	130.98	163.34	163.34	0.00	32.19
MLB5-40-2R	114	1.52	32.42	4.70	33	129.04	161.65	161.64	-0.01	32.41
MLB5-40-3R	102	1.53	32.50	4.70	39	129.61	162.29	162.28	-0.01	32.49
MLB5-40-4R	115	1.56	33.23	4.70	40	125.83	159.24	159.23	-0.01	33.22
MLB5-40-5R	110	1.60	33.99	4.70	15	127.65	161.79	161.79	0.00	33.99
MLB5-40-BR	—	—	34.55	—	82	130.70	165.26	165.07	-0.19	34.36
MLB6-40-1	11	1.18	64.68	1.82	117	255.70	255.71	0.01	64.68	1.82
MLB6-40-2	15	1.15	50.88	2.26	102	237.03	237.03	0.00	50.88	2.26
MLB6-40-3	16	1.18	51.95	2.27	103	242.81	242.81	0.00	51.95	2.27
MLB6-40-4	17	1.22	48.23	2.53	128	237.71	237.70	-0.01	48.23	2.53
MLB6-40-5	18	1.24	52.30	2.37	127	242.37	242.37	0.00	52.30	2.37
MLB6-40-B1	—	—	36.92	—	41	167.45	167.42	-0.03	36.89	—

Table B1. (cont.)

Test Number	Date and Time into oven	Date and Time out of oven	Test Time, hours	Test Time, days	pH (room temp.)	Solution bottle tare, g	Bottle + solution + HNO ₃ , g	Mass solution, g	Total mass acid soak solution, g
MLB1-40-1	2/8/06 13:10	2/9/06 12:20	23.17	0.97	3.69	11.15	37.52	26.37	83.25
MLB1-40-2	1/30/06 13:55	2/1/06 12:40	46.75	1.95	3.69	11.02	36.21	25.19	86.34
MLB1-40-3	1/30/06 13:55	2/2/06 12:35	70.67	2.94	3.70	11.18	35.90	24.72	89.48
MLB1-40-4	1/27/06 14:50	1/31/06 12:10	93.33	3.89	3.70	11.16	32.71	21.55	83.68
MLB1-40-5	1/27/06 14:50	2/1/06 12:40	117.83	4.91	3.71	11.14	34.36	23.22	84.73
MLB1-40-B1	1/27/06 15:10	2/1/06 12:40	117.50	4.90	3.71	11.17	37.44	26.27	not det.
MLB2-40-1	2/8/06 13:10	2/9/06 12:20	23.17	0.97	4.85	11.17	34.40	23.23	41.64
MLB2-40-2	1/30/06 13:55	2/1/06 12:40	46.75	1.95	4.87	11.16	34.97	23.81	32.76
MLB2-40-3	1/30/06 13:55	2/2/06 12:35	70.67	2.94	4.88	11.13	32.95	21.82	32.83
MLB2-40-4	1/27/06 14:50	1/31/06 12:10	93.33	3.89	4.89	11.14	37.46	26.32	33.44
MLB2-40-5	1/27/06 14:50	2/1/06 12:40	117.83	4.91	4.89	11.16	34.70	23.54	33.64
MLB2-40-B1	1/27/06 15:10	2/1/06 12:40	117.50	4.90	4.86	11.15	36.16	25.01	not det.
MLB3-40-1	2/8/06 13:10	2/9/06 12:20	23.17	0.97	6.06	11.18	34.31	23.13	34.52
MLB3-40-2	1/30/06 13:55	2/1/06 12:40	46.75	1.95	6.09	11.20	33.45	22.25	35.92
MLB3-40-3	1/30/06 13:55	2/2/06 12:35	70.67	2.94	6.09	11.18	35.98	24.80	32.94
MLB3-40-4	1/27/06 14:50	1/31/06 12:10	93.33	3.89	6.09	11.19	37.21	26.02	35.03
MLB3-40-5	1/27/06 14:50	2/1/06 12:40	117.83	4.91	6.09	11.13	34.59	23.46	28.35
MLB3-40-B1	1/27/06 15:10	2/1/06 12:40	117.50	4.90	6.09	11.18	36.77	25.59	not det.
MLB4-40-1	2/8/06 13:10	2/9/06 12:20	23.17	0.97	8.55	11.15	36.17	25.02	32.31
MLB4-40-2	1/30/06 13:55	2/1/06 12:40	46.75	1.95	8.51	10.88	32.71	21.83	36.45
MLB4-40-3	1/30/06 13:55	2/2/06 12:35	70.67	2.94	8.54	11.23	34.57	23.34	40.57
MLB4-40-4	1/27/06 14:50	1/31/06 12:10	93.33	3.89	8.56	11.17	38.64	27.47	35.70
MLB4-40-5	1/27/06 14:50	2/1/06 12:40	117.83	4.91	8.56	11.19	32.86	21.67	37.00
MLB4-40-B1	1/27/06 15:10	2/1/06 12:40	117.50	4.90	8.53	11.17	37.35	26.18	not det.
MLB5-40-1	2/8/06 13:10	2/9/06 12:20	23.17	0.97	7.55	11.20	35.23	24.03	30.75
MLB5-40-2	1/30/06 13:55	2/1/06 12:40	46.75	1.95	8.74	11.03	33.99	22.96	36.06
MLB5-40-3	1/30/06 13:55	2/2/06 12:35	70.67	2.94	8.79	11.16	35.14	23.98	37.44
MLB5-40-4	1/27/06 14:50	1/31/06 12:10	93.33	3.89	9.38	11.20	39.72	28.52	35.47
MLB5-40-5	1/27/06 14:50	2/1/06 12:40	117.83	4.91	8.86	11.22	33.77	22.55	32.57
MLB5-40-B1	1/27/06 15:10	2/1/06 12:40	117.50	4.90	8.60	11.14	36.23	25.09	not det.
MLB5-40-1R	3/1/06 16:00	3/2/06 11:00	19.00	0.79	9.38	11.26	34.69	23.43	not det.
MLB5-40-2R	3/1/06 16:00	3/3/06 12:30	44.50	1.85	9.38	11.17	35.93	24.76	not det.
MLB5-40-3R	3/3/06 11:15	3/6/06 12:30	73.25	3.05	9.44	11.20	36.13	24.93	not det.
MLB5-40-4R	3/2/06 11:00	3/6/06 12:30	97.50	4.06	9.49	11.13	37.56	26.43	not det.
MLB5-40-5R	3/1/06 16:00	3/6/06 12:30	116.50	4.85	9.40	11.19	35.58	24.39	not det.
MLB5-40-BR	3/1/06 16:00	3/6/06 12:30	116.50	4.85	not meas.	11.17	34.42	23.25	not det.
MLB6-40-1	2/8/06 13:10	2/9/06 12:20	23.17	0.97	10.94	11.15	37.06	25.91	77.02
MLB6-40-2	1/30/06 13:55	2/1/06 12:40	46.75	1.95	10.92	11.12	37.57	26.45	86.61
MLB6-40-3	1/30/06 13:55	2/2/06 12:35	70.67	2.94	10.83	11.20	37.60	26.40	83.33
MLB6-40-4	1/27/06 14:50	1/31/06 12:10	93.33	3.89	10.83	11.15	39.57	28.42	85.53
MLB6-40-5	1/27/06 14:50	2/1/06 12:40	117.83	4.91	10.89	11.23	38.01	26.78	84.43
MLB6-40-B1	1/27/06 15:10	2/1/06 12:40	117.50	4.90	10.95	11.19	37.54	26.35	not det.

Table B2. Results of Static Dissolution Tests at 40 °C: Measured Concentrations in Test Solutions, µg/L

Test Number	Concentration measured in test solution, µg/L								
	B	Al	Si	Sr	La	Nd	Gd	Hf	Pu 239
MLB1-40-1	161	374	765	48.8	178	169	283	3.11	86.8
MLB1-40-2	197	588	1020	72.5	267	255	417	2.13	96.1
MLB1-40-3	231	776	1200	94.1	348	338	537	1.77	92.0
MLB1-40-4	240	820	1230	103	384	367	582	2.28	97.7
MLB1-40-5	279	671	1510	127	423	432	713	2.13	103
MLB1-40-B1	18.5	13.2	669	0.099	0.039	<0.05	<0.06	<0.19	<0.13
MLB2-40-1	160	307	280	41.2	145	133	212	1.16	20
MLB2-40-2	174	490	462	63.9	224	217	345	0.922	19.7
MLB2-40-3	188	509	502	84.0	266	248	412	0.980	15.9
MLB2-40-4	195	545	544	91.1	294	270	455	1.10	17.6
MLB2-40-5	217	679	707	107	355	337	539	1.06	15.2
MLB2-40-B1	6.9	10.3	124	0.063	0.017	0.055	<0.06	<0.19	<0.13
MLB3-40-1	94.5	21.2	<29	2.16	6.94	7.05	11.2	0.653	2.47
MLB3-40-2	93.6	33.2	<29	2.17	7.52	7.08	11.4	0.691	2.58
MLB3-40-3	95.0	33.4	<29	3.70	12.6	12.0	19.3	0.667	4.52
MLB3-40-4	93.7	32.7	<29	3.53	11.4	11.5	18.1	0.665	3.99
MLB3-40-5	97.4	25.4	29.3	6.50	21.6	19.2	30.0	0.688	8.46
MLB3-40-B1	3.93	<9.23	50.6	0.061	<0.01	<0.05	<0.06	<0.19	<0.13
MLB3-40-1 ^a	20.3	—	83.9	—	—	—	—	—	—
MLB3-40-2 ^a	20.0	—	86.2	—	—	—	—	—	—
MLB3-40-3 ^a	22.3	—	94.6	—	—	—	—	—	—
MLB3-40-4 ^a	22.7	—	97.2	—	—	—	—	—	—
MLB3-40-5 ^a	25.7	—	114	—	—	—	—	—	—
MLB3-40-B1 ^a	20.3	—	83.9	—	—	—	—	—	—
MLB4-40-1	163	41.6	139	2.39	3.86	2.88	3.52	1.05	1.35
MLB4-40-2	161	38.3	137	4.01	1.73	1.09	1.02	1.01	2.32
MLB4-40-3	147	45.3	151	5.87	6.78	3.94	4.71	1.01	3.30
MLB4-40-4	130	51.6	151	6.71	5.45	3.32	3.89	1.01	4.59
MLB4-40-5	129	57.1	160	7.02	10.5	6.72	8.72	1.05	5.36
MLB4-40-B1	33.7	24.8	193	<0.07	0.039	<0.05	0.048	0.101	<0.04
MLB4-40-1 ^a	194	—	304	—	—	—	—	—	—
MLB4-40-2 ^a	198	—	298	—	—	—	—	—	—
MLB4-40-3 ^a	207	—	307	—	—	—	—	—	—
MLB4-40-4 ^a	210	—	317	—	—	—	—	—	—
MLB4-40-5 ^a	207	—	317	—	—	—	—	—	—
MLB4-40-B1 ^a	192	—	285	—	—	—	—	—	—
MLB5-40-1	159	24.9	<52.2	2.86	4.98	3.73	5.21	0.985	2.80
MLB5-40-2	141	32.9	<52.2	4.07	0.566	0.402	0.487	0.984	2.84
MLB5-40-3	141	48.3	<52.2	5.68	0.702	0.490	0.638	0.997	4.09
MLB5-40-4	145	46.0	<52.2	5.84	0.165	0.197	0.172	0.976	3.98
MLB5-40-5	135	69.4	<52.2	3.46	0.306	0.287	0.246	0.968	4.82
MLB5-40-B1	10.5	74.1	<26.1	0.175	0.122	0.16	0.068	<0.07	<0.04
MLB5-40-1R	7.41	28.9	18.0	2.46	0.043	<0.04	0.056	<0.09	1.56
MLB5-40-2R	10.2	48.1	39.6	5.56	0.024	<0.04	0.041	<0.09	5.21
MLB5-40-3R	11.5	60.3	40.0	6.14	0.054	<0.04	0.041	<0.09	3.08
MLB5-40-4R	12.6	82.8	57.5	8.27	0.033	<0.04	0.05	<0.09	3.65
MLB5-40-5R	12.4	69.7	58.0	8.38	0.046	<0.04	0.048	<0.09	3.98
MLB5-40-BR	9.90	7.46	<9.07	0.083	<0.02	<0.04	<0.04	<0.09	<0.02
MLB6-40-1	118	23.9	<52.2	1.68	0.11	0.166	0.129	0.992	0.789
MLB6-40-2	114	26.8	<52.2	2.72	0.152	0.213	0.192	0.989	1.36
MLB6-40-3	113	28.3	<52.2	3.11	0.127	0.203	0.122	0.988	1.76
MLB6-40-4	112	35.0	<52.2	4.34	0.181	0.219	0.258	0.988	2.37
MLB6-40-5	114	46.6	<52.2	7.06	0.139	0.187	0.167	0.978	3.65
MLB6-40-B1	17.3	244	<26.1	0.539	0.536	0.113	0.077	<0.07	<0.04
MLB6-40-1 ^a	18.3	—	21.5	—	—	—	—	—	—
MLB6-40-2 ^a	20.2	—	30.5	—	—	—	—	—	—
MLB6-40-3 ^a	20.1	—	29.4	—	—	—	—	—	—
MLB6-40-4 ^a	21.0	—	36.5	—	—	—	—	—	—
MLB6-40-5 ^a	24.3	—	54.5	—	—	—	—	—	—
MLB6-40-B1 ^a	16.9	—	21.3	—	—	—	—	—	—

^aSolution was reanalyzed without dilution for B and Si concentrations.

Table B3. Results of Static Dissolution Tests at 40 °C: Measured Masses in Test Solutions, µg

Test Number	Mass leachant, g	Mass in test solution, µg								
		B	Al	Si	Sr	La	Nd	Gd	Hf	Pu 239
MLB1-40-1	54.62	8.79	20.4	41.8	2.67	9.72	9.23	15.5	0.170	4.74
MLB1-40-2	58.46	11.5	34.4	59.6	4.24	15.6	14.9	24.4	0.125	5.62
MLB1-40-3	58.23	13.5	45.2	69.9	5.48	20.3	19.7	31.3	0.103	5.36
MLB1-40-4	56.43	13.5	46.3	69.4	5.81	21.7	20.7	32.8	0.129	5.51
MLB1-40-5	59.02	16.5	39.6	89.1	7.49	25.0	25.5	42.1	0.126	6.08
MLB1-40-B1	59.41	1.10	0.784	39.7	0.006	0.002	<0.003	<0.004	<0.011	<0.008
MLB2-40-1	32.98	5.28	10.1	9.23	1.36	4.78	4.39	6.99	0.038	0.660
MLB2-40-2	36.45	6.34	17.9	16.8	2.33	8.17	7.91	12.6	0.034	0.718
MLB2-40-3	30.01	5.64	15.3	15.1	2.52	7.98	7.44	12.4	0.029	0.477
MLB2-40-4	38.83	7.57	21.2	21.1	3.54	11.4	10.5	17.7	0.043	0.683
MLB2-40-5	37.17	8.07	25.2	26.3	3.98	13.2	12.5	20.0	0.039	0.565
MLB2-40-B1	31.79	0.219	0.327	3.94	0.002	0.001	0.002	<0.002	<0.006	<0.004
MLB3-40-1	23.62	2.23	0.501	<0.69	0.051	0.164	0.167	0.265	0.015	0.058
MLB3-40-2	30.22	2.83	1.00	<0.88	0.066	0.227	0.214	0.344	0.021	0.078
MLB3-40-3	32.50	3.09	1.09	<0.95	0.120	0.409	0.390	0.627	0.022	0.147
MLB3-40-4	33.54	3.14	1.10	<0.98	0.118	0.382	0.386	0.607	0.022	0.134
MLB3-40-5	35.88	3.49	0.911	1.05	0.233	0.775	0.689	1.076	0.025	0.304
MLB3-40-B1	30.71	0.121	<0.283	1.55	0.002	<0.000	<0.002	<0.002	<0.006	<0.004
MLB3-40-1 ^a	23.62	0.479	—	1.98	—	—	—	—	—	—
MLB3-40-2 ^a	30.22	0.604	—	2.60	—	—	—	—	—	—
MLB3-40-3 ^a	32.50	0.725	—	3.07	—	—	—	—	—	—
MLB3-40-4 ^a	33.54	0.761	—	3.26	—	—	—	—	—	—
MLB3-40-5 ^a	35.88	0.922	—	4.09	—	—	—	—	—	—
MLB3-40-B1 ^a	30.71	0.577	—	2.36	—	—	—	—	—	—
MLB4-40-1	33.23	5.42	1.38	4.62	0.079	0.128	0.096	0.117	0.035	0.045
MLB4-40-2	30.03	4.84	1.15	4.11	0.120	0.052	0.033	0.031	0.030	0.070
MLB4-40-3	33.50	4.93	1.52	5.06	0.197	0.227	0.132	0.158	0.034	0.111
MLB4-40-4	32.12	4.18	1.66	4.85	0.216	0.175	0.107	0.125	0.032	0.147
MLB4-40-5	31.45	4.06	1.80	5.03	0.221	0.330	0.211	0.274	0.033	0.169
MLB4-40-B1	29.48	0.993	0.731	5.69	<0.002	0.001	<0.001	0.001	0.003	<0.001
MLB4-40-1 ^a	33.23	6.45	—	10.1	—	—	—	—	—	—
MLB4-40-2 ^a	30.03	5.95	—	8.95	—	—	—	—	—	—
MLB4-40-3 ^a	33.50	6.93	—	10.3	—	—	—	—	—	—
MLB4-40-4 ^a	32.12	6.74	—	10.2	—	—	—	—	—	—
MLB4-40-5 ^a	31.45	6.51	—	9.97	—	—	—	—	—	—
MLB4-40-B1 ^a	29.48	5.66	—	8.40	—	—	—	—	—	—
MLB5-40-1	31.76	5.05	0.791	<1.7	0.091	0.158	0.118	0.165	0.031	0.089
MLB5-40-2	31.89	4.50	1.05	<1.66	0.130	0.018	0.013	0.016	0.031	0.091
MLB5-40-3	32.00	4.51	1.55	<1.67	0.182	0.022	0.016	0.020	0.032	0.131
MLB5-40-4	36.05	5.23	1.66	<1.88	0.211	0.006	0.007	0.006	0.035	0.143
MLB5-40-5	33.42	4.51	2.32	<1.74	0.116	0.010	0.010	0.008	0.032	0.161
MLB5-40-B1	30.36	0.319	2.25	<0.79	0.005	0.004	0.005	0.002	<0.002	<0.001
MLB5-40-1R	32.19	0.239	0.930	0.579	0.079	0.001	<0.001	0.002	<0.003	0.050
MLB5-40-2R	32.41	0.331	1.56	1.28	0.180	0.001	<0.001	0.001	<0.003	0.169
MLB5-40-3R	32.49	0.374	1.96	1.30	0.200	0.002	<0.001	0.001	<0.003	0.100
MLB5-40-4R	33.22	0.419	2.75	1.91	0.275	0.001	<0.001	0.002	<0.003	0.121
MLB5-40-5R	33.99	0.421	2.37	1.97	0.285	0.002	<0.001	0.002	<0.003	0.135
MLB5-40-BR	34.36	0.340	0.256	<0.32	0.003	<0.001	<0.001	<0.001	<0.003	<0.001
MLB6-40-1	64.68	7.63	1.55	<3.4	0.109	0.007	0.011	0.008	0.064	0.051
MLB6-40-2	50.88	5.80	1.36	<2.7	0.138	0.008	0.011	0.010	0.050	0.069
MLB6-40-3	51.95	5.87	1.47	<2.8	0.162	0.007	0.011	0.006	0.051	0.091
MLB6-40-4	48.23	5.40	1.69	<2.6	0.209	0.009	0.011	0.012	0.048	0.114
MLB6-40-5	52.30	5.96	2.44	<2.8	0.369	0.007	0.010	0.009	0.051	0.191
MLB6-40-B1	36.89	0.638	9.00	<0.96	0.020	0.020	0.004	0.003	<0.003	<0.001
MLB6-40-1 ^a	64.68	1.18	—	1.39	—	—	—	—	—	—
MLB6-40-2 ^a	50.88	1.03	—	1.55	—	—	—	—	—	—
MLB6-40-3 ^a	51.95	1.04	—	1.53	—	—	—	—	—	—
MLB6-40-4 ^a	48.23	1.01	—	1.76	—	—	—	—	—	—
MLB6-40-5 ^a	52.30	1.27	—	2.85	—	—	—	—	—	—
MLB6-40-B1 ^a	36.89	0.623	—	0.79	—	—	—	—	—	—

^aSolution was reanalyzed without dilution for B and Si concentrations.

Table B4. Results of Static Dissolution tests at 40 °C: Calculated Concentrations in Acid Soak Solutions, µg/L

Test Number	Concentration measured in acid soak solution, µg/L						
	Si	Sr	La	Nd	Gd	Hf	Pu 239
MLB1-40-1	<28.6	<0.15	<0.01	<0.03	<0.04	1.92	13.3
MLB1-40-2	<28.6	<0.15	0.011	<0.03	<0.04	3.52	28.7
MLB1-40-3	<28.6	<0.15	0.033	0.04	0.057	3.84	49.2
MLB1-40-4	<28.6	<0.15	<0.01	<0.03	<0.04	7.23	58.3
MLB1-40-5	<28.6	<0.15	0.012	0.032	<0.04	3.84	75.0
MLB1-40-B1	not det.	not det.	not det.	not det.	not det.	not det.	not det.
MLB2-40-1	<28.6	<0.15	<0.01	<0.03	<0.04	1.36	9.26
MLB2-40-2	<28.6	<0.15	0.142	0.208	0.149	1.86	18.2
MLB2-40-3	<28.6	<0.15	0.287	0.400	0.674	1.48	22.9
MLB2-40-4	<28.6	<0.15	0.072	0.092	0.13	6.55	32.4
MLB2-40-5	<28.6	<0.15	0.733	0.793	1.25	1.57	27.0
MLB2-40-B1	not det.	not det.	not det.	not det.	not det.	not det.	not det.
MLB3-40-1	<28.6	<0.15	0.071	0.127	0.255	<0.05	0.206
MLB3-40-2	<28.6	<0.15	0.073	0.117	0.143	<0.05	0.494
MLB3-40-3	<28.6	1.57	0.166	0.166	0.326	<0.05	0.667
MLB3-40-4	<28.6	<0.15	0.694	0.794	1.23	<0.05	1.00
MLB3-40-5	<28.6	<0.15	0.666	0.777	1.86	<0.05	1.37
MLB3-40-B1	not det.	not det.	not det.	not det.	not det.	not det.	not det.
MLB4-40-1	<28.6	<0.15	0.199	0.239	0.276	<0.05	0.033
MLB4-40-2	<28.6	<0.15	2.31	2.21	3.60	<0.05	0.061
MLB4-40-3	<28.6	<0.15	1.87	2.01	3.77	0.169	0.115
MLB4-40-4	<28.6	<0.15	2.05	2.07	3.50	0.060	0.099
MLB4-40-5	<28.6	<0.15	1.04	1.01	1.85	0.109	0.080
MLB4-40-B1	not det.	not det.	not det.	not det.	not det.	not det.	not det.
MLB5-40-1	<28.6	<0.15	0.310	0.362	0.611	<0.05	0.154
MLB5-40-2	<28.6	<0.15	0.161	0.147	0.175	0.061	0.197
MLB5-40-3	<28.6	<0.15	0.694	0.578	0.799	<0.05	0.139
MLB5-40-4	<28.6	<0.15	0.177	0.161	0.267	<0.05	0.316
MLB5-40-5	<28.6	3.26	2.16	1.45	2.14	<0.05	0.224
MLB5-40-B1	not det.	not det.	not det.	not det.	not det.	not det.	not det.
MLB5-40-1R	not det.	not det.	not det.	not det.	not det.	not det.	not det.
MLB5-40-2R	not det.	not det.	not det.	not det.	not det.	not det.	not det.
MLB5-40-3R	not det.	not det.	not det.	not det.	not det.	not det.	not det.
MLB5-40-4R	not det.	not det.	not det.	not det.	not det.	not det.	not det.
MLB5-40-5R	not det.	not det.	not det.	not det.	not det.	not det.	not det.
MLB5-40-BR	not det.	not det.	not det.	not det.	not det.	not det.	not det.
MLB6-40-1	<28.6	<0.15	0.045	0.052	0.046	0.084	0.153
MLB6-40-2	<28.6	<0.15	0.091	0.106	0.141	<0.05	0.154
MLB6-40-3	<28.6	<0.15	0.026	<0.03	0.046	<0.05	0.159
MLB6-40-4	<28.6	<0.15	0.035	<0.03	<0.04	0.051	0.156
MLB6-40-5	<28.6	<0.15	0.019	0.035	<0.04	0.056	0.126
MLB6-40-B1	not det.	not det.	not det.	not det.	not det.	not det.	not det.

Table B5. Results of Static Dissolution Tests at 40 °C: Calculated Masses in Acid Soak Solutions, µg

Test Number	Mass acid soak solution, g	Mass in acid soak solution, µg						
		Si	Sr	La	Nd	Gd	Hf	Pu 239
MLB1-40-1	83.25	<2.4	<0.02	<0.0008	<0.003	<0.004	0.160	1.11
MLB1-40-2	86.34	<2.5	<0.02	0.00095	<0.003	<0.004	0.304	2.48
MLB1-40-3	89.48	<2.6	<0.02	0.00295	0.0036	0.0051	0.344	4.40
MLB1-40-4	83.68	<2.4	<0.02	<0.0008	<0.003	<0.004	0.605	4.88
MLB1-40-5	84.73	<2.5	<0.02	0.00102	0.0027	<0.004	0.325	6.36
MLB2-40-1	41.64	<1.2	<0.006	<0.0004	<0.002	<0.002	0.0566	0.386
MLB2-40-2	32.76	<1.0	<0.005	0.00465	0.0068	0.0049	0.0609	0.596
MLB2-40-3	32.83	<1.0	<0.005	0.00942	0.0131	0.0221	0.0486	0.752
MLB2-40-4	33.44	<1.0	<0.005	0.00241	0.0031	0.0044	0.219	1.08
MLB2-40-5	33.64	<1.0	<0.005	0.0247	0.0267	0.0421	0.0528	0.908
MLB3-40-1	34.52	<1.1	<0.005	0.0025	0.0044	0.0088	<0.002	0.0071
MLB3-40-2	35.92	<1.1	<0.005	0.0026	0.0042	0.0051	<0.002	0.0177
MLB3-40-3	32.94	<1.0	0.052	0.0055	0.0055	0.0107	<0.002	0.0220
MLB3-40-4	35.03	<1.0	<0.005	0.0243	0.0278	0.0431	<0.002	0.0350
MLB3-40-5	28.35	<0.9	<0.004	0.0189	0.0220	0.0527	<0.001	0.0388
MLB4-40-1	32.31	<1.0	<0.005	0.0064	0.0077	0.0089	<0.002	0.00107
MLB4-40-2	36.45	<1.1	<0.005	0.0842	0.0806	0.1312	<0.002	0.00222
MLB4-40-3	40.57	<1.2	<0.006	0.0759	0.0815	0.1529	0.0069	0.00467
MLB4-40-4	35.70	<1.0	<0.005	0.0732	0.0739	0.1250	0.0021	0.00353
MLB4-40-5	37.00	<1.1	<0.006	0.0385	0.0374	0.0685	0.0040	0.00296
MLB5-40-1	30.75	<0.9	<0.005	0.0095	0.0111	0.0188	<0.002	0.00474
MLB5-40-2	36.06	<1.	<0.005	0.0058	0.0053	0.0063	0.0022	0.00710
MLB5-40-3	37.44	<1.1	<0.006	0.0260	0.0216	0.0299	<0.002	0.00520
MLB5-40-4	35.47	<1.0	<0.005	0.0063	0.0057	0.0095	<0.002	0.0112
MLB5-40-5	32.57	<1.0	0.106	0.0704	0.0472	0.0697	<0.002	0.0073
MLB6-40-1	77.02	<2.2	<0.02	0.0035	0.0040	0.0035	0.0065	0.0118
MLB6-40-2	86.61	<2.5	<0.02	0.0079	0.0092	0.0122	<0.004	0.0133
MLB6-40-3	83.33	<2.4	<0.02	0.0022	<0.002	0.0038	<0.004	0.0132
MLB6-40-4	85.53	<2.5	<0.02	0.0030	<0.003	<0.003	0.0044	0.0133
MLB6-40-5	84.43	<2.5	<0.02	0.0016	0.0030	<0.003	0.0047	0.0106

Table B6. Results of Static Dissolution Tests at 40 °C: Normalized Elemental Mass Losses, g/m²

Test Number	Specimen Area, cm ²	Normalized elemental mass loss, g/m ²								
		B	Al	Si	Sr	La	Nd	Gd	Hf	Pu 239
MLB1-40-1	1.30	1.84	1.48	0.330	1.07	1.19	1.12	1.18	0.0466	0.535
MLB1-40-2	1.38	2.32	2.39	1.22	1.60	1.81	1.70	1.76	0.0590	0.698
MLB1-40-3	1.35	2.81	3.22	1.87	2.11	2.40	2.29	2.31	0.0629	0.861
MLB1-40-4	1.38	2.78	3.23	1.88	2.19	2.51	2.36	2.37	0.1011	0.896
MLB1-40-5	1.42	3.32	2.68	2.86	2.75	2.81	2.82	2.95	0.0604	1.042
MLB2-40-1	1.55	0.819	0.620	0.272	0.456	0.493	0.445	0.449	0.0109	0.0803
MLB2-40-2	1.71	0.911	1.00	0.589	0.708	0.763	0.727	0.731	0.0098	0.0914
MLB2-40-3	1.43	0.989	1.03	0.650	0.918	0.894	0.820	0.863	0.0096	0.102
MLB2-40-4	1.83	1.05	1.12	0.731	1.01	0.998	0.903	0.963	0.0266	0.115
MLB2-40-5	1.73	1.20	1.41	1.03	1.20	1.223	1.142	1.156	0.0095	0.102
MLB3-40-1	1.11	0.583 ^b	0.0192	-0.0641	0.0231	0.0239	0.0242	0.0245	0.00164	0.00659
MLB3-40-2	1.49	0.558	0.0474	-0.0372	0.0223	0.0247	0.0230	0.0234	0.00192	0.0073
MLB3-40-3	1.57	0.581	0.0502	-0.0319	0.0565	0.0423	0.0397	0.0405	0.00192	0.0125
MLB3-40-4	1.59	0.583	0.0501	-0.0299	0.0382	0.0409	0.0409	0.0407	0.00197	0.0123
MLB3-40-5	1.68	0.614	0.0365	-0.0244	0.0715	0.0753	0.0664	0.0667	0.00213	0.0239
MLB3-40-1 ^a	1.11	0.0098	—	0.0124	—	—	—	—	—	—
MLB3-40-2 ^a	1.49	0.0075	—	0.0156	—	—	—	—	—	—
MLB3-40-3 ^a	1.57	0.0223	—	0.0302	—	—	—	—	—	—
MLB3-40-4 ^a	1.59	0.0252	—	0.0352	—	—	—	—	—	—
MLB3-40-5 ^a	1.68	0.0451	—	0.0648	—	—	—	—	—	—
MLB4-40-1	1.60	0.848	0.0399	-0.0548	0.0259	0.0133	0.0102	0.0077	0.0038	0.0034
MLB4-40-2	1.42	0.830	0.0289	-0.0908	0.0442	0.0152	0.0125	0.0112	0.0037	0.0060
MLB4-40-3	1.61	0.749	0.0479	-0.0320	0.0636	0.0300	0.0209	0.0191	0.0045	0.0085
MLB4-40-4	1.55	0.630	0.0586	-0.0443	0.0724	0.0255	0.0183	0.0160	0.0039	0.0116
MLB4-40-5	1.50	0.626	0.0696	-0.0359	0.0767	0.0391	0.0261	0.0226	0.0043	0.0136
MLB4-40-1 ^a	1.60	0.0127	—	0.0323	—	—	—	—	—	—
MLB4-40-2 ^a	1.42	0.0389	—	0.0225	—	—	—	—	—	—
MLB4-40-3 ^a	1.61	0.0958	—	0.0375	—	—	—	—	—	—
MLB4-40-4 ^a	1.55	0.114	—	0.0543	—	—	—	—	—	—
MLB4-40-5 ^a	1.50	0.0965	—	0.0549	—	—	—	—	—	—
MLB5-40-1	1.51	0.9611	-0.0947	<0.05	0.0295	0.0173	0.0130	0.0120	0.0039	0.0074
MLB5-40-2	1.53	0.839	-0.0770	<0.05	0.0424	0.0021	0.0014	0.0013	0.0042	0.0076
MLB5-40-3	1.50	0.857	-0.0460	<0.05	0.0612	0.0048	0.0034	0.0032	0.0040	0.0108
MLB5-40-4	1.71	0.880	-0.0339	<0.06	0.0625	0.0008	0.0007	0.0008	0.0039	0.0108
MLB5-40-5	1.60	0.802	0.0043	<0.05	0.0703	0.0077	0.0051	0.0047	0.0038	0.0125
MLB5-40-1R	1.51	-0.0163	0.0447	0.0161	0.0263	0.0001	<0.0001	0.0001	<0.0004	0.0040
MLB5-40-2R	1.52	0.0020	0.0847	0.0537	0.0607	0.0001	<0.0001	0.0001	<0.0004	0.0132
MLB5-40-3R	1.53	0.0104	0.1102	0.0544	0.0671	0.0002	<0.0001	0.0001	<0.0004	0.0078
MLB5-40-4R	1.56	0.0176	0.1571	0.0849	0.0907	0.0001	<0.0001	0.0001	<0.0004	0.0092
MLB5-40-5R	1.60	0.0163	0.1298	0.0858	0.0919	0.0002	<0.0001	0.0001	<0.0004	0.0101
MLB6-40-1	1.18	1.82	-0.619	<0.2	0.0392	-0.0017	0.0014	0.0008	0.0114	0.0063
MLB6-40-2	1.15	1.38	-0.651	<0.2	0.0537	-0.0017	0.0022	0.0017	0.0083	0.0085
MLB6-40-3	1.18	1.36	-0.626	<0.2	0.0625	-0.0018	0.0008	0.0006	0.0083	0.0106
MLB6-40-4	1.22	1.20	-0.588	<0.2	0.0809	-0.0014	0.0012	0.0008	0.0081	0.0125
MLB6-40-5	1.24	1.32	-0.519	<0.2	0.1467	-0.0016	0.0011	0.0005	0.0086	0.0193
MLB6-40-1 ^a	1.18	0.0235	—	0.0419	—	—	—	—	—	—
MLB6-40-2 ^a	1.15	0.0448	—	0.0664	—	—	—	—	—	—
MLB6-40-3 ^a	1.18	0.0432	—	0.0622	—	—	—	—	—	—
MLB6-40-4 ^a	1.22	0.0497	—	0.0788	—	—	—	—	—	—
MLB6-40-5 ^a	1.24	0.0957	—	0.146	—	—	—	—	—	—

^aTest solution was reanalyzed without dilution for B and Si concentrations.^bResults from reanalyses of test solution were used.

APPENDIX C: DATA AND RESULTS FOR IMMERSION TESTS AT 70 °C

The test data for the initiation and termination of tests at 70 °C are summarized in Table C1. The data given in each column are summarized below.

Test Number	Test number from test matrix
Specimen Number	Specimen number of monolith used in test
Specimen Area	Surface area of monolith specimen, in cm ²
Leachant Mass	Mass leachant solution used in test, in g
S/V	Specimen surface-area-to-solution volume (S/V) ratio, in m ⁻¹ , calculated as $S / V = \frac{\text{Sample Area, cm}^2}{\text{Leachant mass, g}} \times \frac{1 \text{ g solution}}{1 \text{ cm}^3 \text{ solution}} \times \frac{100 \text{ cm}}{m}$
Vessel No.	Number assigned to test vessel
Vessel Mass	
Initial	Total mass of vessel + leachant + specimen at beginning of test, in g
Final	Total mass of vessel + leachant + specimen at end of test, in g
Change	Change in vessel mass, in g, calculated as <i>Change, g = Final Vessel Mass – Initial Vessel Mass</i>
Adjusted	
Leachant Mass	Change in leachant mass due to change in vessel mass (only calculated if change in vessel mass > 0.02 g)
Effective S/V	S/V ratio calculated with adjusted leachant mass
Date and Time into Oven	Calendar date and time vessel placed into oven
Date and Time out of Oven	Calendar date and time vessel removed from oven
Test Time	Test duration calculated in hours as <i>Test Time = Date and Time out of oven – Date and Time into oven</i>
Test Time, days	Test Time, hours divided by 24 hours per day
pH	pH of test solution measured at room temperature
Solution Bottle	Mass empty 30-mL polyethylene solution bottle, g
Bottle + solution + HNO ₃	Total mass solution bottle, test solution, and 5 drops concentrated HNO ₃ . (Note: the small volume dilution due to addition of HNO ₃ is ignored in calculations.)
Mass Solution	Mass test solution, in g, calculated as <i>mass solution = (mass with solution + HNO₃) – Solution bottle tare</i>
Total Mass Acid	
Soak Solution	Mass demineralized water and HNO ₃ added to vessel after specimen and test solution were removed, in g. (Note. Measured directly.)

The concentrations measured in the test solutions are summarized in Table C2. The concentrations are given in $\mu\text{g/L}$ (parts per billion, ppb). Dashes in the field indicate the solution was not analyzed for that element.

The calculated masses of elements in the test solutions are summarized in Table C3, in μg . The masses are calculated as the product of the leachant mass, in g, given in Table C1 and the concentrations given in Table C2 as

$$\text{mass } i \text{ in test solution, } \mu\text{g} = \text{leachant, g} \times \frac{1 \text{ mL leachant}}{\text{g leachant}} \times \text{concentration } i, \mu\text{g/L} \times \frac{1 \text{ L}}{1000 \text{ mL}}.$$

The concentrations measured in the acid soak solutions are summarized in Table C4. The concentrations are given in $\mu\text{g/L}$ (parts per billion, ppb). Dashes in the field indicate the solution was not analyzed for that element.

The calculated masses of elements in the acid soak solutions are summarized in Table C5, in μg . The masses are calculated as the product of the mass acid soak solution, in g, from Table C1 and the concentrations given in Table C4 as

$$\text{mass } i \text{ in acid soak solution, } \mu\text{g} = \text{mass acid soak, g} \times \frac{1 \text{ mL solution}}{\text{g solution}} \times \text{concentration } i, \mu\text{g/L} \times \frac{1 \text{ L}}{1000 \text{ mL}}.$$

Entries of "not det." indicate that the acid soak was not performed for that test.

The normalized elemental mass losses are summarized in Table C6, in g/m^2 . The normalized elemental mass loss was calculated as

$$NL(i) = \frac{\text{mass in test solution} - \text{mass in blank} \left(\frac{\text{blank solution}}{\text{test solution}} \right) + \text{mass in acid soak solution}}{\text{Sample Area} \times \text{Mass fraction in glass}}.$$

The mass measured in the blank test was scaled by the amounts of solution used in the test and the blank test because those amounts differed significantly in some cases.

The mass fractions of elements in the Pu LaBS-B glass used in the calculations are:

B = 0.0326
Al = 0.1020
Si = 0.1222
Sr = 0.0192
La = 0.0626
Nd = 0.0636
Gd = 0.1005
Hf = 0.0526
Pu = 0.0840

Negative values indicate that the concentration in the blank test exceeded the sum of the concentrations in the test solution and acid soak solutions. Less-than values indicate that the analyzed concentration in the test solution, the acid soak solution, or both, were below the detection limit, and the values of NL provide

upper bounds. Values shown as strike-outs were not used in analyses, and were replaced by re-run tests or re-analyses of solutions. Calculated values are given to the four decimal place or 3 significant figures.

Table C1. Test Data for Tests at 70 °C

Test Number	Specimen Number	Specimen Area, cm ²	Leachant mass, g	S/V, m ⁻¹	Vessel No.	Vessel Mass			Adjusted leachant mass, g	Effective S/V, m ⁻¹
						Initial, g	Final, g	Change, g		
MLB1-70-1	21	1.42	61.20	2.32	114	252.91	252.90	-0.01	61.20	2.32
MLB1-70-2	40	1.19	50.57	2.35	109	237.51	237.50	-0.01	50.57	2.35
MLB1-70-3	54	1.09	46.69	2.33	44	176.29	176.23	-0.06	46.63	2.34
MLB1-70-4	49	1.29	56.53	2.28	116	244.51	244.49	-0.02	56.53	2.28
MLB1-70-5	51	1.23	53.21	2.31	115	244.23	244.20	-0.03	53.21	2.31
MLB1-70-B1	—	—	51.99	—	117	242.57	242.56	-0.01	51.99	—
MLB2-70-1	7	1.72	35.83	4.80	69	164.60	164.59	-0.01	35.83	4.80
MLB2-70-2	8	1.48	30.47	4.84	46	159.88	159.87	-0.01	30.47	4.84
MLB2-70-3	9	1.56	32.25	4.83	47	160.67	160.64	-0.03	32.25	4.83
MLB2-70-4	10	1.93	37.08	5.17	5	167.23	167.08	-0.15	37.08	5.20
MLB2-70-5	12	1.52	31.55	4.82	4	159.53	159.51	-0.02	31.55	4.82
MLB2-70- B1	—	—	33.35	—	6	163.39	163.33	-0.06	33.25	—
MLB3-70-1	39	1.11	22.81	4.86	72	151.25	151.22	-0.03	22.81	4.87
MLB3-70-2	33	1.72	36.05	4.77	52	165.00	164.96	-0.04	36.05	4.77
MLB3-70-3	36	1.62	33.38	4.83	53	162.77	162.58	-0.19	33.38	4.85
MLB3-70-4	38	1.54	30.43	5.06	14	158.53	158.52	-0.01	30.43	5.06
MLB3-70-5	41	1.55	32.25	4.80	13	162.93	162.90	-0.03	32.25	4.81
MLB3-70-B1	—	—	34.03	—	15	161.66	161.65	-0.01	34.03	—
MLB4-70-1	58	1.57	32.56	4.82	75	162.94	162.94	0.00	32.56	4.82
MLB4-70-2	60	1.56	32.56	4.79	58	163.00	162.98	-0.02	32.56	4.79
MLB4-70-3	61	1.51	31.20	4.84	59	159.66	159.66	0.00	31.20	4.84
MLB4-70-4	63	1.52	31.57	4.81	23	158.98	158.94	-0.04	31.57	4.81
MLB4-70-5	64	1.49	30.87	4.83	22	158.65	158.65	0.00	30.87	4.83
MLB4-70-B1	—	—	33.29	—	24	162.57	162.57	0.00	33.29	—
MLB5-70-1	76	1.70	36.09	4.71	78	167.46	167.46	0.00	36.09	4.71
MLB5-70-2	77	1.81	38.13	4.74	64	167.33	167.30	-0.03	38.13	4.75
MLB5-70-3	79	1.69	36.35	4.63	65	167.04	166.89	-0.15	36.37	4.65
MLB5-70-4	81	1.58	33.23	4.73	32	161.02	160.86	-0.16	33.23	4.75
MLB5-70-5	82	1.48	31.29	4.73	31	160.93	160.90	-0.03	31.29	4.73
MLB5-70-B1	—	—	30.37	—	33	159.44	159.44	0.00	30.37	—
MLB5-70-1R	106	1.62	34.41	4.70	21	162.46	162.44	-0.02	50.00	4.70
MLB5-70-2R	116	1.63	34.64	4.70	81	165.79	165.79	0.00	50.84	4.70
MLB5-70-3R	118	1.63	34.73	4.70	30	162.17	162.15	-0.02	53.55	4.70
MLB5-70-4R	105	1.69	35.86	4.70	24	165.32	165.31	-0.01	51.96	4.70
MLB5-70-5R	109	1.71	36.30	4.70	6	166.47	166.38	-0.09	53.09	4.71
MLB5-70-BR	—	—	27.55	—	41	158.06	157.54	-0.52	60.24	—
MLB6-70-1	25	1.22	50.00	2.44	80	180.90	180.89	-0.01	61.20	2.44
MLB6-70-2	34	1.24	50.84	2.44	107	241.96	241.94	-0.02	50.57	2.44
MLB6-70-3	52	1.33	53.55	2.48	108	241.62	241.61	-0.01	46.63	2.48
MLB6-70-4	90	1.23	51.99	2.37	125	243.11	243.08	-0.03	56.53	2.37
MLB6-70-5	98	1.32	53.16	2.48	124	243.83	243.76	-0.07	53.21	2.49
MLB6-70-B1	—	—	60.24	—	126	250.07	250.06	-0.01	51.99	—

Table C1. (cont.)

Test Number	Date and Time into oven	Date and Time out of oven	Test Time, hours	Test Time, days	pH (room temp.)	Solution bottle tare, g	Bottle + solution + HNO ₃ , g	Mass solution, g	Total mass acid soak solution, g
MLB1-70-1	2/8/06 13:15	2/9/06 12:20	23.17	0.97	3.70	11.17	39.74	28.57	82.36
MLB1-70-2	1/30/06 14:00	2/1/06 12:35	46.58	1.94	3.73	11.19	36.41	25.22	83.56
MLB1-70-3	1/30/06 14:00	2/2/06 12:30	70.50	2.94	3.73	11.13	35.15	24.02	35.46
MLB1-70-4	1/27/06 15:00	1/31/06 12:15	93.25	3.89	3.73	11.15	39.36	28.21	85.52
MLB1-70-5	1/27/06 15:00	2/1/06 12:35	117.58	4.90	3.74	11.19	35.43	24.24	82.78
MLB1-70-B1	1/27/06 15:10	2/1/06 12:35	117.42	4.89	3.72	11.16	38.12	26.96	not det.
MLB2-70-1	2/8/06 13:15	2/9/06 12:20	23.17	0.97	4.86	11.17	37.34	26.17	39.70
MLB2-70-2	1/30/06 14:00	2/1/06 12:35	46.58	1.94	4.89	11.15	35.03	23.88	34.35
MLB2-70-3	1/30/06 14:00	2/2/06 12:30	70.50	2.94	4.89	11.19	37.50	26.31	32.96
MLB2-70-4	1/27/06 15:00	1/31/06 12:15	93.25	3.89	4.90	11.14	39.00	27.86	42.95
MLB2-70-5	1/27/06 15:00	2/1/06 12:35	117.58	4.90	4.90	10.95	36.97	26.02	40.39
MLB2-70- B1	1/27/06 15:10	2/1/06 12:35	117.42	4.89	4.88	11.15	33.89	22.74	not det.
MLB3-70-1	2/8/06 13:15	2/9/06 12:20	23.17	0.97	6.07	11.21	33.70	22.49	30.88
MLB3-70-2	1/30/06 14:00	2/1/06 12:35	46.58	1.94	6.10	11.16	34.67	23.51	34.01
MLB3-70-3	1/30/06 14:00	2/2/06 12:30	70.50	2.94	6.10	11.20	36.19	24.99	37.75
MLB3-70-4	1/27/06 15:00	1/31/06 12:15	93.25	3.89	6.10	11.12	35.89	24.77	38.89
MLB3-70-5	1/27/06 15:00	2/1/06 12:35	117.58	4.90	6.11	11.17	37.38	26.21	38.70
MLB3-70-B1	1/27/06 15:10	2/1/06 12:35	117.42	4.89	6.10	11.16	36.97	25.81	not det.
MLB4-70-1	2/8/06 13:15	2/9/06 12:20	23.17	0.97	8.56	11.16	34.90	23.74	32.32
MLB4-70-2	1/30/06 14:00	2/1/06 12:35	46.58	1.94	8.58	11.20	35.92	24.72	35.31
MLB4-70-3	1/30/06 14:00	2/2/06 12:30	70.50	2.94	8.58	11.22	35.60	24.38	36.52
MLB4-70-4	1/27/06 15:00	1/31/06 12:15	93.25	3.89	8.58	10.98	34.47	23.49	41.46
MLB4-70-5	1/27/06 15:00	2/1/06 12:35	117.58	4.90	8.58	11.18	34.86	23.68	35.38
MLB4-70-B1	1/27/06 15:10	2/1/06 12:35	117.42	4.89	8.59	11.14	34.98	23.84	not det.
MLB5-70-1	2/8/06 13:15	2/9/06 12:20	23.17	0.97	7.79	11.22	37.07	25.85	33.29
MLB5-70-2	1/30/06 14:00	2/1/06 12:35	46.58	1.94	not meas.	11.23	11.41	0.18	35.78
MLB5-70-3	1/30/06 14:00	2/2/06 12:30	70.50	2.94	9.07	11.20	37.70	26.50	32.94
MLB5-70-4	1/27/06 15:00	1/31/06 12:15	93.25	3.89	8.27	11.19	34.92	23.73	38.05
MLB5-70-5	1/27/06 15:00	2/1/06 12:35	117.58	4.90	8.02	11.13	36.30	25.17	36.66
MLB5-70-B1	1/27/06 15:10	2/1/06 12:35	117.42	4.89	9.30	11.13	34.50	23.37	not det.
MLB5-70-1R	3/1/06 16:00	3/2/06 11:00	19.00	0.79	9.39	11.19	35.23	24.04	not det.
MLB5-70-2R	3/1/06 16:00	3/3/06 12:30	44.50	1.85	9.22	11.15	35.49	24.34	not det.
MLB5-70-3R	3/3/06 11:15	3/6/06 12:30	73.25	3.05	9.49	11.18	38.26	27.08	not det.
MLB5-70-4R	3/2/06 11:00	3/6/06 12:30	97.50	4.06	9.37	11.22	40.06	28.84	not det.
MLB5-70-5R	3/1/06 16:00	3/6/06 12:30	116.50	4.85	9.39	11.20	40.60	29.40	not det.
MLB5-70-BR	3/1/06 16:00	3/6/06 12:30	116.50	4.85	not meas.	11.19	34.65	23.46	not det.
MLB6-70-1	2/8/06 13:15	2/9/06 12:20	23.17	0.97	10.97	11.16	36.84	25.68	31.71
MLB6-70-2	1/30/06 14:00	2/1/06 12:35	46.58	1.94	10.87	11.16	35.69	24.53	84.33
MLB6-70-3	1/30/06 14:00	2/2/06 12:30	70.50	2.94	10.90	11.20	37.80	26.60	81.40
MLB6-70-4	1/27/06 15:00	1/31/06 12:15	93.25	3.89	10.85	11.15	34.10	22.95	77.86
MLB6-70-5	1/27/06 15:00	2/1/06 12:35	117.58	4.90	10.83	11.16	38.64	27.48	83.82
MLB6-70-B1	1/27/06 15:10	2/1/06 12:35	117.42	4.89	11.01	11.18	39.74	28.56	not det.

Table C2. Results of Static Dissolution Tests at 70 °C: Measured Concentrations in Test Solutions, µg/L

Test Number	Concentration measured in test solution, µg/L								
	B	Al	Si	Sr	La	Nd	Gd	Hf	Pu 239
MLB1-70-1	272	863	1530	171	614	557	945	2.73	85
MLB1-70-2	551	1890	2700	307	1270	1260	2020	2.76	86.9
MLB1-70-3	642	2170	3030	348	1430	1360	2250	3.25	101
MLB1-70-4	749	2380	3290	383	1570	1520	2510	3.4	115
MLB1-70-5	884	2940	3930	478	1940	1840	3050	3.55	91.8
MLB1-70-B1	98	18.4	850	<0.15	0.051	0.054	<0.06	<0.19	<0.03
MLB2-70-1	184	263	401	42.3	161	162	244	0.882	7.49
MLB2-70-2	178	432	624	75.5	284	264	429	1.08	8.68
MLB2-70-3	171	500	672	89.3	319	297	511	0.964	6.7
MLB2-70-4	199	675	883	110	405	383	647	1.13	6.96
MLB2-70-5	214	768	1060	120	434	450	711	1.13	5.92
MLB2-70- B1	81.5	56.3	106	<0.15	0.053	0.117	<0.06	<0.19	<0.03
MLB3-70-1	30	68.5	167	9.51	28.9	27.3	42.5	0.355	5.43
MLB3-70-2	53.4	13.9	350	32.5	104	92.6	139	<0.21	14.8
MLB3-70-3	40.8	128	251	20.4	64.2	60.3	93.8	<0.21	10.6
MLB3-70-4	43.1	122	265	21.5	67.7	63.5	97.5	<0.21	14
MLB3-70-5	59.9	57.3	401	37.4	111	108	167	<0.21	28.1
MLB3-70-B1	31.2	22.9	141	0.18	0.055	0.112	<0.05	<0.21	<0.01
MLB4-70-1	78.9	72.3	358	8	7.19	3.71	4.35	<0.21	3.8
MLB4-70-2	75.8	108	352	13.6	9.77	4.06	4.07	<0.21	8.93
MLB4-70-3	79	150	436	19.5	17.3	8.63	9.74	<0.21	12.1
MLB4-70-4	76.8	144	412	17.2	16.6	7.77	7.59	<0.21	12.7
MLB4-70-5	83.6	200	491	22.8	9.22	3.12	2.07	<0.21	21.5
MLB4-70-B1	56.8	47	252	<0.06	0.019	<0.05	<0.05	<0.21	<0.01
MLB5-70-1	11.9	67.6	58.7	8.07	1.25	0.621	0.728	<0.21	6.19
MLB5-70-2	2.55	9.23	<17.1	0.508	0.261	0.212	0.376	<0.21	0.492
MLB5-70-3	19.3	122	109	14.9	1.04	0.466	0.511	<0.21	13.9
MLB5-70-4	28.5	318	170	23.4	0.332	0.165	0.163	<0.21	15.9
MLB5-70-5	22.4	358	142	17.8	0.359	0.152	0.178	<0.21	12.7
MLB5-70-B1	5.1	150	<17.1	0.063	<0.01	<0.05	<0.05	<0.21	<0.01
MLB5-70-1R	30.9	245	122	14.7	0.174	0.121	0.098	<0.09	8.32
MLB5-70-2R	22.9	91.5	79.0	12.1	0.452	0.211	0.261	<0.09	11.9
MLB5-70-3R	20.7	99.7	83.3	12.6	0.128	0.076	0.122	<0.09	11.7
MLB5-70-4R	37.00	410	189	26.3	0.101	0.055	0.078	<0.09	13.7
MLB5-70-5R	28.1	286	145	20.1	0.169	0.081	0.079	<0.09	17.2
MLB5-70-BR	9.17	127	<9.1	0.075	0.021	<0.04	<0.04	<0.09	<0.02
MLB6-70-1	27.5	101	67.8	8.06	0.038	0.067	0.057	<0.21	1.98
MLB6-70-2	37	189	150	22.1	0.132	0.128	0.203	<0.21	3.59
MLB6-70-3	49	300	254	36.4	0.038	<0.05	<0.05	<0.21	5.4
MLB6-70-4	64.1	307	337	50.2	0.387	0.367	0.563	<0.21	6.06
MLB6-70-5	56.8	366	309	46.1	0.092	0.078	0.095	<0.21	7.49
MLB6-70-B1	3.43	4.69	<17.1	0.097	<0.01	<0.05	<0.05	<0.21	<0.01

Table C3. Results of Static Dissolution Tests at 70 °C: Calculated Masses in Test Solutions, µg

Test Number	Mass leachant, g	Mass in test solution, µg								
		B	Al	Si	Sr	La	Nd	Gd	Hf	Pu-239
MLB1-70-1	61.20	16.6	52.8	93.6	10.5	37.6	34.1	57.8	0.167	5.20
MLB1-70-2	50.57	27.9	95.6	137	15.5	64.2	63.7	102	0.140	4.40
MLB1-70-3	46.63	29.9	101	141	16.2	66.7	63.4	105	0.152	4.71
MLB1-70-4	56.53	42.3	135	186	21.7	88.8	85.9	142	0.192	6.50
MLB1-70-5	53.21	47.0	156	209	25.4	103	97.9	162	0.189	4.89
MLB1-70-B1	51.99	5.09	0.957	44.2	<0.008	0.0027	0.0028	<0.004	<0.01	<0.002
MLB2-70-1	35.83	6.59	9.42	14.4	1.52	5.77	5.80	8.74	0.0316	0.268
MLB2-70-2	30.47	5.42	13.2	19.0	2.30	8.65	8.05	13.1	0.0329	0.265
MLB2-70-3	32.25	5.51	16.1	21.7	2.88	10.3	9.58	16.5	0.0311	0.216
MLB2-70-4	37.08	7.38	25.0	32.7	4.08	15.0	14.2	24.0	0.0419	0.258
MLB2-70-5	31.55	6.75	24.2	33.4	3.79	13.7	14.2	22.4	0.0357	0.187
MLB2-70- B1	33.25	2.71	1.87	3.52	<0.005	0.0018	0.0039	<0.002	<0.007	<0.001
MLB3-70-1	22.81	0.684	1.56	3.81	0.217	0.659	0.623	0.969	0.0081	0.124
MLB3-70-2	36.05	1.93	0.501	12.6	1.17	3.75	3.34	5.01	<0.008	0.534
MLB3-70-3	33.38	1.36	4.27	8.38	0.681	2.14	2.01	3.13	<0.007	0.354
MLB3-70-4	30.43	1.31	3.71	8.06	0.654	2.06	1.93	2.97	<0.006	0.426
MLB3-70-5	32.25	1.93	1.85	12.9	1.21	3.58	3.48	5.39	<0.007	0.906
MLB3-70-B1	34.03	1.06	0.779	4.80	0.0061	0.0019	0.0038	<0.002	<0.007	<0.0004
MLB4-70-1	32.56	2.57	2.35	11.7	0.260	0.234	0.121	0.142	<0.007	0.124
MLB4-70-2	32.56	2.47	3.52	11.5	0.443	0.318	0.132	0.133	<0.007	0.291
MLB4-70-3	31.20	2.46	4.68	13.6	0.608	0.540	0.269	0.304	<0.007	0.378
MLB4-70-4	31.57	2.43	4.55	13.0	0.543	0.524	0.245	0.240	<0.007	0.401
MLB4-70-5	30.87	2.58	6.17	15.2	0.704	0.285	0.0963	0.064	<0.006	0.664
MLB4-70-B1	33.29	1.89	1.56	8.39	<0.002	0.0006	<0.002	<0.002	<0.007	<0.0003
MLB5-70-1	36.09	0.429	2.44	2.12	0.291	0.0451	0.0224	0.0263	<0.008	0.223
MLB5-70-2	38.13	0.0972	0.352	<0.7	0.0194	0.0100	0.0081	0.0143	<0.008	0.0188
MLB5-70-3	36.35	0.702	4.44	3.96	0.542	0.0378	0.0169	0.0186	<0.008	0.505
MLB5-70-4	33.23	0.947	10.6	5.65	0.778	0.0110	0.0055	0.0054	<0.007	0.528
MLB5-70-5	31.29	0.701	11.2	4.44	0.557	0.0112	0.0048	0.0056	<0.007	0.397
MLB5-70-B1	30.37	0.155	4.56	<0.6	0.0019	<0.0003	<0.002	<0.002	<0.007	<0.0003
MLB5-70-1R	34.39	1.06	8.43	4.20	0.506	0.0060	0.0042	0.0034	<0.003	0.286
MLB5-70-2R	34.64	0.793	3.17	2.74	0.419	0.0157	0.0073	0.0090	<0.003	0.412
MLB5-70-3R	34.71	0.718	3.46	2.89	0.437	0.0044	0.0026	0.0042	<0.003	0.406
MLB5-70-4R	35.85	1.33	14.7	6.78	0.943	0.0036	0.0020	0.0028	<0.003	0.491
MLB5-70-5R	36.21	1.02	10.4	5.25	0.728	0.0061	0.0029	0.0029	<0.003	0.623
MLB5-70-BR	27.03	0.248	3.43	<0.3	0.0020	0.0006	<0.002	<0.002	<0.003	<0.0005
MLB6-70-1	50.00	1.38	5.05	3.39	0.403	0.0019	0.0034	0.0029	<0.02	0.0990
MLB6-70-2	50.84	1.88	9.61	7.63	1.12	0.0067	0.0065	0.0103	<0.02	0.183
MLB6-70-3	53.55	2.62	16.1	13.6	1.95	0.0020	<0.003	<0.003	<0.02	0.289
MLB6-70-4	51.96	3.33	16.0	17.5	2.61	0.0201	0.0191	0.0293	<0.02	0.315
MLB6-70-5	53.09	3.02	19.4	16.4	2.45	0.0049	0.0041	0.0050	<0.02	0.398
MLB6-70-B1	60.24	0.207	0.283	<1.0	0.0058	<0.0006	<0.003	<0.003	<0.02	<0.0006

Table C4. Results of Static Dissolution Tests at 70 °C: Measured Concentrations in Acid Soak Solutions, µg/L

Test Number	Concentration measured in acid soak solution, µg/L						
	Si	Sr	La	Nd	Gd	Hf	Pu 239
MLB1-70-1	<12.5	0.198	0.048	<0.06	0.057	3.38	34.2
MLB1-70-2	<12.5	<0.15	0.039	0.078	0.091	2.23	56.4
MLB1-70-3	<12.5	<0.15	0.062	0.087	0.099	12.1	86.9
MLB1-70-4	<12.5	0.981	0.053	<0.06	0.065	3.82	56.8
MLB1-70-5	<12.5	0.166	0.060	<0.06	0.114	2.31	72.7
MLB1-70-B1	not det.	not det.	not det.	not det.	not det.	not det.	not det.
MLB2-70-1	<12.5	<0.15	0.094	0.107	0.158	1.50	5.98
MLB2-70-2	<12.5	<0.15	0.254	0.282	0.500	2.15	11.7
MLB2-70-3	<12.5	<0.15	0.264	0.331	0.439	6.78	19.1
MLB2-70-4	<12.5	<0.15	0.245	0.318	0.514	4.32	17.7
MLB2-70-5	<12.5	<0.15	0.319	0.400	0.758	2.78	20.8
MLB2-70- B1	not det.	not det.	not det.	not det.	not det.	not det.	not det.
MLB3-70-1	<12.5	<0.15	0.219	0.281	0.442	<0.05	0.139
MLB3-70-2	<12.5	<0.15	1.48	2.91	9.35	<0.05	0.559
MLB3-70-3	<12.5	<0.15	0.207	0.309	0.586	<0.05	0.157
MLB3-70-4	<12.5	<0.15	0.670	1.06	1.98	<0.05	0.736
MLB3-70-5	<12.5	<0.15	0.637	1.17	3.09	<0.05	0.327
MLB3-70-B1	not det.	not det.	not det.	not det.	not det.	not det.	not det.
MLB4-70-1	<12.5	<0.15	0.460	0.362	0.541	0.084	<0.11
MLB4-70-2	<12.5	<0.15	6.13	4.21	5.92	0.064	<0.11
MLB4-70-3	<12.5	<0.15	2.55	2.37	3.99	<0.05	<0.11
MLB4-70-4	<12.5	<0.15	1.38	1.36	2.84	<0.05	<0.11
MLB4-70-5	<12.5	0.197	14.0	12.1	17.3	<0.05	0.764
MLB4-70-B1	not det.	not det.	not det.	not det.	not det.	not det.	not det.
MLB5-70-1	<12.5	<0.15	0.763	0.590	0.886	<0.05	<0.11
MLB5-70-2	<12.5	<0.15	0.325	0.229	0.340	<0.05	<0.11
MLB5-70-3	<12.5	<0.15	0.285	0.220	0.324	<0.05	<0.11
MLB5-70-4	<12.5	<0.15	1.96	1.19	1.67	<0.05	0.951
MLB5-70-5	<12.5	<0.15	4.17	2.91	3.77	<0.05	1.14
MLB5-70-B1	not det.	not det.	not det.	not det.	not det.	not det.	not det.
MLB5-70-1R	not det.	not det.	not det.	not det.	not det.	not det.	not det.
MLB5-70-2R	not det.	not det.	not det.	not det.	not det.	not det.	not det.
MLB5-70-3R	not det.	not det.	not det.	not det.	not det.	not det.	not det.
MLB5-70-4R	not det.	not det.	not det.	not det.	not det.	not det.	not det.
MLB5-70-5R	not det.	not det.	not det.	not det.	not det.	not det.	not det.
MLB5-70-BR	not det.	not det.	not det.	not det.	not det.	not det.	not det.
MLB6-70-1	<12.5	<0.15	0.071	<0.06	0.083	<0.05	<0.11
MLB6-70-2	<12.5	<0.15	0.051	<0.06	<0.05	<0.05	<0.11
MLB6-70-3	<12.5	0.174	0.084	0.094	0.097	<0.05	<0.11
MLB6-70-4	<12.5	<0.15	0.194	0.177	0.290	0.096	<0.11
MLB6-70-5	<12.5	<0.15	0.033	<0.06	0.065	<0.05	<0.11
MLB6-70-B1	not det.	not det.	not det.	not det.	not det.	not det.	not det.

Table C5. Results of Static Dissolution Tests at 70 °C: Calculated Masses in Acid Soak Solutions, µg

Test No.	Mass acid soak solution, g	Mass in acid soak solution, µg						
		Si	Sr	La	Nd	Gd	Hf	Pu 239
MLB1-70-1	82.36	<1.1	0.0163	0.0040	<0.005	0.0047	0.278	2.82
MLB1-70-2	83.56	<1.1	<0.02	0.0033	0.0065	0.0076	0.186	4.71
MLB1-70-3	35.46	<0.5	<0.005	0.0022	0.0031	0.0035	0.429	3.08
MLB1-70-4	85.52	<1.1	0.084	0.0045	<0.006	0.0056	0.327	4.86
MLB1-70-5	82.78	<1.0	0.014	0.0050	<0.005	0.0094	0.191	6.02
MLB2-70-1	39.70	<0.5	<0.006	0.0037	0.0042	0.0063	0.0596	0.237
MLB2-70-2	34.35	<0.5	<0.005	0.0087	0.0097	0.0172	0.0739	0.402
MLB2-70-3	32.96	<0.5	<0.005	0.0087	0.0109	0.0145	0.224	0.630
MLB2-70-4	42.95	<0.6	<0.006	0.0105	0.0137	0.0221	0.186	0.760
MLB2-70-5	40.39	<0.5	<0.006	0.0129	0.0162	0.0306	0.112	0.840
MLB3-70-1	30.88	<0.4	<0.005	0.0068	0.0087	0.0136	<0.002	0.0043
MLB3-70-2	34.01	<0.5	<0.005	0.0503	0.0990	0.318	<0.002	0.0190
MLB3-70-3	37.75	<0.5	<0.006	0.0078	0.0117	0.0221	<0.002	0.0059
MLB3-70-4	38.89	<0.5	<0.006	0.0261	0.0412	0.0770	<0.002	0.0286
MLB3-70-5	38.70	<0.5	<0.006	0.0247	0.0453	0.120	<0.002	0.0127
MLB4-70-1	32.32	<0.4	<0.005	0.0149	0.0117	0.0175	0.0027	<0.004
MLB4-70-2	35.31	<0.5	<0.005	0.216	0.1487	0.209	0.0023	<0.004
MLB4-70-3	36.52	<0.5	<0.005	0.0931	0.0866	0.146	<0.002	<0.004
MLB4-70-4	41.46	<0.6	<0.006	0.0572	0.0564	0.118	<0.002	<0.005
MLB4-70-5	35.38	<0.5	0.0070	0.495	0.428	0.612	<0.002	0.0270
MLB5-70-1	33.29	<0.5	<0.005	0.0254	0.0196	0.0295	<0.002	<0.004
MLB5-70-2	35.78	<0.5	<0.005	0.0116	0.0082	0.0122	<0.002	<0.004
MLB5-70-3	32.94	<0.5	<0.005	0.0094	0.0072	0.0107	<0.002	<0.004
MLB5-70-4	38.05	<0.5	<0.006	0.0746	0.0453	0.0635	<0.002	0.0362
MLB5-70-5	36.66	<0.5	<0.006	0.153	0.107	0.138	<0.002	0.0418
MLB6-70-1	31.71	<0.4	<0.005	0.0023	<0.002	0.0026	<0.002	<0.003
MLB6-70-2	84.33	<1.1	<0.013	0.0043	<0.005	<0.004	<0.004	<0.009
MLB6-70-3	81.40	<1.0	0.0142	0.0068	0.0077	0.0079	<0.004	<0.009
MLB6-70-4	77.86	<1.0	<0.02	0.0151	0.0138	0.0226	0.0075	<0.009
MLB6-70-5	83.82	<1.1	<0.02	0.0028	<0.005	0.0054	<0.004	<0.009

Table C6. Results of Static Dissolution Tests at 70 °C: Normalized Elemental Mass Losses, g/m²

Test Number	Specimen Area, cm ²	Normalized elemental mass loss, g/m ²								
		B	Al	Si	Sr	La	Nd	Gd	Hf	Pu-239
MLB1-70-1	1.42	2.30	3.57	2.40	3.84	4.23	3.77	4.05	0.0583	0.672
MLB1-70-2	1.19	5.91	7.80	6.43	6.80	8.62	8.42	8.54	0.0505	0.911
MLB1-70-3	1.09	7.14	9.02	7.63	7.75	9.77	9.15	9.58	0.0995	0.851
MLB1-70-4	1.29	8.75	10.1	8.75	8.77	11.0	10.5	10.9	0.0750	1.05
MLB1-70-5	1.23	10.4	12.4	10.9	10.8	13.4	12.5	13.1	0.0572	1.06
MLB2-70-1	1.72	0.655	0.422	0.503	0.461	0.536	0.531	0.506	0.0101	0.0350
MLB2-70-2	1.48	0.611	0.761	0.876	0.814	0.938	0.858	0.883	0.0138	0.0538
MLB2-70-3	1.56	0.568	0.900	0.958	0.964	1.06	0.967	1.05	0.0310	0.0646
MLB2-70-4	1.93	0.694	1.17	1.22	1.10	1.25	1.16	1.24	0.0224	0.0629
MLB2-70-5	1.52	0.844	1.45	1.62	1.30	1.44	1.47	1.47	0.0185	0.0804
MLB3-70-1	1.11	-0.0076	0.0919	0.0437	0.102	0.0957	0.0891	0.0880	0.0008	0.0137
MLB3-70-2	1.72	0.143	-0.0185	0.359	0.354	0.353	0.314	0.308	<0.0008	0.0382
MLB3-70-3	1.62	0.0607	0.212	0.186	0.219	0.212	0.196	0.194	<0.0008	0.0264
MLB3-70-4	1.54	0.0721	0.192	0.201	0.221	0.216	0.201	0.197	<0.0008	0.0351
MLB3-70-5	1.55	0.183	0.0702	0.443	0.405	0.371	0.358	0.353	<0.0008	0.0705
MLB4-70-1	1.57	0.141	0.0514	0.180	0.0880	0.0253	0.0133	0.0101	0.0003	0.0097
MLB4-70-2	1.56	0.122	0.125	0.171	0.145	0.0547	0.0283	0.0218	0.0003	0.0225
MLB4-70-3	1.51	0.141	0.209	0.311	0.212	0.0670	0.0371	0.0296	<0.0008	0.0301
MLB4-70-4	1.52	0.127	0.198	0.272	0.188	0.0611	0.0312	0.0234	<0.0008	0.0318
MLB4-70-5	1.49	0.170	0.311	0.405	0.248	0.0836	0.0553	0.0451	<0.0008	0.0552
MLB5-70-1	1.70	0.0443	-0.172	0.102	0.0901	0.0066	0.0037	0.0032	<0.0008	0.0159
MLB5-70-2	1.81	-0.0165	-0.291	<0.03	0.0064	0.0019	0.0012	0.0014	<0.0008	0.0015
MLB5-70-3	1.69	0.0937	-0.0591	0.192	0.168	0.0044	0.0021	0.0016	<0.0009	0.0358
MLB5-70-4	1.58	0.151	0.346	0.293	0.258	0.0086	0.0049	0.0042	<0.0008	0.0425
MLB5-70-5	1.48	0.112	0.431	0.246	0.197	0.0177	0.0117	0.0096	<0.0008	0.0353
MLB5-70-1R	1.62	0.142	0.246	0.212	0.162	0.0005	0.0003	0.0001	<0.0004	0.0210
MLB5-70-2R	1.63	0.0896	-0.0741	0.138	0.133	0.0015	0.0006	0.0005	<0.0004	0.0301
MLB5-70-3R	1.63	0.0752	-0.0569	0.145	0.139	0.0004	0.0001	0.0002	<0.0004	0.0296
MLB5-70-4R	1.69	0.182	0.590	0.329	0.290	0.0003	0.0001	0.0001	<0.0004	0.0346
MLB5-70-5R	1.71	0.123	0.331	0.252	0.221	0.0005	0.0001	0.0001	<0.0004	0.0434
MLB6-70-1	1.22	0.303	0.387	0.227	0.172	0.0005	0.0004	0.0002	<0.002	0.0100
MLB6-70-2	1.24	0.422	0.741	0.503	0.475	0.0014	0.0014	0.0010	<0.002	0.0184
MLB6-70-3	1.33	0.563	1.17	0.837	0.767	0.0010	0.00009	0.0006	<0.002	0.0266
MLB6-70-4	1.23	0.786	1.25	1.17	1.11	0.0045	0.0039	0.0024	0.0012	0.0313
MLB6-70-5	1.32	0.658	1.42	1.02	0.969	0.0009	0.0008	0.0004	<0.002	0.0366

APPENDIX D: DATA AND RESULTS FOR IMMERSION TESTS AT 90 °C

The test data for the initiation and termination of tests at 90 °C are summarized in Table D1. The data given in each column are summarized below

Test Number	Test number from test matrix
Specimen Number	Specimen number of monolith used in test
Specimen Area	Surface area of monolith specimen, in cm ²
Leachant Mass	Mass leachant solution used in test, in g
S/V	Specimen surface-area-to-solution volume (S/V) ratio, in m ⁻¹ , calculated as $S / V = \frac{\text{Sample Area, cm}^2}{\text{Leachant mass, g}} \times \frac{1 \text{ g solution}}{1 \text{ cm}^3 \text{ solution}} \times \frac{100 \text{ cm}}{m}$
Vessel No.	Number assigned to test vessel
Vessel Mass	
Initial	Total mass of vessel + leachant + specimen at beginning of test, in g
Final	Total mass of vessel + leachant + specimen at end of test, in g
Change	Change in vessel mass, in g, calculated as <i>Change, g = Final Vessel Mass – Initial Vessel Mass</i>
Adjusted	
Leachant Mass	Change in leachant mass due to change in vessel mass (only calculated if change in vessel mass > 0.02 g)
Effective S/V	S/V ratio calculated with adjusted leachant mass
Date and Time into Oven	Calendar date and time vessel placed into oven
Date and Time out of Oven	Calendar date and time vessel removed from oven
Test Time	Test duration calculated in hours as <i>Test Time = Date and Time out of oven – Date and Time into oven</i>
Test Time, days	Test Time, hours divided by 24 hours per day
pH	pH of test solution measured at room temperature
Solution Botle	Mass empty 30-mL polyethylene solution bottle, g
Bottle + solution + HNO ₃	Total mass solution bottle, test solution, and 5 drops concentrated HNO ₃ . (Note: the small volume dilution due to addition of HNO ₃ is ignored in calculations.)
Mass Slution	Mass test solution, in g, calculated as <i>mass solution = (mass with solution + HNO₃) – Solution bottle tare</i>
Total Mass Acid	
Soak Solution	Mass demineralized water and HNO ₃ added to vessel after specimen and test solution were removed, in g. (Note. Measured directly.)

The concentrations measured in the test solutions are summarized in Table D2. The concentrations are given in µg/L (parts per billion, ppb). Dashes in the field indicate the solution was not analyzed for that element.

The calculated masses of elements in the test solutions are summarized in Table D3, in µg. The masses are calculated as the product of the leachant mass, in g, given in Table D1 and the concentrations given in Table D2 as

$$\text{mass } i \text{ in test solution, } \mu\text{g} = \text{leachant, g} \times \frac{1 \text{ mL leachant}}{\text{g leachant}} \times \text{concentration } i, \mu\text{g/L} \times \frac{1 \text{ L}}{1000 \text{ mL}}.$$

The concentrations measured in the acid soak solutions are summarized in Table D4. The concentrations are given in µg/L (parts per billion, ppb). Dashes in the field indicate the solution was not analyzed for that element.

The calculated masses of elements in the acid soak solutions are summarized in Table D5, in µg. The masses are calculated as the product of the mass acid soak solution, in g, from Table D1 and the concentrations given in Table D4 as

$$\text{mass } i \text{ in acid soak solution, } \mu\text{g} = \text{mass acid soak, g} \times \frac{1 \text{ mL solution}}{\text{g solution}} \times \text{concentration } i, \mu\text{g/L} \times \frac{1 \text{ L}}{1000 \text{ mL}}.$$

Entries of "not det." indicate that the acid soak was not performed for that test.

The normalized elemental mass losses are summarized in Table D6, in g/m². The normalized elemental mass loss was calculated as

$$NL(i) = \frac{\text{mass in test solution} - \text{mass in blank} \left(\frac{\text{blank solution}}{\text{test solution}} \right) + \text{mass in acid soak solution}}{\text{Sample Area} \times \text{Mass fraction in glass}}.$$

The mass measured in the blank test was scaled by the amounts of solution used in the test and the blank test because those amounts differed significantly in some cases.

The mass fractions of elements in the Pu LaBS-B glass used in the calculations are:

B = 0.0326
Al = 0.1020
Si = 0.1222
Sr = 0.0192
La = 0.0626
Nd = 0.0636
Gd = 0.1005
Hf = 0.0526
Pu = 0.0840

Negative values indicate the concentration in the blank test exceeded the sum of the concentrations in the test solution and acid soak solutions. Less-than values indicate that the analyzed concentration in the test solution, the acid soak solution, or both, were below the detection limit, and the values of NL provide

upper bounds. Values shown as strike-outs were not used in analyses, and were replaced by re-run tests or re-analyses of solutions. Calculated values are given to the four decimal place or 3 significant figures.

Table D1. Test Data for Tests at 90 °C

Test Number.	Specimen Number	Specimen Area, cm ²	Leachant mass, g	S/V, m ⁻¹	Vessel No.	Vessel Mass			Adjusted leachant mass, g	Effective S/V, m ⁻¹
						Initial, g	Final, g	Change, g		
MLB1-90-1	26	1.32	55.70	2.37	120	245.90	245.90	0.00	55.70	2.37
MLB1-90-2	29	1.36	57.43	2.37	104	246.55	246.51	-0.04	57.39	2.37
MLB1-90-3	35	1.25	54.60	2.29	105	242.42	242.36	-0.06	54.54	2.29
MLB1-90-4	37	1.45	59.45	2.44	112	250.22	250.16	-0.06	59.39	2.44
MLB1-90-5	55	1.35	56.61	2.38	113	248.28	248.20	-0.08	56.53	2.39
MLB1-90-B1	—	—	58.78	—	114	249.94	249.89	-0.05	58.73	—
MLB2-90-1	19	1.86	40.35	4.61	70	169.09	169.05	-0.04	40.31	4.61
MLB2-90-2	20	1.45	31.14	4.66	48	159.33	159.30	-0.03	31.11	4.66
MLB2-90-3	22	1.38	30.50	4.52	49	157.98	157.94	-0.04	30.46	4.53
MLB2-90-4	23	1.39	30.88	4.50	1	159.98	159.88	-0.10	30.78	4.52
MLB2-90-5	24	1.80	37.83	4.76	2	168.68	168.57	-0.11	37.72	4.77
MLB2-90-B1	—	—	35.30	—	3	164.91	164.88	-0.03	35.27	—
MLB3-90-1	42	1.51	32.40	4.66	73	162.83	162.83	0.00	32.40	4.66
MLB3-90-2	43	1.70	36.19	4.70	54	164.38	164.29	-0.09	36.10	4.71
MLB3-90-3	44	1.54	33.18	4.64	55	160.94	160.92	-0.02	33.18	4.64
MLB3-90-4	46	1.52	32.70	4.65	10	158.06	158.00	-0.06	32.64	4.66
MLB3-90-5	47	1.55	32.91	4.71	11	161.12	161.09	-0.03	32.88	4.71
MLB3-90-B1	—	—	34.91	—	12	164.55	164.52	-0.03	34.88	—
MLB4-90-1	65	1.47	30.56	4.81	76	158.04	158.01	-0.03	30.53	4.81
MLB4-90-2	66	1.61	32.46	4.97	60	158.06	157.99	-0.07	32.39	4.98
MLB4-90-3	67	1.62	33.87	4.78	61	161.93	161.89	-0.06	33.83	4.79
MLB4-90-4	68	1.62	34.08	4.76	19	165.37	165.25	-0.12	33.96	4.78
MLB4-90-5	69	1.69	35.68	4.74	20	165.25	165.15	-0.10	35.58	4.75
MLB4-90-B1	—	—	30.60	—	21	158.52	158.39	-0.13	30.47	—
MLB5-90-1	85	1.71	36.01	4.76	79	163.36	163.36	0.00	36.01	4.76
MLB5-90-2	86	1.64	34.21	4.78	66	165.26	165.20	-0.06	34.15	4.79
MLB5-90-3	87	1.68	34.59	4.86	67	166.53	166.43	-0.10	34.49	4.87
MLB5-90-4	88	1.67	35.41	4.73	28	165.37	165.28	-0.09	35.32	4.74
MLB5-90-5	89	1.74	37.02	4.71	29	166.46	166.30	-0.16	36.86	4.73
MLB5-90-B1	—	—	36.18	—	30	163.45	163.42	-0.03	36.15	—
MLB5-90-1R	113	1.72	36.59	4.70	18	163.82	163.81	-0.01	36.58	4.70
MLB5-90-2R	111	1.76	37.34	4.70	27	168.01	167.99	-0.02	37.32	4.70
MLB5-90-3R	112	1.79	38.02	4.70	42	168.97	168.94	-0.03	37.99	4.70
MLB5-90-4R	103	1.82	38.72	4.70	9	167.71	167.67	-0.04	38.68	4.70
MLB5-90-5R	117	2.15	45.76	4.70	12	175.60	175.55	-0.05	45.71	4.71
MLB5-90-BR	—	—	29.28	—	3	158.87	157.01	-1.86	27.42	—
MLB6-90-1	78	1.41	58.26	2.42	126	249.04	249.01	-0.03	58.23	2.42
MLB6-90-2	80	1.38	57.72	2.39	110	245.73	245.64	-0.09	57.63	2.39
MLB6-90-3	83	1.41	56.80	2.48	111	242.82	242.68	-0.14	56.66	2.49
MLB6-90-4	84	1.42	59.16	2.40	121	250.51	250.45	-0.06	59.10	2.40
MLB6-90-5	91	1.44	59.92	2.40	122	251.30	251.23	-0.07	59.85	2.41
MLB6-90-B1	—	—	70.45	—	123	261.49	261.44	-0.05	70.40	—
MLBD-90-1	107	1.18	10.00	11.80	904	328.16	328.16	0.00	10.00	11.80
MLBD-90-2	99	1.39	11.79	11.80	960	327.99	327.98	-0.01	11.78	11.81
MLBD-90-3	95	0.966	8.19	11.80	420	328.38	328.38	0.00	8.19	11.80
MLBD-90-4	96	0.958	8.12	11.80	953	324.56	324.56	0.00	8.12	11.80
MLBD-90-5	97	1.10	9.32	11.80	920	330.18	330.18	0.00	9.32	11.80
MLBD-90-B1	—	—	12.71	—	906	331.97	331.97	0.00	12.71	—
MLBD-90-6	92	1.06	9.16	11.59	734	325.71	325.70	-0.01	9.15	11.60
MLBD-90-7	93	1.09	9.18	11.82	819	324.60	324.62	0.02	9.19	11.81
MLBD-90-8	71	1.84	15.30	12.02	159	331.52	331.52	0.00	15.30	12.02
MLBD-120-1	45	0.923	15.55	5.94	44	332.18	332.17	-0.01	15.54	5.94
MLBD-120-2	94	0.886	15.34	5.78	47	343.31	343.29	-0.02	15.32	5.78

Table D1. (cont.)

Test No.	Date and Time into oven	Date and Time out of oven	Test Time, hours	Test Time, days	pH (room temp.)	Solution bottle tare, g	Bottle + solution + HNO ₃ , g	Mass solution, g	Total mass acid soak solution, g
MLB1-90-1	2/8/06 13:20	2/9/06 12:20	23.00	0.96	3.70	11.16	35.64	24.48	76.18
MLB1-90-2	1/30/06 14:05	2/1/06 12:30	46.42	1.93	3.74	11.20	36.49	25.29	84.37
MLB1-90-3	1/30/06 14:05	2/2/06 12:25	70.67	2.94	3.74	11.22	37.41	26.19	81.35
MLB1-90-4	1/27/06 15:10	1/31/06 12:25	93.25	3.89	3.75	10.92	35.14	24.22	94.78
MLB1-90-5	1/27/06 15:10	2/1/06 12:30	117.33	4.89	3.75	11.16	36.99	25.83	85.43
MLB1-90-B1	1/27/06 15:10	2/1/06 12:30	117.33	4.89	3.72	11.19	37.90	26.71	not det.
MLB2-90-1	2/8/06 13:20	2/9/06 12:20	23.00	0.96	4.86	11.20	38.49	27.29	30.13
MLB2-90-2	1/30/06 14:05	2/1/06 12:30	46.42	1.93	4.89	11.00	35.00	24.00	30.93
MLB2-90-3	1/30/06 14:05	2/2/06 12:25	70.67	2.94	4.89	11.15	36.79	25.64	34.09
MLB2-90-4	1/27/06 15:10	1/31/06 12:25	93.25	3.89	4.89	11.12	36.92	25.80	37.69
MLB2-90-5	1/27/06 15:10	2/1/06 12:30	117.33	4.89	4.89	11.23	35.92	24.69	28.13
MLB2-90-B1	1/27/06 15:10	2/1/06 12:30	117.33	4.89	4.88	11.17	36.20	25.03	not det.
MLB3-90-1	2/8/06 13:20	2/9/06 12:20	23.00	0.96	6.07	11.24	36.07	24.83	33.93
MLB3-90-2	1/30/06 14:05	2/1/06 12:30	46.42	1.93	6.11	11.14	35.15	24.01	33.23
MLB3-90-3	1/30/06 14:05	2/2/06 12:25	70.67	2.94	6.12	11.13	36.26	25.13	30.97
MLB3-90-4	1/27/06 15:10	1/31/06 12:25	93.25	3.89	6.13	11.15	37.04	25.89	38.12
MLB3-90-5	1/27/06 15:10	2/1/06 12:30	117.33	4.89	6.13	11.16	36.46	25.30	29.50
MLB3-90-B1	1/27/06 15:10	2/1/06 12:30	117.33	4.89	6.10	11.17	36.82	25.65	not det.
MLB4-90-1	2/8/06 13:20	2/9/06 12:20	23.00	0.96	8.56	11.17	35.73	24.56	31.51
MLB4-90-2	1/30/06 14:05	2/1/06 12:30	46.42	1.93	8.59	11.17	34.88	23.71	37.40
MLB4-90-3	1/30/06 14:05	2/2/06 12:25	70.67	2.94	8.60	11.22	35.66	24.44	35.28
MLB4-90-4	1/27/06 15:10	1/31/06 12:25	93.25	3.89	8.60	11.17	37.84	26.67	40.75
MLB4-90-5	1/27/06 15:10	2/1/06 12:30	117.33	4.89	8.60	11.18	33.95	22.77	30.39
MLB4-90-B1	1/27/06 15:10	2/1/06 12:30	117.33	4.89	8.59	11.15	34.94	23.79	not det.
MLB5-90-1	2/8/06 13:20	2/9/06 12:20	23.00	0.96	7.64	11.19	37.35	26.16	37.44
MLB5-90-2	1/30/06 14:05	2/1/06 12:30	46.42	1.93	7.80	11.15	36.66	25.51	33.07
MLB5-90-3	1/30/06 14:05	2/2/06 12:25	70.67	2.94	8.40	11.18	36.21	25.03	37.85
MLB5-90-4	1/27/06 15:10	1/31/06 12:25	93.25	3.89	8.49	11.16	33.93	22.77	39.40
MLB5-90-5	1/27/06 15:10	2/1/06 12:30	117.33	4.89	9.09	11.17	35.56	24.39	33.14
MLB5-90-B1	1/27/06 15:10	2/1/06 12:30	117.33	4.89	9.41	11.16	36.02	24.86	not det.
MLB5-90-1R	3/1/06 16:00	3/2/06 10:45	19.00	0.79	9.16	11.21	31.55	20.34	not det.
MLB5-90-2R	3/1/06 16:00	3/3/06 12:30	44.50	1.85	9.18	11.20	35.86	24.66	not det.
MLB5-90-3R	3/3/06 14:10	3/6/06 12:30	70.33	2.93	9.15	11.22	36.82	25.60	not det.
MLB5-90-4R	3/2/06 11:00	3/6/06 12:30	97.50	4.06	9.39	11.18	35.97	24.79	not det.
MLB5-90-5R	3/1/06 16:00	3/6/06 12:30	116.50	4.85	9.23	11.20	39.36	28.16	not det.
MLB5-90-BR	3/1/06 16:00	3/6/06 12:30	116.50	4.85	not meas.	11.16	36.94	25.78	not det.
MLB6-90-1	2/8/06 13:20	2/9/06 12:20	23.00	0.96	10.93	11.16	39.48	28.32	77.21
MLB6-90-2	1/30/06 14:05	2/1/06 12:30	46.42	1.93	10.87	11.18	37.06	25.88	81.51
MLB6-90-3	1/30/06 14:05	2/2/06 12:25	70.67	2.94	10.87	11.18	37.24	26.06	76.56
MLB6-90-4	1/27/06 15:10	1/31/06 12:25	93.25	3.89	10.87	11.14	36.77	25.63	85.87
MLB6-90-5	1/27/06 15:10	2/1/06 12:30	117.33	4.89	10.88	11.15	38.43	27.28	85.92
MLB6-90-B1	1/27/06 15:10	2/1/06 12:30	117.33	4.89	11.01	11.22	37.88	26.66	not det.
MLBD-90-1	3/1/06 16:10	3/2/06 11:00	18.83	0.78	6.3	11.21	20.66	9.45	17.61
MLBD-90-2	3/1/06 16:10	3/3/06 12:30	44.33	1.85	6.3	11.14	22.42	11.28	16.41
MLBD-90-3	3/3/06 11:15	3/6/06 12:30	73.25	3.05	6.6	11.21	18.92	7.71	17.84
MLBD-90-4	3/2/06 11:00	3/6/06 12:30	97.50	4.06	6.6	11.19	18.80	7.61	17.04
MLBD-90-5	3/1/06 16:10	3/6/06 12:30	116.33	4.85	6.6	11.16	19.50	8.34	15.33
MLBD-90-B1	3/1/06 16:10	3/6/06 12:30	116.33	4.85	not meas.	11.19	23.51	12.32	15.43
MLBD-90-6	2/2/06 14:25	3/2/06 10:45	668.33	27.85	7.35	11.18	19.94	8.76	16.58
MLBD-90-7	2/2/06 14:25	3/30/06 14:25	1344.00	56.00	6.92	11.20	19.76	8.56	14.72
MLBD-90-8	2/2/06 14:25	5/4/06 9:00	2178.58	90.77	5.22	11.19	25.34	14.15	15.80
MLBD-120-1	2/2/06 14:25	3/2/06 10:45	668.17	27.84	7.63	11.14	24.16	13.02	12.84
MLBD-120-2	2/2/06 14:25	3/30/06 14:25	1344.00	56.00	5.69	11.16	25.65	14.49	15.19

Table D2. Results of Static Dissolution Tests at 90 °C: Measured Concentrations in Test Solutions, µg/L

Test Number	Concentration measured in test solution, µg/L								
	B	Al	Si	Sr	La	Nd	Gd	Hf	Pu 239
MLB1-90-1	535	2100	4240	334	1210	1100	1710	2.97	44.4
MLB1-90-2	821	3630	6020	515	2120	1900	2980	2.66	47.3
MLB1-90-3	1060	4790	7340	683	2840	2560	4020	2.9	37.6
MLB1-90-4	1340	5860	8680	835	3530	3130	4950	3.82	35.3
MLB1-90-5	1350	5720	8330	835	3600	3130	5040	2.78	28.6
MLB1-90-B1	156	<13.2	2200	0.243	0.045	<0.08	<0.04	0.193	<0.02
MLB2-90-1	97.4	207	548	39.0	127	120	195	1.12	7.36
MLB2-90-2	109	351	712	60.2	202	187	309	1.17	4.47
MLB2-90-3	124	449	853	74.5	244	236	381	1.1	4.19
MLB2-90-4	142	541	956	89.0	293	284	465	1.28	5.06
MLB2-90-5	147	554	1030	96.7	319	307	498	1.07	5.00
MLB2-90-B1	34.9	27.0	280	<0.06	<0.02	<0.08	<0.04	<0.08	<0.02
MLB3-90-1	46.4	115	312	28.1	95.5	83.1	132	0.998	4.63
MLB3-90-2	84.2	143	585	60.4	202	177	268	0.899	15.1
MLB3-90-3	101	299	724	74.5	247	214	324	1.02	19.9
MLB3-90-4	131	127	964	106	338	297	448	0.894	25.4
MLB3-90-5	142	130	1040	115	361	319	487	0.839	33.6
MLB3-90-B1	13.0	15.0	127	<0.06	<0.02	<0.08	<0.04	<0.08	<0.02
MLB4-90-1	48.0	107	333	14.5	10.7	4.75	5.39	<0.11	8.77
MLB4-90-2	58.9	130	469	27.7	10.5	2.7	1.82	<0.11	19.3
MLB4-90-3	55.4	173	444	24.3	19.6	8.33	9.31	0.132	19.9
MLB4-90-4	68.7	235	535	35	23.8	8.2	6.77	<0.11	39.2
MLB4-90-5	67.4	241	535	33.8	22.4	7.69	6.94	<0.11	35.3
MLB4-90-B1	36.3	58.8	326	0.113	<0.12	<0.14	<0.14	<0.11	<0.11
MLB5-90-1	29.7	119	105	15.4	3.07	1.37	1.63	<0.11	15.0
MLB5-90-2	29	121	105	16.2	2.22	1.01	1.21	0.163	19.0
MLB5-90-3	29.2	133	117	17.3	0.993	0.495	0.644	0.157	18.4
MLB5-90-4	55.8	359	326	42.0	1.19	0.734	0.991	<0.11	12.8
MLB5-90-5	40	416	208	29.7	0.504	0.279	0.319	<0.11	13.1
MLB5-90-B1	9.51	137	<8.53	0.061	<0.12	<0.14	<0.14	<0.11	<0.11
MLB5-90-1R	9.92	60.9	44.5	6.79	0.043	<0.04	<0.04	<0.09	5.10
MLB5-90-2R	21.6	430	121	16.8	0.068	<0.04	<0.04	<0.09	15.1
MLB5-90-3R	26.3	455	145	21.4	0.317	0.275	0.441	<0.09	8.88
MLB5-90-4R	20.3	136	197	15.5	0.319	0.209	0.277	<0.09	11.6
MLB5-90-5R	30.9	578	176	26.5	0.089	<0.04	0.041	<0.09	3.56
MLB5-90-BR	8.50	669	<9.07	0.13	<0.02	<0.04	<0.04	<0.09	<0.02
MLB6-90-1	34.8	211	181	28.4	<0.12	<0.14	<0.14	<0.11	3.06
MLB6-90-2	82.8	435	447	70.7	<0.12	<0.14	<0.14	<0.11	2.86
MLB6-90-3	121	629	596	102	<0.12	<0.14	<0.14	<0.11	1.26
MLB6-90-4	132	685	645	114	<0.12	<0.14	<0.14	<0.11	3.21
MLB6-90-5	187	967	901	154	<0.12	<0.14	<0.14	<0.11	2.52
MLB6-90-B1	7.99	8.19	<8.53	0.316	<0.12	<0.14	<0.14	<0.11	<0.11
MLBD-90-1	57.2	16.0	429	42.6	68.0	40.7	53.6	<0.09	7.66
MLBD-90-2	148	12.7	852	127	324	172	206	<0.09	16.0
MLBD-90-3	162	33.7	1020	130	241	95.0	104	0.656	22.1
MLBD-90-4	165	55.2	1070	137	301	118	124	<0.09	16.8
MLBD-90-5	202	43.3	1160	173	338	127	134	<0.09	14.6
MLBD-90-B1	6.67	5.38	171	0.547	<0.02	<0.04	<0.04	<0.09	<0.02
MLBD-90-6	345	19.4	1950	292	485	156	167	0.273	26.6
MLBD-90-7	528	47.6	2290	342	460	214	298	0.928	107
MLBD-90-8	2350	<14.96	9720	1440	2400	1630	2330	0.196	79.2
MLBD-120-1	1010	18.4	3380	662	310	117	130	<0.09	8.68
MLBD-120-2	2140	17.9	6950	1370	1230	507	813	0.73	35.6

Table D3. Results of Static Dissolution Tests at 90 °C: Calculated Masses in Test Solutions, µg

Test Number	Mass leachant, g	Mass in test solution, µg								
		B	Al	Si	Sr	La	Nd	Gd	Hf	Pu-239
MLB1-90-1	55.70	29.8	117	236	18.6	67.4	61.3	95.2	0.165	2.47
MLB1-90-2	57.39	47.1	208	346	29.6	122	109	171	0.153	2.71
MLB1-90-3	54.54	57.8	261	400	37.3	155	140	219	0.158	2.05
MLB1-90-4	59.39	79.6	348	515	49.6	210	186	294	0.227	2.10
MLB1-90-5	56.53	76.3	323	471	47.2	204	177	285	0.157	1.62
MLB1-90-B1	58.73	9.16	<0.8	129	0.0143	0.0026	<0.005	<0.003	0.0113	<0.002
MLB2-90-1	40.31	3.93	8.34	22.1	1.57	5.12	4.84	7.86	0.0451	0.297
MLB2-90-2	31.11	3.39	10.9	22.2	1.87	6.28	5.82	9.61	0.0364	0.139
MLB2-90-3	30.46	3.78	13.7	26.0	2.27	7.43	7.19	11.6	0.0335	0.128
MLB2-90-4	30.78	4.37	16.7	29.4	2.74	9.02	8.74	14.3	0.0394	0.156
MLB2-90-5	37.72	5.54	20.9	38.9	3.65	12.0	11.6	18.8	0.0404	0.189
MLB2-90-B1	35.27	1.23	0.952	9.88	<0.003	<0.0007	<0.003	<0.002	<0.003	<0.0007
MLB3-90-1	32.40	1.50	3.73	10.1	0.910	3.09	2.69	4.28	0.0323	0.150
MLB3-90-2	36.10	3.04	5.16	21.1	2.18	7.29	6.39	9.67	0.0324	0.545
MLB3-90-3	33.18	3.35	9.92	24.0	2.47	8.19	7.10	10.7	0.0338	0.660
MLB3-90-4	32.64	4.28	4.15	31.5	3.46	11.0	9.69	14.6	0.0292	0.829
MLB3-90-5	32.88	4.67	4.27	34.2	3.78	11.9	10.5	16.0	0.0276	1.10
MLB3-90-B1	34.88	0.453	0.523	4.43	<0.003	<0.001	<0.003	<0.002	<0.003	<0.001
MLB4-90-1	30.53	1.47	3.27	10.2	0.443	0.327	0.145	0.165	<0.003	0.268
MLB4-90-2	32.39	1.91	4.21	15.2	0.897	0.340	0.0874	0.059	<0.004	0.625
MLB4-90-3	33.83	1.87	5.85	15.0	0.822	0.663	0.282	0.315	0.0045	0.673
MLB4-90-4	33.96	2.33	7.98	18.2	1.19	0.808	0.278	0.230	<0.004	1.33
MLB4-90-5	35.58	2.40	8.58	19.0	1.20	0.797	0.274	0.247	<0.004	1.26
MLB4-90-B1	30.47	1.11	1.79	9.93	0.0034	<0.004	<0.005	<0.005	<0.004	<0.004
MLB5-90-1	36.01	1.07	4.29	3.78	0.555	0.111	0.0493	0.0587	<0.004	0.540
MLB5-90-2	34.15	0.990	4.13	3.59	0.553	0.0758	0.0345	0.0413	0.0056	0.649
MLB5-90-3	34.49	1.01	4.59	4.04	0.597	0.0343	0.0171	0.0222	0.0054	0.635
MLB5-90-4	35.32	1.97	12.7	11.5	1.48	0.0420	0.0259	0.0350	<0.004	0.452
MLB5-90-5	36.86	1.47	15.3	7.67	1.09	0.0186	0.0103	0.0118	<0.005	0.483
MLB5-90-B1	36.15	0.344	4.95	<0.3	0.0022	<0.005	<0.006	<0.006	<0.004	<0.004
MLB5-90-1R	36.58	0.363	2.23	1.63	0.248	0.0016	0.0015	<0.002	<0.003	0.187
MLB5-90-2R	37.32	0.806	16.0	4.52	0.627	0.0025	0.0015	<0.002	<0.003	0.564
MLB5-90-3R	37.99	0.999	17.3	5.51	0.813	0.0120	0.0104	0.0168	<0.003	0.337
MLB5-90-4R	38.68	0.785	5.26	7.62	0.600	0.0123	0.0081	0.0107	<0.003	0.449
MLB5-90-5R	45.71	1.41	26.4	8.04	1.21	0.0041	0.0018	0.0019	<0.004	0.163
MLB5-90-BR	27.42	0.233	18.3	<0.3	0.0036	<0.0005	<0.002	<0.002	<0.003	<0.0005
MLB6-90-1	58.23	2.03	12.3	10.5	1.65	<0.007	<0.008	<0.008	<0.006	0.178
MLB6-90-2	57.63	4.77	25.1	25.8	4.07	<0.007	<0.008	<0.008	<0.006	0.165
MLB6-90-3	56.66	6.86	35.6	33.8	5.78	<0.007	<0.008	<0.008	<0.006	0.071
MLB6-90-4	59.10	7.80	40.5	38.1	6.74	<0.007	<0.008	<0.008	<0.007	0.190
MLB6-90-5	59.85	11.2	57.9	53.9	9.22	<0.007	<0.008	<0.008	<0.007	0.151
MLB6-90-B1	70.40	0.562	0.577	<0.6	0.0222	<0.009	<0.01	<0.01	<0.008	<0.008
MLBD-90-1	10.00	0.572	0.160	4.29	0.426	0.680	0.407	0.536	<0.0009	0.0766
MLBD-90-2	11.78	1.74	0.150	10.0	1.50	3.82	2.03	2.43	<0.002	0.189
MLBD-90-3	8.19	1.33	0.276	8.35	1.06	1.97	0.778	0.851	0.005	0.181
MLBD-90-4	8.12	1.34	0.448	8.69	1.11	2.44	0.958	1.01	<0.0007	0.136
MLBD-90-5	9.32	1.88	0.404	10.8	1.61	3.15	1.18	1.25	<0.0008	0.136
MLBD-90-B1	10.32	0.069	0.056	1.76	0.006	<0.0002	<0.0004	<0.0004	<0.0009	<0.0002
MLBD-90-6	9.15	3.16	0.178	17.9	2.67	4.44	1.43	1.53	0.0025	0.244
MLBD-90-7	9.19	4.85	0.437	21.0	3.14	4.23	1.97	2.74	0.0085	0.983
MLBD-90-8	15.30	36.0	<0.3	149	22.0	36.7	24.9	35.6	0.0030	1.21
MLBD-120-1	15.54	15.7	0.286	52.5	10.3	4.83	1.82	2.02	<0.002	0.135
MLBD-120-2	15.32	32.8	0.274	106	21.0	18.8	7.77	12.4	0.0112	0.545

Table D4. Results of Static Dissolution Tests at 90 °C: Measured Concentrations in Acid Soak Solutions, µg/L

Test Number	Concentration measured in acid soak solution, µg/L						
	Si	Sr	La	Nd	Gd	Hf	Pu 239
MLB1-90-1	<9.4	<0.05	0.028	0.038	0.0430	1.02	23.2
MLB1-90-2	<9.4	<0.05	0.050	0.082	0.104	<0.3	27.7
MLB1-90-3	<9.4	0.053	0.343	0.329	0.296	0.711	28.1
MLB1-90-4	<9.4	<0.05	0.068	0.108	0.161	0.664	32.1
MLB1-90-5	<9.4	<0.05	0.063	0.087	0.144	<0.3	30.6
MLB1-90-B1	not det.	not det.	not det.	not det.	not det.	not det.	not det.
MLB2-90-1	<9.4	<0.05	0.037	0.052	0.0770	1.20	2.30
MLB2-90-2	<9.4	<0.05	0.375	0.430	0.653	0.959	3.00
MLB2-90-3	<9.4	0.098	0.418	0.533	0.643	0.878	3.38
MLB2-90-4	<9.4	0.068	0.521	0.563	0.786	0.902	3.36
MLB2-90-5	<9.4	<0.05	0.296	0.493	0.965	2.37	9.77
MLB2-90-B1	not det.	not det.	not det.	not det.	not det.	not det.	not det.
MLB3-90-1	<9.4	<0.05	0.236	0.363	0.604	<0.3	0.0320
MLB3-90-2	<9.4	<0.05	0.792	1.71	5.36	<0.3	0.105
MLB3-90-3	<9.4	0.080	3.00	5.61	10.4	<0.3	0.422
MLB3-90-4	<9.4	<0.05	1.44	3.32	10.4	<0.3	0.304
MLB3-90-5	<9.4	0.165	2.86	5.75	16.7	<0.3	0.439
MLB3-90-B1	not det.	not det.	not det.	not det.	not det.	not det.	not det.
MLB4-90-1	<9.4	0.081	0.515	0.466	0.751	<0.3	0.101
MLB4-90-2	9.90	0.543	19.5	13.9	21.1	<0.3	0.413
MLB4-90-3	<9.4	<0.05	0.823	0.829	1.47	<0.3	0.045
MLB4-90-4	<9.4	0.062	8.85	8.11	15.5	<0.3	0.430
MLB4-90-5	17.0	0.096	17.7	15.5	24.7	<0.3	0.208
MLB4-90-B1	not det.	not det.	not det.	not det.	not det.	not det.	not det.
MLB5-90-1	<9.4	0.088	0.258	0.257	0.442	<0.3	<0.03
MLB5-90-2	<9.4	<0.05	0.651	0.590	0.822	<0.3	0.0660
MLB5-90-3	<9.4	0.054	1.03	0.645	0.905	<0.3	0.151
MLB5-90-4	32.0	0.376	1.69	1.02	1.31	0.219	1.75
MLB5-90-5	<9.4	0.393	2.74	1.53	2.05	<0.3	1.01
MLB5-90-B1	not det.	not det.	not det.	not det.	not det.	not det.	not det.
MLB5-90-1R	not det.	not det.	not det.	not det.	not det.	not det.	not det.
MLB5-90-2R	not det.	not det.	not det.	not det.	not det.	not det.	not det.
MLB5-90-3R	not det.	not det.	not det.	not det.	not det.	not det.	not det.
MLB5-90-4R	not det.	not det.	not det.	not det.	not det.	not det.	not det.
MLB5-90-5R	not det.	not det.	not det.	not det.	not det.	not det.	not det.
MLB5-90-BR	not det.	not det.	not det.	not det.	not det.	not det.	not det.
MLB6-90-1	<9.4	<0.05	0.023	<0.03	<0.04	<0.3	<0.03
MLB6-90-2	113	0.313	0.106	0.115	0.117	<0.3	0.125
MLB6-90-3	<9.4	0.258	0.180	0.143	0.201	<0.3	0.692
MLB6-90-4	<9.4	<0.05	0.024	<0.03	<0.04	<0.3	0.062
MLB6-90-5	<9.4	<0.05	0.031	0.031	<0.04	<0.3	<0.03
MLB6-90-B1	not det.	not det.	not det.	not det.	not det.	not det.	not det.
MLBD-90-1	42.0	0.490	27.9	31.3	41.9	0.240	6.66
MLBD-90-2	351	0.790	64.2	116	190	1.42	19.5
MLBD-90-3 ^a	130	1.85	73.3	119	193	2.42	50.2
MLBD-90-4 ^b	126	5.13	121	165	255	11.4	105
MLBD-90-5 ^c	140	3.32	481	417	444	5.92	63.4
MLBD-90-B1	27.3	0.348	0.114	0.393	<0.04	<0.03	<0.01
MLBD-90-6	64.3	0.415	143	186	266	1.15	91.9
MLBD-90-7 ^d	232	5.34	1210	934	924	6.98	270
MLBD-90-8	151	32.9	2170	2230	3340	0.897	303
MLBD-120-1	574	<0.04	508	459	625	0.684	361
MLBD-120-2 ^e	33100	6220	20600	19500	30600	9130	16100

^aAnalyzed as solution MLBD-90-5A, values reassigned to test MLBD-90-3.

^bAnalyzed as solution MLBD-90-7A, values reassigned to test MLBD-90-4.

^cAnalyzed as solution MLBD-90-3A, values reassigned to test MLBD-90-5.

^dAnalyzed as solution MLBD-120-2A, values reassigned to test MLBD-90-7.

^eAnalyzed as solution MLBD-90-4A, values reassigned to test MLBD-120-2.

Table D5. Results of Static Dissolution Tests at 90 °C: Calculated Masses in Acid Soak Solutions, µg

Test Number	Mass acid soak solution, g	Mass in acid soak solution, µg						
		Si	Sr	La	Nd	Gd	Hf	Pu 239
MLB1-90-1	76.18	<0.8	<0.004	0.0021	0.0029	0.0033	0.0777	1.77
MLB1-90-2	84.37	<0.8	<0.004	0.0042	0.0069	0.0088	<0.02	2.34
MLB1-90-3	81.35	<0.8	0.0043	0.0279	0.0268	0.0241	0.0578	2.29
MLB1-90-4	94.78	<0.9	<0.005	0.0064	0.0102	0.0153	0.0629	3.04
MLB1-90-5	85.43	<0.8	<0.004	0.0054	0.0074	0.0123	<0.02	2.61
MLB2-90-1	30.13	<0.3	<0.002	0.0011	0.0016	0.0023	0.0362	0.0693
MLB2-90-2	30.93	<0.3	<0.002	0.0116	0.0133	0.0202	0.0297	0.0928
MLB2-90-3	34.09	<0.4	0.0033	0.0142	0.0182	0.0219	0.0299	0.115
MLB2-90-4	37.69	<0.4	0.0026	0.0196	0.0212	0.0296	0.0340	0.127
MLB2-90-5	28.13	<0.3	<0.001	0.0083	0.0139	0.0271	0.0667	0.275
MLB3-90-1	33.93	<0.4	<0.002	0.0080	0.0123	0.0205	<0.008	0.0011
MLB3-90-2	33.23	<0.4	<0.002	0.0263	0.0568	0.178	<0.007	0.0035
MLB3-90-3	30.97	<0.3	0.0025	0.0929	0.174	0.322	<0.007	0.0131
MLB3-90-4	38.12	<0.4	<0.002	0.0549	0.127	0.396	<0.008	0.0116
MLB3-90-5	29.50	<0.3	0.0049	0.0844	0.170	0.493	<0.007	0.0130
MLB4-90-1	31.51	<0.3	0.0026	0.0162	0.0147	0.0237	<0.007	0.0032
MLB4-90-2	37.40	0.370	0.0203	0.729	0.520	0.7891	<0.008	0.0155
MLB4-90-3	35.28	<0.4	<0.002	0.0290	0.0292	0.0519	<0.008	0.0016
MLB4-90-4	40.75	<0.4	0.0025	0.361	0.330	0.632	<0.009	0.0175
MLB4-90-5	30.39	0.517	0.0029	0.538	0.471	0.751	<0.007	0.0063
MLB5-90-1	37.44	<0.4	0.0033	0.0097	0.0096	0.0165	<0.008	<0.002
MLB5-90-2	33.07	<0.4	<0.002	0.0215	0.0195	0.0272	<0.007	0.0022
MLB5-90-3	37.85	<0.4	0.0020	0.0390	0.0244	0.0343	<0.008	0.0057
MLB5-90-4	39.40	1.26	0.0148	0.0666	0.0402	0.0516	0.0086	0.0690
MLB5-90-5	33.14	<0.4	0.0130	0.0908	0.0507	0.0679	<0.007	0.0335
MLB6-90-1	77.21	<0.8	<0.004	0.0018	<0.002	<0.003	<0.02	<0.003
MLB6-90-2	81.51	9.21	0.0255	0.0086	0.0094	0.0095	<0.0	0.0102
MLB6-90-3	76.56	<0.8	0.0198	0.0138	0.0109	0.0154	<0.02	0.0530
MLB6-90-4	85.87	<0.8	<0.004	0.0021	<0.003	<0.003	<0.02	0.0053
MLB6-90-5	85.92	<0.8	<0.004	0.0027	0.0027	<0.003	<0.02	<0.003
MLBD-90-1	17.61	0.740	0.0086	0.491	0.551	0.738	0.0042	0.117
MLBD-90-2	16.41	5.76	0.0130	1.05	1.90	3.12	0.0233	0.320
MLBD-90-3	15.33	2.32	0.0330	1.31	2.12	3.44	0.0432	0.896
MLBD-90-4	14.72	2.15	0.0874	2.06	2.81	4.35	0.194	1.79
MLBD-90-5	17.84	2.15	0.0509	7.37	6.39	6.81	0.0908	0.972
MLBD-90-B1	15.43	0.421	0.0054	0.0018	0.0061	<0.0006	<0.0005	<0.0002
MLBD-90-6	16.58	1.07	0.0069	2.37	3.08	4.41	0.0191	1.52
MLBD-90-7	15.19	3.42	0.0786	17.8	13.7	13.6	0.103	3.97
MLBD-90-8	15.80	2.39	0.520	34.3	35.2	52.8	0.0142	4.79
MLBD-120-1	12.84	7.37	<0.0005	6.52	5.89	8.03	0.0088	4.64
MLBD-120-2	17.04	503	94.5	313	296	465	139	245

Table D6. Results of Static Dissolution Tests at 90 °C: Normalized Elemental Mass Losses, g/m²

Test Number	Specimen Area, cm ²	Normalized elemental mass loss, g/m ²								
		B	Al	Si	Sr	La	Nd	Gd	Hf	Pu-239
MLB1-90-1	1.32	4.91	8.63	7.04	7.34	8.16	7.30	7.18	0.0335	0.382
MLB1-90-2	1.36	8.61	15.0	13.2	11.3	14.3	12.6	12.5	0.0223	0.442
MLB1-90-3	1.25	12.1	20.4	18.4	15.5	19.8	17.6	17.5	0.0313	0.413
MLB1-90-4	1.45	14.9	23.5	21.7	17.8	23.1	20.2	20.2	0.0365	0.422
MLB1-90-5	1.35	15.3	23.4	21.0	18.2	24.1	20.6	21.0	0.0231	0.373
MLB2-90-1	1.86	0.416	0.382	0.475	0.440	0.440	0.409	0.421	0.0080	0.0234
MLB2-90-2	1.45	0.488	0.682	0.759	0.673	0.694	0.632	0.661	0.0083	0.0190
MLB2-90-3	1.38	0.603	0.913	1.04	0.857	0.862	0.821	0.838	0.0084	0.0209
MLB2-90-4	1.39	0.728	1.116	1.23	1.03	1.04	0.991	1.03	0.0097	0.0241
MLB2-90-5	1.80	0.721	1.08	1.29	1.06	1.07	1.01	1.04	0.0110	0.0306
MLB3-90-1	1.51	0.220	0.210	0.325	0.315	0.328	0.282	0.283	0.0050	0.0119
MLB3-90-2	1.70	0.464	0.266	0.796	0.668	0.688	0.596	0.577	0.0044	0.0384
MLB3-90-3	1.54	0.581	0.600	1.05	0.837	0.860	0.743	0.715	0.0050	0.0520
MLB3-90-4	1.52	0.777	0.236	1.47	1.19	1.17	1.02	0.983	0.0047	0.0658
MLB3-90-5	1.55	0.839	0.239	1.58	1.27	1.23	1.08	1.06	0.0041	0.0858
MLB4-90-1	1.47	0.0745	0.098	0.0120	0.158	0.0373	0.0171	0.0127	<0.0004	0.0219
MLB4-90-2	1.61	0.139	0.140	0.235	0.296	0.106	0.0592	0.0523	<0.0004	0.0473
MLB4-90-3	1.62	0.122	0.234	0.202	0.265	0.0683	0.0302	0.0225	<0.0005	0.0496
MLB4-90-4	1.62	0.208	0.361	0.358	0.382	0.115	0.0590	0.0528	<0.0004	0.0989
MLB4-90-5	1.69	0.201	0.376	0.360	0.371	0.126	0.0692	0.0587	<0.0004	0.0889
MLB5-90-1	1.71	0.130	-0.0371	0.181	0.169	0.0112	0.0054	0.0044	<0.002	0.0376
MLB5-90-2	1.64	0.125	-0.0328	0.179	0.177	0.0095	0.0052	0.0042	0.0015	0.0474
MLB5-90-3	1.68	0.124	-0.0081	0.197	0.186	0.00696	0.0039	0.0033	0.0015	0.0454
MLB5-90-4	1.67	0.300	0.459	0.563	0.466	0.0104	0.0062	0.0051	0.0010	0.0371
MLB5-90-5	1.74	0.198	0.579	0.360	0.331	0.0100	0.0055	0.0046	0.0012	0.0353
MLB5-90-1R	1.72	0.0093	-1.268	0.0617	0.0738	0.0001	0.0001	<0.0001	<0.0004	0.0129
MLB5-90-2R	1.76	0.0855	-0.498	0.195	0.185	0.0002	0.0001	<0.0001	<0.0004	0.0382
MLB5-90-3R	1.79	0.116	-0.446	0.237	0.236	0.0011	0.0009	0.0009	<0.0004	0.0225
MLB5-90-4R	1.82	0.0769	-1.11	0.327	0.170	0.0011	0.0007	0.0006	<0.0004	0.0294
MLB5-90-5R	2.15	0.146	-0.190	0.290	0.292	0.0003	0.0001	0.0001	<0.0004	0.0090
MLB6-90-1	1.41	0.340	0.821	0.583	<0.7	<0.0008	<0.0009	<0.0006	<0.0009	0.0152
MLB6-90-2	1.38	0.958	1.75	1.50	<1.5	<0.0008	0.0011	0.0007	<0.0009	0.0151
MLB6-90-3	1.41	1.39	2.45	1.93	<2.1	<0.0008	0.0012	0.0011	<0.0008	0.0105
MLB6-90-4	1.42	1.58	2.76	2.17	<2.5	<0.0008	<0.0009	<0.0006	<0.0009	0.0164
MLB6-90-5	1.44	2.28	3.91	3.04	<3.4	<0.0008	0.0003	<0.0006	<0.0009	0.0127
MLBD-90-1	1.18	0.131	0.0088	0.230	0.189	0.159	0.128	0.107	<0.0007	0.0195
MLBD-90-2	1.39	0.367	0.0061	0.811	0.563	0.559	0.444	0.396	<0.004	0.0435
MLBD-90-3	0.966	0.404	0.0235	0.785	0.589	0.542	0.472	0.442	0.0094	0.133
MLBD-90-4	0.958	0.412	0.0414	0.807	0.650	0.751	0.619	0.556	<0.04	0.239
MLBD-90-5	1.10	0.508	0.0315	0.846	0.785	1.53	1.08	0.729	<0.02	0.120
MLBD-90-6	1.06	0.894	0.0118	1.34	1.31	1.02	0.668	0.556	0.0037	0.198
MLBD-90-7	1.09	1.35	0.0350	1.73	1.54	3.24	2.28	1.50	0.0194	0.544
MLBD-90-8	1.84	5.98	<0.005	6.60	6.38	6.16	5.14	4.78	0.0016	0.388
MLBD-120-1	0.923	5.18	0.0215	5.07	5.80	1.96	1.31	1.08	0.0018	0.615
MLBD-120-2	0.886	11.3	0.0212	56.0	67.9	59.8	53.9	53.6	29.8	32.9

APPENDIX E: PROPAGATION OF ERRORS

The uncertainties in calculated values were estimated from the measured values using the propagation of errors method. For a property P that is a function of measured values x_1, x_2, x_3 , etc., the probable error associated with P (Q_P) can be expressed in terms of the probable error in the means of the measured values (q_1, q_2, q_3 , etc.) as

$$Q_P^2 = \left(\frac{\partial P}{\partial x_1} \right)^2 \cdot q_1^2 + \left(\frac{\partial P}{\partial x_2} \right)^2 \cdot q_2^2 + \left(\frac{\partial P}{\partial x_3} \right)^2 \cdot q_3^2 + \dots \quad (\text{E-1})$$

The estimated uncertainties for measured and calculated values are listed below.

E.1 ELEMENTAL MASS FRACTION

The uncertainty in the elemental mass fraction $f(i)$ is due to uncertainty in the mass of glass dissolved for analysis, the volume of the solution used to dissolve the glass, and the analysis of the solution. The uncertainty in the values of $f(i)$ are estimated to be 6% for all elements. This is based on the analytical uncertainty in analyzing any particular sample and the possible heterogeneity in the distribution of PuO_2 inclusions, which will affect the normalization of the glass composition to 100%. The values of $f(B)$ and $f(Si)$ used for calculations in this report are 0.0326 and 0.122, respectively, and the corresponding uncertainties are 0.0020 and 0.0073.

E.2 GLASS SURFACE AREA

The uncertainty in the surface area of monolithic specimens is due to uncertainties in the measured dimensions, in drawing and weighing the paper cut-outs to estimate the facial area, and using the geometric surface area without accounting for the surface roughness. The area was calculated as the sum of the 4 or 5 sides and twice the area of the face. The area of each side is simply the length (l) times the average thickness at the corners (h):

$$A = l \times h. \quad (\text{E-2a})$$

Applying Equation E-1 to the area calculated with Equation E-2a gives

$$Q_A^2 = (h)^2 \cdot q_l^2 + (l)^2 \cdot q_h^2. \quad (\text{E-2b})$$

All dimensions were measured to ± 0.0005 inches, so that $q_l = 0.0005$ in. and $q_h = 0.0005$ in. For Specimen 1 with an edge length $l = 0.4470$ in. and thicknesses $h_l = 0.0285$ in. and $h_l = 0.0335$ in., the average thickness is $h = 0.0310$ in. and the area is 0.01386 in.^2 . Inserting the experimental values gives

$$Q_A^2 = (0.0310)^2 \cdot (0.0005)^2 + (0.4470)^2 \cdot (0.0005)^2 = 5.00 \times 10^{-8}. \quad (\text{E-2c})$$

The uncertainty in the calculated area of the side is $Q_A = 2.24 \times 10^{-4} \text{ in.}^2$ ($1.45 \times 10^{-3} \text{ cm}^2$). The area of the side is $1.39 \times 10^{-2} \text{ in.}^2$ ($8.94 \times 10^{-2} \text{ cm}^2$). The relative uncertainty in the area of the side is $100 \cdot (0.00145/0.0894) = 1.62\%$.

The area of the specimen face was irregular and was not calculated geometrically. Instead, the dimensions of the specimen were measured with a caliper with a scale in inches, and the specimen faces were drawn on paper using a caliper with a scale in mm. The dimensions that had been measured in inches were

multiplied by 20 and the values drawn in that number of cm. For example, the side of Specimen 1 that was measured to be 0.744 inches was drawn 8.94 cm long. That is, the drawings of the specimens were scaled so that 1 inch on the specimen was drawn as 20 cm on the drawing (an expansion scale of 20/2.54). The shape of each specimen face was drawn based on the measured dimensions of the sides and diameters using the caliper and a compass. The sketched outlines of the specimens were cut out of the paper and were weighed using a 4-place balance. Squares drawn with 5, 7, and 10 cm on each side were also cut out and weighed. The mass and area (in scaled units) were related by the calibration equation that was determined by weighing the pieces of paper sized to 25, 49, and 100 cm². The linear regression equation for the three pieces is

$$area = \frac{(mass + 0.00873)}{0.00785} . \quad (E-2d)$$

The uncertainty in the area determined by weighing is calculated as

$$Q_{area}^2 = \left(\frac{1}{0.00785} \right)^2 \bullet q_{mass}^2 . \quad (E-2e)$$

The uncertainty in the measured mass is assumed to be ± 0.0005 g, so the uncertainty in the area is 0.0637 scaled units. The mass of the paper for Specimen 1 was 0.3019 g. The area of Specimen 1 that was determined by weighing was 39.57 scaled units, and the uncertainty in the calculated area of the face is $Q_{area} = 0.0637$ scaled units. The actual area in cm² is obtained by multiplying the area that was determined in scaled units by the factor $(2.54 \text{ cm/inch} \div 20 \text{ scaled units/inch})^2 = 0.01613 \text{ cm}^2/\text{scaled unit}^2$. This gives an area of 0.638 cm² for the face of Specimen 1, with an uncertainty of 0.00103 cm² and a relative uncertainty of 0.16%. This is an unreasonably small uncertainty that does not include the uncertainty in the drawing and cutting of the paper.

As an alternate measure of the uncertainty, Specimen 99 was dimensioned and weighed twice (the second measurements are referred to as Specimen 99R). The facial areas of Specimens 99 and 99R were determined to be 0.5789 and 0.5823 cm², respectively, which is a difference of $100 \times (0.5823 - 0.5789)/0.5789 = 0.59 \%$.

The uncertainty due to the surface roughness is neglected because all specimens were prepared with the same surface finish. Although the uncertainty in the area of each side (which is about 1.6%) is about 3 times the uncertainty in each face (which is about 0.6%), the areas of the 2 faces are about 5 times the areas of the 4 or 5 sides for most specimens. Therefore, the uncertainty in the total surface area is taken to be 1% of the calculated area.

E.3 SOLUTION VOLUME

The amounts of leachant solution added to the tests and the amounts of nitric acid solution in the acid strip analyses were determined by mass. The uncertainty in mass due to the difference in two mass measurements is used as the uncertainty in volume by presuming a solution density of 1.00 g/mL for all test solutions. The masses were measured to the nearest 0.01 g, which is taken to be the uncertainty. The solution mass was calculated as the difference between the mass of the test vessel or bottle without solution and the mass of the vessel or bottle with the added solution. The uncertainty in the mass determination is calculated using propagation of errors formula in Equation E-1 for the equation $M = mass_1 - mass_2$ is as follows:

$$Q_M^2 = \left(\frac{\partial M}{\partial M_{mass\ 1}}\right)^2 \cdot q_1^2 + \left(\frac{\partial M}{\partial M_{mass\ 2}}\right)^2 \cdot q_2^2. \quad (E-3a)$$

If the uncertainty in each measured mass is $q_1 = q_2 = 0.01$ g, then

$$\frac{\partial M}{\partial mass_1} = 1 \quad (E-3b)$$

$$\frac{\partial M}{\partial mass_2} = -1 \quad (E-3c)$$

Inserting the experimental values gives

$$Q_M^2 = (1)^2 \cdot (0.01)^2 + (-1)^2 \cdot (0.01)^2 = 0.0002. \quad (E-3d)$$

The uncertainty in the difference of two masses is estimated to be $q_M = (0.0002)^{0.5} = 0.014$ g. The uncertainty in volume is estimated to be 0.014 mL. Tests were conducted with between about 30 and 60 g of water, and the relative uncertainties in these mass measurements range between 0.05% and 0.1%. The uncertainty in the volume is taken to be 0.02 mL for all tests.

$$q_V = 0.02 \text{ mL}. \quad (E-3e)$$

E.4 SOLUTION CONCENTRATIONS

The uncertainties in the measured concentrations of all analytes were estimated by the ICP-MS analyst to be 10% of the measured values:

$$q_C = 0.1 \times C(i). \quad (E-4a)$$

E.5 MASS RELEASED

The mass released from the glass is calculated from the difference in the concentration measured in the test and the background concentration from the blank test. The total mass is the product of the measured concentration and the volume of test solution. The background mass is the product of the concentration measured in the blank test and the **volume of the test solution**. The mass of Si released from the glass is calculated as

$$m(Si) = [C_{test\ solution}(Si) - C^\circ(Si)] \times V_{test\ solution} + C_{acid\ soak}(Si) \times V_{acid\ soak\ solution} \quad (E-5a)$$

$$Q_{C_{test\ solution}} = \frac{\partial m(Si)}{\partial C_{test\ solution}(Si)} = V_{test\ solution} \quad (E-5b)$$

$$Q_{C^\circ} = \frac{\partial m(Si)}{\partial C^\circ(Si)} = -V_{test\ solution} \quad (E-5c)$$

$$Q_{V_test\ solution} = \frac{\partial m(Si)}{\partial V_{test\ solution}} = C_{test\ solution}(Si) - C^{\circ}(Si) \quad (E-5d)$$

$$Q_{C_acid\ soak\ solution} = \frac{\partial m(Si)}{\partial C_{acid\ soak\ solution}(Si)} = V_{acid\ soak\ solution} \quad (E-5e)$$

$$Q_{V_acid\ soak\ solution} = \frac{\partial m(Si)}{\partial V_{acid\ soak\ solution}} = C_{acid\ soak\ solution}(Si) \quad (E-5f)$$

As a sample calculation, for test MLB1-70-1:

$$\begin{aligned} C_{test\ solution}(Si) &= 1530 \mu\text{g/L} (1.53 \times 10^{-3} \text{ g/L}) \text{ with an uncertainty of 10\%, } (1.53 \times 10^{-4} \text{ g/L}) \\ C^{\circ}(Si) &= 850 \mu\text{g/L} (8.50 \times 10^{-4} \text{ g/L}) \text{ with an uncertainty of 10\%, } (8.50 \times 10^{-5} \text{ g/L}) \\ V_{test\ solution} &= 61.20 \text{ mL} (0.06120 \text{ L}) \text{ with uncertainty of 0.02 mL} (0.00002 \text{ L}) \\ C_{acid\ soak\ solution}(Si) &= 0 \mu\text{g/L} \end{aligned}$$

$$Q_{m(Si)}^2 = (0.0612)^2 \cdot (1.53 \times 10^{-4})^2 + (-0.0612)^2 \cdot (8.50 \times 10^{-5})^2 + (6.8 \times 10^{-4})^2 \cdot (0.00002)^2 \quad (E-5g)$$

$Q_{m(Si)}^2 = 1.147 \times 10^{-10}$ and $Q_{m(Si)} = 1.07 \times 10^{-5} \text{ g}$. The calculated mass is

$$(1.53 - 0.85) \times \left(\frac{1 \times 10^{-3} \text{ g}}{\text{L}} \right) \times 0.0612 \text{ L} = 4.16 \times 10^{-5} \text{ g} \quad (E-5h)$$

and the relative uncertainty is 25.7%.

Note: The uncertainties in the absolute amounts of Si released from the glass are high because the net concentration is the small difference of two large numbers. However, because the leachants used in a series of tests were taken as aliquots from the same source, the background concentrations in a series of tests can be considered constant, and the *relative* Si concentrations and masses in a series of tests, which are used to determine the release rates, are more reliable than appears from the propagated uncertainty.

E.6 NL(SI) IN IMMERSION TESTS

Although normalized elemental mass losses are calculated for other glass components, the glass dissolution rate calculated from the loss of silicon is of primary importance and considered here. The uncertainty in the value of NL(Si) is due to uncertainties in the measured solution concentration, the specimen surface area, the solution volume, and the mass fraction of Si in the glass. The uncertainty in NL(Si) is determined by propagation of errors and applying Equation E-1 to the function given in Equation 9, which is expressed in terms of measured values as:

$$NL(i) = \frac{(C(i)_{test\ solution} - C^{\circ}(i)) \times V_{test\ solution} + C(i)_{acid\ soak\ solution} \times V_{acid\ soak\ solution}}{S \times f(i)} \quad (E-6a)$$

Since the Si concentrations in the acid soak solutions were negligible compared with the Si concentrations in almost all test solutions, the contributions of uncertainties in the acid soak solutions are ignored. (The contributions of other elements in the acid soak solutions are significant, but those elements are not used to determine dissolution rates or rate coefficient values.) Differentiating Equation E-6a gives the following terms:

$$Q_{C(Si)_{test\ solution}} = \frac{\partial NL}{\partial C(Si)_{test\ solution}} = \frac{V_{test\ solution}}{S \times f(Si)} \quad (E-6b)$$

$$Q_{C^o(Si)} = \frac{\partial NL}{\partial C^o(Si)} = \frac{-V_{test\ solution}}{S \times f(Si)} \quad (E-6c)$$

$$Q_{V_{test\ solution}} = \frac{\partial NL}{\partial V_{test\ solution}} = \frac{C(Si)_{test\ solution} - C^o(Si)}{S \times f(Si)} \quad (E-6d)$$

$$Q_S = \frac{\partial NL}{\partial S} = \frac{-(C(Si)_{test\ solution} - C^o(Si)) \times V_{test\ solution}}{S^2 \times f(Si)} \quad (E-6e)$$

$$Q_{f(Si)} = \frac{\partial NL}{\partial f(Si)} = \frac{-(C(Si)_{test\ solution} - C^o(Si)) \times V_{test\ solution}}{S \times f(Si)^2} \quad (E-6f)$$

As a sample calculation, for test MLB1-70-1:

$$\begin{aligned} C_{test\ solution}(Si) &= 1530 \mu\text{g/L} (1.53 \times 10^{-3} \text{ g/L}) \text{ with an uncertainty of } 10\%, (1.53 \times 10^{-4} \text{ g/L}) \\ C^o(Si) &= 850 \mu\text{g/L} (8.50 \times 10^{-4} \text{ g/L}) \text{ with an uncertainty of } 10\%, (8.50 \times 10^{-5} \text{ g/L}) \\ V_{test\ solution} &= 61.20 \text{ mL} (0.06120 \text{ L}) \text{ with uncertainty of } 0.02 \text{ mL} (0.00002 \text{ L}) \\ C_{acid\ soak\ solution}(Si) &= 0 \mu\text{g/L} \\ S &= 1.42 \text{ cm}^2 \text{ with an uncertainty of } 1\% = 0.0142 \text{ cm}^2, \\ f(Si) &= 0.122 \text{ with an uncertainty of } 0.0073. \end{aligned}$$

Inserting the experimental values for the partial derivatives gives

$$\frac{V}{(S \bullet f)} = 3533; \frac{-V}{(S \bullet f)} = -3533; \frac{(C - C^o)}{(S \bullet f)} = 39.25; \frac{-(C - C^o) \bullet V}{(S^2 \bullet f)} = -1692; \frac{-(C - C^o) \bullet V}{(S \bullet f^2)} = -19.69 \quad (E-6g)$$

Inserting these values and the uncertainties into Eq. E-1 gives

$$\begin{aligned} Q_{NL}^2 &= (0.292) \bullet (2.34 \times 10^{-8}) + (0.0902) \bullet (4.48 \times 10^{-9}) + (6.16 \times 10^{-7}) \bullet (4.00 \times 10^{-10}) \\ &\quad + (5.77 \times 10^4) \bullet (2.02 \times 10^{-12}) + (0.0207) \bullet (5.33 \times 10^{-5}) = 0.404 \end{aligned} \quad (E-6h)$$

The uncertainty is $Q_{NL} = (0.404)^{0.5} = 0.635 \text{ g/m}^2$. The calculated value of NL(Si) is 2.40 g/m^2 , so the relative uncertainty is 26.4 %.

The uncertainties in the measured values for all immersion tests are summarized in Table F1, and the propagated uncertainties are summarized in Table F2. The uncertainty is dominated by the uncertainty in the released mass (through the solution concentrations). The uncertainty in the mass fraction of Si is important in most tests at 70 and 90 °C (up to about 25% of the uncertainty). The uncertainty in the surface area contributes less than 1% to the uncertainty in NL(Si) in the immersion tests.

Note: The uncertainties in the absolute amounts of Si released from the glass are high because the net concentration is the small difference of two large numbers. However, because the leachants used in a series of tests were taken as aliquots from the same source, the background concentrations in a series of tests can be considered constant, and the *relative* Si concentrations and masses in a series of tests, which are used to determine the release rates, are more reliable than appears from the propagated uncertainty. For this reason, the plotted values of NL(Si) are shown with uncertainty bars drawn at 15% of the calculated value.

E.7 TIME

The test duration is determined by the time between when the test vessel was placed in the oven and when it was removed from the oven, to the nearest 5 minutes. The time required for the solution and glass to heat from room temperature to the test temperature is not known, but is estimated to be the same for all tests at that temperature. The uncertainty in test duration is estimated to be 10 minutes (0.007 days).

E.8 NR(Si)

The uncertainty in the value of NR(Si) is due to a combination of the uncertainties in the values of NL(Si) and the reaction time, uncertainty in the regression of NL(Si), and which values were included in the regression. Some values were excluded from the regression subjectively based on whether they appeared to be affected by the affinity term (that is, whether the value fell below the regression fit by an amount that was more than could be attributed to testing uncertainty) or if they were significant outliers. The uncertainty in the regression fit was calculated by the KaleidaGraph software routine as the goodness of fit R^2 . These values are included with the equations of the fitted lines in Figures 5 – 7 and in Tables 5 and 6. The regressions for tests at 70 °C at pH 6.10 and pH 9.37 are statistically poor for NR(Si), while the R^2 values for tests at other pH values are above 0.80, which indicates that less than 20% of the uncertainty is due to the regression. Most of the uncertainty in NR(Si) is due to the uncertainties in NL(Si).

Table E1. Summary of Solution Concentrations, Volumes, and Specimen Areas and Their Uncertainties

Test Number	C, g/L	q _c ²	C°, g/L	q _{co} ²	V, L	q _v ²	S, m ²	q _s ²
Immersion Tests at 40 °C								
MLB1-40-1	7.65E-04	5.85E-09	6.69E-04	4.48E-09	5.46E-02	4.00E-10	1.30E-04	1.69E-12
MLB1-40-2	1.02E-03	1.04E-08	6.69E-04	4.48E-09	5.85E-02	4.00E-10	1.38E-04	1.90E-12
MLB1-40-3	1.20E-03	1.44E-08	6.69E-04	4.48E-09	5.82E-02	4.00E-10	1.35E-04	1.82E-12
MLB1-40-4	1.23E-03	1.51E-08	6.69E-04	4.48E-09	5.64E-02	4.00E-10	1.38E-04	1.90E-12
MLB1-40-5	1.51E-03	2.28E-08	6.69E-04	4.48E-09	5.90E-02	4.00E-10	1.42E-04	2.02E-12
MLB2-40-1	2.80E-04	7.84E-10	1.24E-04	1.54E-10	3.30E-02	4.00E-10	1.55E-04	2.40E-12
MLB2-40-2	4.62E-04	2.13E-09	1.24E-04	1.54E-10	3.65E-02	4.00E-10	1.71E-04	2.93E-12
MLB2-40-3	5.02E-04	2.52E-09	1.24E-04	1.54E-10	3.00E-02	4.00E-10	1.43E-04	2.04E-12
MLB2-40-4	5.44E-04	2.96E-09	1.24E-04	1.54E-10	3.88E-02	4.00E-10	1.83E-04	3.34E-12
MLB2-40-5	7.07E-04	5.00E-09	1.24E-04	1.54E-10	3.72E-02	4.00E-10	1.73E-04	2.98E-12
MLB3-40-1	8.39E-05	7.04E-11	7.68E-05	5.90E-11	2.36E-02	4.00E-10	1.11E-04	1.23E-12
MLB3-40-2	8.62E-05	7.43E-11	7.68E-05	5.90E-11	3.02E-02	4.00E-10	1.49E-04	2.22E-12
MLB3-40-3	9.46E-05	8.95E-11	7.68E-05	5.90E-11	3.25E-02	4.00E-10	1.57E-04	2.46E-12
MLB3-40-4	9.72E-05	9.45E-11	7.68E-05	5.90E-11	3.35E-02	4.00E-10	1.59E-04	2.53E-12
MLB3-40-5	1.14E-04	1.30E-10	7.68E-05	5.90E-11	3.59E-02	4.00E-10	1.68E-04	2.84E-12
MLB4-40-1	3.04E-04	9.24E-10	2.85E-04	8.12E-10	3.35E-02	4.00E-10	1.60E-04	2.56E-12
MLB4-40-2	2.98E-04	8.88E-10	2.85E-04	8.12E-10	3.00E-02	4.00E-10	1.42E-04	2.02E-12
MLB4-40-3	3.07E-04	9.42E-10	2.85E-04	8.12E-10	3.35E-02	4.00E-10	1.61E-04	2.59E-12
MLB4-40-4	3.17E-04	1.00E-09	2.85E-04	8.12E-10	3.21E-02	4.00E-10	1.55E-04	2.40E-12
MLB4-40-5	3.17E-04	1.00E-09	2.85E-04	8.12E-10	3.14E-02	4.00E-10	1.50E-04	2.25E-12
MLB5-40-1R	1.80E-05	3.24E-12	8.73E-06	7.62E-13	3.22E-02	4.00E-10	1.51E-04	2.29E-12
MLB5-40-2R	3.96E-05	1.57E-11	8.73E-06	7.62E-13	3.24E-02	4.00E-10	1.52E-04	2.32E-12
MLB5-40-3R	4.00E-05	1.60E-11	8.73E-06	7.62E-13	3.25E-02	4.00E-10	1.53E-04	2.33E-12
MLB5-40-4R	5.75E-05	3.31E-11	8.73E-06	7.62E-13	3.32E-02	4.00E-10	1.56E-04	2.44E-12
MLB5-40-5R	5.80E-05	3.36E-11	8.73E-06	7.62E-13	3.40E-02	4.00E-10	1.60E-04	2.55E-12
MLB6-40-1	2.15E-05	4.62E-12	2.13E-05	4.54E-12	6.47E-02	4.00E-10	1.55E-04	2.40E-12
MLB6-40-2	3.05E-05	9.30E-12	2.13E-05	4.54E-12	5.09E-02	4.00E-10	1.15E-04	1.32E-12
MLB6-40-3	2.94E-05	8.64E-12	2.13E-05	4.54E-12	5.19E-02	4.00E-10	1.18E-04	1.39E-12
MLB6-40-4	3.65E-05	1.33E-11	2.13E-05	4.54E-12	4.82E-02	4.00E-10	1.22E-04	1.49E-12
MLB6-40-5	5.45E-05	2.97E-11	2.13E-05	4.54E-12	5.23E-02	4.00E-10	1.24E-04	1.54E-12
Immersion Tests at 70 °C								
MLB1-70-1	1.53E-03	2.34E-08	8.50E-04	7.23E-09	6.12E-02	4.00E-10	1.42E-04	2.02E-12
MLB1-70-2	2.70E-03	7.29E-08	8.50E-04	7.23E-09	5.06E-02	4.00E-10	1.19E-04	1.42E-12
MLB1-70-3	3.03E-03	9.18E-08	8.50E-04	7.23E-09	4.67E-02	4.00E-10	1.09E-04	1.19E-12
MLB1-70-4	3.29E-03	1.08E-07	8.50E-04	7.23E-09	5.65E-02	4.00E-10	1.29E-04	1.66E-12
MLB1-70-5	3.93E-03	1.54E-07	8.50E-04	7.23E-09	5.32E-02	4.00E-10	1.23E-04	1.51E-12
MLB2-70-1	4.01E-04	1.61E-09	1.06E-04	1.12E-10	3.58E-02	4.00E-10	1.72E-04	2.96E-12
MLB2-70-2	6.24E-04	3.89E-09	1.06E-04	1.12E-10	3.05E-02	4.00E-10	1.48E-04	2.18E-12
MLB2-70-3	6.72E-04	4.52E-09	1.06E-04	1.12E-10	3.23E-02	4.00E-10	1.56E-04	2.43E-12
MLB2-70-4	8.83E-04	7.80E-09	1.06E-04	1.12E-10	3.72E-02	4.00E-10	1.93E-04	3.71E-12
MLB2-70-5	1.06E-03	1.12E-08	1.06E-04	1.12E-10	3.16E-02	4.00E-10	1.52E-04	2.31E-12
MLB3-70-1	1.67E-04	2.79E-10	1.41E-04	1.99E-10	2.28E-02	4.00E-10	1.11E-04	1.23E-12
MLB3-70-2	3.50E-04	1.23E-09	1.41E-04	1.99E-10	3.61E-02	4.00E-10	1.72E-04	2.96E-12
MLB3-70-3	2.51E-04	6.30E-10	1.41E-04	1.99E-10	3.36E-02	4.00E-10	1.62E-04	2.62E-12
MLB3-70-4	2.65E-04	7.02E-10	1.41E-04	1.99E-10	3.04E-02	4.00E-10	1.54E-04	2.37E-12
MLB3-70-5	4.01E-04	1.61E-09	1.41E-04	1.99E-10	3.23E-02	4.00E-10	1.55E-04	2.40E-12
MLB4-70-1	3.58E-04	1.28E-09	2.52E-04	6.35E-10	3.26E-02	4.00E-10	1.57E-04	2.46E-12
MLB4-70-2	3.52E-04	1.24E-09	2.52E-04	6.35E-10	3.26E-02	4.00E-10	1.56E-04	2.43E-12
MLB4-70-3	4.36E-04	1.90E-09	2.52E-04	6.35E-10	3.12E-02	4.00E-10	1.51E-04	2.28E-12
MLB4-70-4	4.12E-04	1.70E-09	2.52E-04	6.35E-10	3.16E-02	4.00E-10	1.52E-04	2.31E-12
MLB4-70-5	4.91E-04	2.41E-09	2.52E-04	6.35E-10	3.09E-02	4.00E-10	1.49E-04	2.22E-12
MLB5-70-1R	1.22E-04	1.49E-10	9.00E-06	8.10E-13	3.44E-02	4.00E-10	1.62E-04	2.62E-12
MLB5-70-2R	7.90E-05	6.24E-11	9.00E-06	8.10E-13	3.46E-02	4.00E-10	1.63E-04	2.65E-12
MLB5-70-3R	8.33E-05	6.94E-11	9.00E-06	8.10E-13	3.47E-02	4.00E-10	1.63E-04	2.66E-12
MLB5-70-4R	1.89E-04	3.57E-10	9.00E-06	8.10E-13	3.59E-02	4.00E-10	1.69E-04	2.84E-12
MLB5-70-5R	1.45E-04	2.10E-10	9.00E-06	8.10E-13	3.62E-02	4.00E-10	1.71E-04	2.91E-12
MLB6-70-1	6.78E-05	4.60E-11	1.71E-05	2.92E-12	5.00E-02	4.00E-10	1.22E-04	1.49E-12
MLB6-70-2	1.50E-04	2.25E-10	1.71E-05	2.92E-12	5.08E-02	4.00E-10	1.24E-04	1.54E-12
MLB6-70-3	2.54E-04	6.45E-10	1.71E-05	2.92E-12	5.36E-02	4.00E-10	1.33E-04	1.77E-12

Table E1. (cont.)

Test Number	C, g/L	q_c^2	C° , g/L	q_{co}^2	V, L	q_v^2	S, m ²	q_s^2
MLB6-70-4	3.37E-04	1.14E-09	1.71E-05	2.92E-12	5.20E-02	4.00E-10	1.23E-04	1.51E-12
MLB6-70-5	3.09E-04	9.55E-10	1.71E-05	2.92E-12	5.32E-02	4.00E-10	1.32E-04	1.74E-12
Immersion Tests at 90 °C								
MLB1-90-1	4.24E-03	1.80E-07	2.20E-03	4.84E-08	5.57E-02	4.00E-10	1.32E-04	1.74E-12
MLB1-90-2	6.02E-03	3.62E-07	2.20E-03	4.84E-08	5.74E-02	4.00E-10	1.36E-04	1.85E-12
MLB1-90-3	7.34E-03	5.39E-07	2.20E-03	4.84E-08	5.45E-02	4.00E-10	1.25E-04	1.56E-12
MLB1-90-4	8.68E-03	7.53E-07	2.20E-03	4.84E-08	5.94E-02	4.00E-10	1.45E-04	2.10E-12
MLB1-90-5	8.33E-03	6.94E-07	2.20E-03	4.84E-08	5.65E-02	4.00E-10	1.35E-04	1.82E-12
MLB2-90-1	5.48E-04	3.00E-09	2.80E-04	7.84E-10	4.03E-02	4.00E-10	1.86E-04	3.46E-12
MLB2-90-2	7.12E-04	5.07E-09	2.80E-04	7.84E-10	3.11E-02	4.00E-10	1.45E-04	2.10E-12
MLB2-90-3	8.53E-04	7.28E-09	2.80E-04	7.84E-10	3.05E-02	4.00E-10	1.38E-04	1.90E-12
MLB2-90-4	9.56E-04	9.14E-09	2.80E-04	7.84E-10	3.08E-02	4.00E-10	1.39E-04	1.93E-12
MLB2-90-5	1.03E-03	1.06E-08	2.80E-04	7.84E-10	3.77E-02	4.00E-10	1.80E-04	3.24E-12
MLB3-90-1	3.12E-04	9.73E-10	1.27E-04	1.61E-10	3.24E-02	4.00E-10	1.51E-04	2.28E-12
MLB3-90-2	5.85E-04	3.42E-09	1.27E-04	1.61E-10	3.61E-02	4.00E-10	1.70E-04	2.89E-12
MLB3-90-3	7.24E-04	5.24E-09	1.27E-04	1.61E-10	3.32E-02	4.00E-10	1.54E-04	2.37E-12
MLB3-90-4	9.64E-04	9.29E-09	1.27E-04	1.61E-10	3.26E-02	4.00E-10	1.52E-04	2.31E-12
MLB3-90-5	1.04E-03	1.08E-08	1.27E-04	1.61E-10	3.29E-02	4.00E-10	1.55E-04	2.40E-12
MLB4-90-1	3.33E-04	1.11E-09	3.26E-04	1.06E-09	3.05E-02	4.00E-10	1.47E-04	2.16E-12
MLB4-90-2	4.69E-04	2.20E-09	3.26E-04	1.06E-09	3.24E-02	4.00E-10	1.61E-04	2.60E-12
MLB4-90-3	4.44E-04	1.97E-09	3.26E-04	1.06E-09	3.38E-02	4.00E-10	1.62E-04	2.62E-12
MLB4-90-4	5.35E-04	2.86E-09	3.26E-04	1.06E-09	3.40E-02	4.00E-10	1.62E-04	2.64E-12
MLB4-90-5	5.35E-04	2.86E-09	3.26E-04	1.06E-09	3.56E-02	4.00E-10	1.69E-04	2.86E-12
MLB5-90-1R	4.45E-05	1.98E-11	9.07E-06	8.23E-13	3.66E-02	4.00E-10	1.72E-04	2.96E-12
MLB5-90-2R	1.21E-04	1.46E-10	9.07E-06	8.23E-13	3.73E-02	4.00E-10	1.76E-04	3.08E-12
MLB5-90-3R	1.45E-04	2.10E-10	9.07E-06	8.23E-13	3.80E-02	4.00E-10	1.79E-04	3.19E-12
MLB5-90-4R	1.97E-04	3.88E-10	9.07E-06	8.23E-13	3.87E-02	4.00E-10	1.82E-04	3.31E-12
MLB5-90-5R	1.76E-04	3.10E-10	9.07E-06	8.23E-13	4.57E-02	4.00E-10	2.15E-04	4.62E-12
MLB6-90-1	1.81E-04	3.28E-10	8.53E-06	7.28E-13	5.82E-02	4.00E-10	1.41E-04	1.99E-12
MLB6-90-2	4.47E-04	2.00E-09	8.53E-06	7.28E-13	5.76E-02	4.00E-10	1.38E-04	1.90E-12
MLB6-90-3	5.96E-04	3.55E-09	8.53E-06	7.28E-13	5.67E-02	4.00E-10	1.41E-04	1.99E-12
MLB6-90-4	6.45E-04	4.16E-09	8.53E-06	7.28E-13	5.91E-02	4.00E-10	1.42E-04	2.02E-12
MLB6-90-5	9.01E-04	8.12E-09	8.53E-06	7.28E-13	5.98E-02	4.00E-10	1.44E-04	2.07E-12
MLBD-90-1	4.29E-04	1.84E-09	1.71E-04	2.92E-10	1.00E-02	4.00E-10	1.18E-04	1.39E-12
MLBD-90-2	8.52E-04	7.26E-09	1.71E-04	2.92E-10	1.18E-02	4.00E-10	1.39E-04	1.94E-12
MLBD-90-3	1.02E-03	1.04E-08	1.71E-04	2.92E-10	8.19E-03	4.00E-10	9.66E-05	9.33E-13
MLBD-90-4	1.07E-03	1.14E-08	1.71E-04	2.92E-10	8.12E-03	4.00E-10	9.58E-05	9.18E-13
MLBD-90-5	1.16E-03	1.35E-08	1.71E-04	2.92E-10	9.32E-03	4.00E-10	1.10E-04	1.21E-12
MLBD-90-6	1.95E-03	3.80E-08	1.71E-04	2.92E-10	9.15E-03	4.00E-10	1.06E-04	1.13E-12
MLBD-90-7	2.29E-03	5.24E-08	1.71E-04	2.92E-10	9.19E-03	4.00E-10	1.09E-04	1.18E-12
MLBD-90-8	9.72E-03	9.45E-07	1.71E-04	2.92E-10	1.53E-02	4.00E-10	1.84E-04	3.39E-12
MLBD-120-1	3.38E-03	1.14E-07	1.71E-04	2.92E-10	1.55E-02	4.00E-10	9.23E-05	8.52E-13
MLBD-120-2	6.95E-03	4.83E-07	1.71E-04	2.92E-10	1.53E-02	4.00E-10	8.86E-05	7.85E-13

Table E2. Summary of Variance in Each Term, Uncertainty, and Relative Uncertainty^a

Test Number	Q_C^2	$Q_{C^0}^2$	Q_V^2	Q_S^2	Q_f^2	Q_{NL}^2	Q	NL(Si)	Q/NL(Si)
Immersion Tests at 40 °C									
MLB1-40-1	6.94E-02	5.31E-02	1.47E-08	1.09E-05	3.91E-04	1.23E-01	3.51E-01	3.31E-01	106.0%
MLB1-40-2	1.25E-01	5.40E-02	1.74E-07	1.49E-04	5.32E-03	1.85E-01	4.30E-01	1.22E+00	35.3%
MLB1-40-3	1.80E-01	5.60E-02	4.16E-07	3.53E-04	1.26E-02	2.49E-01	4.99E-01	1.88E+00	26.6%
MLB1-40-4	1.70E-01	5.03E-02	4.44E-07	3.54E-04	1.27E-02	2.33E-01	4.83E-01	1.88E+00	25.7%
MLB1-40-5	2.65E-01	5.19E-02	9.43E-07	8.21E-04	2.94E-02	3.47E-01	5.89E-01	2.86E+00	20.6%
MLB2-40-1	2.38E-03	4.68E-04	2.72E-08	7.40E-06	2.65E-04	3.12E-03	5.59E-02	2.72E-01	20.5%
MLB2-40-2	6.51E-03	4.69E-04	1.05E-07	3.48E-05	1.25E-03	8.26E-03	9.09E-02	5.90E-01	15.4%
MLB2-40-3	7.47E-03	4.56E-04	1.88E-07	4.24E-05	1.52E-03	9.49E-03	9.74E-02	6.51E-01	15.0%
MLB2-40-4	8.98E-03	4.67E-04	1.42E-07	5.36E-05	1.92E-03	1.14E-02	1.07E-01	7.32E-01	14.6%
MLB2-40-5	1.56E-02	4.78E-04	3.06E-07	1.06E-04	3.79E-03	1.99E-02	1.41E-01	1.03E+00	13.7%
MLB3-40-1	2.14E-04	1.79E-04	1.10E-10	1.53E-08	5.49E-07	3.94E-04	1.99E-02	1.24E-02	160.3%
MLB3-40-2	2.06E-04	1.63E-04	1.07E-10	2.44E-08	8.75E-07	3.70E-04	1.92E-02	1.56E-02	123.0%
MLB3-40-3	2.59E-04	1.70E-04	3.47E-10	9.15E-08	3.28E-06	4.32E-04	2.08E-02	3.03E-02	68.7%
MLB3-40-4	2.82E-04	1.76E-04	4.42E-10	1.24E-07	4.45E-06	4.63E-04	2.15E-02	3.53E-02	61.0%
MLB3-40-5	3.96E-04	1.80E-04	1.31E-09	4.22E-07	1.51E-05	5.91E-04	2.43E-02	6.49E-02	37.4%
MLB4-40-1	2.72E-03	2.39E-03	3.79E-10	1.06E-07	3.80E-06	5.11E-03	7.15E-02	3.26E-02	219.4%
MLB4-40-2	2.67E-03	2.44E-03	2.25E-10	5.08E-08	1.82E-06	5.11E-03	7.15E-02	2.25E-02	317.2%
MLB4-40-3	2.74E-03	2.36E-03	5.02E-10	1.41E-07	5.04E-06	5.11E-03	7.15E-02	3.75E-02	190.5%
MLB4-40-4	2.90E-03	2.34E-03	1.15E-09	2.95E-07	1.06E-05	5.25E-03	7.25E-02	5.43E-02	133.4%
MLB4-40-5	2.97E-03	2.40E-03	1.22E-09	3.02E-07	1.08E-05	5.38E-03	7.33E-02	5.50E-02	133.4%
MLB5-40-1R	9.85E-06	2.32E-06	1.01E-10	2.61E-08	9.36E-07	1.31E-05	3.62E-03	1.62E-02	22.4%
MLB5-40-2R	4.77E-05	2.32E-06	1.10E-09	2.90E-07	1.04E-05	6.06E-05	7.79E-03	5.38E-02	14.5%
MLB5-40-3R	4.86E-05	2.32E-06	1.13E-09	2.97E-07	1.06E-05	6.19E-05	7.87E-03	5.45E-02	14.4%
MLB5-40-4R	1.00E-04	2.32E-06	2.62E-09	7.23E-07	2.59E-05	1.29E-04	1.14E-02	8.50E-02	13.4%
MLB5-40-5R	1.02E-04	2.32E-06	2.56E-09	7.38E-07	2.64E-05	1.32E-04	1.15E-02	8.59E-02	13.4%
MLB6-40-1	5.41E-05	5.31E-05	4.47E-14	4.68E-11	1.68E-09	1.07E-04	1.04E-02	6.84E-04	1513.2%
MLB6-40-2	1.22E-04	5.97E-05	1.72E-10	1.11E-07	3.99E-06	1.86E-04	1.36E-02	3.34E-02	40.9%
MLB6-40-3	1.13E-04	5.91E-05	1.27E-10	8.54E-08	3.06E-06	1.75E-04	1.32E-02	2.92E-02	45.2%
MLB6-40-4	1.40E-04	4.76E-05	4.17E-10	2.43E-07	8.69E-06	1.96E-04	1.40E-02	4.93E-02	28.5%
MLB6-40-5	3.55E-04	5.42E-05	1.93E-09	1.32E-06	4.72E-05	4.58E-04	2.14E-02	1.15E-01	18.6%
Immersion Tests at 70 °C									
MLB1-70-1	2.92E-01	9.02E-02	6.16E-07	5.77E-04	2.07E-02	4.04E-01	6.35E-01	2.40E+00	26.4%
MLB1-70-2	8.85E-01	8.77E-02	6.50E-06	4.15E-03	1.49E-01	1.13E+00	1.06E+00	6.39E+00	16.5%
MLB1-70-3	1.13E+00	8.91E-02	1.07E-05	5.86E-03	2.10E-01	1.44E+00	1.20E+00	7.65E+00	15.7%
MLB1-70-4	1.40E+00	9.32E-02	9.61E-06	7.68E-03	2.75E-01	1.77E+00	1.33E+00	8.76E+00	15.2%
MLB1-70-5	1.94E+00	9.10E-02	1.69E-05	1.19E-02	4.28E-01	2.47E+00	1.57E+00	1.09E+01	14.4%
MLB2-70-1	4.69E-03	3.28E-04	7.91E-08	2.54E-05	9.08E-04	5.95E-03	7.71E-02	5.04E-01	15.3%
MLB2-70-2	1.12E-02	3.22E-04	3.31E-07	7.69E-05	2.75E-03	1.43E-02	1.20E-01	8.77E-01	13.6%
MLB2-70-3	1.30E-02	3.24E-04	3.54E-07	9.23E-05	3.30E-03	1.67E-02	1.29E-01	9.61E-01	13.5%
MLB2-70-4	1.96E-02	2.82E-04	4.37E-07	1.51E-04	5.42E-03	2.54E-02	1.59E-01	1.23E+00	13.0%
MLB2-70-5	3.25E-02	3.25E-04	1.06E-06	2.63E-04	9.43E-03	4.26E-02	2.06E-01	1.62E+00	12.7%
MLB3-70-1	7.93E-04	5.66E-04	1.47E-09	1.92E-07	6.88E-06	1.37E-03	3.70E-02	4.39E-02	84.3%
MLB3-70-2	3.62E-03	5.88E-04	3.97E-08	1.29E-05	4.63E-04	4.69E-03	6.85E-02	3.59E-01	19.0%
MLB3-70-3	1.82E-03	5.73E-04	1.24E-08	3.49E-06	1.25E-04	2.52E-03	5.02E-02	1.87E-01	26.9%
MLB3-70-4	1.84E-03	5.22E-04	1.74E-08	4.03E-06	1.44E-04	2.51E-03	5.01E-02	2.01E-01	25.0%
MLB3-70-5	4.69E-03	5.79E-04	7.56E-08	1.97E-05	7.05E-04	5.99E-03	7.74E-02	4.44E-01	17.4%
MLB4-70-1	3.70E-03	1.83E-03	1.23E-08	3.25E-06	1.16E-04	5.66E-03	7.52E-02	1.80E-01	41.7%
MLB4-70-2	3.63E-03	1.86E-03	1.10E-08	2.93E-06	1.05E-04	5.59E-03	7.48E-02	1.71E-01	43.7%
MLB4-70-3	5.45E-03	1.82E-03	3.99E-08	9.71E-06	3.48E-04	7.63E-03	8.74E-02	3.12E-01	28.0%
MLB4-70-4	4.93E-03	1.85E-03	2.98E-08	7.44E-06	2.66E-04	7.05E-03	8.40E-02	2.73E-01	30.8%
MLB4-70-5	6.95E-03	1.83E-03	6.91E-08	1.65E-05	5.90E-04	9.39E-03	9.69E-02	4.06E-01	23.9%
MLB5-70-1R	4.52E-04	2.46E-06	1.31E-08	3.88E-06	1.39E-04	5.97E-04	2.44E-02	1.97E-01	12.4%
MLB5-70-2R	1.90E-04	2.46E-06	4.97E-09	1.49E-06	5.34E-05	2.47E-04	1.57E-02	1.22E-01	12.9%
MLB5-70-3R	2.11E-04	2.46E-06	5.57E-09	1.68E-06	6.00E-05	2.75E-04	1.66E-02	1.30E-01	12.8%
MLB5-70-4R	1.09E-03	2.46E-06	3.06E-08	9.85E-06	3.53E-04	1.45E-03	3.81E-02	3.14E-01	12.1%
MLB5-70-5R	6.36E-04	2.45E-06	1.71E-08	5.60E-06	2.00E-04	8.45E-04	2.91E-02	2.37E-01	12.3%
MLB6-70-1	5.19E-04	3.30E-05	4.64E-09	2.90E-06	1.04E-04	6.59E-04	2.57E-02	1.70E-01	15.1%
MLB6-70-2	2.54E-03	3.30E-05	3.09E-08	1.99E-05	7.14E-04	3.31E-03	5.75E-02	4.47E-01	12.9%
MLB6-70-3	7.03E-03	3.18E-05	8.53E-08	6.11E-05	2.19E-03	9.31E-03	9.65E-02	7.82E-01	12.3%

Table E2. (cont.)

Test Number	Q_C^2	$Q_{C^\circ}^2$	Q_V^2	Q_S^2	Q_f^2	Q_{NL}^2	Q_{NL}	NL(Si)	Q/NL(Si)
MLB6-70-4	1.36E-02	3.51E-05	1.82E-07	1.23E-04	4.40E-03	1.82E-02	1.35E-01	1.11E+00	12.2%
MLB6-70-5	1.04E-02	3.19E-05	1.31E-07	9.28E-05	3.32E-03	1.39E-02	1.18E-01	9.64E-01	12.2%
Immersion Tests at 90 °C									
MLB1-90-1	2.15E+00	5.79E-01	6.42E-06	4.98E-03	1.78E-01	2.91E+00	1.71E+00	7.06E+00	24.2%
MLB1-90-2	4.34E+00	5.79E-01	2.12E-05	1.75E-02	6.25E-01	5.56E+00	2.36E+00	1.32E+01	17.8%
MLB1-90-3	6.89E+00	6.19E-01	4.54E-05	3.38E-02	1.21E+00	8.75E+00	2.96E+00	1.84E+01	16.1%
MLB1-90-4	8.49E+00	5.45E-01	5.37E-05	4.73E-02	1.69E+00	1.08E+01	3.28E+00	2.18E+01	15.1%
MLB1-90-5	8.18E+00	5.70E-01	5.54E-05	4.43E-02	1.59E+00	1.04E+01	3.22E+00	2.10E+01	15.3%
MLB2-90-1	9.45E-03	2.47E-03	5.58E-08	2.26E-05	8.09E-04	1.27E-02	1.13E-01	4.75E-01	23.8%
MLB2-90-2	1.57E-02	2.42E-03	2.39E-07	5.77E-05	2.07E-03	2.02E-02	1.42E-01	7.60E-01	18.7%
MLB2-90-3	2.38E-02	2.57E-03	4.63E-07	1.08E-04	3.85E-03	3.03E-02	1.74E-01	1.04E+00	16.8%
MLB2-90-4	3.01E-02	2.58E-03	6.36E-07	1.51E-04	5.39E-03	3.82E-02	1.96E-01	1.23E+00	15.9%
MLB2-90-5	3.13E-02	2.31E-03	4.67E-07	1.66E-04	5.94E-03	3.97E-02	1.99E-01	1.29E+00	15.5%
MLB3-90-1	3.01E-03	4.99E-04	4.03E-08	1.06E-05	3.79E-04	3.90E-03	6.24E-02	3.25E-01	19.2%
MLB3-90-2	1.04E-02	4.89E-04	1.95E-07	6.35E-05	2.27E-03	1.32E-02	1.15E-01	7.97E-01	14.4%
MLB3-90-3	1.63E-02	5.03E-04	4.04E-07	1.11E-04	3.98E-03	2.09E-02	1.45E-01	1.05E+00	13.7%
MLB3-90-4	2.88E-02	5.00E-04	8.15E-07	2.17E-04	7.77E-03	3.73E-02	1.93E-01	1.49E+00	13.1%
MLB3-90-5	3.27E-02	4.88E-04	9.32E-07	2.52E-04	9.02E-03	4.25E-02	2.06E-01	1.59E+00	13.0%
MLB4-90-1	3.21E-03	3.08E-03	6.09E-11	1.42E-08	5.08E-07	6.29E-03	7.93E-02	1.19E-02	665.8%
MLB4-90-2	5.96E-03	2.88E-03	2.11E-08	5.54E-06	1.98E-04	9.04E-03	9.51E-02	2.35E-01	40.4%
MLB4-90-3	5.78E-03	3.11E-03	1.43E-08	4.08E-06	1.46E-04	9.04E-03	9.51E-02	2.02E-01	47.1%
MLB4-90-4	8.41E-03	3.12E-03	4.45E-08	1.28E-05	4.60E-04	1.20E-02	1.10E-01	3.58E-01	30.6%
MLB4-90-5	8.51E-03	3.16E-03	4.10E-08	1.30E-05	4.65E-04	1.22E-02	1.10E-01	3.60E-01	30.6%
MLB5-90-1R	6.02E-05	2.50E-06	1.14E-09	3.82E-07	1.37E-05	7.67E-05	8.76E-03	6.18E-02	14.2%
MLB5-90-2R	4.45E-04	2.50E-06	1.09E-08	3.81E-06	1.36E-04	5.87E-04	2.42E-02	1.95E-01	12.4%
MLB5-90-3R	6.38E-04	2.50E-06	1.55E-08	5.61E-06	2.01E-04	8.47E-04	2.91E-02	2.37E-01	12.3%
MLB5-90-4R	1.18E-03	2.50E-06	2.87E-08	1.07E-05	3.84E-04	1.57E-03	3.97E-02	3.27E-01	12.1%
MLB5-90-5R	9.40E-04	2.50E-06	1.62E-08	8.46E-06	3.03E-04	1.25E-03	3.54E-02	2.91E-01	12.2%
MLB6-90-1	3.75E-03	8.34E-06	4.02E-08	3.41E-05	1.22E-03	5.02E-03	7.08E-02	5.84E-01	12.1%
MLB6-90-2	2.34E-02	8.53E-06	2.71E-07	2.25E-04	8.07E-03	3.17E-02	1.78E-01	1.50E+00	11.9%
MLB6-90-3	3.85E-02	7.89E-06	4.67E-07	3.74E-04	1.34E-02	5.23E-02	2.29E-01	1.93E+00	11.8%
MLB6-90-4	4.84E-02	8.47E-06	5.40E-07	4.71E-04	1.69E-02	6.58E-02	2.56E-01	2.17E+00	11.8%
MLB6-90-5	9.42E-02	8.44E-06	1.03E-06	9.24E-04	3.31E-02	1.28E-01	3.58E-01	3.04E+00	11.8%
MLBD-90-1	8.88E-04	1.41E-04	1.29E-07	3.21E-06	1.15E-04	1.15E-03	3.39E-02	1.79E-01	18.9%
MLBD-90-2	3.50E-03	1.41E-04	6.43E-07	2.23E-05	8.00E-04	4.46E-03	6.68E-02	4.73E-01	14.1%
MLBD-90-3	5.02E-03	1.41E-04	2.08E-06	3.48E-05	1.25E-03	6.44E-03	8.03E-02	5.90E-01	13.6%
MLBD-90-4	5.52E-03	1.41E-04	2.37E-06	3.90E-05	1.40E-03	7.10E-03	8.43E-02	6.24E-01	13.5%
MLBD-90-5	6.49E-03	1.41E-04	2.17E-06	4.72E-05	1.69E-03	8.37E-03	9.15E-02	6.87E-01	13.3%
MLBD-90-6	1.90E-02	1.46E-04	7.54E-06	1.58E-04	5.65E-03	2.49E-02	1.58E-01	1.26E+00	12.6%
MLBD-90-7	2.53E-02	1.41E-04	1.02E-05	2.16E-04	7.74E-03	3.34E-02	1.83E-01	1.47E+00	12.4%
MLBD-90-8	4.39E-01	1.36E-04	7.24E-05	4.24E-03	1.52E-01	5.95E-01	7.71E-01	6.51E+00	11.9%
MLBD-120-1	2.18E-01	5.57E-04	3.25E-05	1.96E-03	7.02E-02	2.90E-01	5.39E-01	4.43E+00	12.2%
MLBD-120-2	9.70E-01	5.87E-04	1.57E-04	9.23E-03	3.31E-01	1.31E+00	1.14E+00	9.61E+00	11.9%

^aColumn headings:

$$Q_C^2 = \left(\frac{V_{\text{test solution}}}{S \times f(\text{Si})} \right)^2 \times q_C^2 \quad Q_{C^\circ}^2 = \left(\frac{-V_{\text{test solution}}}{S \times f(\text{Si})} \right)^2 \times q_{C^\circ}^2 \quad Q_V^2 = \left(\frac{C(\text{Si})_{\text{test solution}} - C^\circ(\text{Si})}{S \times f(\text{Si})} \right)^2 \times q_V^2$$

$$Q_S^2 = \left(\frac{-(C(\text{Si})_{\text{test solution}} - C^\circ(\text{Si})) \times V_{\text{test solution}}}{S^2 \times f(\text{Si})} \right)^2 \times q_S^2 \quad Q_{NL}^2 = Q_C^2 + Q_{C^\circ}^2 + Q_V^2 + Q_S^2 + Q_{f(\text{Si})}^2$$

$$Q_{f(\text{Si})}^2 = \left(\frac{-(C(\text{Si})_{\text{test solution}} - C^\circ(\text{Si})) \times V_{\text{test solution}}}{S \times f(\text{Si})^2} \right)^2 \times q_{f(\text{Si})}^2$$

APPENDIX F: TEST DATA FOR VAPOR HYDRATION TESTS

The test data for the initiation and termination of vapor hydration tests at 120 and 200 °C are summarized in Table F1. The data given in each column are summarized below

Test Number	Test number from test matrix
Duration	Number of days vessel was in oven
Vessel Number	Number of vessel used in test
Specimen number	Alpha-numeric assigned to each specimen
LaBS-B contacting	Specimen of Pu LaBS-B glass tied with specimen of SRL 418 glass
SRL 418 contacting	Specimen of SRL 418 glass tied with specimen of Pu LaBS glass
LaBS-B separated	Specimen of Pu LaBS-B glass not contacting another glass
Water mass, g	Mass demineralized water added to vessel
Date In/Time	Calendar date and time of day vessel was placed in oven
Date Out/Time	Calendar date and time of day vessel was removed from oven

Table F1. Test Data for Vapor Hydration Tests

Test Number	Duration, d	Vessel number	Specimen numbers			Water mass, g	Date In Time	Date Out Time
			LaBS-B contacting	SRL 418 contacting	LaBS-B separated			
VHT at 120 °C with LaBS-B and SRL 418 glass								
VLB-120-1	72	169	B1a	S1	B1b	0.20	3/24/06 16:30	6/4/06 10:00
VLB-120-2	72	843	B2a	S2	B2b	0.20	3/24/06 16:30	6/4/06 10:00
VLB-120-3	54	743	B3a	S3	B3b	0.20	3/24/06 16:30	5/17/06 10:00
VLB-120-4	35	820	B4a	S4	B4b	0.20	3/24/06 16:30	4/28/06 11:00
VLB-120-5	21	805	B5a	S5	B5b	0.20	3/24/06 16:30	4/14/06 10:00
VHT at 200 °C with LaBS-B and SRL 418 glass								
VLB-200-1	24	87	B6a	S6	B6b	0.25	3/24/06 16:30	4/17/06 10:00
VLB-200-2	24	833	B7a	S7	B7b	0.25	3/24/06 16:30	4/17/06 10:00
VLB-200-3	24	182	B8a	S8	B8b	0.25	3/24/06 16:30	4/17/06 10:00
VLB-200-4	21	807	B9a	S9	B9b	0.25	3/24/06 16:30	4/14/06 10:00
VLB-200-5	14	803	B10a	S10	B10b	0.25	3/31/06 10:00	4/14/06 10:00
VHT at 120 °C with SRL 418 glass								
VBB-120-1	65	108	S11	—	S12	0.20	3/31/06 10:00	6/4/06 10:00
VBB-120-2	35	823	S13	—	S14	0.20	3/31/06 10:00	5/5/06 15:40
VHT at 200 °C with SRL 418 glass								
VBB-200-1	14	755	S15	—	S16	0.25	3/31/06 10:00	4/14/06 10:00
VBB-200-2	24	759	S17	—	S18	0.25	3/31/06 10:00	4/17/06 10:00

Distribution for ANL/06-35

Internal (Electronic Copy Only):

D. B. Chamberlain
J. C. Cunnane
N. L. Dietz
W. L. Ebert
J. A. Fortner
D. J. Graziano
J. L. Jerden, Jr.
M. T. Peters
M. C. Regalbuto
V. S. Sullivan
Y. Tsai

External (Electronic Copies Only):

M. A. Buckley, ANL Library-E

N. E. Bibler, Savannah River National Laboratory, Aiken, SC
C. L. Crawford, Savannah River National Laboratory, Aiken, SC
J. C. Marra, Savannah River National Laboratory, Aiken, SC
D. M. Strachan, Pacific Northwest National Laboratory, Richland, WA



Chemical Engineering Division

Argonne National Laboratory
9700 South Cass Avenue, Bldg. 205
Argonne, IL 60439-4837

www.anl.gov



THE UNIVERSITY OF
CHICAGO

A U.S. Department of Energy laboratory
managed by The University of Chicago